Métabolisme des acides aminés dans l'échappement de Francisella tularensis du phagosome des macrophages infectés

Elodie Ramond

Université Paris Descartes - Faculté de Médecine

Thèse de doctorat en Sciences présentée par

Elodie Ramond

Pour obtenir le grade de Docteur de l'Université Paris Descartes

Ecole doctorale Gc2iD - Spécialité : Infectiologie

Métabolisme des acides aminés dans l'échappement de *Francisella tularensis* du phagosome des macrophages infectés.

Soutenue publiquement le 30 septembre 2014, devant le jury composé de :

Pr Xavier NASSIF	Président du jury
Dr Alain CHARBIT	Directeur de thèse
Dr Jost ENNINGA	Rapporteur
Dr Stéphane MERESSE	Rapporteur
Pr Isabelle MARTIN-VERSTRAETE	Examinateur
Pr Oliver NÜSSE	Examinateur

Unité de pathogénie des infections systémiques, INSERM U1151, équipe 11
Université Paris Descartes - Sorbonne Paris Cité
Faculté de médecine Necker
BATIMENT LERICHE – PORTE 9
14 Rue Maria Helena Vieira Da Silva CS61431
75993 Paris cedex 14
FRANCE

« Les rêves donnent du travail »

Paulo Coelho

Remerciements

Je voudrais tout d'abord remercier grandement mon directeur de thèse, Alain Charbit, pour m'avoir accueillie dans son équipe et pour m'avoir fait confiance, pour son aide et ses conseils tout au long de cette thèse et enfin pour la liberté et l'autonomie qu'il m'a laissé pendant ces trois ans. J'espère avoir été à la hauteur de la tâche attendue. Je suis ravie d'avoir travaillé avec vous.

Cette thèse n'aurait pas été possible sans le soutien de la Région Ile-de-France (DIM Malinf) que je remercie.

Mes remerciements vont au professeur Xavier Nassif, pour son aide et sa confiance lors de cette thèse et pour avoir accepté d'être membre de mon jury.

Je remercie les rapporteurs de cette thèse, le docteur Jost Enninga et le docteur Stéphane Méresse, ainsi que les examinateurs, le professeur Isabelle Martin-Verstraete et le professeur Oliver Nüsse pour avoir accepté d'évaluer ce travail et pour l'intérêt qu'ils y ont porté.

Je remercie tous les membres de l'équipe *Francisella* pour m'avoir aidée dans mes travaux scientifiques et pour leur bonne humeur : Gaël Gesbert, mon coloc' de laboratoire, Monique Barel, Fabiola Tros, très bonne organisatrice de repas, et Marion Dupuis. Une pensée et des remerciements aussi pour les anciens qui ont contribué à ma formation : Karin Meibom, Iharilalao Dubail, Jennifer Dieppedale et Terry Brissac. Une pensée pour tous les membres de l'équipe *Neisseria*. Mathieu, pour tes conseils, Emmanuelle, Eric et Daniel pour m'avoir convertie à la course à pied, Julie, contente de t'avoir rencontrée, Anne, Olivier, Hervé, Elena, Florence, Jean-Philippe et Zoé. Bonne continuation à vous tous.

J'adresse mes remerciements aux personnes qui ont collaboré à mes travaux de recherche de près ou de loin : Mélanie Rigard et son directeur Thomas Henry (Centre International de Recherche en Infectiologie, Lyon), Julien Dairou (Unité de Biologie Fonctionnelle, Paris), Loredana Saveanu (Institut Necker Enfants Malades, Paris), Chiarra Guerrera et Cerina Chhuon (Plateforme de protéomique, Institut Necker Enfants Malades).

Une pensée pour les stagiaires avec qui j'ai travaillé : Alexandra Baumard (bravo pour ton diplôme), Morgane Grand et Clément Argiewicz.

Je termine ces remerciements en dédiant cette thèse à mes parents qui m'ont donné le goût des Sciences. Pas d'inquiétude, la Suisse ça n'est pas si loin!

Enfin, je la dédie aussi à Damien, pour son amour et son soutien, merci de me faire confiance dans mon projet professionnel.

Résumé

Francisella tularensis, l'agent étiologique de la tularémie, est une bactérie à multiplication intracellulaire facultative capable d'infecter de nombreux types cellulaires avec un tropisme particulier pour les macrophages. Cette bactérie est responsable d'infections graves chez de nombreuses espèces animales mais aussi chez l'homme. En particulier, la sous-espèce *F. tularensis* ssp *tularensis* a été classée comme agent de bioterrorisme de type A du fait de son pouvoir pathogène extrêmement élevé avec une faible dose infectieuse.

Des approches de mutagénèse aléatoire et de criblage de banques de mutants ont suggéré l'importance des gènes impliqués dans les fonctions métaboliques et nutritionnelles dans le cycle intracellulaire de *Francisella.* Parmi ces gènes, on retrouve de très nombreux systèmes de transport d'acides aminés dont la sous-famille de transporteurs amino-polyamine-organocation (APC).

Dans un premier temps, nous nous sommes intéressés à un transporteur APC codé par le gène *FTN_0571*, que nous avons appelé GadC. Pour comprendre l'importance de GadC dans la virulence de *F. tularensis*, nous avons réalisé un mutant chromosomique, délété du gène *gadC*, chez la sous-espèce *novicida*. Nous avons démontré que GadC est un importeur de glutamate et qu'il est nécessaire à la multiplication intracellulaire et à la virulence de *Francisella*, en assurant une sortie normale de la bactérie du phagosome. Ce phénomène s'explique par l'implication de GadC dans la résistance au stress oxydant généré dans le phagosome. De façon remarquable, la multiplication du mutant *gadC* est restaurée dans un contexte gp91phox$^{-/-}$, incapable de générer des espèces réactives de l'oxygène, aussi bien *in vitro* qu'*in vivo*. Enfin, nous avons montré que l'activité de GadC modifie la production de certains intermédiaires du cycle de Krebs, et la transcription de l'enzyme qui leur est associée, démontrant un lien étroit entre la résistance au stress oxydant, le métabolisme du glutamate et la virulence de *F. tularensis*.

Ces résultats nous ont conduits à nous intéresser à un autre transporteur appartenant à la sous-famille APC, présentant une homologie de 33% avec GadC, et que nous avons nommé ArgP. Nous montrons qu'un mutant *argP* présente un défaut de multiplication intracellulaire et de virulence résultant d'un retard sévère de sortie du phagosome. Ce phénotype s'explique par un défaut d'import d'arginine. L'inactivation du gène *argP* dans sous-espèce *holarctica* LVS provoque des défauts de multiplication intracellulaire similaires à ceux observés dans la sous-espèce *novicida*, suggérant un rôle conservé du transporteur ArgP dans les différentes sous-espèces de *F. tularensis*.

Comme l'arginine constitue un acide aminé essentiel pour la bactérie, nous nous sommes posés la question de l'importance de cet acide aminé durant la phase phagosomale. Une analyse du protéome bactérien du mutant *argP* de *F. novicida*, dans des conditions mimant les conditions nutritionnelles phagosomales, révèle que l'arginine joue un rôle prépondérant dans la traduction des protéines en affectant la synthèse des protéines ribosomales.

L'ensemble des travaux réalisés au cours de cette thèse constitue la première démonstration de l'importance de l'acquisition d'acides aminés durant la phase phagosomale du cycle intracellulaire de *F. tularensis*.

Mots-clés : *F. tularensis*, GadC, ArgP, échappement phagosomal

Abréviations

8-oxo-dA/dG :8-oxo-7,8-dihydrodésoxyadénine/guanine
4-HNE : 4-hydroxy-2-nonénal
ABC : ATP binding cassette
ADN : acide désoxyribonucléique
Ahp : alkylhydroperoxide réductase
AIM2 : absent in melanoma 2
APC : amino acid-polyamine organication
ARN : acide ribonucléique
ATG : autophagy related genes
ATP : adénosine triphosphate
Bcl-2 : B-cell lymphoma 2
BCP : bacterioferritine comigratory protein
CDC : cholesterol dependent pore-forming cytolysin
Cu : cuivre
DAMPs : danger-associated molecular patterns
Dps : DNA binding protein
Dsb : disulfide bond formation protein
EEA-1 : early endosome antigen 1
ERA : espèces réactives de l'azote
ERK : extracellular signal-regulated kinases
ERO : espèces réactives de l'oxygène
FCP : *Francisella* containing phagosome
FCV : *Francisella* containing vacuole
Fe : fer
FevR : *Francisella* effector of virulence regulation
FPI : *Francisella* pathogenicity island
FTL : *Francisella tularensis* ssp *holarctica* LVS
FTN : *Francisella tularensis* ssp *novicida*
FTT : *Francisella tularensis* ssp *tularensis*
Ggt : γ-glutamyl transpeptidase
Gpx : glutathion peroxydase
GTP : guanosine triphosphate
HAAAP : hydroxyl/aromatic amino acid permease
Igl : intracellular growth locus
iNOS : inducible nitric oxyde synthase
Km : constante d'affinité
KO : knock-out
LAMP : Lysosomal-associated membrane protein
LC3 : microtubule –associated protein light chain 3
LPO : peroxyde lipidique
LPS : lipolysaccharide
LVS : live vaccine strain
MAPK : mitogen activated protein kinases
MDA : malondialdéhyde
MEK : MAPK/ERK kinase
MFS : major facilitator superfamily
MglA : macrophage growth locus
Mn : manganese
MR : mannose receptor
Msr : methionine sulfoxyde reductase
NADPH : nicotinamide adenine dinucléotide phophate
NDP52 : nuclear dot protein 52
NF-κB : nuclear factor-kappa B
NHEJ : non-homologous end-joining
NOD1/2 : nucleotide-binding oligomerization domain 1/2
NRAMP1 : natural resistance-associated macrophage protein 1
PAM : peptides anti-microbiens
PAMPs : pathogen-associated molecular patterns
PGA : poly-gamma-d-glutamate
PHOX : phagocyte oxydase
PI(3)P : phosphatidylinositol-3-phosphate
PLP : phospholipase
PigR : pathogenicity island gene regulator
PLP : phospholipase
POT : proton-dependent oligopeptide
PUFA : polyunsaturated fatty acids
RNS : reactive nitrogen species
ROS : reactive oxygen species
Sdh : serine 3 deshydrogenase
SLC1A5 : solute carrier family 1 A member 5
SOD : superoxyde dismutase
SNARE : N-ethylmaleimide-sensitive factor attachment protein receptor
Ssp : sous-espèce
TLR : toll-like receptor
TSC : two component systems
VSP45 : vacuole sorting protein 45
XO : xanthine oxydase
Zn : zinc

Illustrations

Table des matières

Introduction générale

Une introduction bibliographique présentera, dans un premier chapitre, les bactéries à multiplication intracellulaire, leur mode de survie dans la cellule phagocytaire et en particulier dans le phagosome face au stress oxydant. Un second chapitre présentera le modèle *Francisella tularensis*, bactérie à multiplication intracellulaire facultative que nous étudions au laboratoire.

La deuxième partie de ce travail présentera deux articles qui ont constitué mon principal travail de thèse, et qui portent sur l'identification de deux transporteurs d'acides aminés essentiels à la virulence de *F. tularensis*.

Enfin, les autres travaux auxquels j'ai participé, et qui ont donné lieu à des publications, seront regroupés en annexe.

Chapitre I

Introduction bibliographique

I. Stress oxydant et bactéries à multiplication intracellulaire.

1. Infection des bactéries à multiplication intracellulaire

Les bactéries à multiplication intracellulaire sont généralement classées en deux catégories : les bactéries à multiplication intracellulaire facultative et les bactéries à multiplication intracellulaire obligatoire. Certaines d'entre elles, comme *F. tularensis,* sont capables de disséminer de façon systémique en utilisant notamment les macrophages circulants comme véhicules.

1.1 Présentation des bactéries à multiplication intracellulaire

1.1.1 Facultative ou obligatoire ?

Les bactéries à multiplication intracellulaire obligatoire, aussi appelées endosymbiotes obligatoires, ont la particularité d'être incapables de survivre en dehors de leur hôte ou dans un milieu de culture synthétique. Le seul moyen pour elles de se multiplier est d'infecter un organisme hôte et de se répliquer dans un contexte intracellulaire. Elles se sont adaptées au fil du temps au métabolisme de leurs hôtes en utilisant de nombreux constituants présents dans les cellules infectées. On parle alors d'inter-dépendance métabolique qui se caractérise par l'extinction de nombreuses voies métaboliques, liée à l'apparition de nombreux pseudogènes (J. O. Andersson et al., 1999).

A l'inverse, les bactéries à multiplication intracellulaire facultative ont gardé la capacité de se répliquer aussi en milieu extracellulaire (Suter, 1956). Cette double compétence est un atout de virulence majeur puisqu'elle leur permet de persister, de transmettre efficacement la maladie dont elles sont responsables (Eswarappa, 2009; Honer zu Bentrup et al., 2001) et également de survivre dans l'environnement (Yildiz, 2007).

Toutes ces bactéries peuvent être à l'origine de maladies extrêmement infectieuses. Les principales bactéries appartenant à ces deux sous catégories sont référencées dans le tableau n°1 ci-dessous.

	Cellules infectées	Maladie associée
Ordre des *Rickettsiales*		
Rickettsia ans spp	Cellules endothéliales	Rickettsiose
Ehrlichia and spp	Monocytes et granulocytes	Ehrlichiose
Anaplasma and spp	Leucocytes, érythrocytes	Anaplasmose
Ordre des *Legionellales*		
Coxiella burnetii	Macrophages	Fièvre Q
Ordre des *Chlamydiales*		
Chlamydia and spp	Cellules épithéliales	Lymphogranulome vénérien

Table 1 ***Bactéries à multiplication intracellulaire obligatoire***

	Cellules infectées	Maladie associée
Ordre des *Bacillales*		
Listeria and spp	Cellules intestinales Cellules phagocytaires	Listériose
Ordre des *Rhizobiales*		
Brucella and spp	Cellules phagocytaires	Brucellose
Ordre des *Legionellales*		
Legionella and spp	Cellules phagocytaires	Legionellose
Ordre des *Enterobacteriales*		
Salmonella and spp	Cellules intestinales Cellules phagocytaires	Salmonellose : Gastroentérite Fièvre typhoïde

Table 2 ***Bactéries à multiplication intracellulaire facultative***

Dans cette introduction bibliographique, j'ai choisi de discuter à titre d'exemples six bactéries à multiplication intracellulaire facultative (*Salmonella, Legionella, Listeria, Mycobacterium, Brucella* et *Francisella*) qui se multiplient soit à l'intérieur d'un compartiment vacuolaire soit directement dans le cytosol des cellules infectées.

1.1.2 Les quatre phases du cycle intracellulaire

Il est possible de diviser le cycle intracellulaire de ces bactéries en quatre parties. On distingue dans un premier temps l'*entrée* dans la cellule. Il s'agit d'une étape de transition entre l'espace extracellulaire et l'espace intracellulaire. Cette étape est généralement « microbe active ». En effet, la majorité des bactéries à multiplication intracellulaire sont capables de réarranger le cytosquelette de la cellule hôte pour entrer, comme par exemple *Salmonella* spp (Tujulin et al., 1998). Dans un deuxième temps, il s'agit pour la bactérie de *survivre* dans cet environnement hostile que constitue la vacuole phagosomale. En effet, dans ce compartiment, celle-ci est soumise à de nombreux stress microbicides générés par la cellule. Ces stress constituent notre sujet d'intérêt, ils seront détaillés dans les paragraphes

suivants. On distingue dans un troisième temps la *multiplication* intracellulaire. Certaines bactéries ont acquis des mécanismes qui leurs permettent de perforer la membrane phagosomale pour atteindre le cytosol, tandis que d'autres créent leur propre environnement vacuolaire propice à leur multiplication. Enfin, les bactéries ont développé plusieurs stratégies de *dissémination* pour atteindre les cellules voisines, on appelle ce phénomène la paracytophagie. Il s'agit d'une étape cruciale dans la pathogénie des bactéries intracellulaires. A titre d'exemples, alors que *L. monocytogenes* est propulsée de cellule en cellule grâce à ce qu'on appelle des « comètes d'actine » qui lui évitent de passer par le compartiment extracellulaire (Ireton, 2013), *Francisella* spp, qui est incapable de polymériser l'actine, conduit de façon contrôlée son hôte à la mort cellulaire (par apoptose et pyroptose) pour sa libération dans le milieu extérieur et l'infection de nouvelles cellules (Lai et al., 2001).

1.1.3 Adaptation à la vie intracellulaire et modification du génome

L'étude des génomes des nombreuses bactéries à multiplication intracellulaire a révélé que, lorsque le pathogène a acquis la capacité d'utiliser certains nutriments présents chez l'hôte, celui-ci à généralement tendance à perdre ses propres capacités de biosynthèse. En effet, la délétion de voies métaboliques entières est observée chez certains génomes bactériens. Par exemple, chez la bactérie *Rickettsia* ssp, la perte des voies impliquées dans le métabolisme des sucres, des purines et des acides aminés, est associée à l'apparition et au polymorphisme de transporteurs membranaires (Renesto et al., 2005). Pour ces pathogènes, on parle de « patho-adaptation ». Plusieurs articles émettent l'hypothèse que ce phénomène provoque la transition des bactéries à multiplication intracellulaire facultative vers des bactéries à multiplication intracellulaire obligatoire car la délétion de séquences génomiques empêcherait la bactérie de survivre à l'extérieur de l'hôte (Casadevall, 2008). De façon symétrique, il semblerait que les pathogènes possédant les plus grands génomes sont les plus aptes à s'adapter dans l'environnement (Wren et al., 2000).

Cependant, on peut aussi assister dans certaines situations à un « gain de gène ». On retrouve cette particularité, entre autres, chez la bactérie *L. pneumophila*. Cazalet et collaborateurs ont mis en évidence chez cette bactérie l'acquisition de onze gènes déterminant des sérine/thréonine kinases d'origine eucaryote qui jouent un rôle essentiel dans la survie et l'échappement phagosomal de la bactérie (Doumith et al., 2004).

1.2 Interactions hôte-pathogène : que le meilleur gagne.

1.2.1 Le phagosome

Lors de l'internalisation du pathogène dans la cellule hôte, le phagosome constitue la première ligne de défense de l'hôte. En effet, on assiste dans cette organelle à la naissance de molécules bactéricides comme des molécules pro-oxydantes, les espèces réactives de l'oxygène (ERO). Celles-ci constituent notre sujet d'étude et seront décrites plus en détail dans les paragraphes suivants. On retrouve aussi des espèces réactives de l'azote (ERA) induites par les NO synthases.

Ce recrutement d'ERO et d'ERA s'accompagne également d'une diminution du pH, associé à la production de peptides anti-microbiens (PAMs). On peut diviser les PAMs en deux sous-groupes, les défensines et les cathélicidines. Toutes deux conduisent à la lyse de la bactérie en formant des pores dans sa membrane, mais aussi à la dégradation de l'ADN bactérien (Hancock et al., 2000; Lehrer et al., 1993). Les PAMs jouent aussi un rôle pro-inflammatoire et chimio-attractant pour la mise en place de la réponse immunitaire macrophagique (Mendez-Samperio, 2008).

1.2.2 Dialogue métabolique

Les interactions entre le pathogène et la cellule hôte durant l'infection sont à l'origine d'une adaptation métabolique chez ces deux entités. L'importance de ce type d'adaptation lors de l'infection des cellules phagocytaires a été mise en évidence pour la première fois par Beisel et collaborateurs en 1975 (Beisel, 1975). Cependant ce sujet n'a pris un essor considérable qu'à partir des années 2.000, avec l'arrivée des techniques à grande échelle de protéomique, d'analyses par puces à ADN (ou « microarrays ») et des études métabolomiques qui consistent à suivre l'incorporation des radio-isotopes dans les différents intermédiaires métaboliques.

Eisenreich et collaborateurs se sont particulièrement intéressés à ces mécanismes d'adaptation mutuelle dans le modèle infectieux *L. monocytogenes*. Ils ont ainsi mis en évidence les modifications et adaptations métaboliques de l'hôte mises en jeu pour détruire les bactéries intracellulaires (Eisenreich et al., 2013), et celles déclenchées chez la bactérie pour s'adapter à l'environnement de la cellule qu'elle a infectée (voir pour revues (Eisenreich et al., 2010; Fuchs et al., 2012). Les grandes modifications observées dans ce contexte sont récapitulées dans la figure 1 ci-dessous.

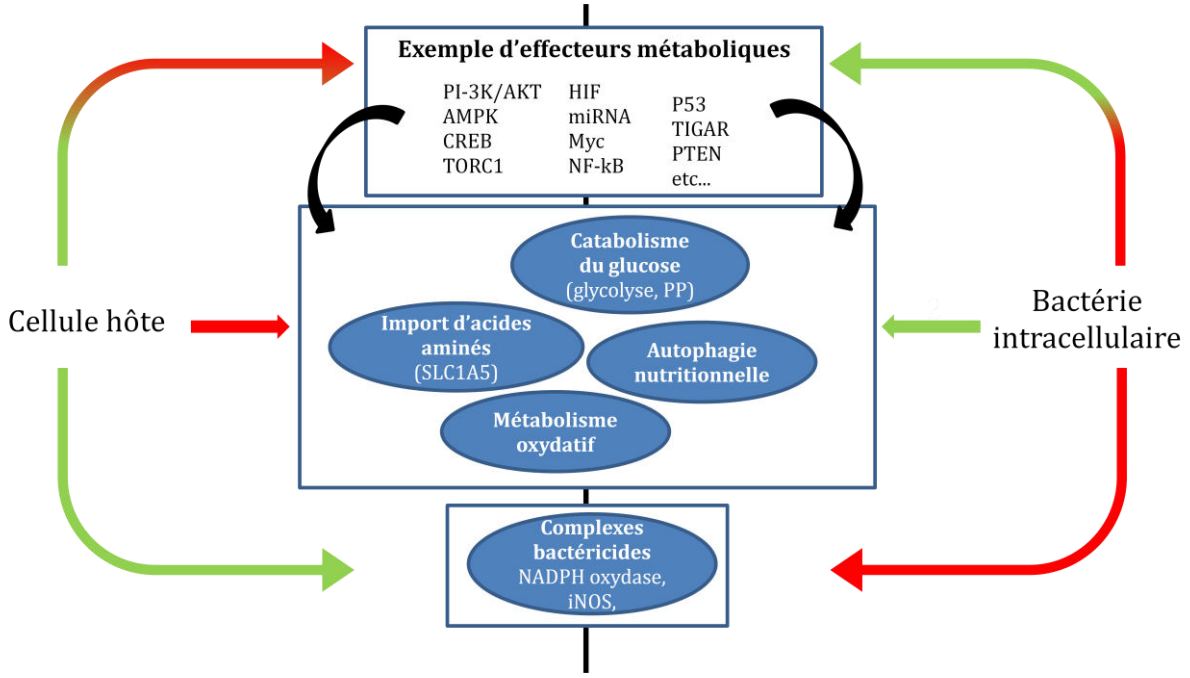

Figure 1 ***Résumé des modifications métaboliques observées dans un contexte d'infection macrophagique par une bactérie à multiplication intracellulaire (en vert : activation des effecteurs, en rouge : inactivation des effecteurs).***

Lors de l'infection, la cellule hôte module l'expression et l'activité de nombreux effecteurs intermédiaires dans son cytosol qui vont eux-mêmes moduler l'expression des voies métaboliques (1ère case de la figure 1). Parmi ces effecteurs, on retrouve des facteurs reconnus comme des suppresseurs de tumeurs ou des oncogènes avec par exemple HIF (Hypoxia-inducible factors) (Rupp et al., 2005) ou P53 (Wu et al., 2010) qui jouent un rôle dans la régulation du cycle cellulaire et de l'apoptose. On retrouve aussi des effecteurs reconnus comme modulant les flux métaboliques comme l'AMPK (AMP-activated protein kinase) (Shackelford et al., 2009) et qui modulent l'entrée et le métabolisme des sucres, des acides gras et des acides aminés.

A l'inverse, la bactérie est capable de manipuler ces flux à son avantage. On assiste par exemple à une activation de la production d'intermédiaires glucidiques et oxydatifs eucaryotes que la bactérie va pouvoir utiliser. La bactérie peut aussi provoquer une autophagie cellulaire de façon à augmenter le pool de nutriments disponibles. C'est notamment le cas pour *L. pneumophila* (Otto et al., 2004) et *F. tularensis* (Steele et al., 2013). Enfin, la bactérie a la possibilité de provoquer l'augmentation de la production et l'adressage de transporteurs d'acides aminés, c'est aussi le cas pour *L. pneumophila* et *F. tularensis* avec l'induction du transporteur SLC1A5 (Barel et al., 2012). Enfin, alors que la cellule exacerbe la formation de complexes bactéricides, la bactérie a la capacité de limiter leur formation ou de limiter leur fonctionnement (NADPH oxydase, iNOS, voir l'exemple de *F. tularensis* décrit plus loin).

1.2.3 Echappement de l'autophagie

L'autophagie est une voie catabolique qui joue un rôle essentiel dans la dégradation des pathogènes intracellulaires. On retrouve une forme d'autophagie constitutive dans tous les types cellulaires qui permet de maintenir une homéostasie à travers la dégradation des protéines et organelles qui ne sont plus essentielles. Cette voie devient inductible en condition de stress, et en particulier en carence nutritionnelle, par la présence de PI(3)P (Phosphatidylinositol-3-Phosphate) via le recrutement de Vsp34 (He et al., 2009). Dans ce cas, les protéines d'autophagie Atg5, Atg12 et Atg16 vont être activées et provoquer la formation d'une vésicule autour des produits à dégrader en recyclant des portions de membrane provenant soit du réticulum endoplasmique, soit de l'appareil de Golgi, soit des mitochondries (Rubinsztein et al., 2012). On parle alors d'« autophagosome » (Hanada et al., 2007). Dans un second temps, LC3 (appelé aussi Atg8) va adresser cette vésicule vers les lysosomes pour en dégrader son contenu (Dunn, 1990).

Pour améliorer ce processus, les cellules phagocytaires ont mis au point une machinerie capable de reconnaitre des molécules spécifiques de chaque bactérie, soit dans le cytosol, avec par exemple la participation de la protéine p62 qui reconnait *L. monocytogenes* (Yoshikawa et al., 2009) et *S. typhimurium* (Y. T. Zheng et al., 2009) ou NDP52 (nuclear dot protein 52) qui reconnait *Shigella* (Mostowy et al., 2011), mais aussi à la membrane, avec NOD1 et NOD2 (nucleotide-binding oligomerization domain) qui reconnaissent *Shigella* lors de son entrée (Travassos et al., 2010). Les bactéries à multiplication intracellulaire ont développé des mécanismes leur permettant d'échapper à cette voie de dégradation. On peut assister à une inhibition de l'autophagie avec la sécrétion de facteurs de virulence qui vont cliver les protéines pro-autophagiques, par exemple LC3 avec *L. pneumophila* (Choy et al., 2012). Ou encore, on peut assister à une adaptation à l'autophagie avec les bactéries *Coxiella* et *B. abortus* qui ont acquis la capacité de se multiplier dans ce type de vacuole (Heinzen et al., 1996; Starr et al., 2008).

1.2.4 Manipulation de l'apoptose

Pour se défendre contre les bactéries à multiplication intracellulaire, les cellules ont mis au point un mécanisme de défense qui consiste à programmer leur mort : c'est l'apoptose. Elle se caractérise par une segmentation de l'ADN eucaryote et le maintien de l'intégrité membranaire de façon à y intégrer aussi les corps étrangers. Ces corps apoptotiques serviront ainsi à la présentation antigénique et l'activation de l'immunité adaptative.

A l'inverse, le but ultime d'une bactérie à multiplication intracellulaire est de trouver une niche de réplication idéale. Pour cela, les bactéries ont développé des mécanismes de manipulation de la mort de leur hôte en faisant en sorte qu'elle n'arrive pas trop tôt pour qu'elles aient le temps de se multiplier, mais qu'elle n'arrive pas trop tard non plus pour permettre leur dissémination alors qu'elles sont encore viables.

On distingue presque autant de mécanismes d'activation ou d'inhibition de la mort de l'hôte que de types de bactéries différentes. Les plus remarquables sont les suivants :

- Voie de mort cellulaire dépendante des mitochondries (voie intrinsèque)

Lorsque la cellule est infectée, elle active la sécrétion de protéines pro-inflammatoires telles que Bcl-2 homology (appelée aussi BH3) qui vont provoquer l'oligomérisation des facteurs pro-apoptotiques Bax et Bak, la formation de pores dans la membrane mitochondriale et le relarguage du cytochrome C. On assiste alors à l'activation des pro-caspases 9 en caspases 9 et l'activation du processus d'apoptose (Arnoult et al., 2011). La bactérie *L. pneumophila* est capable de décaler la mort cellulaire. En effet, celle-ci sécrète les protéines SdhA et SidF qui vont venir fixer Bcl-2 et inhiber le processus d'apoptose et permettre leur multiplication (Banga et al., 2007; Laguna et al., 2006).

- Facteur NF-κB

NF-κB est l'un des régulateurs majeurs de la réponse immunitaire innée et de la réponse au stress cellulaire. De plus il est connu pour déclencher la transcription de gènes anti-apoptotiques (par exemple A20, Mn-SOD, Gadd45b, ...) (Bubici et al., 2006). Plusieurs pathogènes ont mis en place des mécanismes qui leur permettent de manipuler ce facteur dans le but de promouvoir leur réplication intracellulaire. La bactérie *M. tuberculosis* est capable de réguler positivement le complexe TLR2/NF-κB, qui induit une hyper régulation de la protéine FLIP, un puissant inhibiteur de la signalisation induisant la mort cellulaire (Loeuillet et al., 2006).

- Activation de l'inflammasome à travers la reconnaissance de l'hôte

Un autre mécanisme affectant la mort cellulaire et dépendant de l'inflammation a été mis en évidence plus récemment, il est appelé pyroptose. Il est utilisé par de nombreuses bactéries telles que *Legionella* et spp, *Salmonella* et spp, *Francisella* et spp... Il implique le relargage par les bactéries de molécules effectrices appelées PAMPs (Pathogen-Associated Molecular Patterns) et DAMPs (Danger-Associated molecular patterns) qui vont être identifiés par des molécules de reconnaissance appelées PRR pour « Pattern-recognition receptors » et qui vont successivement activer la caspase 1. Par exemple, on distingue parmi les PAMPs la flagelline pour la bactérie *L. pneumophila* ou l'ADN pour les bactéries *F. tularensis* et *L.*

monocytogenes. Ces PAMPs vont être reconnues dans le cytosol cellulaire par des PRR spécifiques. On distingue par exemple, les molécules IPAF/Naip5 pour la bactérie *L. pneumophila*, AIM2 (pour « Absent in melanoma 2 ») pour *F. tularensis* et NLRP3 et AIM2 pour *L. monocytogenes* (Henry et al., 2007). De plus, il a été montré que beaucoup de bactéries nécessitent la présence de la molécule de reconnaissance ASC (pour « an associated speck-like protein containing a caspase recruitment domain ») (Mariathasan et al., 2005; Mariathasan et al., 2006). Une fois la caspase 1 activée, celle-ci va provoquer le clivage et l'activation des cytokines IL-1β et IL-18 pour induire la mort de la cellule (Mariathasan et al., 2007).

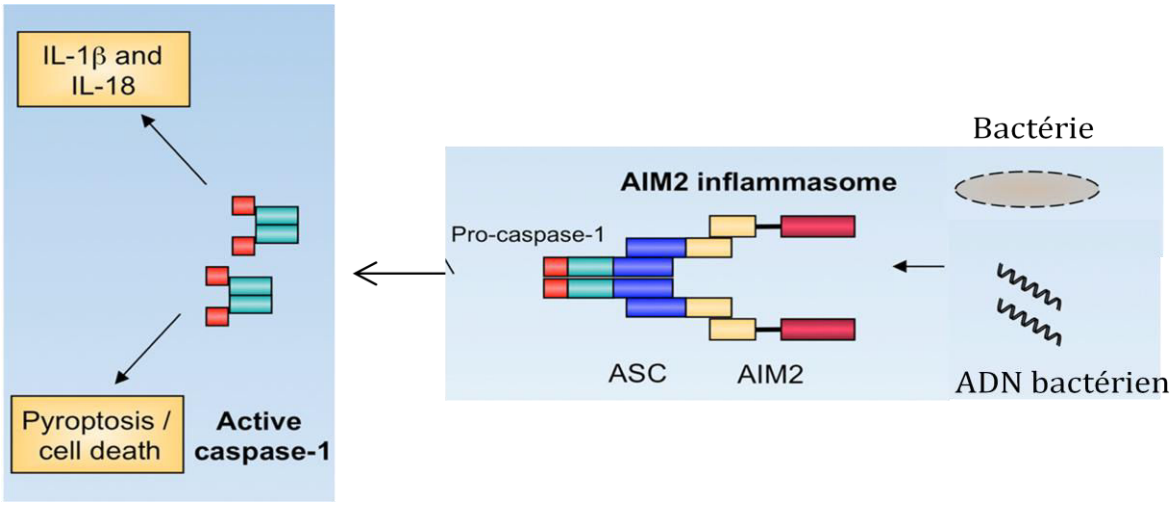

Figure 2 ***Activation de l'inflammasome par F. tularensis (inspiré de Jones et al., 2011)***

1.3 Le phagosome, un organite stratégique

La phagocytose joue un rôle central dans la clairance cellulaire et dans la mise en place de l'immunité innée et adaptative. Dans ce chapitre seront développées dans un premier temps les particularités de ces espaces vacuolaires hostiles. Dans un second temps, nous présenterons les principaux systèmes mis en jeu par les bactéries à multiplication intracellulaire pour y survivre.

1.3.1 Mécanismes microbicides du phagosome

Le phénomène de phagocytose est défini initialement comme l'ingestion de particules par des cellules phagocytaires professionnelles. Il a été décrit pour la première fois par Elie Metchnikoff en 1884 (Metschnikoff, 1884). Parmi ces cellules, on distingue essentiellement les neutrophiles, les macrophages et les cellules dendritiques. Dans les cellules phagocytaires, on assiste successivement : i) au relargage de cytokines pro-

inflammatoires ; ii) à la migration des cellules lymphoïdes par chimiotactisme ; et aussi ii) à la présentation d'antigènes dérivés de la dégradation des bactéries phagocytées pour les présenter à ces cellules lymphoïdes. Bien qu'elles ne soient pas définies comme telles, les cellules épithéliales et endothéliales, et même les fibroblastes, peuvent internaliser des pathogènes pour permettre leur élimination.

Le processus de phagocytose se caractérise par une maturation qui permet un remodelage de la vacuole et l'acquisition successive de marqueurs biochimiques donnant naissance à une organelle microbicide (Pitt et al., 1992). On distingue trois étapes successives dans la maturation du phagosome : le phagosome précoce, le phagosome tardif et le phagolysosome.

- Le phagosome précoce

La modification du phagosome commence immédiatement après la scission entre cette vacuole naissante et la membrane plasmique. On assiste à la formation d'un phagosome précoce qui provient de la fusion d'un phagosome naissant et d'un endosome précoce. Ce trafic vésiculaire est coordonné par une famille de molécules, les Rab GTPases (Stenmark, 2009), qui s'activent les unes les autres successivement par un processus appelé « Rab conversion ». Ces molécules jouent un rôle prépondérant dans le trafic vésiculaire, la fusion entre les vésicules et la fission. Cette première étape se caractérise par l'acquisition de Rab5, une molécule essentielle puisqu'elle est initiatrice de la maturation (Vieira et al., 2003). Il a aussi été mis en évidence la présence nécessaire de la molécule EEA-1 (Early Endosome Antigen 1) et de la molécule VPS45 dans l'activation de Rab5 par interaction directe mais aussi du PI(3)P (Christoforidis et al., 1999; Kummel et al., 2014; Ohya et al., 2009). On retrouve ces deux molécules au niveau de la membrane du phagosome. Elles constituent d'ailleurs des cibles de choix en immufluorescence pour le suivi de la maturation phagosomale. Enfin, on distingue comme grande famille de molécules intervenant dans ce processus, la famille des SNARE (N-ethylmaleimide-sensitive factor attachment protein receptor) (McBride et al., 1999). Elles interviennent dans la fusion des membranes en apportant l'énergie nécessaire à la modification des membranes lipidiques. A ce stade, on distingue en particulier dans cette famille les protéines VAMP4, syntaxin13, Vit1A et Syntaxin6 (Bethani et al., 2007).

Plusieurs équipes se sont intéressées aux modifications intervenant dans l'endosome précoce et pouvant affecter la viabilité des pathogènes. Li et collaborateurs ont mis en évidence la production de molécules pro-oxydantes par la NADPH oxydase durant cette étape (Li et al., 2001). On appelle ce phénomène le « burst oxydatif » et il est particulièrement important chez les neutrophiles. On inclut dans ce burst oxydatif la production des espèces réactives de

l'oxygène (ERO) et de l'azote (ERA). Les mécanismes de production et d'action de ces composés seront développés plus en détail plus loin.

- Le phagosome tardif

La naissance de ce phagosome résulte de la fusion des phagosomes précoces avec les endosomes tardifs. Ce compartiment se caractérise par l'acquisition de pompes à protons, appelées vATPases, qui permettent de faire descendre le pH autour de 5,5 (Maxfield et al., 1987). Il se caractérise aussi par un enrichissement en enzymes hydrolytiques et une morphologie vésiculaire. Ces compartiments migrent vers le noyau cellulaire.

Le phagosome tardif est reconnaissable grâce à l'acquisition de Rab7 (Rink et al., 2005; Vonderheit et al., 2005) et la perte de Rab5 (Vonderheit et al., 2005) qui va être recyclé. Il s'agit d'un échange de machinerie de fusion qui empêcherait la mise en contact des phagosomes tardifs avec des endosomes précoces. On retrouve aussi Rab9 qui joue un rôle dans la taille de ce compartiment (Ganley et al., 2004) et les molécules LAMP (LAMP-1 et LAMP-2). Le rôle respectif de ces molécules n'a pas encore été déterminé. En effet, la délétion de LAMP-1 ou de LAMP-2, chez des souris, n'a aucun effet sur l'internalisation de pathogènes ni sur la maturation du phagosome. De façon surprenante, un double KO est à l'origine d'une létalité embryonique, suggérant un rôle essentiel de ces deux partenaires (Huynh et al., 2007). L'étude des macrophages, délétés pour l'une ou l'autre molécule, suggère très fortement un rôle dans l'intégrité de la membrane lysosomale.

Enfin, on assiste dans ce compartiment à l'arrivée massive de peptides et protéines anti-microbiens destinés à compromettre l'intégrité des bactéries. On distingue, tout d'abord, les protéines qui ont un rôle de séquestreurs de nutriments. Celles-ci ont été particulièrement étudiées chez les neutrophiles (Borregaard et al., 1995). Parmi celles-ci on retrouve la lactoferrine, une glycoprotéine qui séquestre le fer, un nutriment essentiel pour les bactéries (Cassat et al., 2013). On distingue également NRAMP1 (natural resistance-associated macrophage protein 1 (aussi connue sous le nom de SLC11A1). Cette protéine membranaire exerce un effet bactériostatique et permet l'excrétion des ions Fe^{2+}, Zn^{2+} et Mn^{2+} de la vacuole phagosomale (Cellier et al., 2007). Fe^{2+} et Zn^{2+} sont des cofacteurs d'enzymes bactériennes et le Mn^{2+} est requis pour l'activité de la superoxyde dismutase, une enzyme anti-oxydante. On distingue encore les défensines et les cathélicidines qui induisent une perméabilité membranaire de la bactérie. Enfin, on retrouve des endopeptidases (cystéine and aspartate protéases), des exopeptidases (cystéine and sérine protéases) (Pillay et al., 2002) et des hydrolases qui vont dégrader les sucres (α-hexosaminidase et β-glucuronidase) et les lipides (phospholipase A2).

De façon remarquable, les phagosomes résultant directement de la fission de la membrane plasmique sont réfractaires à interagir avec les endosomes tardifs, appuyant l'idée d'une maturation progressive.

- Le phagolysosome

Les endosomes tardifs sont voués à être transformés en phagolysosomes par fusion avec des vésicules d'hydrolyse provenant de l'appareil de Golgi. On assiste cette fois à l'acquisition massive de vATPases qui font descendre le pH autour de 4,5, mais aussi de protéases et lipases, de molécules LAMP et de la cathepsine D (qui constitue un marqueur de ces vésicules classiquement utilisé en immunofluorescence). La cathepsine D est une protéase qui joue un rôle dans la dégradation des protéines du pathogène mais aussi dans la présentation de peptides au complexe majeur d'histocompatibilité (Deussing et al., 1998).

Le phagolysosome dirige les particules dégradées soit vers : i) des compartiments de recyclage ; ii) la membrane plasmique, dans le but de les présenter au système immunitaire ; iii) le réticulum endoplasmique, pour les réutiliser.

Toutes les étapes de cette maturation sont résumées dans la figure 3.

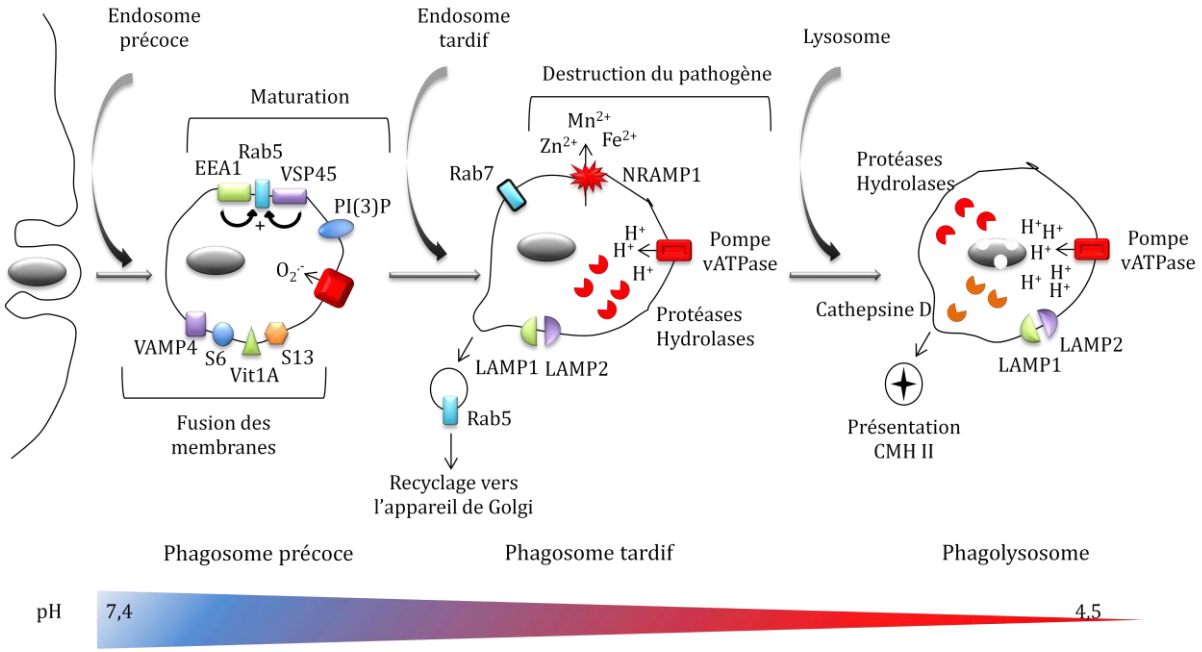

Figure 3 ***Etapes de la maturation phagosomale.***
EEA1, Early Endosome Antigen 1; PI(3)P, PhosphatidylInositol-3-Phosphate; VSP45, Vacuole Sorting Protein 45 ; VAMP4, ; LAMP, Lysosomal-Associated Membrane Protein; NRAMP1, Natural Resistance-Associated Macrophage Protein 1; CMH II, Complexe Majeur d'Histocompatibilité de type II.

1.3.2 Moyens de survie des bactéries à multiplication intracellulaire dans le phagosome

Qu'elles soient obligatoires ou facultatives, toutes les bactéries intracellulaires ont développé des stratégies qui leur permettent de survivre dans cette vacuole phagosomale extrêmement agressive. On distingue trois mécanismes d'adaptation qui seront détaillés succinctement ici :

- Arrêt de la maturation phagosomale par inhibition de la fusion avec les lysosomes

Dans ce cas de figure, les bactéries sont capables de limiter la maturation à l'étape de phagosome (précoce ou tardif), de façon à empêcher le pH de diminuer considérablement mais aussi de voir arriver les enzymes lytiques. Il s'agit d'une stratégie employée par plusieurs bactéries dont *L. pneumophila*. En effet, une étude a montré que la maturation de son phagosome s'arrêtait à l'étape de phagosome précoce car il n'y avait pas d'acquisition de Rab7 (Roy et al., 1998). La littérature scientifique assimile souvent ce type de situation à un « cheval de troie » puisqu'en effet cette stratégie permettrait à ces bactéries d'être cachées du système immunitaire (Nguyen et al., 2005).

- Persistance dans le phagolysosome

A priori très peu de bactéries, et aucune parmi celles qui constituent le sujet de cette première partie, peuvent être classées dans cette catégorie. Cependant, il est intéressant de souligner que deux équipes ont mis en évidence la fusion de la vacuole phagosomale contenant *M. tuberculosis* ou *M. Leprae* avec le lysosome (McDonough et al., 1993; van der Wel et al., 2007) pour former un phagolysosome, avec une persistance pendant 48 heures. Il s'agit là de deux études extrêmement controversées puisqu'aucune autre équipe n'a mis en évidence ce phénomène. Au contraire, un arrêt de la maturation au stade de phagosome précoce a même été décrit pour *M. bovis* (Via et al., 1997).

- Sortie de la vacuole phagosomale

L'échappement vers le cytosol constitue une stratégie simple pour accéder à un environnement moins hostile. Les bactéries capables d'accéder au compartiment cytosolique ont développé des stratégies qui leur permettent de dégrader la membrane phagosomale. Les mécanismes moléculaires mis en jeu lors de l'échappement phagosomal ont été particulièrement bien décrits chez *L. monocytogenes*. En effet, il a été montré que celle-ci sécrétait une cytolysine, appelée Listeriolysine O (LLO), qui se fixe à la membrane plasmique de la cellule avant même que *L. monocytogenes* soit rentrée. Ce facteur de virulence appartient à la famille des CDCs (Cholesterol-Dependent pore-forming Cytolysins). La LLO se fixe sur le cholestérol de la membrane vacuolaire pour désorganiser son réseau lipidique (Kayal et al., 2006). On assiste alors à la formation de larges oligomères (certains membres des CDC forment des pores qui font entre 250 et 350 nm). A ce jour, aucun mécanisme

impliqué dans la dégradation de la membrane phagosomale par *F. tularensis* n'a encore été mis en évidence.

2. Le stress oxydant dans les cellules phagocytaires

L'oxygène moléculaire est un composant essentiel de la vie depuis près de deux milliards d'années. L'oxygène est indispensable à de très nombreux être vivants car il est à l'origine de la production d'énergie par l'intermédiaire de chaines de transport d'électrons, un processus appelé "respiration cellulaire". Depuis plusieurs années, de nombreuses publications s'accordent pour souligner l'importance du stress oxydant comme stratégie de défense contre le pathogène durant l'infection.

2.1 Caractérisation du stress oxydant.

2.1.1 Définition

Le stress oxydant est couramment défini comme un déséquilibre entre la production massive d'espèces réactives de l'oxygène (ERO ou ROS pour "Reactive Oxygen Species" en anglais) et les capacités anti-oxydantes de la cellule. Elle est synonyme en générale de situation pathologique. Par définition, ces ERO dérivent du métabolisme de l'oxygène et sont donc générées dans des organismes de type aérobie (bactéries, cellules eucaryotes...).

Cependant, il est important de noter que la production d'ERO ne constitue pas dans tous les cas une situation délétère. En effet, il a été montré la présence constitutive et nécessaire de ces molécules dans de nombreux types cellulaires. La respiration des bactéries est d'ailleurs à l'origine d'une production fine d'ERO.

2.1.2 Naissance des radicaux primaires et leurs dérivés

L'oxygène que nous respirons subit pour sa majeure partie une réduction tétravalente, c'est-à-dire une addition de 4 électrons, pour conduire à la formation d'une molécule d'eau. Cette réaction est catalysée par la cytochrome oxydase, une enzyme placée à la fin de la chaîne de transport des électrons, au niveau du complexe IV. La cytochrome oxydase est localisée dans la membrane interne des mitochondries et dans la membrane cytoplasmique des bactéries. Il arrive que cette chaîne de transport laisse passer quelques électrons qui vont venir réduire une petite partie du pool d'oxygène (environ 2%). Ce processus conduit à la formation du radical superoxyde ($O_2^{\circ -}$) puis, par l'addition successive d'un ou plusieurs électrons et/ou protons, mène à la formation de nombreuses autres molécules pro-oxydantes. On peut classer

ces molécules en deux groupes. Le premier regroupe les espèces radicalaires qui possèdent un ou plusieurs électrons non appariés. Parmi ces espèces, on retrouve les molécules suivantes :

- L'anion superoxyde : $O_2^{\circ -}$

L'anion superoxyde provient de la réaction d'une molécule de dioxygène avec un électron (cf. Fig. 3). Cette espèce n'est pas extrêmement réactive avec les différents constituants cellulaires en tant que telle mais elle constitue un passage obligatoire pour la formation d'autres espèces hautement réactives, en particulier le radical hydroxyle (HO°, décrit ci-après).

- Le radical hydroxyle : HO°

Le radical hydroxyle provient de la dismutation de deux molécules de peroxyde d'hydrogène (réaction de deux mêmes molécules entre elles). Il s'agit de l'une des ERO les plus réactives et les plus dangereuses car elle peut réagir avec tous les constituants cellulaires en modifiant leur conformation chimique ou en s'y attachant.

D'autre part, on distingue des espèces non radicalaires, considérées aussi comme molécules pro-oxydantes. Ces molécules sont composées de liaisons O-H, qui sont des liaisons facilement modulables. La principale espèce classée sous cette nomination est le peroxyde d'hydrogène (H_2O_2). Comme l'anion superoxyde, il ne s'agit pas d'une molécule extrêmement réactive. Sa dangerosité réside plutôt dans le fait qu'il constitue une transition vers le radical hydroxyle, molécule hautement réactive. La particularité de cette molécule est qu'elle traverse très facilement les membranes cellulaires.

La cellule utilise aussi la réaction de Fenton (voir figure 4 ci-dessous) pour transformer les ERO et augmenter leur potentiel toxique. L'ion superoxyde, qui initialement n'est pas extrêmement réactif, lorsqu'il est en excès peut réagir avec des molécules de fer menant à la production d'ions hydroxyles qui sont beaucoup plus réactifs.

En plus de toutes ces ERO bien connues et définies, il a été montré que ces molécules pouvaient réagir avec d'autres classes chimiques et en particulier des molécules azotées pour donner ce qu'on appelle des espèces réactives de l'azote (ERA ou "RNS" pour Reactive Nitrogen Species) tout aussi toxiques (Patel et al., 1999). Parmi ces espèces, on distingue en particulier le peroxynitrite (ONOOH) issu de la réaction d'un ion superoxyde et d'une molécule de monoxyde d'azote (NO). Cette molécule est extrêmement nocive puisqu'elle peut mener à l'oxydation, la nitrosation (addition de NO) ou la nitration (addition de NO_2) de produits cellulaires. Les sources de NO sont assez limitées dans le macrophage puisqu'elles se limitent à la NO synthase. On distingue : i) des NO synthase de type I et III, qui sont

constitutives et retrouvées respectivement dans les cellules neuronales et les cellules endothéliales, et ii) une NO synthase de type II inductible (iNOS), retrouvée dans les cellules phagocytaires (Andrew et al., 1999).

La formation de ces intermédiaires semble jouer un rôle prépondérant dans la réponse inflammatoire à l'infection chez plusieurs bactéries intracellulaires telles que *S. typhimurium* (Prior et al., 2009) ou *F. tularensis* (H. Lindgren et al., 2004b)

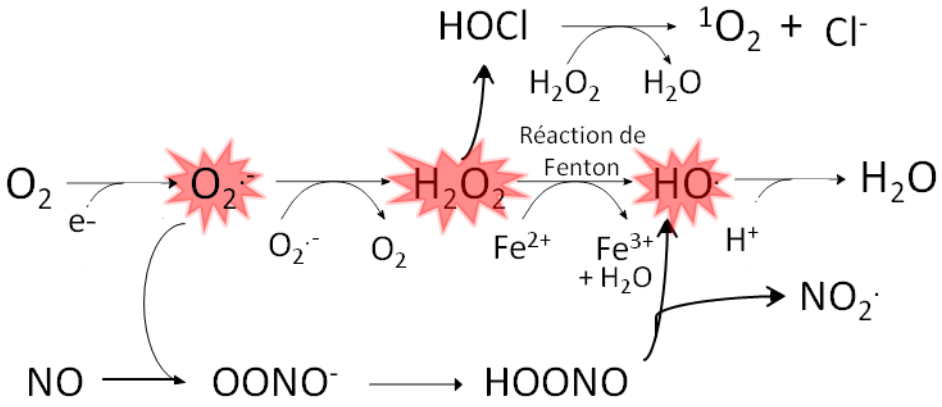

Figure 4 ***Réactions menant à la formation des espèces réactives de l'oxygène et de l'azote.***

2.1.3 Utilité des espèces réactives de l'oxygène dans la cellule phagocytaire.

Il a été également montré dans de nombreuses publications que ces ERO étaient nécessaires pour l'activation de voies de signalisation ou dans l'activation de la transcription de facteurs nécessaires à l'activité pro-inflammatoire et à la survie du macrophage. De nombreuses familles de molécules sont mises en jeu dans ces situations :

- Famille NF-κB/Rel

Il a été montré que les ERO provoquent la dissociation du complexe [IκBα]-[NF-κB]. Une fois libéré, le dimère NF-κB est dirigé vers le noyau pour jouer sa fonction de facteur de transcription anti-apoptotique (Morgan et al., 2011). De façon très intéressante, une équipe a montré l'impossibilité d'activer la voie NF-κB dans des souris p47^{phox} KO où la NADPH oxydase est inactive (Koay et al., 2001).

- Voie des MAPK

L'activation de la voie des MAPK (Mitogen Activated Protein Kinases), aussi connue sous le nom de voie "Ras-Raf-MEK-ERK", a été montrée dans plusieurs articles comme étant activée en réponse à un stimulus pro-oxydant. Cette voie de signalisation est composée d'une chaîne de protéines kinases, activées par phosphorylations successives, et qui vont provoquer

l'activation de la protéine p38 responsable de l'arrêt de l'activité mitogène de la cellule (Noguchi et al., 2008).

2.2 Génération du stress oxydant dans la cellule phagocytaire

La première preuve de l'existence d'un « burst » oxydatif en tant que ligne de défense contre les pathogènes a été mis en évidence en 1932, par Baldridge et Gerard (Baldridge et al., 1932). En effet, ces deux chercheurs ont montré que des neutrophiles de chien exposés à une bactérie répondaient en produisant des espèces réactives pendant 10 à 15 minutes, très rapidement après la mise en contact. D'autre part, 27 ans plus tard, il a été démontré que cette production de ROS était indépendante de la chaîne de transport mitochondriale puisqu'elle n'était pas inhibée par le cyanide (une molécule impliquée dans l'arrêt du fonctionnement de la cytochrome C oxydase) (Sbarra et al., 1959). Aux vues de ces découvertes, la communauté scientifique s'est attachée à comprendre les mécanismes et à connaître les enzymes impliqués dans ce burst oxydatif lié à la phagocytose.

2.2.1 Rôle de la NADPH oxydase

La NADPH oxydase est une enzyme membranaire qu'on retrouve aussi bien dans des cellules phagocytaires que dans les lymphocytes B (Babior, 2004). Elle catalyse la production de l'ion superoxyde ($O_2^{\circ-}$) en utilisant une molécule de NAPDH comme donneur d'électron. Comme décrit plus haut et indiqué sur la figure 4, cet ion va donner naissance à de nombreuses autres molécules bien plus nocives. Cette enzyme est composée de 5 sous-unités. A l'état basal, on retrouve un dimère au niveau de la membrane des vésicules sécrétées en continu. Il comprend les sous-unités $p22^{PHOX}$ et $gp91^{PHOX}$ (*PHOX* pour PHagocyte OXidase). On parle alors de cytochrome b_{558} pour ce complexe. D'autre part, on retrouve libre dans le cytosol, un trimère comprenant les 3 autres sous-unités, désignées sous les noms $p40^{PHOX}$, $p47^{PHOX}$ et $p67^{PHOX}$.

Lors de l'internalisation d'un organisme étranger, celui-ci est intégré dans une vacuole phagosomale. La sous-unité $p47^{PHOX}$ acquiert alors trois phosphorylations qui vont jouer comme signal pour adresser le complexe cytosolique vers la membrane phagosomale et ainsi former une NADPH oxydase complète.

Enfin, deux molécules de faible poids moléculaire, et appartenant à la famille des "Guanine nucleotide binding proteins" (ou "G proteins"), ont été identifiées comme étant essentielles au fonctionnement de ce complexe. D'une part Rap1A, qui fait partie de la famille des protéines Ras (GTPases), se retrouve dans la membrane des vésicules sécrétées (Maly et al., 1994).

D'autre part Rac, qui appartient à la famille des protéines Rho (Diekmann et al., 1994) et qui se retrouve liée au complexe GDP/GDI mais non intégré à la membrane.

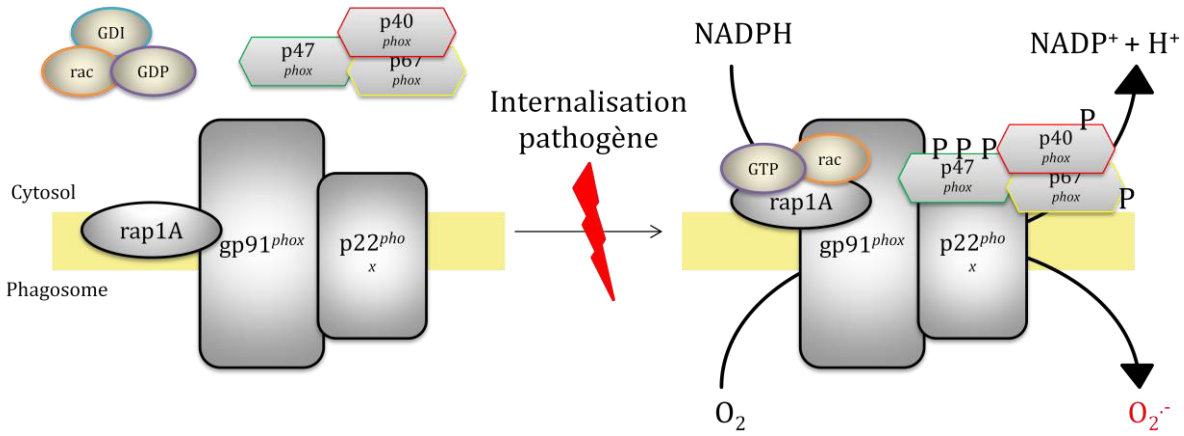

Figure 5 ***Schéma récapitulatif du fonctionnement de la NADPH oxydase dans les cellules phagocytaires.***

2.2.2 Autres contributions mineures : miélopéroxydase et xanthine oxydase

La génération du stress oxydant dans la cellule phagocytaire peut avoir lieu suite à l'activation d'autres enzymes, cependant leur contribution reste mineure. La première enzyme qu'on peut citer est la myélopéroxidase. Il s'agit d'une protéine hémique tétramérique qu'on retrouve au niveau des granules des cellules phagocytaires, en particulier les neutrophiles. En effet, celle-ci peut représenter jusqu'à 5% de leur poids secs (Pham et al., 2003). Cette enzyme a la particularité de générer des molécules extrêmement bactéricides, puisqu'elle provoque l'oxydation de ce qu'on appelle des "ions halides", comme les ions bromide (Br^-), iodide (I^-) mais surtout chloride (Cl^-) par le peroxyde d'hydrogène. A titre d'exemple, la réaction d'un ion chloride avec le peroxyde d'hydrogène donnera un ion hypochloreux (HOCl). Cependant, il est à noter que son activité antimicrobienne n'a pas été clairement démontrée dans des macrophages murins.

Comme autre contributeur endogène dans la génération d'espèces dérivées de l'oxygène, on distingue aussi la xanthine oxydase (XO). Cette enzyme est à l'origine de la production d'acide urique par l'oxydation de l'hypoxanthine ou de la xanthine avec comme substrat le dioxygène. Dans les deux cas, cette enzyme est à l'origine de la production de peroxyde d'hydrogène. Enfin, il a été démontré l'importance de l'activation de cette enzyme dans la mise en place de la réponse inflammatoire (Gibbings et al., 2011).

2.3 Impacts moléculaires et conséquences sur la bactérie

2.3.1 Impact sur l'ADN bactérien

Parmi les différentes espèces réactives de l'oxygène, le radical hydroxyle est reconnu pour être la molécule la plus réactive vis-à-vis de l'ADN. On distingue communément quatre altérations intervenant dans la dégradation de l'ADN (Chatgilialoglu et al., 2001; Dizdaroglu, 2012) :

- Oxydation des bases

Le radical hydroxyle réagit de façon différente selon la nature chimique de la base (purine ou pyrimidine). Il a été montré que la guanine était la base la plus sensible à ce type de réaction. Si on considère les molécules pyrimidines (cytosine et thymine), le radical peut s'additionner au niveau des carbones C5 et C6 pour donner des pyrimidines glycol. Dans le cas des purines (adénine et guanine), il a été montré qu'il peut s'additionner sur la doubles liaison N7-C8 pour former le 8-oxo-7,8-dihydrodésoxyguanine (8-oxo-dG) et le 8-oxo-7,8-dihydrodésoxyadénine (8-oxo-dA) mais en quantité moins importante. Il peut aussi s'additionner en position C5 ou C6 pour donner des purines glycol. Ces altérations donnent naissance à des bases modifiées ou même à une perte de la base.

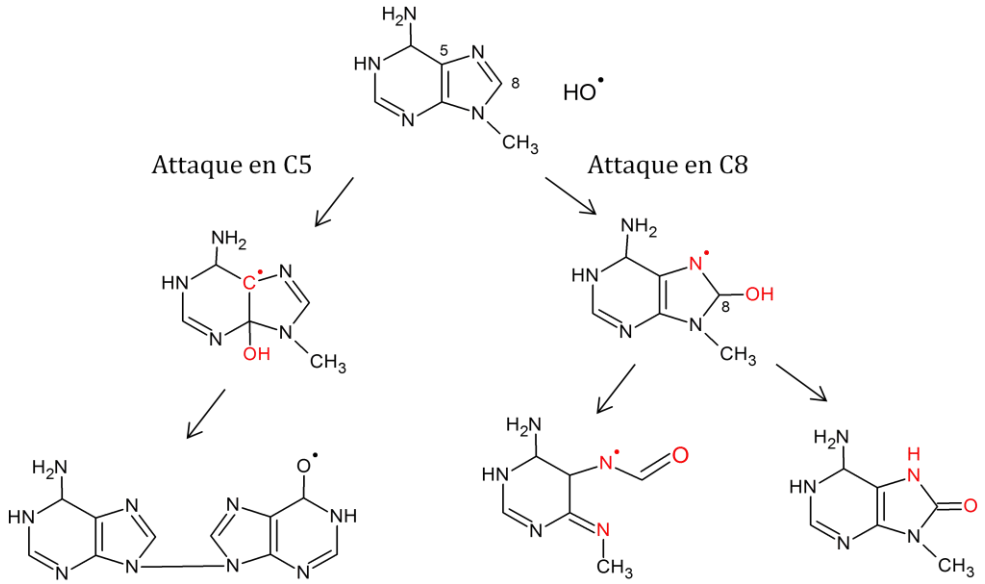

Figure 6 ***Exemples de réactions du radical hydroxyle avec des bases de type purine (adénine et guanine)***

- Cassure de brins

Cette situation est la conséquence de l'attaque des liaisons entre les bases et les désoxyriboses. Elle a comme conséquences la coupure de chaîne simple brin ou double brin.

- Formation d'adduits intra-caténaire

Il a été montré que le phénomène d'oxydation des lipides, couramment appelé "peroxydation" et décrit plus loin est à l'origine de la naissance d'aldéhydes mutagènes, et que ces produits réagissent avec les bases pour donner des adduits de type lipide oxydé-guanine ou éthénodérivés.

- Formation de pontages ADN-protéine

Ce dommage résulte de la réaction de l'ADN avec des protéines oxydées. En effet, sont particulièrement impliqués dans ce phénomène des histones oxydés, des enzymes et des facteurs de réplication ou transcription. On observera alors des pontages de type lysinoguanine.

Toutes ces modifications sont résumées dans la figure 7.

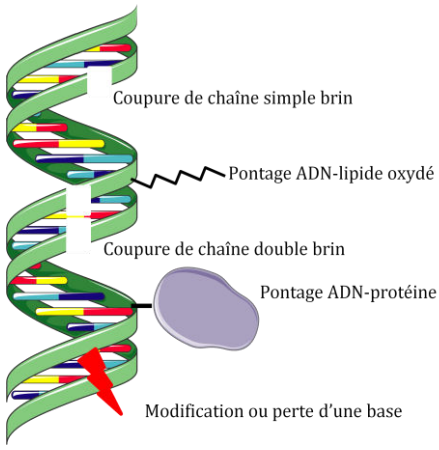

Figure 7 ***Schéma récapitulatif des différentes altérations de l'ADN par un stress oxydant***

2.3.2 Impact sur les protéines bactériennes

L'étude des protéines oxydées a commencé en 1906 lors de la découverte par Fenton de l'oxydation des acides aminés. Le premier cas d'étude d'acide aminé fût l'oxydation de la cystéine par Hopkins, en 1925 (R. T. Dean et al., 1997).

- Oxydation de la structure carbonée de la protéine

Ce phénomène résulte de la réaction d'un radical hydroxyle sur le carbone central. Il en résulte un carbone centré oxydé. On observe ensuite l'addition d'une molécule de dioxygène sur ce carbone pour former successivement un radical alkylperoxyl, un radical alkoxyl puis une protéine hydroxyle. Dans certains cas, on observe même la réaction de ce carbone centré avec d'autres acides aminés.

- Fragmentation des protéines

On observe très souvent, à la suite du schéma décrit précédemment, une fragmentation des protéines. En effet, les protéines hydroxyles sont très fragiles et peuvent être fragmentées par les voies de diamide ou α-déamidation. La première implique une cassure en C terminal du carbone centré, la seconde en N-terminal du carbone centré.

La fragmentation des protéines peut aussi résulter de l'attaque d'un radical hydroxyle avec des extrémités glutamyl, aspartyl et prolyl.

- Oxydation des chaînes latérales

On distingue comme autre altération l'oxydation des chaînes latérales par le radical hydroxyle de nombreux acides aminés. Les cystéines et les méthionines, deux acides-aminés soufrés, y sont extrêmement sensibles. Cependant leur oxydation est réversible c'est pourquoi ils constituent des acides aminés protecteurs (Luo et al., 2009).

Les acides-aminés aromatiques sont aussi très affectés par ce type de modification.

Acides aminés	Produits d'oxydation
Cystéine	Disulfides et acide cystéique
Méthionine	Méthionine sulfoxyde et méthionine sulfone
Tryptophane	2-, 4-, 5-, 6-, et 7-Hydroxytryptophan, nitrotryptophane, kynurénine, 3-hydroxykynurinine et formylkynurinine
Phénylalanine	2,3-Dihydroxyphénylalanine, 2-, 3-, et 4-hydroxyphénylalanine
Tyrosine	3,4-Dihydroxyphenylalanine, ponts tyrosine-tyrosine, Tyr-*O*-Tyr et nitrotyrosine
Histidine	2-Oxohistidine, asparagine et acide aspartique
Arginine	Acide glutamique semialdehyde
Lysine	α-Aminoadipic semialdéhyde
Proline	2-Pyrrolidone, acide 4- et 5-hydroxyproline pyroglutamique, acide glutamique semialdéhyde
Thréonine	Acide 2-Amino-3-cétobutyrique
Glutamine	Acide oxalic, acide pyruvique

Table 3 : Liste des produits issus de l'oxydation des acides aminés, inspiré de (Cabiscol et al., 2000).

Les conséquences de ces modifications chimiques sont la modification, voire la perte, des propriétés biologiques des protéines. Ces modifications sont être extrêmement délétères car elles peuvent toucher des récepteurs, des enzymes, des facteurs de transcription, etc... Dans des cas plus extrêmes, les protéines oxydées initialement hydrophiles deviennent hydrophobes, par exemple suite à l'extériorisation des zones hydrophobes. Ce phénomène aura pour conséquence la formation d'amas anormaux (Berlett et al., 1997).

2.3.3 Impact sur les lipides bactériens

Les lipides constituent la classe moléculaire la plus affectée par le stress oxydant. On parle alors de "peroxydation lipidique". Ce phénomène concerne principalement les acides gras polyinsaturés (PUFA ou "polyunsaturated fatty acids") ou estérifiés des membranes (esters de cholestérols, phospholipides et triglycérides).

La peroxydation lipidique est une réaction en chaîne en 3 phases (cf. figure 8):

1. Phase d'initiation : elle se caractérise par l'attaque des structures lipidiques par des ERO, soit par un radical hydroxyle, des peroxynitrites, etc... La conséquence de cette

réaction est l'arrachement d'un hydrogène et la production d'un radical pentandiényl qui après addition avec le dioxygène peut donner le radical peroxyle ($LOO^{\cdot}$).

2. Phase de propagation : il s'agit de la réaction d'un radical peroxyle avec un autre PUFA pour former un hydroperoxyde ($LOO^{\cdot}$ + LOOH → $L^{\cdot}$ + LOOH). Ces hydroperoxydes appartiennent à la famille des peroxydes lipidiques (LPO).
3. Phase de terminaison : il s'agit de l'ajout d'un hydrogène au niveau du radical hydroxyle, mettant fin au processus de propagation.

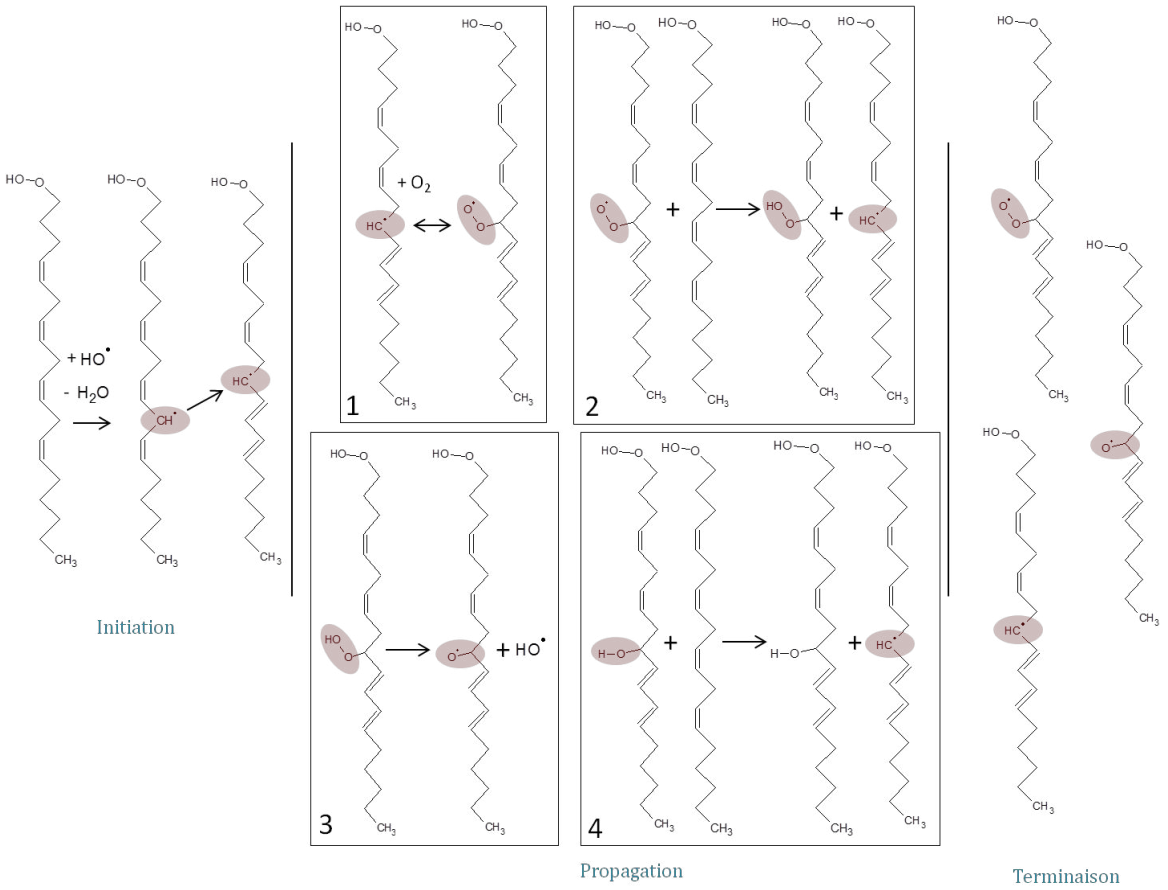

Figure 8 ***Schéma récapitulatif de la peroxydation des acides gras polyinsaturés. Présentation des 3 étapes intermédiaires de l'oxydation des acides gras polyinsaturés qui sont l'initiation, la propagation et la terminaison.***

Un aspect très particulier de la peroxydation lipidique est la fragmentation des LPO suivi de la production de produits secondaires. Ils sont malheureusement tout aussi nocifs que les radicaux oxygénés puisqu'ils réagissent particulièrement avec l'ADN et les lipides. On regroupe ces réactions sous le nom de "lipo-oxydation". On distingue parmi ces produits deux espèces majoritaires (cf. figure 8) :

1. Le malondialdehyde (MDA) est une molécule qui réagit avec l'adénine mais surtout la guanine pour former des adduits d'ADN extrêmement mutagènes (Marnett, 1999).

2. Le 4-hydroxy-2-nonénal (4-HNE) est très réactif vis-à-vis des protéines. En effet, il est responsable de la formation de produits d'addition stables avec l'histidine, la lysine et la cystéine. Les effets biochimiques du 4-HNE sont majoritairement dus à sa réaction avec les groupements thiol et amine. Ainsi, il peut réagir aussi avec le glutathion et modifier négativement l'état d'oxydation de la cellule.

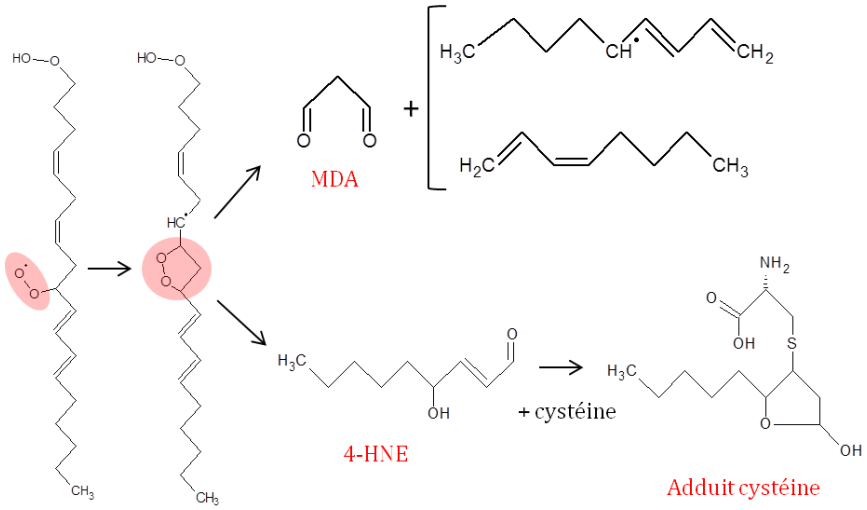

Figure 9 ***Devenir des lipides péroxydés (MDA, malondialdéhyde ; 4-HNE, 4-hydroxy-2E-nonenal ; Inspiré de Bocci et al., 2011).***

Le cholestérol est une molécule aussi très affectée par le stress oxydant. Elle peut donner naissance à des produits tels que des époxydes et des alcools.

La peroxydation des lipides est un phénomène dramatique pour la bactérie puisqu'elle est dirigée vers sa membrane plasmique. Celle-ci, dans le cas où elle accumule ces lipides altérés, devient rigide, perd de sa perméabilité sélective et, en condition de stress extrême, peut perdre son intégrité.

En conclusion, on peut voir que la présence d'ERO constitue une condition extrêmement délétère pour toutes les bactéries. Celles-ci doivent donc acquérir des systèmes de réparations et de neutralisation des ERO. Ils seront développés dans les paragraphes suivants.

Par ailleurs, les produits résultant de réactions d'oxydation sont une aide précieuse pour la recherche en laboratoire. En effet, de nombreux tests permettant d'évaluer des degrés d'oxydation de façon ciblée sont basés sur la détection d'intermédiaires oxydés avec en particulier le marquage des MDA, 4-HNE (lipides oxydés) et de la 8-oxo-dG (ADN oxydé).

3. Moyen de défense de la bactérie contre le stress oxydant

Au cours de l'évolution, les êtres vivants aérobies se sont adaptés à la naissance de ces composés toxiques et ont mis au point une armée de molécules dites "anti-oxydantes". Celles-

ci ont pour fonction d'empêcher ces dérivés de l'oxygène et de l'azote d'atteindre des cibles précieuses telles que l'ADN, les protéines ou les lipides.

3.1 Enzymes anti-oxydantes

3.1.1 La catalase

Les catalases sont des enzymes essentielles dans les défenses anti-oxydantes mises en place par les bactéries. Il s'agit d'une oxydoréductase qui catalyse la dismutation du peroxyde d'hydrogène (c'est-à-dire une réaction sur lui même) en eau et dioxygène. Les catalases sont divisées en trois groupes (Goldberg et al., 1989) :

- les catalases monofonctionnelles : aussi appelées catalases typiques, elles représentent la majorité des catalases. Elles sont constituées d'un groupement héminique, d'une grande et d'une petite sous-unité. Elles peuvent être inactivées si la concentration en peroxyde d'hydrogène est trop forte.
- les catalases-peroxydases : elles se présentent sous la forme d'un homodimère et possèdent aussi un groupement héminique.
- les catalases à manganèse : il s'agit de protéines homohexamériques avec un centre catalytique constitué de deux atomes de manganèse à la place de l'hème. Elles n'ont été observées que chez les bactéries. Même si elles jouent un rôle de détoxificateur, elles restent tout de même moins efficaces que les deux autres types de catalases.

Toutes les bactéries à multiplication intracellulaire facultative possèdent au moins une catalase et chaque bactérie a développé son propre système de détoxification mettant en jeu une catalase (voir tableau ci-dessous) :

Bactérie		Particularités	Réf.
B. abortus	KatE	Cytoplasmique	Base de données KEGG
F. tularensis	KatG	Catalase-peroxydase Role mineur chez SchuS4	(H. Lindgren et al., 2007)
L. pneumophila	KatA KatB	Catalase-peroxydase, périplasmique, Catalase-peroxydase, cytosolique	(St John et al., 1996) (Sadosky et al., 1994)
L. monocytogenes	Kat	Non requis pour la virulence chez l'Homme	(Chatterjee et al., 2006) (Bubert et al., 1997)
M. tuberculosis	KatE	?	(Wayne et al., 1988)

	KatG	Catalase peroxydase	
S. typhimurium	KatE KatG KatN	Régulé par RpoS Catalase-peroxydase Catalase à manganèse	(Hébrard, 2010) (Hebrard et al., 2009)

Table 4 : Récapitulatif des catalases retrouvées chez les bactéries à multiplication intracellulaire.

3.1.2 Les superoxydes dismutases

La famille des superoxydes dismutases (SOD) peut être considérée comme la deuxième famille la plus importante parmi les enzymes anti-oxydantes. Les SOD ont pour rôle de convertir les radicaux superoxydes en peroxyde d'hydrogène moins dangereux. Chez les bactéries, on distingue plusieurs types de SOD fonctionnant avec différents cofacteurs : Cu,Zn-SOD, Fe-SOD, Mn-SOD et Fe-Mn-SOD. Suivant la bactérie à multiplication intracellulaire considérée, elles sont annotées différemment et ont une localisation qui varie. Celles-ci sont présentées dans le tableau suivant avec leurs caractéristiques respectives.

Bactérie	Nom du gène	Particularité moléculaire	Situation sub-cellulaire	
B. abortus	*sodA* *sodC*	Fe-Mn SOD Cu-Zn SOD	Cytoplasme Périplasme	(Martin et al., 2012) (Gee et al., 2005)
F. tularensis	*sodB* *sodC*	Fe-Mn SOD Cu-Zn SOD	? Périplasme	(Bakshi et al., 2006) (A. A. Melillo et al., 2009)
L. pneumophila	*sodA* *sodB*	Cu,Zn-SOD Fe-SOD	Périplasme Cytoplasme	(Steinman, 1992)
L. monocytogenes	*sod*	Mn-SOD	?	(Haas et al., 1992)
M. tuberculosis	*sodB*	Fe-Mn SOD	Sécrétion à l'extérieur grâce au système SecA2	(Jackson et al., 1998)
	sodC	Cu-Zn SOD	Périplasme	(Piddington et al., 2001)
S. typhimurium	*sodA*	Fe-Mn SOD	Périplasme	(Tsolis et al., 1995)

Table 5 : Récapitulatif des superoxydes dismutases retrouvées chez les bactéries à multiplication intracellulaire.

3.1.3 Autres enzymes

Certaines bactéries à multiplication intracellulaire possèdent également d'autres types d'enzymes anti-oxydantes qui ont été jusqu'ici très peu -voire pas du tout- étudiées. Parmi celles-ci on retrouve :

- La glutathion peroxydase (Gpx) qui permet la réduction du glutathion oxydé (GSSG) en glutathion réduit (GSH), lui même un élément clé dans la détoxification des ERO. Aucune donnée n'a encore été publiée sur l'importance de cette enzyme chez les bactéries à multiplication intracellulaire de cette première partie à l'inverse de la bactérie *E. coli*. Il a été montré son rôle essentiel dans la croissance de cette bactérie, dans l'osmoadaptation et la résistance au stress oxydant (McLaggan et al., 1990; Smirnova et al., 2000).
- L'alkylhydroperoxide réductase (Ahp)
- La bacterioferritine comigratory protein (BCP). Il s'agit d'une thiol peroxydase. Son monde d'action contre le stress oxydant n'est pas encore clairement défini. En effet, il a été montré qu'elle a un rôle détoxifiant vis-à-vis du peroxyde d'hydrogène (Km = 50 µM), cependant elle aurait un rôle plus important dans la détoxification des lipides oxydés (Km = 10 µM pour les acides linoléiques) (Jeong et al., 2000).

	Gpx	Ahp	BCP
B. abortus	Non	Oui, *ahpC*, *ahpD*	Oui
F. tularensis	Oui	Oui, *ahpC*	Oui
L. pneumophila	Non	Oui, *ahpC*	Oui
L. monocytogenes	Oui	Non	Non
M. tuberculosis	Non	Oui, *ahpC*, *ahpD*, *ahpE*	Oui, *bcp*, *bcpB*
S. typhimurium	Oui, *btuE*	Oui	Non

Table 6 : Table récapitulative des enzymes anti-oxydantes des différentes bactéries à multiplication intracellulaire par analyse systématique de leur génome (d'après la base de données KEGG)

3.2 Réponses transcriptionelles

Les bactéries ont acquis des systèmes d'activation de toutes ces enzymes pour répondre très rapidement à un stress oxydant. Parmi ces systèmes, on en distingue deux en particulier, les systèmes Oxy-R et Sox-R qui sont présentés ci-après.

3.2.1 Système Oxy-R

Le facteur OxyR a été mis en évidence pour la première fois dans la bactérie *E.coli*. Il s'agit d'un régulateur transcriptionnel de type LysR. Il est activé par la présence de peroxyde d'hydrogène, à la suite de l'oxydation de ses cystéines n°199 et n°208 (M. Zheng et al., 1998). La cystéine 199 a d'ailleurs été mise en évidence comme jouant un rôle essentiel dans l'activité d'OxyR (Toledano et al., 1994). OxyR a la capacité de se fixer à l'ADN. En effet, il reconnaît un motif conservé ATAG. La forme réduite se fixe au promoteur du gène *oxyR* mais

avec une affinité limitée alors que la forme oxydée se fixe au promoteur du gène *katG* qui code pour une catalase et au promoteur du gène *ahpC* qui code pour une peroxiredoxine, avec une affinité plus importante. Dans ce cas, OxyR améliore la fixation de l'ARN polymérase aux promoteurs en se fixant à leur extrémité C-terminale (Storz et al., 1999). Ce système et son importance dans la réponse au stress oxydant ont été mis en évidence chez plusieurs bactéries à multiplication intracellulaire telles que *S. typhimurium* (Christman et al., 1985), *B. abortus* (Kim et al., 2000), *M. tuberculosis* (Pagan-Ramos et al., 1998) et *F. tularensis* (Moule et al., 2010)

3.2.2 Système Sox-R

On distingue comme deuxième régulon majeur de réponse au stress oxydant, le système Sox-R (pour « superoxide response ») qui répond à la production d'ions superoxyde. Il a la capacité d'activer la transcription de la Mn-SOD. La protéine SoxR est un homodimère composé de centres 2Fe-2S dans chacune de ses sous-unités. L'oxydation de ces centres active la protéine SoxR et permet sa fixation au promoteur du gène *soxS*. SoxS active la transcription des enzymes impliquées dans la réponse au stress oxydant (Green et al., 2004; Lushchak, 2011).

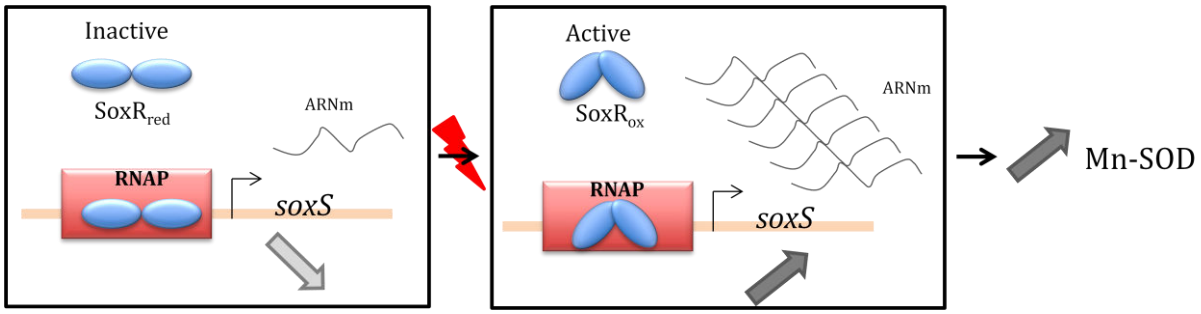

Figure 10 ***Régulon SoxR activé dans la réponse au stress oxydant, inspiré de (Green et al., 2004) (RNAP : RNA polymérase)***

3.3 Systèmes de réparation

Tout comme les systèmes de détoxification, les systèmes de réparation des différentes molécules oxydées sont tout aussi importants dans la résistance au stress oxydant pour la bactérie.

3.3.1 Réparation de l'ADN

Toutes les espèces bactériennes ont besoin de systèmes de réparation de l'ADN, et de leur voie d'activation, à la fois pour préserver leur intégrité génomique, mais aussi pour répondre aux dommages causés lors de l'exposition à des stress et assurer leur virulence.

Plusieurs protéines et voies de signalisation ont été identifiées comme jouant un rôle important dans la réparation des bases oxydées et des cassures de l'ADN.

- Enzymes impliquées dans la réparation directe des bases
    - Réparation des cassures par le système « non-homologous end-joining » (NHEJ)

Il s'agit d'un système à deux composants : la protéine Ku et la protéine multifonctionnelle ligase/polymérase/nucléase LigD, une ADN ligase. La protéine Ku se fixe à chaque extrémité endommagée. Elle permet le recrutement de la ligase LigD, qui se fixe de façon spécifique au niveau des phosphates 5'. On assiste ainsi à la réunification des deux extrémités double-brins. On retrouve ce système chez de nombreuses bactéries dont *L. pneumophila* (Popa et al., 2011) et *M. tuberculosis* (Della et al., 2004). Cependant, il semblerait absent chez *B. abortus*, d'après une étude de son génome (Bowater et al., 2006).

- Réparation des bases altérées par excision

Ce système permet l'élimination de bases altérées jusqu'à 4 nucléotides. Il nécessite l'action de l'ADN glycosylase. Celle-ci coupe la liaison N-glycosidique entre la base anormale et le désoxyribose (Jacobs et al., 2012). L'ADN polymérase vient par la suite rajouter une base (Dianov et al., 2003).

- Voies de signalisation activées après oxydation des bases
    - La réponse SOS

La réponse SOS constitue une voie induite par les cassures de l'ADN. On distingue deux protéines majeures impliquées dans cette voie : LexA, un répresseur, et RecA, un activateur. En l'absence de dommages causés à l'ADN, le dimère LexA se fixe de manière constitutive et dans un but répressif à une boite SOS, c'est-à-dire une séquence consensus palyndromique située en amont d'une cinquantaine de gène associée à la réponse SOS. Lorsque l'ADN est altéré, et qu'il y a production d'ADN simple brin, RecA est activé, il va provoquer l'auto-clivage de LexA, permettant l'arrêt de la répression de la boite SOS (Butala et al., 2009). D'autre part, il a été suggéré chez *S. typhimurium* que le système de réparation RecA était plus important que les enzymes anti-oxydantes dans la résistance au stress oxydant (Buchmeier et al., 1995).

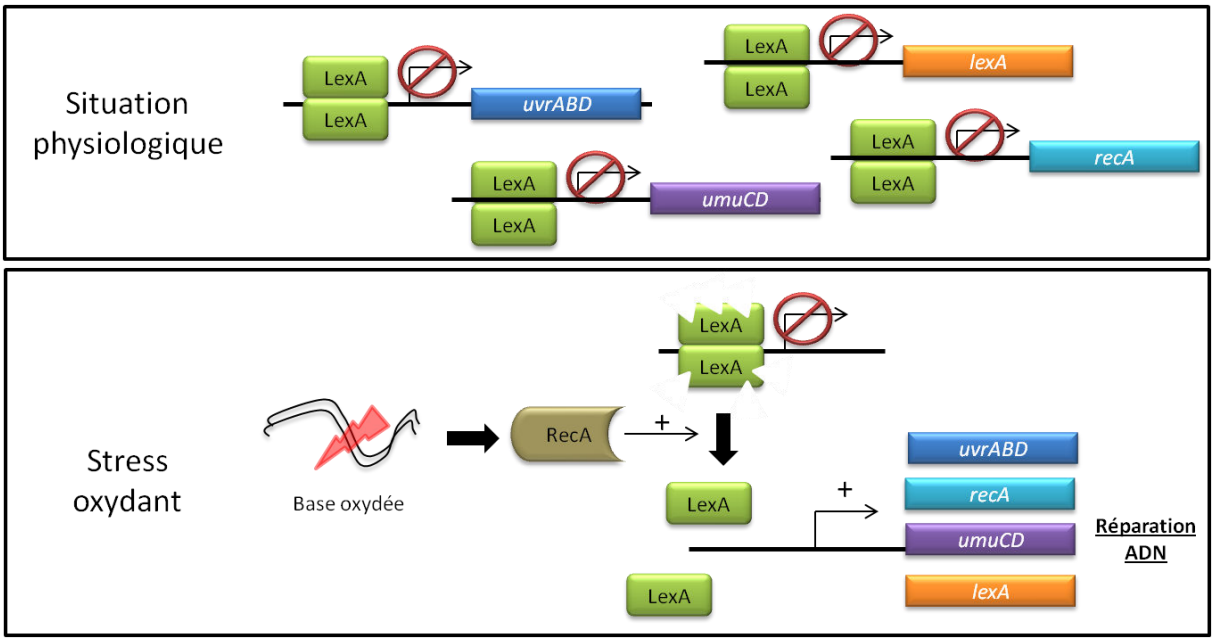

Figure 11 ***Mise en place du système SOS (inspiré de (Dallo et al., 2010))***

- Génération d'un système préventif

Enfin, il a été montré que les bactéries sont capables de mettre en place un système préventif qui limite l'oxydation de protéines : le système « DNA binding protein » ou Dps.

Les premières expériences de mise en évidence de ce système et de l'existence de la molécule Dps ont été réalisées chez la bactérie *E.coli* par l'équipe de Kolter en 1992. Ils ont démontré que Dps était capable de former une structure microcrystalline autour de la chromatine protégeant ainsi l'ADN en particulier en condition de stress oxydant. De plus, ils ont montré que cette protection était dépendante de la fixation du fer(II) par Dps, empêchant ainsi la réaction de Fenton (Grant et al., 1998).

On retrouve ce type de système chez *S. typhimurium* (Halsey et al., 2004), *L. monocytogenes* (Bozzi et al., 1997), *L. pneumophila* (Yu et al., 2009), *B. abortus* (Al Dahouk et al., 2013) et *M. tuberculosis* (Ceci et al., 2005).

3.3.2 Réparation des protéines

La réparation des protéines se limite à trois types de mécanismes qui permettent la réduction de certains produits d'oxydation et la bonne conformation des protéines. On peut les répertorier comme suit:

- Réduction des ponts disulfures

Dans ce remaniement, la bactérie va tenter de contrecarrer la sur-oxydation des cystéines et donc la formation trop importante de ponts disulfures susceptibles d'altérer la conformation des protéines. On distingue le complexe thiorédoxine/thiorédoxine réductase et le complexe glutarédoxine/glutathion réductase, qui jouent un rôle dans le contrôle de l'état redox des

groupements thiols des cystéines, mais aussi la disulfide isomérase qui réarrange les ponts disulfures (Biteau et al., 2003).

- Réparation des acides aminés

Ce type de réparation concerne essentiellement la méthionine. Il met en jeu la méthionine sulfoxyde réductase (Msr) qui va réduire les sulfoxydes de méthionine. Elle est toujours présente sous forme de deux énantiomères, permettant ainsi une réduction optimale des méthionines oxydées.

- Repliement des protéines

Le repliement correct des protéines est un phénomène contrôlé par les protéines chaperonnes. Elles permettent le maintien de la conformation et de la solubilité des protéines sous forme active. On peut citer en exemple les protéines DnaL ou GroEL. Elles sont à l'origine aussi de la prévention des mésappariements et agrégation des protéines oxydées.

Comme nous venons de le voir, la bactérie est très peu armée pour faire face à l'accumulation de protéines oxydées. Elle peut donc faire appel en dernier recours à la protéolyse pour dégrader les protéines endommagées dans son cytoplasme. Ce mécanisme évite aussi l'accumulation dans le cytoplasme de ponts intra et inter-chaînes et ainsi empêche leur agrégation (Grune et al., 1997). Ce type de protéolyse a d'abord été décrit chez *E.coli* (Chung, 1993; Kanemori et al., 1997) puis chez d'autres bactéries à multiplication intracellulaire telles que *S. typhimurium* (Takaya et al., 2003), *M. tuberculosis* (Lee et al., 2008). Elle implique la protéase ATP-dépendante La codée par le gène *lon* et le locus heat-shock VU, homologue du protéasome eucaryote.

3.3.3 Réparation des lipides

Aucune étude n'a été réalisée à ce jour à propos de la réparation des lipides peroxydés chez les bactéries. Ce phénomène constitue pourtant un élément essentiel de la survie des bactéries puisque des lipides, même modifiés, peuvent s'intégrer au sein de ses membranes. A l'inverse, ce phénomène a été étudié chez les eucaryotes. Il a été mis en évidence l'implication de deux enzymes et donc de deux voies de réparation (Girotti, 1998) :

- Première voie : excision, réduction et réparation

On assiste d'abord à une excision de la chaîne oxydée par la phospholipase, puis une réaction de réduction par la glutathion peroxydase. Enfin, une chaine latérale « normale » est réassemblée à l'acide gras par une acyltransférase.

- Deuxième voie : réduction, excision et réparation

Cette deuxième voie propose la réaction inverse, une réduction de la chaine oxydée par la glutathion peroxydase, l'excision de la chaine réparée par une phospholipase puis l'ajout d'une chaine latérale « normale ».

L'étude du génome des principales bactéries à multiplication intracellulaire montre l'existence d'une -voire des deux- enzyme(s) nécessaire(s) à ces réactions. On peut imaginer que ces bactéries ont acquis la capacité de réparer les lipides oxydés, en particulier lorsque les deux gènes sont présents. Ces gènes sont répertoriés dans le tableau suivant :

Souche	Glutathion peroxydase	Phospholipase
B. abortus	Ø	Ø
F. tularensis	*FTT_0733*	*acpA*/*plpC*
L. pneumophila	Ø	*plpC* (phosholipase C)
L. monocytogenes	*bsaA*	*plpB* (phosholipase B), *plpC*
M. tuberculosis	Ø	*plpA* (phospholipase A), *plpB*, *plpC*
S. typhimurium	*btuE*	*pldA* (phospholipase A1)

Table 7 : Enzymes de détoxification des lipides oxydés chez les bactéries à multiplication intracelllulaire (d'après la base de données KEGG)
Phospholipase A : coupe la chaine latérale en carbone 1
Phospholipase B : coupe la chaine latérale en carbone 2
Phospholipase C : coupe la chaine latérale en carbone 3

II. Etude d'un cas particulier : *Francisella tularensis*

1. *Francisella*, l'agent étiologique de la tularémie

1.1 Contexte

1.1.1 Historique

Les premiers cas rapportés de tularémie chez diverses espèces animales s'apparentant à une infection à *F. tularensis* ont été décrits au Japon en 1818 (Kurokawa et al., 1961), en Norvège en 1890 et en 1908 aux Etats-Unis (Morner, 1992). Cependant, il semblerait que le premier réel cas de tularémie ait été présenté en 1911 par McCoy chez des écureuils, dans le conté de Tulare en Californie. La souche fût isolée en 1912 par Edward Francis, qui la nomma alors Bacterium tularense, en rapport avec le lieu de sa première découverte. Son nom fût ensuite changé en *F. tularensis*, en l'honneur d'E. Francis.
Chez l'Homme, le premier cas rapporté fût en Ohio, en 1914 (Wherry et al., 2004).

1.1.2 *Francisella* : une arme de bioterrorisme

Depuis les années 1940, la sous-espèce *F. tularensis* ssp *tularensis* est considérée comme un agent de bioterrorisme. En 1966, l'Organisation Mondiale pour la Santé (OMS) a développé un modèle prédictif visant à déterminer les conséquences d'une attaque terroriste avec cette bactérie. Il a été estimé que la dissémination par voie aérienne de 50 kg de cette bactérie dans le métro, en imaginant un passage de 5 millions de personnes, rendrait 250 000 personnes malades et causerait la mort d'environ 20 000 personnes, sans prévoir les disséminations potentielles qui pourraient s'en suivre.

1.2 Le genre *Francisella*

1.2.1 Taxonomie

La position taxonomique de *F. tularensis* a longtemps été discutée. En effet, au début du XXème siècle, elle était classée dans le genre *Bacterium* par Edward Francis. Après des études sérologiques, elle a été classée dans le genre *Pasteurella* puis *B. abortus*. Les études phylogénétiques ont montré qu'elle est assez éloignée d'autres pathogènes ou bactérie commensale de la flore intestinale. Ce n'est qu'en 1947 que Dorofe'eva a proposé de créer le genre *Francisella* comportant comme unique espèce *F. tularensis* (Olsufjev, 1970).

Aujourd'hui, grâce à des analyses de séquences de l'ARN ribosomal 16S, *F. tularensis* est finalement classée comme appartenant au genre *Francisella*, genre unique de la famille des

Francisellaceae, elle est membre de la sous-classe des *gamma-Proteobacteria* (Forsman et al., 1994; Sjostedt, 2007). Il semblerait que l'organisme le plus proche de *F. tularensis* est *Wolbachia persica*, un endosymbiote des arthropodes (Sjostedt, 2007).

Une étude de l'ADN et de la composition en acides gras a permis de mettre en évidence deux espèces dans le genre *Francisella* : *tularensis* et *philomiragia*. On distingue généralement quatre sous-espèces (ssp) dans l'espèce *F. tularensis* : la ssp *tularensis* (aussi appelé *F. tularensis* Schu S4 ou type A), la ssp *holarctica* (aussi appelé *F* type B) et les ssp *novicida* et *mediasiatica* (Forsman et al., 1994; Svensson et al., 2005). La souche vaccinale LVS (Live Vaccine Strain) a été utilisée comme modèle dans de très nombreuses études. Il s'agit d'un variant atténué de *F. tularensis* ssp *holarctica*, manipulable au laboratoire en conditions de sécurité de niveau 2 (BSL2). Les origines de son atténuation sont encore mal connues. Cependant Rohmer et collaborateurs ont déterminé 35 variations de gènes s'expliquant par des délétions ou des insertions de larges fragments ou des mutations de type SNP entre les souches virulentes *holarctica* FSC200, *holarctica* OSU18 et *tularensis* SCHU S4 et la souche horlarctica LVS. Parmi les protéines altérées on distingue des protéines de membrane, une protéine impliquée dans la mise en place des pili de type IV, une peroxydase, une glycosyltransférase, etc... (Rohmer et al., 2006).

Très récemment, de nouvelles sous-espèces prélevées dans l'environnement ont été identifiées, en particulier chez des animaux marins. Elles présentent toutes un fort taux d'identité nucléotidique ave la sous-espèce *novicida*. Tout d'abord en 2005, une première souche a été ré-isolée de mollusques marins au Japon. Cette souche a été nommée *Francisella halioticida* ssp *novicida*. Puis en 2007, une autre bactérie a été retrouvée dans un élevage norvégien de cabillauds. Elle fût nommée *Francisella piscida* ssp *novicida* (Caipang et al., 2010; Ottem et al., 2007a; Ottem et al., 2007b). Enfin, en 2010, l'étude d'une souche isolée de sang humain en 2003 (appelée à ce moment là FhSp1T) par analyse de son ARN 16S et séquençage du gène *recA* a permis de faire entrer une nouvelle sous-espèce : *Francisella hispaniensis* ssp *novicida* (Huber et al., 2010).

1.2.2 Caractéristiques phénotypiques et bactériologiques

F. tularensis est un petit coccobacille Gram négatif (0,2 µm de large à 0,7 µm de long), non mobile, non sporulé et aérobie strict. Il est catalase négatif et oxydase positif. Les formes virulentes de *F. tularensis* sont entourées d'une capsule de 0.02 à 0.04 µm d'épaisseur dont la perte peut s'accompagner d'une perte de virulence. Les pourcentages en lipides de la capsule et de la paroi sont assez élevés, ils sont respectivement de 50 % et 70 %.

F. tularensis possède un lipopolysaccharide (LPS) très particulier. En effet, il est composé de 4 chaînes longues allant de 16 à 18 carbones alors que, par exemple, on en retrouve 6 chez *E.coli* présentant entre 12 et 14 carbones (Okan et al., 2013). Celui-ci est présenté en détail plus loin.

Les génomes des souches hautement virulentes de *F. tularensis* sont associés à la présence de nombreux pseudogènes s'expliquant par des insertions, des substitutions et/ou des délétions (dans environ 10 % des gènes) ayant entrainé diverses pertes de fonctions métaboliques. C'est pourquoi cette bactérie reste difficile à cultiver au laboratoire (d'où la désignation de « fastidious growth »). Ces difficultés sont notables pour les sous-espèces *tularensis*, *holarctica* et *mediasiatica*. Elles le sont un peu moins pour la sous-espèce *novicida* et l'espèce . *philomiragia*. De par leur exigence métabolique, on les cultive de façon systématique sur -ou dans- des milieux très riches. Les principaux milieux retrouvés dans la littérature sont, pour les milieux solides, des géloses « infusion cœur-cervelle » (Brain heart infusion agar) ou des géloses « chocolat » enrichies (PolyViteX^{TM} ou IsoVitaleX^{TM}). Pour les milieux liquides, on distingue le milieu Chamberlain (Chamberlain, 1965), le bouillon Mueller-Hinton (il peut être supplémenté avec : 0.1% glucose, 2 % IsoVitalex, 0.025 % pyrophosphate de fer) et le milieu TSB pour Triptic Soy Broth (supplémenté avec 0.1% glucose et 0.4 % cystéine).

1.3 Epidémiologie

1.3.1 Distribution géographique

Les différentes sous-espèces de *F. tularensis* présentées précédemment se distinguent par leur situation géographique et leur virulence (Titball et al., 2003). On distingue dans un premier temps la sous-espèce *tularensis*. Elle constitue, comme indiqué précédemment, la sous-espèce la plus pathogène pour l'homme. En effet, sa dose infectieuse est extrêmement faible : 10 bactéries par voie sous-cutanée et 25 bactéries par aérosol (McCrumb, 1961). Cette sous-espèce est retrouvée principalement en Amérique du Nord et au Mexique. La sous-espèce *holarctica* est retrouvée sur la majorité de l'hémisphère Nord. La sous-espèce *mediasiatica* a été isolée au Kazakhstan et au Turkmenistan. Ces deux sous-espèces sont pathogènes pour l'homme mais leur virulence est plus modérée. En ce qui concerne la sous-espèce *novicida*, elle est très rarement virulente pour l'homme sauf dans des cas particulier d'immuno-dépression (Hollis et al., 1989). On la retrouve principalement aux Etats-Unis et en Australie. Il s'agit d'ailleurs de la seule souche identifiée dans l'hémisphère Sud (Hollis et al.,

1989). La souche *F. philomiragia,* comme la sous-espèce *novicida,* est très peu infectieuse pour l'Homme. On la retrouve dans les mers très salées, et notamment la Méditerranée.

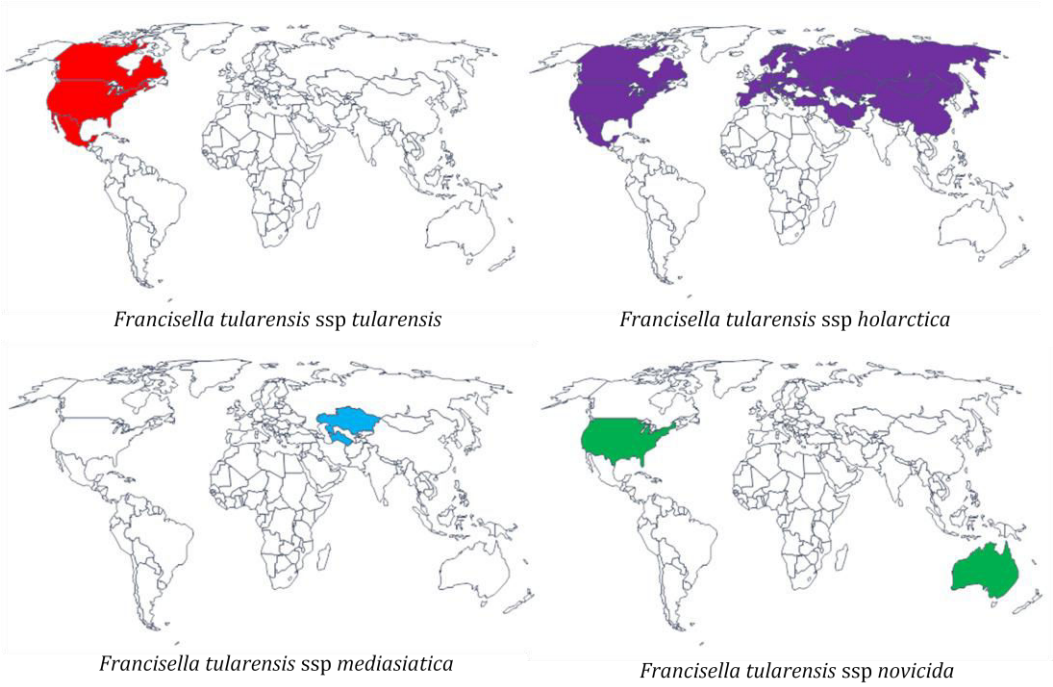

Figure 12 ***Répartition géographique des principales souches de Francisella tularensis (Inspiré de (Oyston et al., 2004))***

En France, des cas de tularémie sont répertoriés sur l'ensemble du territoire et en particulier dans le Nord-Est et le Centre (d'après les données du Ministère des affaires sociales et de la santé et de l'Institut de veille sanitaire). Ces cas se déclarent principalement en été et automne. Ce recensement s'explique par des activités se rapportant à la chasse (manipulation de gibiers) ou à la promenade en campagne.

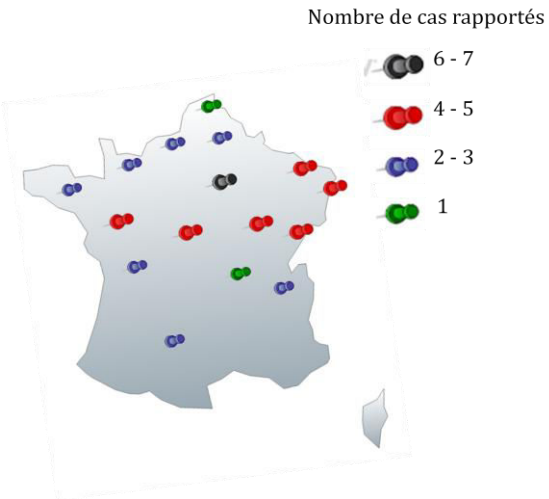

Figure 13 ***Répartition géographique des cas de tularémie déclarés en France en 2012, patients âgés de 6 à 87 ans. (Données épidémiologiques de l'Institut de Veille Sanitaire)***

1.3.2 Réservoirs et vecteurs

On distingue trois types de réservoirs pour la bactérie *F. tularensis* : les animaux, les arthropodes et l'environnement.

Parmi les animaux, on distingue plus d'une centaine d'espèces qui sont susceptibles d'être infectées. Aux Etats-Unis, on recense principalement des épizooties chez les lapins sauvages, les rats musqués et les castors (Sjostedt, 2007). En Europe, on isole *F. tularensis* à partir de petits mammifères terrestres comme des écureuils, des campagnols, des souris ou encore des lagomorphes, en particulier des lièvres. Les oiseaux migrateurs sont un vecteur prépondérant mis en évidence en 2002 (Hansson et al., 2002). Enfin d'autres animaux peuvent être ajoutés à cette liste, mais y jouent un rôle mineur, c'est-à-dire les animaux carnivores vivant en campagne comme les renards ou les furets, mais aussi les poules. En France, les petits rongeurs constituent le principal réservoir animal car ils sont extrêmement sensibles à ce type d'infection. On distingue aussi les animaux domestiques tels que les chiens ou les chats (Eliasson et al., 2002), mais aussi les ruminants (vaches et moutons).

D'autre part on distingue les arthropodes hématophages (*e.g.* tiques, moustiques, puces et poux) comme second réservoir (Petersen et al., 2005). Les tiques ont été identifiées dans la contamination des bovins, ovins et chiens. Ils constituent la principale cause de transmission entre l'animal et l'homme.

Enfin on distingue un troisième réservoir : l'environnement. *F. tularensis* est dépendante de la température du milieu dans lequel elle se trouve. En effet, plus la température est basse (proche de 0°C), plus *F. tularensis* a de chance de persister, en particulier dans l'eau (Colquhoun et al., 2011). On peut la retrouver aussi dans les déjections animales.

L'Homme constitue un hôte accidentel. Enfin, on retrouve souvent une association entre la déclaration importante de cas chez les animaux, à un moment donné, et la déclaration de cas chez l'Homme.

1.4 Aspects cliniques de la tularémie

1.4.1 Transmission et manifestations cliniques

La tularémie est décrite comme une zoonose, ce qui signifie qu'elle est naturellement transmissible de l'animal à l'homme. De nombreuses voies de contamination ont été décrites dans la littérature. On distingue des transmissions par voie cutanée ou voie conjonctivale. Elles peuvent se produire par exemple avec la manipulation d'animaux malades ou la piqure d'insectes infectés. On distingue aussi une transmission par voie respiratoire médiée par l'inhalation d'aérosols. Cette voie de contamination est d'ailleurs la plus infectante à très faible dose. On retrouve enfin une contamination possible par voie orale, après l'ingestion de

nourriture ou d'eau contaminées, mais l'inoculum bactérien dans ce cas doit être beaucoup plus important.

Certaines populations sont plus à risque que d'autres comme par exemple les agriculteurs, les chasseurs et promeneurs en forêt (Levesque et al., 1995; Petersen et al., 2005). On considère également que les bouchers, les vétérinaires et les personnels de laboratoire sont des personnes pouvant être exposées à ce type de maladie. A ce titre, la tularémie est reconnue comme une maladie professionnelle.

La période de temps entre la contamination et l'infection dépend du mode de contamination. Il varie en général entre 3 et 5 jours et dans de rares cas peut aller jusqu'à 21 jours. Les symptômes généraux sont : une fièvre soudaine, des frissons, des maux de tête, des douleurs musculaires, une toux sèche, un mal de gorge et une faiblesse progressive. Les principaux organes cibles de *F. tularensis* sont les poumons, la rate, le foie, les reins, les nœuds lymphatiques et la plèvre.

On distingue en général six formes cliniques principales qui sont dépendantes du mode de contamination (Dennis et al., 2001; Petersen et al., 2005).

- Infection **cutanée**
    - Forme **ulcéro-glandulaire** et **glandulaire** (87%) : il s'agit d'une atteinte de la peau, elle se caractérise par un ulcère au point d'infection et/ou une tuméfaction des ganglions lymphatiques.
    - Forme **oculo-ganglionnaire** (3%): il s'agit d'une atteinte des yeux, on verra l'apparition d'une conjonctivite avec possibilité de tuméfaction des glanglions lymphatiques.
- Infection par **voie orale** :
    - Forme **oro-pharyngée** ; pharyngite avec adénopathie cervicale, parfois signes digestifs
    - Forme **typhoïde** (8%) : forme systémique avec fièvre et « tuphos »
- Infection par **voie aérienne**
    - Forme **pulmonaire** : pleuro-pneumonie

En cas d'évolution aggravée de l'infection, ou suite à un traitement inadapté ou mis en place trop tardivement, toute les formes de tularémie peuvent évoluer vers de graves complications telles qu'une inflammation pulmonaire, une intoxication du sang et entraîner la mort.

Du fait d'une prévalence relativement faible et de l'absence de spécificité des signes cliniques,

la tularémie est en général une maladie plutôt difficile à diagnostiquer.
Aujourd'hui, il existe différents moyens d'établir un diagnostic biologique. On utilise en première intention des tests sérologiques avec analyse des anticorps dans le sang. Il peut être aussi utilisé dans un deuxième temps, des tests par PCR, la spectrométrie de masse MALDI-TOF, la culture ou la coloration de Gram.

1.4.2 Traitements préventifs et curatifs

Un vaccin vivant atténué utilisant la souche LVS (Live Vaccine Strain) de *F. tularensis* ssp *holarctica* est à disposition et peut être utilisé pour des individus soumis à des risques importants (Sandstrom, 1994), ce type de traitement confère une immunité après 2 semaines. Cependant sa mise sur le marché est encore interdite dans de nombreux pays dont la France car ses mécanismes d'atténuation sont mal définis et il peut engendrer de nombreux effets secondaires.
Il existe de nombreux traitements curatifs. On distingue principalement un traitement par antibiothérapie. Il inclut, pour les adultes en première intention, des antibiotiques de la classe des fluoroquinolones comme la ciprofloxacine, l'ofloxacine et la lévofloxacine, pendant 2 à 3 semaines. Pour les cas de forme sévère, il a longtemps été administré de la streptomycine, un antibiotique de la famille des aminoglycosides. Cependant, au vue de sa toxicité, il a été remplacé par de la gentamycine, un antibiotique qui a démontré son efficacité dans des études plus récentes (Dennis et al., 2001).

2. Cycle intracellulaire de *F. tularensis*

F. tularensis est capable de survivre et de se multiplier dans de nombreux types cellulaires. On distingue les cellules phagocytaires, comme par exemple les macrophages et les cellules dendritiques, mais aussi des cellules non phagocytaires comme les hépatocytes ou les cellules épithéliales des poumons. Cependant, les macrophages restent la cellule de prédilection de la bactérie *F. tularensis*. Dans les paragraphes à venir, nous allons présenter en détail les différentes étapes qui composent ce cycle intracellulaire.

2.1 Entrée de *Francisella* dans la cellule phagocytaire

2.1.1 Processus d'attachement à la cellule hôte

Bien que de nombreux récepteurs cellulaires et bactériens aient été identifiés, les molécules impliquées dans l'arrimage de la bactérie *F. tularensis* restent encore mal

caractérisées. Un complexe protéique semble jouer un rôle majeur dans ce processus : les pili de type IV. Cette classe de molécules a été bien définie chez de nombreuses espèces bactériennes. Il a été montré, pour la première fois en 2004, la présence de fibres ayant les caractéristiques typiques des pili de type IV en surface de la souche de *F. tularensis* ssp *holarctica* LVS. Cette observation a été confirmée par une analyse génomique comparative avec le génome de la bactérie *Neisseria* meningitidis (Gil et al., 2004). De telles structures ont été observées chez les souches *tularensis* SCHU S4, *holarctica* LVS et *novicida* U112. Une équipe américaine a notamment mis en évidence l'importance de la protéine FsaP dans l'adhérence de la bactérie vis-à-vis de cellules épithéliales pulmonaires type A549 (A. Melillo et al., 2006). Enfin, notre équipe a montré la présence d'un ligand EF-Tu (elongation factor) bactérien qui lie la nucléoline de la cellule hôte et qui facilite l'adhésion de *F. tularensis* ssp *holarctica* LVS (Barel et al., 2008).

2.1.2 Processus d'internalisation

Les mécanismes d'adhésion et d'entrée de la bactérie *F. tularensis* ont été particulièrement étudiés par Clemens et collaborateurs dans des macrophages dérivés de monocytes de sang périphérique (MDM) et des THP1 (correspondant à une lignée de monocytes humains), en utilisant la souche atténuée *F. tularensis* ssp *holarctica* LVS, et un dérivé clinique de la sous-espèce hautement virulente de type A. Plusieurs de leurs travaux ont démontré, par microscopie à fluorescence et microscopie électronique, que *F. tularensis* était internalisée par un mécanisme unique d'enveloppement mettant en jeu de grandes boucles asymétriques de pseudopodes. La fusion de la boucle avec la membrane plasmique de la cellule permet l'internalisation de la bactérie dans de larges vacuoles à la surface du macrophage. Ce processus appelé "looping phagocytosis" implique un réarrangement de l'actine et une signalisation dépendante de la phosphatidylinositol 3-kinase. De plus cette même équipe a montré que dans le cas de bactéries opsonisées, c'est-à-dire ayant été en contact avec du sérum, on assistait à un mécanisme d'internalisation dépendant de la présence du complément C3 et de son récepteur CR3 (Clemens et al., 2007; Clemens et al., 2005).
D'autres équipes ont mis en évidence l'importance des récepteurs Fcγ (Balagopal et al., 2006), des récepteurs "scavenger" de classe A (Pierini, 2006) et de la nucléoline (Barel et al., 2008).
Dans le cas d'une bactérie non opsonisée, il a été montré qu'on se trouvait en présence d'un mécanisme dépendant du récepteur au mannose (MR), en particulier pour les sous-espèces *F. tularensis* ssp *holarctica* LVS et *novicida* U112 (Schulert et al., 2006). Il a d'ailleurs été

montré qu'une lignée tumorale de macrophages murins (J774.1) surexprimant le MR fixait beaucoup mieux la souche *holarctica* LVS.

Comme de nombreuses bactéries, *F. tularensis* est capable aussi de manipuler ce qu'on appelle des radeaux lipidiques pour optimiser son internalisation. Les radeaux lipidiques sont des domaines particuliers de la membrane plasmique qui regroupent des glycosphingolipides (GSL) et des molécules de cholestérol. On assimile communément ces domaines à des plateformes où sont disposés des récepteurs et des protéines prêts à réagir entre autres avec les bactéries. Ils constituent par conséquent une porte d'entrée pour celles-ci. L'équipe de S. Daefler a montré récemment que la souche *F. tularensis* ssp *holarctica* LVS recrutait ces domaines en association avec la cavéoline-1 pour son internalisation (Tamilselvam et al., 2008).

Ce comportement observé chez *F. tularensis* diffère de ceux observés chez d'autres bactéries à multiplication intracellulaire. En effet, avant ces découvertes, on distinguait trois grands mécanismes d'entrée. Deux d'entre eux furent proposés pour la première fois en 1995 (Swanson et al., 1995). L'un est appelé « zipper» pour symboliser une fermeture éclair. Il consiste en un contact direct entre la cellule et la bactérie, ce qui n'est pas le cas de *F. tularensis*, et il est associé, entre autres, aux bactéries *Yersinia* et *L. monocytogenes.* L'autre mécanisme identifié est appelé « trigger » pour symboliser un déclenchement. Il implique la sécrétion d'effecteurs vers la cellule cible et il concerne les bactéries *Shigella* et *P. aeruginosa*. Le troisième mécanisme a été identifié encore plus tôt par Horwitz (Horwitz, 1984). Il décrit un mécanisme dit « coiling », c'est-à-dire qu'il implique l'extension et l'enroulement d'un pseudopode autour de la bactérie. Il concerne en particulier la bactérie *L. pneumophila* (Abu Kwaik, 1996).

2.2 Phase phagosomale

La phagocytose est un processus mis en place par la cellule hôte pour détruire toute particule étrangère. On distingue différentes étapes successives se caractérisant par l'état de maturation de la vacuole contenant la bactérie. Cette maturation résulte de la fusion de la première vacuole avec d'autres vacuoles (voir paragraphes précédents). Les techniques d'immunofluorescence, de microscopie électronique et d'immuno-électron microscopie, ont permis d'avoir une vision assez claire du devenir de *F. tularensis* dans la cellule phagocytaire, et en particulier dans la voie d'endocytose.

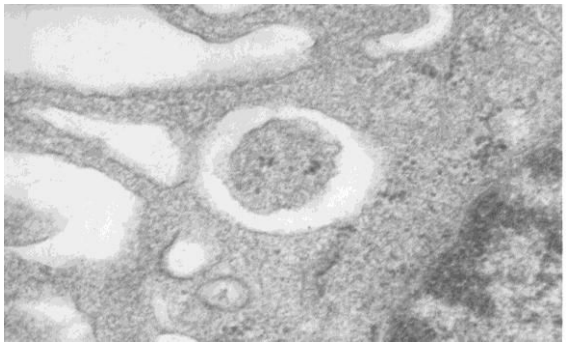

Figure 14 ***Phagocytose de F. tularensis ssp novicida par des macrophages murins J774.1, après 1 h d'infection (image prise au laboratoire, grossissement x 40 000)***

2.2.1 Inhibition de la maturation du phagosome et échappement

L'étude du cycle intracellulaire de *F. tularensis* a permis de mettre en évidence un arrêt précoce de la maturation phagosomale. En effet, à la suite de son internalisation, *F. tularensis* se retrouve piégée dans ce qu'on appelle un « phagosome contenant *Francisella* » ou « FCP ». L'équipe de Clemens a démontré que cette FCP fusionnait dès 15 minutes avec un endosome précoce, symbolisé par la présence du marqueur « early endosomal antigen 1 » (EEA-1) au niveau de sa membrane, et de la GTPase Rab5. Dans un second temps, 15 à 30 minutes après le début de l'infection, on assiste à la fusion entre cette vacuole et un endosome tardif symbolisé par l'acquisition des marqueurs CD63, LAMP-1, LAMP-2 et Rab7 GTPase. Cependant, ce type d'interaction se fait de façon limitée, en témoignent la quantité restreinte de cathepsine D et de molécules LAMPs à la surface de la membrane phagosomale. Il a surtout été montré que *F. tularensis* était capable d'inhiber la fusion avec les lysosomes (Checroun et al., 2006; Chong et al., 2008a; Clemens et al., 2004). De façon très intéressante, la formation de phagolysosomes est observée uniquement lors de l'internalisation de bactéries *F. tularensis* mortes (Checroun et al., 2006; Clemens et al., 2004; Santic et al., 2005a). Il est à noter que pour la souche *holarctica* LVS, ces événements se produisent sur une période de temps plus longue, allant de 1 h à 4 h.

A ce jour, deux molécules ont été identifiées comme jouant un rôle dans ce processus d'inhibition de maturation. La première est la molécule eucaryote SHIP. Une inhibition de la fusion entre le FCP et les endosomes tardifs est observée dans des BMM $SHIP^{-/-}$. La deuxième molécule est la molécule AKT. Il l a été montré une augmentation de la fusion FCP-endosomes tardifs dans des BMM exprimant de façon constitutive la molécule AKT (Rajaram et al., 2009). Cette étude suggère que *F. tularensis* manipulerait l'expression de ces deux molécules pour inhiber cette fusion.

On assiste ensuite à une rupture de la membrane phagosomale dont les mécanismes à ce jour n'ont pas encore été mis en évidence. *F. tularensis* atteint alors le cytosol et peut se multiplier.

2.2.2 Contrôle du pH phagosomal

Plusieurs équipes se sont penchées sur l'importance de l'acidification de la vacuole phagosomale dans la survie intracellulaire de *F. tularensis*. Cette acidification est effective grâce à la fusion entre la FCP naissante et un endosome précoce. En effet, les endosomes précoces possèdent au niveau de leur membrane des pompes ATPases vacuolaires (vATPase) à l'origine de l'entrée de protons. La nouvelle FCP passe alors d'un pH physiologique à une valeur se situant entre un pH 4 et un pH 5,5. Cette acidification est nécessaire au bon fonctionnement de nombreuses enzymes bactéricides, à la dégradation des constituants de *F. tularensis* (Clemens et al., 2004) et à la maturation phagosomale (Huynh et al., 2007).

Il a été démontré, chez les souches *tularensis* Schu 4 et *holarctica* LVS (dans des macrophages humains et des macrophages J774.1 issus de lignées tumorales), une résistance à l'acidification s'expliquant par des phagosomes qui acquièrent un nombre limité de pompes vATPases (Clemens et al., 2004). Cependant, deux études réalisées sur les sous-espèces *tularensis* et *novicida,* démontrent que les FCPs acquièrent ces pompes à protons « de façon normale » avant la libération de *F. tularensis* (Chong et al., 2008b; Santic et al., 2008). Il semblerait que ces résultats, apparemment contradictoires, soient dépendants de l'opsonisation préalable de la bactérie. L'opsonisation de *F. tularensis* serait responsable de la diminution de l'acquisition des pompes vATPases à la membrane vacuolaire. Ces données s'ajoutent à la démonstration que l'échappement phagosomal de *F. tularensis* n'est pas altéré par la présence de ces pompes à protons (Clemens et al., 2009).

D'un point de vue moléculaire, certaines de ces études suggèrent l'importance de l'acidification phagosomale dans l'induction de facteurs en jeu dans la lyse de la membrane phagosomale. En effet, à l'aide de mutants, il a été démontré l'importance des gènes *iglC*, *iglD* (gènes de l'ilôt de virulence) et leur régulateur *mglA* dans la prévention de l'acidification de la FCP (Bonquist et al., 2008). De plus, Chong et collaborateurs ont démontré une hyper expression de ces gènes pendant la phase phagosomale et suggèrent un rôle pour ces protéines dans la production de molécules impliquées dans la lyse de la paroi vacuolaire (Chong et al., 2008b).

2.2.3 Inhibition du « burst oxydatif »

Comme nous l'avons décrit précédemment, l'une des stratégies de la cellule phagocytaire pour éliminer un pathogène est de générer un stress oxydant avec la production d'ions superoxydes dans la vacuole phagosomale. Ce burst oxydatif regroupe aussi les dérivés nitrés. Le principal complexe protéique responsable de ce burst oxydatif est la « NADPH-dependent phagocytic oxydase » ou « NADPH oxydase » appelée aussi Phox ou Nox2. Pour rappel, celle-ci pompe des électrons dans le compartiment phagosomal pour réduire des molécules d'oxygène en ions superoxydes. On distingue aussi l'enzyme « inducible nitric oxyde synthase », ou iNOS. Celle-ci utilise l'arginine et l'oxygène comme substrats pour produire des dérivés nitrés (Fang, 2004). *F. tularensis* a développé deux stratégies principales de survie face à ce burst oxydatif :

- L'inhibition du fonctionnement de la NAPDH oxydase.

Plusieurs équipes ont montré que l'inhibition du burst oxydatif par *F. tularensis* constituait une stratégie de survie dans le macrophage, et ce quelque soit la sous-espèce (Lofgren et al., 1980; McCaffrey et al., 2006; Proctor et al., 1975; Vestvik et al., 2013). Reilly et collaborateurs ont mis en évidence l'importance de l'enzyme AcpA, une phosphatase acide, dans cette inhibition. Cette enzyme a été retrouvée dans différents pathogènes comme jouant un rôle dans la survie intracellulaire, en inhibant la production d'ERO par la NADPH oxydase. Parmi ces pathogènes, on distingue *Coxiella burnetii* (Baca et al., 1993) ou encore *Legionella micdadei* (Saha et al., 1985). Chez *F. tularensis*, l'enzyme AcpA joue un rôle similaire (Reilly et al., 1996). AcpA, située dans le périplasme bactérien, et libérée sous forme soluble, empêcherait l'assemblage du complexe NADPH oxydase en déphosphorylant ses sous-unités $p47^{phox}$ et $p40^{phox}$ (Reilly et al., 1996). L'activité phospholipase de l'AcpA pourrait également empêcher son ancrage correct à la membrane (Mohapatra et al., 2007a). D'autres études plus récentes, réalisées par Mohapatra et collaborateurs, ont montré que l'inactivation du gène *acpA* conférait une susceptibilité accrue à l'action des ERO, empêchant sa sortie du phagosome. Il existe en tout cinq ou six acides phosphatases selon les sous-espèces (AcpA, AcpB, AcpC, AcpD, HapA and HapB). Cependant, leurs rôles respectifs n'ont pas été encore clairement définis. Il semblerait que toutes ces enzymes fonctionnent ensemble dans l'inhibition du burst oxydatif (Mohapatra et al., 2013).

D'autres enzymes ont été mis en évidence comme jouant un rôle prépondérant dans l'inhibition de la production d'ERO. Cependant, leur mode d'action n'a pas encore été déterminé. Parmi celles-ci, on distingue les gènes *carA*, *carB* et *pyrB,* codant respectivement

pour la petite et la grande sous-unité de la carbamoylphosphate synthase et l'aspartate carbamoyl transférase, et étant impliquées dans le métabolisme de l'uracile. Trois mutants inactivés respectivement pour l'une de ces enzymes montrent une production normale d'ERO (Schulert et al., 2009).

- La production d'enzymes anti-oxydantes :

La bactérie *F. tularensis* possède aussi un panel d'enzymes pour faire face à la production d'ERO car le blocage de l'action de la NADPH oxydase n'est probablement pas total et pour lui permettre de s'adapter rapidement au contexte redox qui l'entoure dès son entrée dans le phagosome. Parmi celles-ci, on distingue principalement la catalase KatG (H. Lindgren et al., 2007; A. A. Melillo et al., 2010) et les superoxydes dismutase SodB (Bakshi et al., 2006) et SodC (A. A. Melillo et al., 2009).

2.3 Phase cytosolique

F. tularensis est capable de rejoindre rapidement le cytosol, en effet il est observé généralement une sortie entre 30 minutes et 1 heure après le début de l'infection. On distingue, après 8 heures d'infection, un pic de multiplication intracellulaire qui peut perdurer jusqu'à 12 à 24 heures post-infection, selon les sous-espèces.

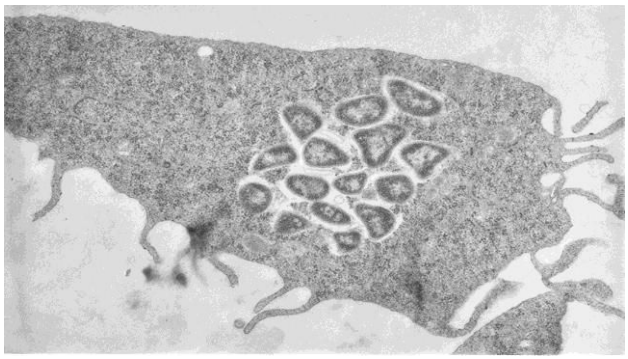

Figure 15 ***Infection de macrophage murin J774.1 par F. tularensis ssp novicida (après 10 heures d'infection, image prise au laboratoire, grossissement x 10000).***

A ce stade assez avancé de multiplication, l'équipe de Jean Celli a pu mettre en évidence, dans des macrophages de moelle osseuse de souris BALB/c, des bactéries encapsulées dans une large structure vacuolaire appelée FCV ou *Francisella* Containing Vacuole (Checroun et al., 2006; Wehrly et al., 2009). Ces vacuoles multi-membranaires, situées près du noyau cellulaire, expriment à leur membrane le marqueur LAMP-1, mais aussi la protéine LC3, un marqueur de l'autophagie. Elles n'altèrent en rien la survie et la croissance de *F. tularensis*.

Il est encore difficile de déterminer si cette FCV joue un rôle précis dans le devenir de *F. tularensis* et/ou s'il s'agit d'un mécanisme dirigé par le macrophage pour contrôler la multiplication de la bactérie. Cette explication semble peu probable puisqu'il a été montré que

ce mécanisme était absent dans des macrophages dérivés de monocytes (Chong et al., 2010; Edwards et al., 2010). De plus, malgré la présence de LC3, plusieurs équipes ont démontré que de nombreux gènes liés à l'autophagie étaient sous-exprimés lors de l'infection à *F. tularensis* ssp *novicida* et *F. tularensis* ssp *tularensis*.

De façon très intéressante, un lien a été établi entre la phase phagosomale et la multiplication efficace de cette bactérie en démontrant qu'un mutant qui a subi de nombreux dommages pendant la phase phagosomale (H. Lindgren et al., 2004a; Santic et al., 2005a; Schmerk et al., 2009) et un mutant qui s'échappe tardivement (Chong et al., 2008a) présentent une multiplication cytosolique altérée.

De nombreux gènes ont été identifiés comme jouant un rôle essentiel dans la réplication cytosolique de *F. tularensis* grâce aux techniques de mutagenèse dirigée. Ils sont énumérés dans le tableau suivant.

Nom associé		Référence
iglD	Intracellular growth locus protein D	(Santic et al., 2007)
iglB	Intracellular growth locus protein B	(Gray et al., 2002)
iglA	Intracellular growth locus protein A	(de Bruin et al., 2007)
mglB	ClpXP protease specificity-enhancing factor	(Baron et al., 1998)
pmrA	two-component response regulator	(Mohapatra et al., 2007b) (Sammons-Jackson et al., 2008)
FTT_0989	Hypothetical protein	(Brotcke et al., 2006)
dsbB	Disulfide bond formation protein	(Maier et al., 2006) (Tempel et al., 2006) (Weiss et al., 2007) (Qin et al., 2009)
pdpB	Hypothetical protein	(Brotcke et al., 2006) (Tempel et al., 2006)
cds2	Hypothetical protein	(Brotcke et al., 2006)

Table 8 : Liste des gènes jouant un rôle essentiel dans la réplication cytosolique de Francisella tularensis.

2.4 Induction de la mort cellulaire

Lorsque la bactérie a atteint son pic de multiplication intracellulaire (environ 24 heures p.i.), pour des raisons d'espace disponible dans la cellule mais aussi à cause de la limitation en ressources disponibles dans le cytosol, celle-ci a la capacité de mener son hôte à la mort cellulaire (Lai et al., 2001). Ce phénomène est extrêmement bien réglé dans le temps car il s'agit pour la bactérie d'assurer une multiplication optimale (en évitant que ce processus arrive trop précocement) mais aussi sa dissémination optimale. Des études ont été menées sur le

modèle de macrophages murins J774.1. Plusieurs équipes ont mis en évidence l'implication de deux voies de mort cellulaire induites par *F. tularensis* :

1. La voie intrinsèque apoptotique : on assiste à une activation de cette voie de façon très précoce, entre 9 heures et 12 heures p.i.. Elle se manifeste par le relargage du cytochrome *c* dans le cytosol, une perturbation du potentiel mitochondrial puis par l'activation successive des caspases 9 et 3.
2. La voie pyroptotique : de façon simplifiée, ce mécanisme met en jeu la molécule AIM2. Celle-ci a pour rôle de reconnaitre des séquences d'ADN bactérien libérées dans le cytosol par un mécanisme probablement passif résultant de la lyse de quelques bactéries. Elle s'associe alors à l'adaptateur ASC pour activer la caspase 1 et successivement les cytokines pro-inflammatoires IL-1β et IL-18 (Jones et al., 2011).

3. Eléments de virulence de *F. tularensis*

3.1 Structures de surface

Une vingtaine de gènes d'enveloppe ont été identifiés comme étant impliqués dans la formation soit de la capsule, soit du lipopolysaccharide (LPS), soit des protéines de membrane externe. Tous ces gènes ont été identifiés par des approches génétiques réalisées *in vitro* et *in vivo* permettant ainsi de relier ces éléments indispensables dans sa structure membranaire à sa pathogénicité et démontrant ainsi leur effet dans la protection contre les activités bactéricides de l'organisme hôte.

3.1.1 La capsule

La présence, la composition et le rôle de la capsule dans le cycle intracellulaire de *F. tularensis* sont des éléments extrêmement discutés. La première démonstration de la présence d'une capsule autour de *F. tularensis* eut lieu il y a plus de 40 ans, basée sur l'isolement de polysaccharides antigéniques typiques de capsule à partir de la souche virulente *tularensis* SCHU S4 (Carlisle et al., 1962). Ces résultats ont été confirmé quelques années plus tard par la découverte de la présence de mannose et de rhamnose. L'équipe de Gibson a montré par spectrométrie de masse qu'elle était composée d'un polymère de répétitions de tétrasaccharides permettant la classification de cette capsule comme une "O-antigen capsular polysaccharide". Ils ont de plus démontré l'absence de lipide A et de sucres dans ce domaine et présents habituellement dans le LPS, confirmant ainsi la réelle existence d'une capsule (Apicella et al., 2010). Cette capsule semble être présente uniquement chez les sous-espèces *tularensis* et *holarctica*. Il a été mis en évidence par Su et collaborateurs la présence du locus

capBCA qui correspond aux gènes *FTT_0805 - FTT_0807* (ssp *tularensis*) et *FTL_1416 - FTL_1414* (ssp *holarctica* LVS) et qui présente une homologie forte avec les gènes *capB*, *capC* et *capA* de *Vibrio cholera* (Chen et al., 2007; Sarkar et al., 2014; Su et al., 2011). Chez *Bacillus anthracis*, les protéines CapB et CapC sont impliquées dans la synthèse du poly-gamma-d-glutamate (PGA), un élément de la capsule. CapA (au même titre que CapD et CapE) sont des protéines impliquées dans l'ancrage du PGA.

En termes de pathogénicité, ces protéines jouent un rôle très important dans la virulence de *F. tularensis*. En effet, il a été démontré que l'inactivation du locus *capBCA* chez *F. tularensis* ssp *holarctica* LVS ou ssp *tularensis* entrainait un défaut de virulence dans le modèle murin lors d'une infection par voie aérienne (Su et al., 2011). Ce phénotype s'expliquerait par un défaut de sortie du phagosome.

3.1.2 Le lipopolysaccharide (LPS)

Le LPS de *F. tularensis* a suscité un grand intérêt au sein de la communauté scientifique du fait de ses propriétés biologiques et structurelles très particulières. Comme la plupart des LPS bactériens, le LPS de *F. tularensis* est composé de lipides A qui permettent l'ancrage du LPS à la membrane externe, d'un complexe oligosaccharidique lié au lipide A et appelé "3-deoxy-d-*manno*-octulosonic acid" ou plus communément Kdo et d'un O-polysaccharide, appelé aussi O-antigène.

Les mécanismes impliqués dans l'activation du système immunitaire lors de l'infection mettent en jeu : i) du côté de la bactérie, de nombreuses protéines et en particulier le LPS et son lipide A, et ii) du côté de la cellule, les TLR ou Toll-like receptors, des molécules de reconnaissance d'antigènes bactériens. On distingue en particulier le TLR4 spécifiquement impliqué dans la reconnaissance du LPS. La structure du LPS bactérien joue donc un rôle essentiel et potentiellement stimulant dans l'activation de la réponse inflammatoire. Il a été démontré chez *F. tularensis* ssp *novicida* que son LPS lui permettait l'échappement à la réponse immunitaire de la cellule hôte. Ce phénomène s'explique par une modification de la structure du lipide A (Miller et al., 2005), ayant pour effet la limitation de l'interaction avec le TLR4. En effet, il a été montré que *F. tularensis* synthétisait un lipide A précurseur ayant des caractéristiques structurales classiques et que celui-ci était modifié pour présenter en fin de biosynthèse, des chaînes d'acides gras : i) plus longues que les autres bactéries (16 à 18 carbones contre 12 à 14 carbones), ii) au nombre de 4, au lieu de 6 pour *E. coli* par exemple, iii) contenant un groupement phosphate, au lieu de 2 classiquement, mais aussi un sucre Kdo (Raetz et al., 2009).

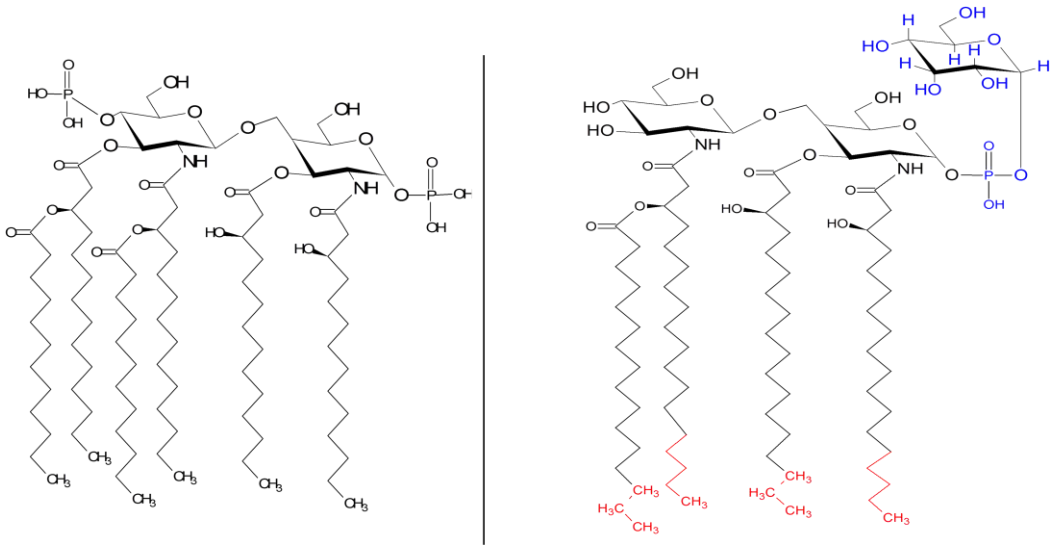

Figure 16 ***Structures des lipides A de E. coli et F. tularensis.***
Structures des lipides A de E. coli (gauche) et F. tularensis (droite).
Les modifications majeures du lipide A sont colorées en rouge pour les chaînes latérales et en bleu pour le sucre Kdo.

L'importance structurale du lipide A a été démontrée par l'analyse de mutants menant à la production de lipides A altérés. Dans tous les cas, on observe des phénotypes similaires, à savoir une clairance rapide de la bactérie (Wang et al., 2007). De la même façon, des souris déficientes pour le récepteur TLR4 montrent une sensibilité accrue pour la souche *horlactica* LVS (Anthony et al., 1988; Macela et al., 1996).

3.1.3 Glycosylation des protéines

Ces dix dernières années, l'étude des modifications post-traductionnelles et en particulier de la glycosylation des protéines chez les bactéries, est devenue de plus en plus importante grâce à l'évolution des techniques (Electrophorèse 2D, Spectrométrie de masse en tandem, bioinformatique...). Ces modifications jouent un rôle majeur dans la reconnaissance bactérie-bactérie et bactérie-cellule, le repliement des protéines et la réponse immunitaire. En effet, il a été mis en évidence chez plusieurs bactéries comme *Campylobacter* (Goon et al., 2003) ou *Helicobacter pylori* (Josenhans et al., 2002), une perte de pathogénicité intracellulaire et d'interaction hôte-pathogène associées à un défaut de glycosylation des flagelles.

Une première étude chez *F. tularensis*, parue en 2011, a révélé l'importance de la glycosylation de la protéine PilA impliquée dans la formation des pili (Egge-Jacobsen et al., 2011). Une seconde étude, basée sur une identification large des protéines glycosylées (Balonova et al., 2010), a révélé que de multiples protéines de *F. tularensis*, aux fonctions extrêmement variées, sont glycosylées. A titre d'exemples, parmi celles-ci, on distingue des

protéines de l'ilôt de virulence telles que IglB et PdpB, des protéines faisant partie des pili telles que PilA et PilE ou des protéines de membrane telles que OmpA et FopA.

3.2 Le génome

Le génome de la souche *F. tularensis* ssp *tularensis* SCHU S4 fût le premier à avoir été entièrement séquencé en 2005. Les séquences des génomes des trois autres sous-espèces ont été publiés plus récemment (Larsson et al., 2005; Rohmer et al., 2007). Les particularités des trois sous-espèces *tularensis*, *holarctica* et *novicida* sont présentées dans la table 9.

Souche	Taille du génome (pb)	Nombre de protéines codées	Contenu G+C (%)	Nombre de pseudogènes
F. tularensis ssp *tularensis* SCHU S4	1 892 819	1145	32,25	254
F. tularensis ssp *holarctica* LVS	1 895 998	1380	32,15	303
F. tularensis ssp *novicida*	1 910 031	1731	32,47	14

Table 9 : Caractéristiques génomiques des trois sous-espèces tularensis Schu S4, holarctica LVS et novicida, inspiré de (Kingry et al., 2014)

Comme indiqué dans la table 9, *F. tularensis* présente un faible pourcentage de (G+C), ce qui est assez courant chez les petits génomes bactériens. De plus, le génome de *F. tularensis* comprend un îlot de pathogénicité (« Fancisella Pathogenicity Island » ou FPI) qui sera décrit dans le paragraphe suivant. Le FPI, qui est dupliqué chez les ssp *tularensis* et *holarctica* mais présent en une seule copie chez la ssp *novicida*, présente un pourcentage de (G+C) encore plus bas que celui du génome complet (27,5%), suggérant une acquisition par transfert horizontal.

Les deux types de séquences d'insertions trouvées dans les génomes de *F. tularensis* sont nommés ISFtu1 et ISFtu2. Elles ont la particularité d'être retrouvées aux points de rupture génomique suggérant leur implication dans les réarrangements chromosomiques (Champion et al., 2009; Rohmer et al., 2007).

Même si les différentes sous-espèces de *F. tularensis* présentent un haut degré d'identité nucléotidique (≥ 97,7%), on distingue cependant quelques différences appelées « Regional différences » ou RD. Elles sont au nombre de 22. Les huit premières (RD1 à RD8) ont été mises en évidence en 2003 grâce aux techniques de puces à ADN (Broekhuijsen et al., 2003). Il est à noter que ces régions sont absentes de la souche *holarctica* LVS. Plus tard, l'analyse de 45 isolats de *F. tularensis* par PCR a permis d'identifier les régions RD9 à RD22. RD1 et

RD6 (contenant le gène *pdpD* appartenant au FPI) sont deux régions qui sont aujourd'hui utilisées pour l'identification de souches (Svensson et al., 2005).

Enfin, les études sur le génome de *F. tularensis* ont permis de comprendre de façon partielle l'atténuation de virulence particulière de la souche *F. tularensis* ssp *holarctica* LVS. Une équipe a mis en évidence des mutations dans 35 gènes permettant d'expliquer cette atténuation. Ces mutations sont pour la majorité des « single nucléotide polymorphism » (ou SNP), ou des délétions d'1, 2, 12 ou 90 paire(s) de base et qui peuvent aller jusqu'à 500 voire 1500 paires de base (Rohmer et al., 2006).

3.3 Le FPI

Le FPI (en français, ilôt de pathogénicité de *Francisella*) est une région de 33 kb (Barker et al., 2007; Nano et al., 2004). Le fait que le FPI soit présent en une seule copie chez la sous-espèce *novicida* et en deux copies chez les autres sous-espèces, pourrait expliquer la nature non pathogène pour l'homme de cette sous-espèce spécifiquement. Une hypothèse serait qu'un génome ancestral similaire à celui de la sous-espèce *novicida*, dans lequel le FPI était en simple copie, aurait subit une duplication par recombinaison non réciproque (Champion et al., 2009). Une étude comparative des FPI de différentes souches a permis de montrer une grande conservation de sa séquence. Le FPI est constitué de 17 gènes répartis en deux opérons. Le premier rassemble les gènes *pdpD, iglA, iglB, iglC* et *iglD*. Le second est orienté dans le sens inverse et comprend les gènes *pdpA, pdpB, iglE, vgrG, ilgF, iglG, iglH, dotU, iglI, iglJ* et *pdpC* (Barker et al., 2007). On remarquera que le gène *pdpD* est tronqué chez la souche *F. tularensis* ssp. *holarctica*.

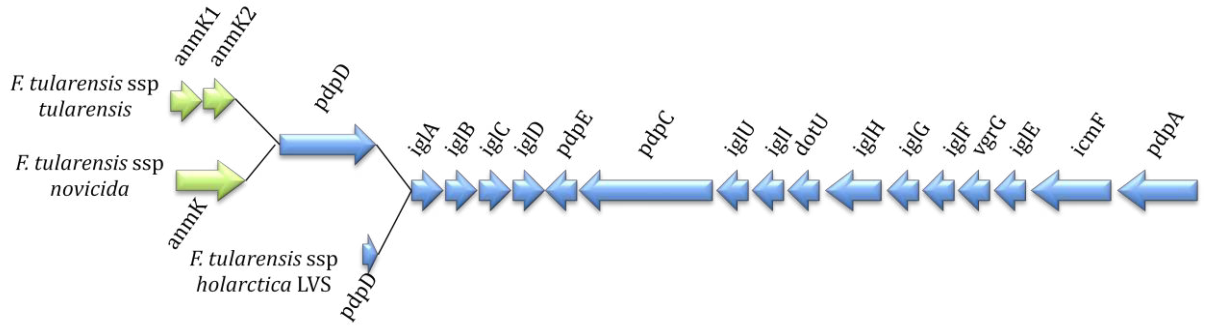

Figure 17 ***Francisella pathogenicity island (FPI).***
Représentation schématique de l'îlot de pathogénicité de Francisella. (inspiré de Bröms et al., 2010)

Le FPI joue un rôle crucial dans la virulence et la multiplication intracellulaire de *F. tularensis*, en témoignent les nombreuses analyses génomiques identifiant des gènes de cette région. De nombreux mutants ont été réalisés au cours des dernières années afin de mieux

caractériser le rôle de chaque gène. On attribue à chacun de ces gènes de nombreuses fonctions importantes dans la virulence de *F. tularensis* :

Souche	Gène	Référence
Echappement phagosomal		
F. tularensis ssp *tularensis* SCHU S4	i*glE*	(Robertson et al., 2013)
F. tularensis ssp *holarctica* FSC200	*iglH*	(Straskova et al., 2012)
F. tularensis ssp *holarctica* LVS	*iglC*	(H. Lindgren et al., 2004a)
F. tularensis ssp *holarctica* LVS	*pdpC*	(M. Lindgren et al., 2013a)
F. tularensis ssp *holarctica* LVS	*dotU* et *vgrG*	(Broms et al., 2012)
F. tularensis ssp *holarctica* LVS	*iglG* et *iglI*	(Broms et al., 2011)
F. tularensis ssp *novicida*	*pdpA*	(Schmerk et al., 2009)
F. tularensis ssp *novicida*	*iglD*	(Santic et al., 2007)
Multiplication cytosolique		
F. tularensis ssp *tularensis* SCHU S4	*iglJ*	(Long et al., 2013)
F. tularensis ssp *holarctica* LVS	*pdpC*	(M. Lindgren et al., 2013a)
F. tularensis ssp *novicida*	*iglA*	(de Bruin et al., 2007)
F. tularensis ssp *novicida*	*iglB*	(Read et al., 2008)
Cytotoxicité		
F. tularensis ssp *novicida*	*iglC*, *iglI* et *iglG*	(M. Lindgren et al., 2013b)
Résistance aux stress		
F. tularensis ssp *holarctica* LVS	*iglC*	(Lenco et al., 2005)

Table 10 : Liste des gènes du FPI impliqués dans le cycle intracellulaire de Francisella tularensis.

3.4 Eléments de sécrétion

Les êtres vivants possèdent de nombreuses machineries de sécrétion de molécules et partagent en particulier le système «Sec» (ou machinerie générale de sécrétion) pour la sécrétion de protéines non repliées possédant une séquence signal N-terminal Sec-dépendante et, pour quelques unes, le système « Tat » (Twin Arginine translocation) pour les protéines repliées possédant une séquence signal N-terminale Tat-dépendante. Les bactéries à Gram négatif possèdent en plus 8 systèmes différents de sécrétion désignés sous le nom de système de sécrétion de type I à VI, (ou SST I à SST VI) (Desvaux et al., 2009; Thanassi et al., 2012). Il a été montré que la plupart d'entre eux étaient impliqués dans les interactions bactérie-cellule eucaryote, en médiant notamment le passage de molécules effectrices dans le cytosol eucaryote.

Des analyses *in silico* ont démontré chez *F. tularensis*, en plus du système Sec, la présence de 3 types de systèmes de sécrétion, le système de sécrétion de type I et de type II, mais aussi un système de sécrétion de type VI qui de façon surprenante aurait un lien avec le FPI, c'est

pourquoi il sera développé séparément. D'autre part, *F. tularensis* présente d'autres éléments de sécrétion, à savoir des vésicules de la membrane externe.

3.4.1 Sécrétion de type I et de type II

Le système de sécrétion de type I ou SSTI a été caractérisé pour la première fois chez la bactérie *E.coli.* Il s'agit d'un système d'export de l'hémolysine (HlyA) nécessitant la présence de 3 protéines : une ABC ATPase cytoplasmique accrochée à la membrane interne, HlyB ; une protéine liée à la membrane externe, TolC ; et une molécule faisant le lien entre ces deux protéines dans l'espace externe, HlyD (Holland et al., 2005). Il a été montré chez *F. tularensis* qu'il existait 3 paralogues de la protéine TolC : TolC, FtlC et SilC. Il a été démontré que TolC et FtlC participaient à la résistance vis-à-vis de nombreux antibiotiques mais aussi que TolC était nécessaire dans la virulence de la ssp *horlactica* LVS. De plus, dans la même sous-espèce, TolC contribue à une diminution de la cytotoxicité de *Francisella* dans un modèle de macrophages murins et humains, permettant un décalage de la mort de l'hôte (Platz et al., 2010). Cependant, de façon inattendue, cette protéine semble avoir une contribution mineure dans la virulence de la sous-espèce *tularensis* (Kadzhaev et al., 2009).

Comme pour toutes les bactéries, le système de sécrétion de type II (SSTII) constitue un système majeur pour le transport de molécules depuis le périplasme vers l'extérieur (celles-ci ayant été transportées à travers la membrane cytoplasmique par le système sec). Le SSTII est composé de 12 à 15 protéines, regroupées en trois multimères, et formant un assemblage assez complexe que nous ne détaillerons pas ici. De plus, il a été montré que le SSTII établissait un lien étroit avec les pili de type IV (Nunn, 1999). Très peu de données sont disponibles sur ce SSTII. Cependant, la présence de ce système chez la sous-espèce *novicida* a pu être montrée de façon indirecte. En effet, la sécrétion de plusieurs protéines est abolie chez des mutants de *F. tularensis* ssp *novicida* n'exprimant plus des facteurs de pili de type IV.

3.4.2 Sécrétion de type VI

Le système de sécrétion de type VI a été découvert pour la première fois chez *Vibrio Cholerae* (Pukatzki et al., 2006). Il a maintenant été identifié dans plus d'un quart des génomes bactériens séquencés. Les bactéries pathogènes utilisent ce système pour injecter des protéines effectrices dans le cytosol de leur hôte. Des analyses *in silico* réalisées par Barker et collaborateurs ont suggéré que les protéines codées par le FPI formaient un système de sécrétion de type VI (SST VI) phylogénétiquement différent de ce qui a pu être décrit précédemment (Barker et al., 2007). En effet, on retrouve des petites homologies entre des

protéines du FPI et des protéines des systèmes classiques SST VI : DotU et IcmH, PdpB et IcmF, IglA et VipA, IglB et VipB. PdpE et Hcp. Plusieurs protéines codées par les gènes du FPI sont retrouvées au niveau de la membrane externe, comme par exemple PdpD et IglC, leur distribution est affectée par l'absence de *pdpB* ou *dotU* (Ludu et al., 2008). Plus récemment, il a été montré que les protéines VgrG et IglI étaient aussi sécrétées dans le cytosol de la cellule hôte (Barker et al., 2009). Enfin, il a été montré plus récemment que la protéine DotU a une structure très proche de TssL, un composant essentiel du SST VI (Robb et al., 2012). L'équipe suédoise de Söjstedt et collaborateurs a démontré que la souche *F. tularensis* ssp *novicida* sécrétait dans le cytosol du macrophage les protéines IglE, IglC, VgrG, IglI, PdpE, PdpA, IglJ et IglF et que cette sécrétion dépendait de la présence des protéines DotU, VgrG, et IglC qui font partie du core du système de sécrétion (Broms et al., 2012).

3.4.3 Vésicules de la membrane externe

Les vésicules de membrane externe sont produites de façon ubiquitaire dans toutes les bactéries Gram négatif et tout au long de leur cycle infectieux. Ce système constitue pour elles un moyen rapide et efficace de sécréter des facteurs de virulence, des toxines et des effecteurs, pour répondre aux différentes situations qu'elles rencontrent. Il s'agit de structures sphériques (50 à 250 nm de diamètre) (Kulp et al., 2010).

Il a été démontré que *F. tularensis* sécrétait ce type de vésicules durant sa phase stationnaire, en milieu liquide. Une analyse spectrométrique de ces vésicules chez les sous-espèces *novicida* et *philomiragia* a démontré qu'elles étaient composées d'une centaine de protéines dont 166 étaient communes. Parmi ces protéines, on distingue majoritairement des protéines cytoplasmiques (60%), en particulier des chaperonnes (GroEL, DnaK et KatG). Parmi les protéines de membrane, on retrouve entre autres PilQ et des protéines du FPI (PdpA, B, D et IglA, B et C) (Pierson et al., 2011). D'autre part, une étude récente montre que la production de ces vésicules est stimulée lors de l'infection par *F. tularensis* ssp *novicida*, et qu'elles provoquent le relargage de cytokines pro-inflammatoires (McCaig et al., 2013).

3.5 Facteurs de transcription

Les facteurs de transcription sont des régulateurs essentiels permettant à la bactérie *F. tularensis* de survivre dans des environnements très différents. De multiples facteurs ont été identifiés et à ce jour, on distingue principalement MglA, SspA, FevR, MigR, (p)ppGpp, PmrA, MigR et la chaperonne Hfq. L'inactivation individuelle de ces gènes entraîne une forte

atténuation de virulence, illustrant ainsi l'importance de chacun de ces régulateurs dans la pathogénicité de *F. tularensis*.

3.5.1 MglA, SspA et l'ARN polymerase

MglA, pour Macrophage Growth Locus A, fût le premier facteur de transcription à avoir été décrit. En effet, l'équipe de Nano en 1998 a montré que la sous-espèce *novicida* délétée pour le gène *mglA* présentait un défaut sévère de multiplication. Quelques années après, l'équipe de Kwaik démontra que ce défaut de pathogénicité s'expliquait par un défaut de sortie du phagosome (Santic et al., 2005b).

En 2004, il a été montré que chez un mutant n'exprimant pas *mglA*, on assistait à une sous-expression des gènes *iglA*, *iglC*, *iglD*, *pdpA* et *pdpC* (Lauriano et al., 2004). D'autre part, une analyse transcriptionnelle réalisée aussi dans ce même mutant a montré qu'il était responsable de la régulation de 102 gènes, et confirmait son influence sur les gènes du FPI (Brotcke et al., 2006). Des travaux ultérieurs ont démontré que MglA était impliqué dans la résistance à l'acidification du phagosome (Bonquist et al., 2008; Santic et al., 2005b) mais aussi dans la réponse au stress oxydant et au stress de type carence nutritionnelle (Guina et al., 2007; Honn et al., 2012). Enfin, chez *F. tularensis* ssp *novicida*, d'autres facteurs de virulence tels que la métalloprotéase PepO sont régulés par MglA.

MglA présente une homologie faible (21,8% d'identité peptidique) avec une autre protéine codée par le génome de *F. tularensis*, désignée SspA (pour Stringent starvation protein A) du fait de son homologie avec les protéines SspA d'autres espèces (Brotcke et al., 2006). SspA est un facteur de transcription identifié pour la première fois chez *E.coli*. Il répond aux limitations nutritionnelles ressenties par la bactérie et est impliqué dans la régulation des gènes de réponse à ce stress. Il a été démontré que MglA et SspA formaient un complexe qui s'associe à l'ARN polymérase pour contrôler positivement la transcription de nombreux gènes de virulence. Une analyse transcriptomique a confirmé le lien étroit entre ces deux protéines en montrant que leur mutation respective affecte quasiment les mêmes gènes (Charity et al., 2007).

3.5.2 FevR/PigR

La protéine désignée FevR pour "*Francisella* effector of virulence regulation" (ou PigR pour "pathogenicity island gene regulator") constitue un autre acteur essentiel dans la transcription des gènes du FPI. Il a été montré que cette protéine était nécessaire à la multiplication intracellulaire et à la virulence de *F. tularensis* dans un modèle murin (Charity et al., 2009). FevR est positivement régulée par MglA, et interagit directement avec le

complexe MglA/SspA pour moduler l'expression des gènes en aval (Brotcke et al., 2008; Rohlfing et al., 2014).

Enfin, il a été montré dans la souche *tularensis* SCHUS4 que FevR joue un rôle majeur dans l'inhibition de l'assemblage de la NADPH oxydase (McCaffrey et al., 2010).

3.5.3 (p)ppGpp

Dans des conditions de carence nutritionnelle importante, certaines bactéries ont la capacité de faire face en exprimant une guanosine diphosphate hyperphosphorylée ou guanosine pentophasphate, autrement appelée (p)ppGpp. On la retrouve par exemple chez *E. coli* et *L. monocytogenes* où elle a été mise en évidence pour la première fois en 1970 (Cashel et al., 1970). Le mode de fonctionnement de cette alarmone est le suivant : en condition de stress métabolique, et en particulier lors d'une carence en acides aminés, on assiste à la liaison d'ARNt non chargés aux ribosomes, conduisant à un blocage de la traduction. La molécule RelA se fixe à ces ribosomes et provoque la synthèse de (p)ppGpp, qui est ensuite converti en ppGpp. RelA se fixe successivement à plusieurs ribosomes pour permettre une production suffisante de (p)ppGpp (Braeken et al., 2006). ppGpp se fixe à l'ARN polymérase en association avec le complexe MglA/SspA et la molécule FevR (Charity et al., 2009). On retrouve le même type de mécanisme avec la molécule SpoT, mais dans le cadre d'une restriction en sucres et acides gras. De plus, SpoT est aussi impliqué dans la dégradation de cette molécule signal, évitant une accumulation trop importante (Jain et al., 2006).

Ces deux molécules, RelA et SpoT, sont retrouvées dans le génome de *F.tularensis* ssp *novicida* et ssp *tularensis* Schu S4 (R. E. Dean et al., 2009; Larsson et al., 2005; Rohmer et al., 2006). Une équipe a réalisé un mutant n'exprimant pas la protéine RelA et ainsi pu montrer que RelA jouait un rôle dans la résistance au stress *in vitro*, dans la formation des biofilms (R. E. Dean et al., 2009), mais surtout qu'elle était importante dans la multiplication de la bactérie *in vitro* et *in vivo*. La délétion simultanée de *relA* et *spoT* dans la souche LVS, empêchant la production de ppGpp, provoque aussi un défaut de multiplication mais de façon moins accentuée. Enfin, il a été montré que le ppGpp améliorait les interactions entre FevR et le complexe MglA/SspA (Charity et al., 2009).

3.5.4 PmrA

Les bactéries ont développé des systèmes senseurs appelés "système à deux composants" (ou "Two Component Systems", TCS), capables de répondre rapidement aux conditions environnementales. On distingue un récepteur membranaire possédant une activité

kinase, associé à un régulateur cytoplasmique. Toutes les molécules intégrées dans ce système proviennent de gènes généralement très proches.

La présence de deux TCS a été mise en évidence chez *F. tularensis*. L'un d'entre eux a suscité un intérêt majeur puisqu'il est homologue à un TCS retrouvé chez *S. enterica enterica*. Il met en jeu la molécule PmrA et le FPI (Gunn, 2008; Mohapatra et al., 2007b). Mohapatra et collaborateurs ont montré qu'un mutant du gène *pmrA* avait une susceptibilité accrue aux peptides anti-microbiens, une altération de la multiplication intracellulaire s'expliquant par une altération de la sortie du phagosome, et une altération de la virulence dans le modèle murin. Mais surtout, ils ont montré une diminution de l'expression des gènes du FPI (Mohapatra et al., 2007b).

Une étude plus récente chez la sous-espèce *novicida* a permis de mieux comprendre le fonctionnement de cette molécule. Il semblerait que PmrA co-précipite avec le complexe MglA/SspA pour augmenter l'expression des gènes de l'ilôt de virulence. Elle se fixe en particulier sur le gène *pdpD*. On comprend ainsi mieux le phénotype observé dans un mutant Δ*pmrA*. Il est montré aussi que cette molécule se fixe sur son propre promoteur pour activer sa transcription, et que cette fixation est dépendante d'une phosphorylation sur l'acide aspartique en position 51. Cette réaction a lieu grâce à la tyrosine kinase KdpD, l'autre acteur majeur du TCS (Bell et al., 2010).

3.5.5 MigR/CaiC

Un autre régulateur positif, appelé MigR (pour "Macrophage Intracellular Growth Regulator", et appelé aussi CaiC), a également été mis en évidence plus récemment chez *F. tularensis*. Une étude par qRT-PCR dans la sous-espèce *holarctica* a montré une diminution de l'expression des gènes du FPI tels que *iglA*, *iglB*, *iglC* et *iglD* dans un mutant Δ*migR*. Ce mutant présente un défaut de multiplication dans des macrophages murins s'expliquant par un défaut de sortie du phagosome. De façon surprenante, un mutant Δ*migR* dans la sous-espèce *tularensis* SCHU S4 ne présente aucun phénotype particulier sinon une diminution de l'activation de FevR et des gènes du FPI cités précédemment (Buchan et al., 2009). MigR ne possédant aucun domaine de fixation à l'ADN, une hypothèse serait que MigR affecterait RelA ou SpoT, ce qui induirait la synthèse de (p)ppGpp et successivement l'expression de *fevR* (Charity et al., 2009).

3.5.6 La chaperonne Hfq

La molécule Hfq est un régulateur post-transcriptionnel pléiotropique, considérée comme une chaperonne à ARN. Elle a été découverte pour la première fois chez la bactérie

E.coli (Tsui et al., 1994). L'une des principales fonctions qui lui est attribuée est qu'elle facilite les interactions entre des petits ARN (sARN) et leur ARN messagers (ARNm) correspondants, permettant ainsi la mise sous silence du gène cible. Hfq peut également modifier la conformation d'un ARNm afin de limiter sa traduction ou se lier à l'ADN de façon à moduler directement la production d'ARNm. Enfin, Hfq peut faire intervenir le facteur de terminaison de transcription Rho pour modifier la terminaison des ARNm et ainsi modifier leur survie dans le cytoplasme bactérien (Sobrero et al., 2012).

On retrouve la protéine Hfq dans toutes les principales bactéries à multiplication intracellulaire. Pour ne citer que quelques exemples par rapport à la très large littérature sur le sujet, il a été mis en évidence qu'elle avait un rôle important dans la croissance, en particulier en phase stationnaire, chez *L. monocytogenes*, *L. pneumophila* (Christiansen et al., 2004; McNealy et al., 2005), dans la résistance à des stress acide, osmotique, oxydant chez *L. monocytogenes* (Christiansen et al., 2004; Sittka et al., 2007), la formation de biofilm chez *S. enterica* (Monteiro et al., 2012) et la résistance aux antibiotiques en règle générale (Hayashi-Nishino et al., 2012).

Enfin, il a été démontré par notre laboratoire que la protéine Hfq de *F. tularensis* contrôlait l'expression de nombreux gènes et notamment régulait négativement l'expression d'une partie des gènes du FPI (Meibom et al., 2009) chez la sous-espèce *holarctica*, jouant ainsi un rôle essentiel dans la pathogénicité de *F. tularensis*.

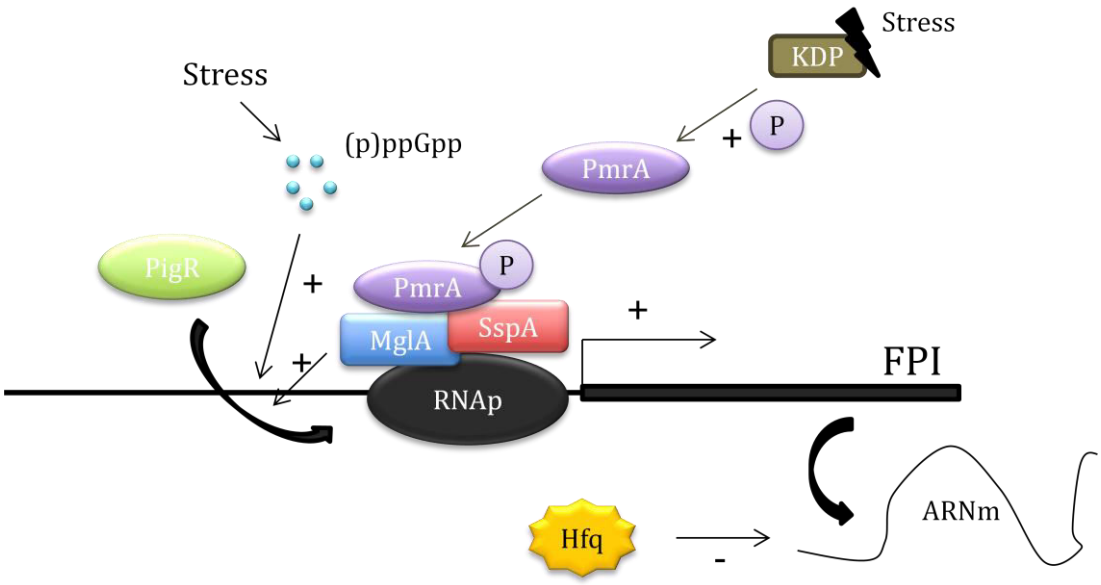

Figure 18 Régulation du FPI

3.6 Adaptation aux stimuli extérieurs

La bactérie *F. tularensis* a développé de nombreux mécanismes pour répondre aux modifications extérieures qu'elle subit. De nombreux profils transcriptionnels, à la fois dans des milieux de culture bien définis mais aussi lors de l'infection de modèles cellulaires, ont été réalisés et permettent de mieux comprendre les réponses de ce pathogène. Dans cette partie seront développés les différents évènements auxquels est confrontée *F. tularensis* lors d'un cycle infectieux et les réponses qu'elle a mises en place pour y faire face.

3.6.1 Température

La bactérie *F. tularensis* peut être confrontée à d'importantes variations de température. En effet, comme décrit précédemment, il s'agit d'une bactérie environnementale qui est capable d'infecter de nombreuses espèces animales et des insectes. Elle peut donc subir des températures allant globalement de 0°C à 37°C. Une étude réalisée chez la sous-espèce *horlactica*, a évalué les modifications transcriptionnelles en fonction de la température (Horzempa et al., 2008). Elle a montré que 95 gènes étaient surexprimés et 125 autres étaient réprimés si on se plaçait à une température inférieure à 37°C. Parmi ces gènes, on distingue en particulier des gènes codant pour des protéines chaperonnes mais aussi des protéines impliquées dans le métabolisme des acides aminés. De façon surprenante, cette étude ne relève pas d'effet de la température sur la modification de l'expression des gènes de l'ilot de virulence. Or une autre étude, réalisée plus récemment, démontre une augmentation de l'expression des gènes *IglC*, *IglD* et *PdpC* lorsqu'on abaisse la température (Lenco et al., 2009). Enfin, d'autres chercheurs ont aussi mis en évidence une modification du LPS température-dépendante. En effet, ils ont montré que le gène *deoB,* impliqué dans la production de LPS, était plus induit à 37 °C. Ce résultat est en adéquation avec la nécessité pour *F. tularensis* d'avoir une membrane en parfait état lors de l'infection de cellules hôtes qui survivent à 37 °C (Shaffer et al., 2007). Les mécanismes de régulation sous-jacents à ces modifications sont encore méconnus. Une étude, réalisée dans notre laboratoire, suggère l'implication du facteur sigma alternatif RpoH, dans la réponse au stress thermique (Grall et al., 2009).

3.6.2 Fer

La présence de fer est une nécessité vitale pour toutes les bactéries puisqu'il est impliqué dans de nombreuses réactions chimiques. Il participe aux réactions métaboliques, en particulier au niveau du cycle de Krebs, au transport d'oxygène, à la régulation génique et à la

biosynthèse d'ADN (via la ribotide synthase) (Collins, 2003). Capter le fer est aussi un moyen pour la bactérie de limiter la réaction de Fenton qui peut se produire dans la cellule hôte et qui est particulièrement délétère pour elle.

Disponible en général de manière illimitée dans l'environnement, elle devient une ressource limitée volontairement lors de l'infection (10^{-9} M). En effet, la cellule phagocytaire est composée d'un récepteur transferrine (TfR) qui lie la molécule transferrine (Tf) et est capable d'importer le fer avec une haute affinité. La cellule hôte est capable de limiter l'infection en limitant la présentation de ce récepteur à la membrane (Ryu et al.), de même qu'elle est capable d'adresser les complexes Tfr-fer subsistant aux phagosomes. En effet, la cellule utilise le fer pour augmenter l'activité de la NADPH oxydase (Lieu et al., 2001).

F. tularensis possède un système senseur du fer, composé d'un répresseur transcriptionnel Fur qui se lie au fer. En conditions où le fer est en excès, les complexes Fur-Fer se fixent avec une haute affinité aux « boites Fur » situées en amont des gènes qu'ils régulent et répriment ainsi (le plus généralement) leur expression. En conditions de carence en fer, le répresseur Fur perd son affinité pour les boites Fur, libérant alors la transcription des gènes cibles (comprenant notamment des systèmes d'acquisition du fer). Pour identifier ces gènes, Deng et collaborateurs ont réalisé une analyse transcriptomique de la souche *F. tularensis* ssp *holarctica* LVS soumise à une basse concentration en fer (Deng et al., 2006). Ils ont montré une augmentation de la présence de protéines chaperonnes, de ribosomes, de protéines du métabolisme ferrique, d'enzymes du métabolisme mais aussi de protéines du FPI en corrélation avec une autre étude (Lenco et al., 2007).

Des travaux ont montré que le complexe Fur-Fer se fixait en amont d'un premier opéron appelé soit *fsl* pour « *Ft* siderophore locus », soit *fig* pour « *Ft* iron genes » ou même *fsl/fig* ABCD car il est constitué de 4 gènes. Il se fixe en amont et l'active en particulier quand le fer devient indisponible, et provoque la synthèse et la sécrétion de protéines sidérophores de type rhizoferrine qui vont « attraper » le fer extracellulaire (Kiss et al., 2008). Le complexe Fur-Fer peut se fixer aussi sur le promoteur du gène *fsl/fig E*, un cinquième gène essentiel puisqu'il code pour un récepteur de la membrane externe capable de fixer le complexe Sidérophore-fer (Ramakrishnan et al., 2008).

3.6.3 Stress oxydant

Comme précisé précédemment, lors de son cycle intracellulaire *F. tularensis* est confrontée au stress oxydant durant son passage dans le phagosome. Deux études ont permis de mettre en évidence des mécanismes qui lui permettent à la fois de sentir, de répondre et de

limiter la production d'espèces réactives. La première, réalisée en 1994, a montré par des techniques protéomiques d'électrophorèse 2D l'activation de nombreuses chaperonnes de stress et d'enzymes anti-oxydantes (Ericsson et al., 1994). Une autre analyse par microarray a confirmé que tous ces gènes se retrouvaient eux aussi surexprimés durant l'infection et en particulier durant les temps précoces (H. Andersson et al., 2006). Pour mieux comprendre l'importance des enzymes anti-oxydantes, plusieurs équipes ont réalisé des mutants délétés pour un ou plusieurs gènes (*katG, sodC*). De façon surprenante, des mutants ne comportant la délétion que d'un seul gène ont globalement une virulence très peu affectée (Kadzhaev et al., 2009; H. Lindgren et al., 2007). Ces résultats suggèrent la mise en place par *F. tularensis* de plusieurs outils extrêmement sophistiqués pour faire face à ce type de stress.

Des chercheurs ont montré la capacité de *F. tularensis* ssp *horlactica* LVS à stopper la formation de la NADPH oxydase (voire chapitre correspondant) au niveau de la membrane du phagosome des neutrophiles (McCaffrey et al., 2006). Il serait intéressant de savoir si ces travaux s'appliquent à toutes les sous-espèces de *F. tularensis*, mais aussi dans tous les types de cellules macrophagiques.

3.6.4 Divers

De nombreux autres stimuli peuvent être considérés comme importants dans l'expression de la virulence de *F. tularensis* mais qui à ce jour ont été peu développés.

Par exemple, contrairement au stress oxydant, la réponse au pH acide a été très peu étudiée. En effet, cette bactérie peut faire face au pH acide dans deux situations : la première dans le phagosome, la deuxième dans l'estomac puisqu'une de ses voies d'entrée est la voie digestive. L'analyse du génome de *F. tularensis* laisse penser qu'elle possède de nombreux systèmes de détoxification identifiés comme des transporteurs d'acides aminés (comme par exemple des importeurs d'arginine, de lysine, …). Le pH acide semblerait cependant être un élément important dans la virulence de la bactérie. En effet, il a été montré qu'il active des chaperonnes impliqués elles-mêmes dans l'activation de l'îlot de virulence (Dieppedale et al., 2011).

Une autre molécule, la spermine, a été présentée comme un senseur du milieu environnant. En effet, il s'agit d'un polyamine produit seulement chez les eucaryotes. Sa présence permettrait d'alerter *F. tularensis* d'un « environnement eucaryote » en affectant significativement l'expression de nombreuses protéines bactériennes (Carlson et al., 2009).

4. La « virulence nutritionnelle »

La nutrition est un aspect de la virulence des micro-organismes pathogènes (parasites, bactéries) de plus en plus étudié ces cinq dernières années et notamment chez les bactéries à multiplication intracellulaires. Lors son cycle infectieux, *F. tularensis* est confrontée à des environnements très différents tels que des organes aux fonctions variées (foie, rate, système lymphatique, sang, etc... et par conséquent elle est dans l'obligation de s'adapter aux nutriments disponibles. Par ailleurs, dans la cellule hôte, *F. tularensis* doit faire face à deux espaces sensiblement différents : le phagosome et le cytosol. A ce jour aucune étude n'a permis de décrire de façon précise les composants nutritionnels de cette vacuole bactéricide. Cependant, il est vraisemblable qu'elle constitue un espace limité en sucres, lipides et acides aminés. A l'inverse, le cytosol est considéré comme un espace où les nutriments sont présents en quantité suffisante. Les études génétiques menées ces dix dernières années ont permis de mettre en évidence de nombreux gènes impliqués dans la virulence de *F. tularensis.* Parmi ces gènes, on retrouve en quantité relativement importante des gènes reliés aux fonctions métaboliques et à la nutrition (Ahlund et al., 2010; Akimana et al., 2010; Asare et al., 2010a; Asare et al., 2010b; Lai et al., 2010; Meibom et al., 2010; Peng et al., 2010). Leur distribution est présentée dans la figure 18.

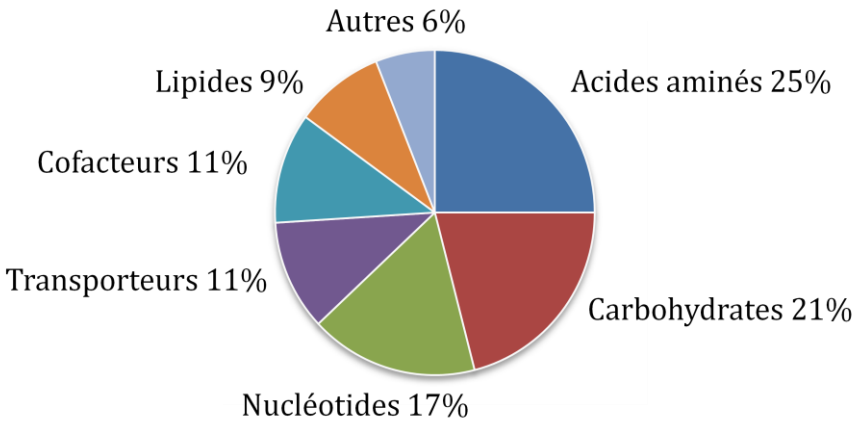

Figure 19 ***Classification fonctionnelle des gènes impliqués dans le métabolisme de Francisella tularensis ssp holarctica LVS (inspiré de Raghunathan et al., 2010).***

Ainsi, l'expression « virulence nutritionnelle » a été proposée récemment pour illustrer le rôle essentiel du métabolisme dans la virulence de *F. tularensis* (Santic et al., 2013).

Dans ce chapitre, nous allons présenter les différents besoins de la bactérie *F. tularensis* ainsi que la façon dont elle manipule l'hôte pour subvenir à ses besoins nutritionnels. Enfin, nous nous attacherons à décrire une famille de protéines qui constitue l'objet d'étude principal de ma thèse : les transporteurs d'acides aminés.

4.1 Besoins nutritionnels de *F. tularensis*

Au cours de l'évolution, les bactéries à multiplication intracellulaire ont développé un réseau métabolique dépendant du type d'hôte qu'elles infectent. Elles utilisent les acides aminés, les sucres et les lipides comme sources de carbone et d'azote, avec potentiellement une préférence pour les acides aminés (voir paragraphes suivants).

4.1.1 Les lipides

Très peu de données sont disponibles sur l'utilisation des lipides en tant que nutriments. Une seule étude parue récemment a démontré que *F. tularensis* utilisait les lipides en tant que source de nutriments au cours de l'infection macrophagique, en particulier après un temps long (24h d'infection) (Raghunathan et al., 2010). Cependant *F. tularensis* ne possède pas toutes les voies métaboliques nécessaires à l'utilisation de ces molécules. Par exemple il a été montré que la bactérie *S. enterica* était capable de générer du glyoxylate à partir de lipides (avec le glyoxylate shunt). Cette molécule a pour rôle d'alimenter le Cycle de Krebs pour revenir vers la néoglucogenèse (Fang et al., 2005). *F. tularensis* ne possède pas les enzymes particulières impliquées dans ce mécanisme. Il reste donc à expliquer pourquoi elle utilise si peu les lipides, et comment trouve-t-elle dans les autres molécules les ressources nécessaires pour répondre à ses besoins nutritionnels ?

4.1.2 Les sucres

On distingue trois voies métaboliques majeures concernant le glucose : la double voie glycolyse/néoglucogenèse (cf. figure 20), la voie des pentoses-phosphates et la voie Entner-Doudoroff. Il a été longtemps considéré que le glucose était la source de carbone principale de *F. tularensis*. En effet, il représente une source de carbone rapidement assimilable, utilisable immédiatement et qui fournit de l'énergie. Les études génétiques réalisées sur *F. tularensis* ont montré en particulier l'importance des enzymes inclues dans la voie de glycolyse/néoglucogenèse (Kraemer et al., 2009; Maier et al., 2007; Peng et al., 2010; Su et al., 2007; Weiss et al., 2007). Par exemple, un mutant délété du gène *pgm* codant pour la phosphoglucomutase et catalysant la conversion du glucose-1-phosphate en glucose-6-phosphate perd sa virulence (Weiss et al., 2007). De façon très surprenante, un mutant délété du gène *pckA* codant pour la phosphoénolpyruvate carboxykinase, et faisant donc le lien entre le Cycle de Krebs et la voie de la néoglucogenèse, ne montre aucun défaut de virulence dans un modèle murin (Kadzhaev et al., 2009). Enfin, des données très récentes de notre laboratoire (manuscrit en préparation) confirment l'importance de la gluconéogenèse dans la virulence de *F. tularensis*. En effet, un mutant délété du gène *glpX*, n'exprimant pas la

fructose-1,6-bisphosphatase et empêchant la néoglucogenèse, présente un sévère défaut de virulence *in vitro* et *in vivo* en absence de glucose. On peut donc imaginer que la néoglucogenèse pourrait être alimentée par des composés entrant en amont du Cycle de Krebs comme par exemple le glycérol.

Par ailleurs, une analyse transcriptomique de la souche *F. tularensis* ssp *tularensis* SCHU S4 dans des macrophages de moelle osseuse de souris a montré une augmentation significative des gènes impliqués dans le métabolisme des sucres et en particulier dans la double voie glycolyse/néoglucogenèse (Wehrly et al., 2009).

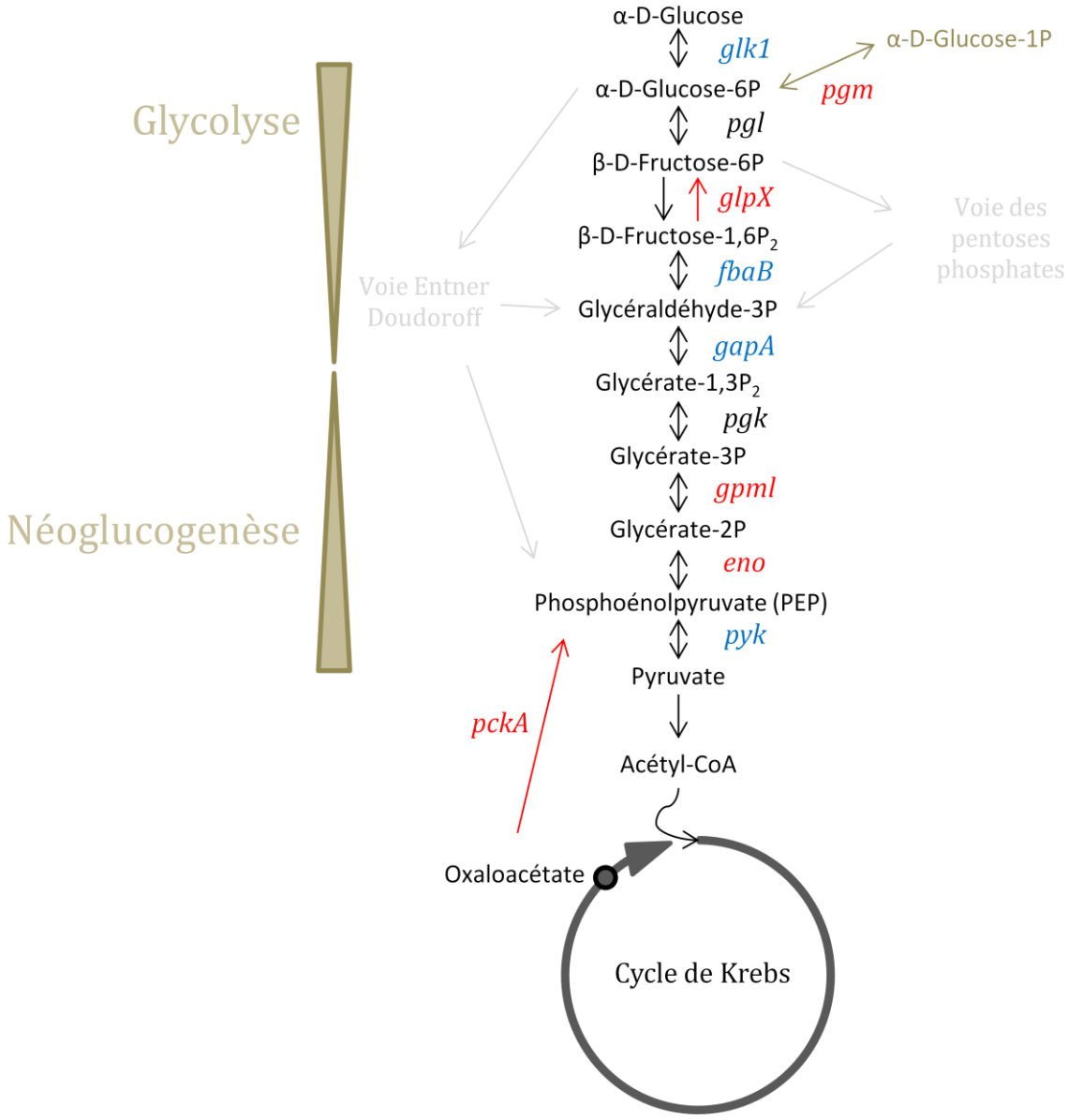

Figure 20 ***Voies de glycolyse et de néoglucogenèse chez F. tularensis, inspiré de (Meibom et al., 2010).***

A ce jour, aucun travail n'a encore mis en évidence l'importance des enzymes des voies des pentoses phosphates ou Entner-Doudoroff dans la virulence de *F. tularensis*.

4.1.3 Les acides aminés

La réalisation de nombreux cribles *in vitro* et *in vivo*, ainsi que les études *in silico* des génomes de *F. tularensis*, ont permis de mettre en évidence la présence ou l'absence des voies de biosynthèse des acides aminés de cette bactérie. Il a ainsi été démontré que *F. tularensis* était auxotrophe pour plusieurs acides aminés (aas). De façon opérationnelle, on parlera d' « auxotrophie » pour les aas qu'elle est obligée d'importer de l'extérieur pour se multiplier dans un milieu synthétique. Parmi ceux-ci, on distingue : i) les aas indispensables à la croissance de la bactérie, ils sont appelés « essentiels » et correspondent en général à l'inactivation des voies de biosynthèse correspondantes ; et ii) les aas qui permettent d'améliorer la croissance, ils sont appelés « utiles non essentiels ». On parle de « prototrophie » pour les aas que *F. tularensis* sait produire car elle possède les voies complètes de biosynthèse et qu'elle n'a pas besoin d'obtenir du milieu de culture pour se multiplier normalement. Ces aas sont dits « non essentiels ».

Dans la table ci-dessous sont présentés les auxotrophies et prototrophies de la bactérie *F. tularensis* ssp *novicida*.

Auxotrophie stricte (essentiel)	Auxotrophie limitée (utile non essentiel)	Prototrophie (non essentiel)
Arginine	Aspartate	Alanine
Cystéine	Isoleucine	Asparagine
Histidine	Leucine	Glutamate
Lysine	Proline	Glutamine
Méthionine	Sérine	Glycine
Tyrosine	Thréonine	Phénylalanine
	Valine	Tryptophane

Table 11 : Classification des acides-aminés en fonction de leur importance pour la croissance de* F. tularensis *ssp* novicida *en milieu synthétique.

On retrouve des différences d'auxotrophie entre les différentes sous-espèces. Les différences remarquables entre les sous-espèces *horlactica* et *novicida* que nous manipulons au laboratoire sont présentées dans la table 11. La connaissance de ces particularités métaboliques a permis de mettre au point un milieu minimum adapté du « milieu Chamberlain » (Chamberlain, 1965).

Acide aminé	*Francisella* ssp *holarctica* LVS	*Francisella* ssp *novicida*
Arginine	Oui	Oui

Asparagine	Non	Non
Aspartate	Oui	Oui
Cystéine	Oui	Oui
Glutamate	Non	Non
Glutamine	Non	Non
Glycine	Non	Non
Histidine	Oui	Oui
Leucine	Oui	Oui
Isoleucine	Oui	Oui
Lysine	Oui	Oui
Méthionine	Oui	Oui
Phénylalanine	Non	Non
Proline	Oui	Oui
Sérine	Oui	Oui
Thréonine	**Oui**	**Non**
Tryptophane	Non	Non
Tyrosine	Non	Non
Valine	**Oui**	**Non**

Table 12 : Liste des caractères essentiels des acides aminés

Même si on imagine un cytosol eucaryote riche en acides aminés, la cellule macrophagique a elle aussi ses particularités métaboliques. En effet, elle est auxotrophe pour l'histidine, l'isoleucine, la leucine, la lysine, la méthionine, la phénylalanine, le tryptophane, la valine et la thréonine (Price et al., 2014). De façon surprenante on retrouve parmi ces 9 aas l'histidine, la lysine et la méthionine pour lesquels *F. tularensis* est strictement auxotrophe et l'isoleucine, la leucine, la thréonine et la valine, pour lesquels elle présente une certaine auxotrophie. La concentration de tous ces aas est donc dépendante de la concentration du milieu extérieur est peut par conséquent atteindre des valeurs hautes comme basses. On peut donc imaginer que *F. tularensis* a acquis des transporteurs à très haute affinité vis-à-vis de ces aas pour s'adapter à ces concentrations.

Les acides aminés constituent une source nutritionnelle très intéressante car ils sont capables d'intégrer le cycle de Krebs (aussi appelé cycle du citrate ou cycle tricarboxylique) à différents niveaux. Cette voie métabolique est essentielle puisqu'elle constitue la source majeure d'énergie (ATP) pour la bactérie. Ce cycle est présenté sur la figure 21.

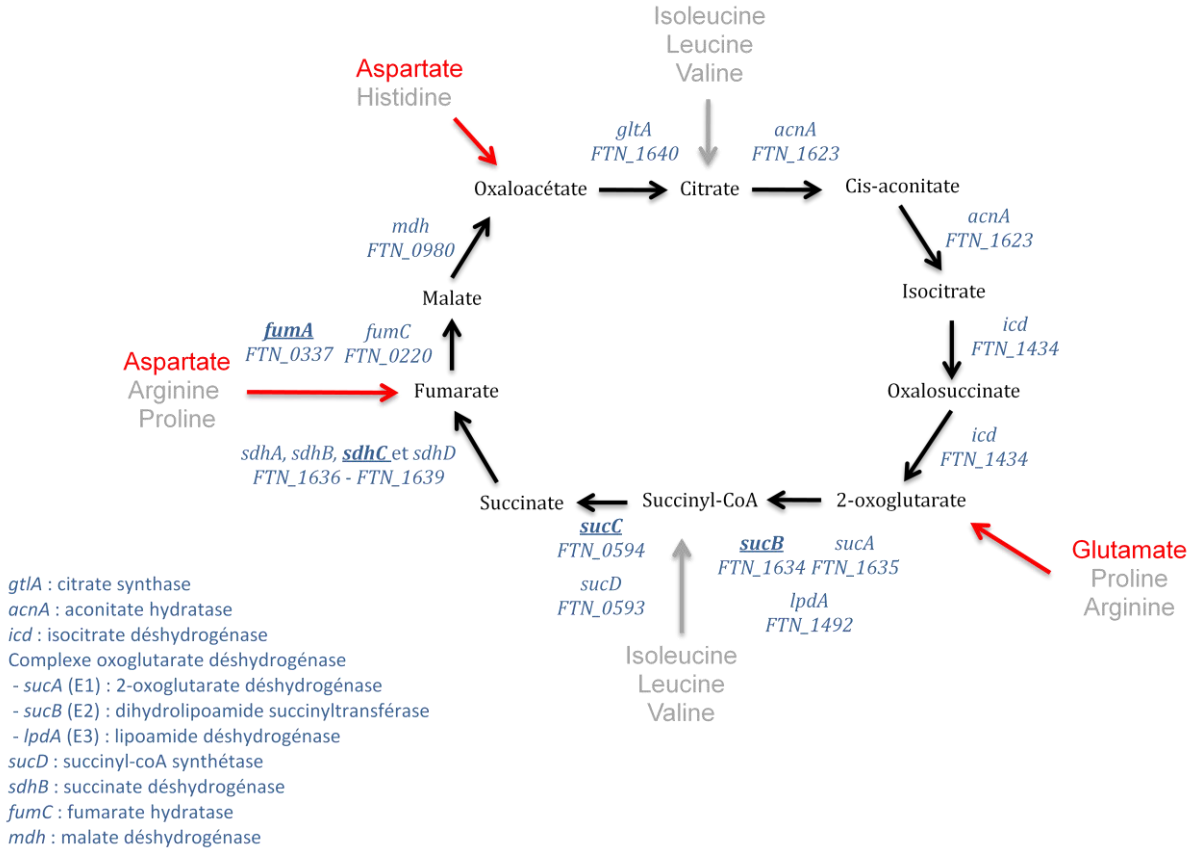

Figure 21 ***Cycle de Krebs.***
Les produits intermédiaires sont notés en noir, les enzymes en bleu. Les gènes ayant été identifiés dans des cribles génétiques comme jouant un rôle dans la pathogénicité de F. tularensis sont en gras. Chez les bactéries il existe de multiples points d'entrée dans le cycle de Krebs pour les aas.. Les acides aminés capables d'intégrer le Cycle de Krebs chez la souche novicida sont notés en rouge

Plusieurs études ont mis en évidence l'importance de ce cycle dans la virulence de *F. tularensis* (voir pour revue récente (Pechous et al., 2009)). La table 13 récapitule les gènes codant pour des enzymes du cycle de Krebs qui sont impliqués dans la pathogénicité de *F. tularensis* (voir également figure 21).

Numéro et nom du gène	Fonction	Modèle d'atténuation
FTN_0337, fumA	Fumarate hydrolase, classe 1	Cellules : J774.1, RAW, BMM Animaux : souris Balb/C
FTN_0594, sucC	Succinyl-coenzyme A synthétase	Cellules : RAW
FTN_1634, sucB	Dihydrolipoamide succinyltransférase, sous-unité n°2 de la 2-oxoglutarate déshydrogénase	Animaux : souris C57Bl/6J
FTN_1639, sdhC	Succinate déshydrogénase, cytochrome b556	Animaux : souris C57Bl/6J

Table 13 : Liste des gènes codant pour des enzymes du cycle de Krebs étant impliqués dans la virulence de F. tularensis ssp novicida. (inspiré de Pechous et al., 2009)

On distingue de nombreux points d'entrées des acides aminés dans le cycle de Krebs (figure 21). Des résultats obtenus au laboratoire (données non publiées) suggèrent que certains d'entre eux constitueraient des substrats neoglucogéniques.

4.2 Stratégies de survie mettant en jeu les acides aminés

Il a longtemps été considéré que le cytosol de la cellule hôte constituait un « paradis nutritionnel » pour toutes les bactéries à multiplication intracellulaire facultative. Depuis quelques années, cette théorie est remise en cause par différentes études indiquant que le milieu intracellulaire contient de nombreux éléments nécessaires à la croissance de ces bactéries mais qu'ils sont présents en conditions limitantes.

4.2.1 Utilisation des nutriments de l'hôte

Une étude réalisée dans notre laboratoire en 2009 a montré que *F. tularensis*, auxotrophe pour la cystéine, un acide aminé présent en quantité très limitée dans les cellules eucaryotes, importait et utilisait le glutathion de la cellule hôte pour constituer son propre pool de cystéine. En effet, le glutathion est un tri-peptide (L-γ-L-glutamyl-L-Cysteinyl-glycine) qui une fois métabolisé donne de la cystéine. En particulier, *F. tularensis* utilise une enzyme, la γ-glutamyl transpeptidase (gène *ggt*) pour cliver spécifiquement le glutathion. Un mutant inactivé pour le gène *ggt* est d'ailleurs incapable de se multiplier à l'intérieur des macrophages, en absence de supplémentation du milieu de culture par de la cystéine (Alkhuder et al., 2009).

4.2.2 Manipulation de l'hôte

Pour répondre à ses besoins, la bactérie a développé des stratégies de manipulation de l'hôte. A ce jour, deux études ont démontré comment *F. tularensis* utilisait à son avantage les réserves nutritionnelles de l'hôte. La première étude, réalisée au sein du laboratoire, a démontré que *F. tularensis* est capable d'augmenter l'expression d'un transporteur eucaryote, SLC1A5, responsable de l'entrée d'acides aminés neutres et en particulier de la glutamine (Barel et al., 2012). De façon très intéressante, ces travaux ont montré lors de l'infection à *F. tularensis* une diminution de la transcription du transporteur SLC7A5 identifié comme un exporteur de glutamine.

Une seconde étude, parue très récemment, a démontré que *F. tularensis* était capable de manipuler la voie canonique de l'autophagie de la cellule hôte dans le but de dégrader plus de protéines et d'avoir à disposition un pool plus important d'aas utilisables immédiatement (Steele et al., 2013).

4.3 Les systèmes d'acquisition des acides aminés de *F.tularensis*

La disponibilité en aas dans le phagosome et le cytosol de la cellule hôte n'a d'intérêt pour la bactérie que si elle possède des systèmes d'acquisition adaptés à ses besoins. *F. tularensis* possède un nombre important de transporteurs d'aas (Meibom et al., 2010) qu'on peut diviser en quatre sous-familles. On distingue tout d'abord les transporteurs actifs primaires ou ATP-dépendant, La deuxième grande famille correspond aux transporteurs dits « secondaires ». Elle constitue la famille la plus grande. On distingue encore la famille des canaux ioniques et une quatrième famille qui regroupe des transporteurs aux fonctions uniques et variées. Ces familles sont présentées dans la table 14 avec leurs sous-familles respectives.

Familles de transporteurs	Nombre total de transporteurs	Nombre de transporteurs ou de sous-unités identifiés dans des screens génétiques
Transporteurs actifs I^{aires}	48	25
Famille ABC	15	16 (sous-unités)
Famille F-ATPase	10	4
Famille IISP	2	1
Famille SSPTS	1	0
Transporteurs II^{aires}	100	50
Famille MFS	31	18
Famille APC	11	7
Famille POT	8	4
Famille HAAP	7	4
Autres familles	43	17
Canaux ioniques	6	4
Inclassables	4	2

Table 14 : Liste des familles et sous-familles de transporteurs d'acides aminés identifiés chez F. tularensis et nombre de protéines identifiées dans des screens génétiques (inspiré de Meibom et Charbit, 2010).

Nom	***Définition***
ABC	***ATP binding cassette superfamily***
F-ATPase	***H+ or Na+ translocating F-type, V-type and A-type ATPase superfamily***
IISP	***Type II (General) secretory pathway family***
SSPTS	***Sugar specific phosphotransferase system***
MFS	***Major facilitator superfamily***
APC	***Amino acid polyamine organocation family***
POT	***Proton dépendent oligopeptide transporter family***
HAAAP	***Hydroxy/aromatic amino acid perméase family***

4.3.1 Transporteurs actifs primaires

Les transporteurs actifs primaires ont la particularité d'hydrolyser une molécule d'ATP pour faire passer les nutriments à travers la membrane cytoplasmique. Ils comportent

les quatre sous-familles ABC, F-ATPase, IISP et SSPTS, indiquées dans table 14. La sous-famille ABC est la plus importante parmi les transporteurs actifs primaires. Elle comprend une perméase imbriquée dans la membrane, liée à une sous-unité cytoplasmique qui fixe l'ATP pour l'hydrolyser et une protéine affine du substrat, periplasmique pour les bactéries Gram-négatif. Il existe 15 systèmes complets chez *F. tularensis* ssp *tularensis* SCHU S4 qui sont dédiés à l'import (3), à l'export (5), à des processus autres que du transport (4) ou à des fonctions encore inconnues (3) (Atkins et al., 2006). *F. tularensis* a la particularité de présenter peu de transporteurs ABC. En effet, on en retrouve 37 chez la bactérie *L. pneumophila* et jusqu'à 69 chez *E. coli*.

Le seul transporteur ABC impliqué dans l'import d'acides aminés ayant été identifié de façon répétée dans des cribles génétiques, est un transporteur prédit de méthionine dont l'inactivation entraine un sévère défaut de multiplication *in vitro* (Maier et al., 2007) et de virulence *in vivo* (Kraemer et al., 2009; Su et al., 2007).

4.3.2 Transporteurs secondaires

Les transporteurs secondaires sont dépendants soit de la différence de potentiel électrochimique soit de la différence de concentration des différentes molécules pour fonctionner. Ils constituent la plus grande famille de transporteurs chez *F. tularensis.* Celle-ci est divisée en quatre sous-familles bien identifiées et une cinquième dans laquelle on retrouve toutes les autres protéines aux fonctions uniques ou très peu représentées (cf table 14). Les transporteurs MFS (31 protéines) représentent la plus importante sous-famille. Ils jouent un rôle dans l'import ou l'export de molécules de nature très variée (aas, carbohydrates, antibiotiques…). La deuxième sous-famille la plus représentée correspond aux transporteurs APC, au nombre de 11. Ils sont prédits pour permettre l'antiport d'aas tels que glutamate/GABA ou le symport d'un acide aminé aromatique avec un proton. On distingue également la sous-famille POT qui comprend 8 transporteurs de dipeptide, tripeptide ou oligopeptide. Parmi eux, 4 ont été identifiés dans les mêmes cribles. Enfin, la sous-famille HAAAP comprend 7 transporteurs d'acides aminés, dont 4 ont été identifiés dans des cribles génétiques, et qui jouent un rôle dans le transport d'acides aminés aromatiques, de sérine ou de tyrosine.

L'importance des transporteurs secondaires dans la virulence de *F. tularensis* a été mise en évidence au travers de nombreux cribles génétiques décrits dans le paragraphe précédent, en particulier pour les sous-familles MFS (18/31 protéines) et APC (8/11 protéines) (cf table 14).

Pour toutes ces raisons, notre laboratoire a choisi de s'intéresser tout particulièrement au rôle de ces deux sous-familles dans le cycle infectieux de cette bactérie.

4.4 Stress oxydant, métabolisme et virulence

Le cycle de Krebs joue un rôle essentiel chez tous les organismes aérobies. Notamment, plusieurs enzymes ont été identifiées comme permettant la réduction des ERO.

- L'activité enzymatique de l'aconitase semble contribuer de façon majeure aux défenses contre le stress oxydant, en particulier chez *S. typhimurium*. On distingue deux aconitases appelées AcnA et AcnB qui ont des rôles physiologiques distincts (Bradbury et al., 1996; Cunningham et al., 1997). AcnB est activée de façon constitutive à l'inverse de l'enzyme AcnA qui est activée seulement en phase stationnaire. AcnB joue le rôle le plus important dans le cycle de Krebs. Cette protéine possède un centre $[4Fe\text{-}4S]^{2+}$ sensible au stress oxydant et qui, lorsqu'il est oxydé, lui permet de passer d'un rôle d'enzyme à un rôle de régulateur transcriptionnel. On parle alors de la molécule Apo-AcnB. On assiste dans ce cas à l'initiation d'une cascade de régulation où Apo-AcnB va diminuer la synthèse de la molécule FTsH, provoquant successivement l'augmentation de la quantité de facteur σ32 s'expliquant par une diminution de sa dégradation, puis une augmentation de la production de DnaK, une chaperonne qui stabilise les protéines affectées par le stress oxydant (Tang et al., 2004).
- La production de nicotinamide adénine dinucléotide phosphate (NADPH) constitue aussi une aide précieuse pour la neutralisation des ERO (Singh et al., 2007). En effet cette molécule permet le retour à l'état réduit du glutathion et de la thiorédoxine oxydés. Ainsi, un grand nombre d'enzymes générant du NADPH (et un proton H^+) appartiennent au cycle de Krebs ou ont un lien plus ou moins directe avec celui-ci. Parmi elles, on distingue l'isocitrate déshydrogénase (Icd), l'enzyme malique (ME), la glucose-6-phosphate déshydrogénase (G_6PDH), la 6-phosphogluconate déshydrogénase (6-PGDH), l'aldéhyde déshydrogénase (ADH) et la glutamate déshydrogénase (GDH) (Pollak et al., 2007; Singh et al., 2007).

Enfin, plusieurs articles ont établi un lien entre la présence des acides aminés et la résistance au stress oxydant, soit parce qu'ils : i) sont transformés en glutathion (glutamine et glutamate) ; ii) mènent à la production de NADPH,H+ (glutamate) ; iii) protègent de façon indirecte en passant par une neutralisation du pH (arginine) ; iv) détournent les ERO (méthionine) ; v) ou encore intégrant le cycle de Krebs par métabolisation (histidine, arginine,

proline et glutamine qui deviennent du glutamate). Ces travaux sont regroupés dans la table 15.

Acide aminé impliqué	Bactérie	Article
Histidine	*Pseudomonas fluorescens*	(Lemire et al., 2010)
Glutamate	*Pseudomonas fluorescens* *L. monocytogenes*	(Mailloux et al., 2009) (Feehily et al., 2013)
Arginine	*E.coli*	(Bearson et al., 2009)
Méthionine	*E.coli*	(Luo et al., 2009)
Glutamine	*E.coli*	(Amores-Sanchez et al., 1999)

Table 15 : Articles proposant un rôle aux acides-aminés dans la résistance au stress oxydant.

Chapitre II

Résultats, perspectives et conclusion

I. Résultats expérimentaux

Lors de l'infection d'un hôte mammifère, *F. tularensis* peut aussi bien résider à l'intérieur des cellules hôtes et se propager de cellule en cellule qu'être libre dans des fluides type sang, système lymphatique, etc… *In vivo*, *F. tularensis* infecte préférentiellement les macrophages. Comme de nombreuses bactéries à multiplication intracellulaire cytosolique, après être entrée en contact avec la membrane plasmique de la cellule, *F. tularensis* est internalisée dans une vacuole phagosomale d'où elle réussit à s'échapper rapidement, entre 30 et 60 minutes (Chong et al., 2010; Golovliov et al., 1997). Elle atteint alors le cytosol où elle se multiplie et induit la mort cellulaire de son hôte, son seul moyen de dissémination vers les cellules et tissus adjacents.

Ainsi, **la facilité de *F. tularensis* à s'échapper rapidement du phagosome va déterminer sa capacité à se multiplier efficacement dans le cytosol.**

L'acquisition de nutriments *in vivo* constitue l'un des aspects fondamentaux de la virulence des bactéries à multiplication intracellulaire. En effet, plusieurs études basées sur le criblage de banques de mutants de *F. tularensis* (Kraemer et al., 2009; Maier et al., 2007; Peng et al., 2010; Weiss et al., 2007) ont permis d'identifier de nombreux gènes (>10% du génome bactérien) potentiellement impliqués dans la virulence de cette bactérie. De façon remarquable, parmi les gènes candidats identifiés, on retrouve de nombreux gènes appartenant à la famille des transporteurs secondaires traduisant l'importance des mécanismes d'acquisition de nutriments dans la pathogénèse microbienne. Ainsi, nous avons choisi de nous intéresser à une famille de gènes déterminant des transporteurs d'acides aminés appartenant à la sous-famille des transporteurs APC. Notre objectif a été de comprendre l'importance de ces transporteurs dans la pathogénicité de *F. tularensis*.

Article n°1

Glutamate Utilization Couples Oxidative Stress Defense and the Tricarboxylic Acid Cycle in *Francisella* Phagosomal Escape

Elodie Ramond, Gael Gesbert, Mélanie Rigard, Julien Dairou, Marion Dupuis, Iharilalao Dubail, Karin Meibom, Thomas Henry, Monique Barel et Alain Charbit.

Parmi les onze membres de la famille APC, huit d'entre eux ont été identifiés dans des études génétiques Dans un premier temps, nous nous sommes intéressés à un transporteur revenant régulièrement parmi les différentes études dédiées : le transporteur prédit d'acides aminés codé par le gène *FTN_0571*, appelé par la suite GadC. Ce transporteur GadC a été identifié quatre fois soit chez *F.tularensis* ssp *holarctica* (Maier et al., 2007), soit chez *F .tularensis* ssp *novicida* (Kraemer et al., 2009; Peng et al., 2010; Weiss et al., 2007).

Nos travaux ont permis de montrer que l'inactivation du transporteur GadC, un membre de la famille des échangeurs glutamate:γ-aminobutyrate, conduisait à une réduction drastique de la multiplication intracellulaire dans les macrophages et à une atténuation sévère de la virulence dans le modèle murin. Nous démontrons que le gène *gadC* est essentiel pour l'échappement phagosomal de *F. tularensis* et plus particulièrement pour la défense contre le stress oxydant. En effet, le mutant *gadC* présente une sensibilité accrue au stress oxydant *in vitro* et un défaut de contrôle des espèces réactives de l'oxygène (ERO) générées dans les phagosomes de cellules infectées. De façon remarquable, la virulence du mutant *gadC* est rétablie dans des modèles *in vitro* et *in vivo* incapables de générer des ERO au niveau phagosomal ($gp91^{phox-/-}$). Enfin, nous résultats montrent que l'activité du transporteur GadC modifie l'expression des gènes métaboliques du cycle de Krebs et la production de ses intermédiaires, ce qui pourrait expliquer les observations précédentes.

Ce travail constitue la première démonstration de l'importance d'un transporteur d'acide aminé dans la phase précoce de l'infection de *F. tularensis*.

OPEN ACCESS Freely available online

PLOS | PATHOGENS

Glutamate Utilization Couples Oxidative Stress Defense and the Tricarboxylic Acid Cycle in *Francisella* Phagosomal Escape

Elodie Ramond[1,2], Gael Gesbert[1,2], Mélanie Rigard[3,4], Julien Dairou[5], Marion Dupuis[1,2], Iharilalao Dubail[1,2], Karin Meibom[1,2], Thomas Henry[3,4], Monique Barel[1,2], Alain Charbit[1,2]*

1 Université Paris Descartes, Sorbonne Paris Cité, Bâtiment Leriche, Paris, France, **2** INSERM, U1002, Unité de Pathogénie des Infections Systémiques, Paris, France, **3** Centre international de recherche en infectiologie, Université de Lyon, Lyon, France, **4** Bacterial Pathogenesis and Innate Immunity Laboratory, INSERM U851 "Immunity, Infection and Vaccination", Lyon, France, **5** Platform "Bioprofiler" Université Paris Diderot, Paris, France

Abstract

Intracellular bacterial pathogens have developed a variety of strategies to avoid degradation by the host innate immune defense mechanisms triggered upon phagocytocis. Upon infection of mammalian host cells, the intracellular pathogen *Francisella* replicates exclusively in the cytosolic compartment. Hence, its ability to escape rapidly from the phagosomal compartment is critical for its pathogenicity. Here, we show for the first time that a glutamate transporter of *Francisella* (here designated GadC) is critical for oxidative stress defense in the phagosome, thus impairing intra-macrophage multiplication and virulence in the mouse model. The *gadC* mutant failed to efficiently neutralize the production of reactive oxygen species. Remarkably, virulence of the *gadC* mutant was partially restored in mice defective in NADPH oxidase activity. The data presented highlight links between glutamate uptake, oxidative stress defense, the tricarboxylic acid cycle and phagosomal escape. This is the first report establishing the role of an amino acid transporter in the early stage of the *Francisella* intracellular lifecycle.

Citation: Ramond E, Gesbert G, Rigard M, Dairou J, Dupuis M, et al. (2014) Glutamate Utilization Couples Oxidative Stress Defense and the Tricarboxylic Acid Cycle in *Francisella* Phagosomal Escape. PLoS Pathog 10(1): e1003893. doi:10.1371/journal.ppat.1003893

Editor: David Weiss, Emory University School of Medicine, United States of America

Received July 1, 2013; **Accepted** December 5, 2013; **Published** January 16, 2014

Funding: These studies were supported by INSERM, CNRS and Université Paris Descartes Paris Cité Sorbonne. Elodie Ramond was funded by a fellowship from the "Région Ile de France" and Gael Gesbert by a fellowship from the "Délégation Générale à l'Armement" (DGA). The funders had no role in study design, data collection and analysis, decision to publish, or preparation of the manuscript.

Competing Interests: The authors have declared that no competing interests exist.

* E-mail: alain.charbit@inserm.fr

Introduction

Francisella tularensis is a Gram-negative bacterium causing the disease tularemia in a large number of animal species. This highly infectious bacterial pathogen can be transmitted to humans in numerous ways [1], including direct contact with sick animals, inhalation, ingestion of contaminated water or food, or by bites from ticks, mosquitoes or flies. Four different subspecies (subsp.) of *F. tularensis* that differ in virulence and geographic distribution exist, designated subsps. *tularensis*, *holarctica*, *mediasiatica* and *novicida*, respectively. The *tularensis* subspecies is the most virulent causing a severe disease in humans [2,3]. *F. tularensis* subsp. *novicida* (*F. novicida*) is rarely pathogenic to non-immuno-compromized humans but is fully virulent for mice and is therefore widely used as a model to study *Francisella* intracellular parasitism.

F. novicida has the capacity to evade host defenses and to replicate to high numbers within the cytosol of eukaryotic cells [4]. The bacterium is able to enter and to replicate inside a variety of cells, and in particular in macrophages. After a transient passage through a phagosomal compartment, bacteria are released within 30–60 minutes in the host cell cytosol where they undergo several rounds of active replication [1]. Upon *Francisella* entry into macrophages, the phagosomal compartment transiently acidifies and the activation of NADPH oxidase leads to the production of noxious oxygen reactive species [5]. Although several genes required for phagosomal escape have been identified ([6,7] and references therein), the molecular mechanisms underlying this complex process are still very poorly understood.

Protection against oxidative stress includes the production of anti-oxidant molecules (such as glutathione and NADPH) and of enzymes (such as catalases, superoxide dismutases glutaredoxin-related protein and alkylhydroperoxide reductases). *Francisella* subspecies encode a whole set of such oxidative stress-related enzymes [8]. Inactivation of the corresponding genes generally leads to increased sensitivity to oxidative stress, defective intracellular multiplication, and attenuated virulence [9,10,11]. Protection against oxidative and other stress also involves a number of dedicated protein chaperones and chaperone complexes [12].

In contrast, the importance of acid-resistance mechanisms in *Francisella* intracellular survival remains controversial [13,14,15] and their possible contribution to pathogenesis still largely unknown. One of the best characterized acid-resistance systems in bacteria couples the glutamate:γ-aminobutyrate exchanger GadC with the glutamate decarboxylase(s) GadA and/or GadB [16]. The decarboxylase replaces the α-carboxyl group of its amino acid substrate with a proton that is consumed from the cytoplasmic pool [17]. The capacity to produce γ-aminobutyric

Author Summary

Intracellular bacterial pathogens have developed a variety of strategies to avoid degradation by the host innate immune defense mechanisms triggered upon phagocytocis. We show here for the first time that glutamate acquisition is essential for phagosomal escape and virulence of an intracellular pathogen. Remarkably, inactivation of the glutamate transporter GadC of *Francisella* impaired the capacity of the bacterium to neutralize reactive oxygen species (ROS) production in the phagosome. Virulence of the *gadC* mutant was partially restored in mice with a defective NADPH oxidase. Importantly, we found that impaired glutamate uptake affected the production of tricarboxylic acid (TCA) cycle intermediates, highlighting novel links between the TCA cycle and bacterial phagosomal escape. Amino acid transporters are, thus, likely to constitute underscored players in microbial intracellular parasitism.

acid (GABA) through glutamate decarboxylation has been observed in both Gram-negative and Gram-positive bacteria. The GadC/GadB glutamate decarboxylase (GAD) system has been shown to play an essential role in acid tolerance in food-borne bacterial pathogens that must survive the potentially lethal acidic environments of the stomach before reaching the intestine. Some bacteria possess a unique permease-decarboxylase pair whereas others, like *Listeria monocytogenes* [18], encode several paralogues of each component.

Recent genome sequence analyses and genome-scale genetic studies suggest that an important proportion of genes related to metabolic and nutritional functions participate to *Francisella* virulence [19]. However, the relationship between nutrition and the *in vivo* life cycle of *F. tularensis* remain poorly understood. *Francisella* is predicted to possess numerous nutrient uptake systems to capture its necessary host-derived nutrients, some of which are probably available in limiting concentrations. Notably, we showed very recently that an asparagine transporter of the major facilitator superfamily of transporters was specifically required for cytoslic multiplication of *Francisella* and its systemic dissemination [20].

The amino acid-polyamine-organocation family of transporters (APC) is specifically involved in amino acid transport [19]. Remarkably, eight of the 11 APC members have been identified at least once in earlier genetic studies, and are likely to be involved in bacterial virulence. In particular, the gene encoding the GadC permease has been identified in several different genome-wide screens, performed in either *F. tularensis* subsp. *holarctica* [21] or *F. novicida* [22,23,24].

In the present work, we elucidate the functional role of the GadC protein in *Francisella* pathogenesis. We show that glutamate uptake plays a critical role in *Francisella* oxidative stress defense in the phagosomal compartment. Strikingly, the activity of GadC influences the expression of metabolic genes and the production of tricarboxylic acid (TCA) cycle intermediates, unraveling a relationship between oxidative stress defense, metabolism and *Francisella* virulence.

Results

The Gad system of *Francisella*

F. tularensis subspecies possess a unique putative GAD system, composed of the antiporter GadC and a decarboxylase GadB (encoded by genes *FTN_0571* and *FTN_1701* in *F. novicida* and hereafter designated *gadC* and *gadB*, respectively for simplification) (**Figure S1A**). The transcription of *gadC* is initiated 27 nucleotides upstream of the translational start from a predicted σ^{70} promoter (**Figure S1B**). This genetic organization is highly conserved in all the available *F. tularensis* genomes (not shown). The gene *gadC* encodes a protein of 469 amino acids sharing 98.7%, 99.1% and 99.6% identity with its orthologues in the subspecies *mediasiatica* (*FTM_*1423), *holartica* (*FTL_1583*) and *tularensis* (*FTT_0480c*), respectively.

The *Francisella* GadC protein is predicted as a putative glutamate:γ-aminobutyric acid (GAD) antiporter (KEGG database). Although it shows only modest homology (approximately 25% amino acid identity) with GadC of *E. coli* [25], secondary structure prediction (using the method for prediction of transmembrane helices HMM available at the internet site www.cbs.dtu.dk) indicates that the GadC transporter of *Francisella* also comprises 12 transmembrane helixes and has its N and C-terminal ends facing the cytoplasm (not shown).

The *gadB* gene encodes a putative glutamate decarboxylase protein of 448 amino acid residues that is highly conserved in *F. tularensis* subsp. *tularensis* (98.7% amino acid identity with FTT_1722c). However, the corresponding protein is truncated at its C-terminal end in the subspecies *holarctica* (FTL_1863) and *mediasiatica* (FTM_1673, and noted as a pseudogene in the KEGG database).

Role of GadC in bacterial intracellular multiplication and virulence

We constructed a strain with chromosomal deletion of the entire *gadC* gene in *F. novicida* by allelic replacement [26]. We confirmed that the Δ*gadC* mutation did not have any polar effect on the downstream gene *FTN_0570* by quantitative qRT-PCR (**Figure S1C**). The growth kinetics of the parental *F. novicida* strain and the Δ*gadC* mutant were indistinguishable in tryptic soya broth (TSB) and chemically defined medium (CDM) [27] liquid media at 37°C (**Figure S2**), indicating that inactivation of *gadC* had no impact on bacterial growth in broth.

We examined the ability of wild-type *F. novicida*, the Δ*gadC* mutant and a Δ*gadC* mutant strain complemented with a plasmid-encoded copy of wild-type *gadC*, to survive in murine and human macrophage cell lines and primary bone marrow-derived mouse macrophages, over a 24 h-period. The Δ*gadC* mutant showed a severe growth defect in J774.1 cells, comparable to that of a mutant deleted of the entire *Francisella* pathogenicity island (Δ*FPI* mutant), with more than a 30-fold reduction of intracellular bacteria after 10 h and a 1,000-fold reduction after 24 h (**Figure 1A**). Impaired multiplication of the Δ*gadC* mutant was also observed in THP-1 macrophages (**Figure 1B**) as well as in bone marrow-derived macrophages (**Figure 1C**). In all cell types tested, introduction of the complementing plasmid (pKK-*gadC*) restored bacterial viability to same level as in the wild-type parent, confirming the specific involvement of the *gadC* gene in intracellular survival.

Next, *in vivo* competition assays in BALB/c mice were performed to determine if the GadC protein played a role in the ability of *Francisella* to cause disease. Five mice (6- to 8-week old) were inoculated by the intraperitoneal (i.p.) route with a 1:1 mixture of wild-type *F. novicida* and Δ*gadC* mutant strains. Bacterial multiplication in the liver and spleen was monitored at day 2 post-infection (**Figure 1D**). The Competition Index (CI), calculated for both organs, was extremely low (10^{-6}) demonstrating that the gene *gadC* played an essential role in *Francisella* virulence in the mouse model.

Upon *Francisella* entry into cells, *Francisella* initially resides in a phagosomal compartment that transiently acidifies and that

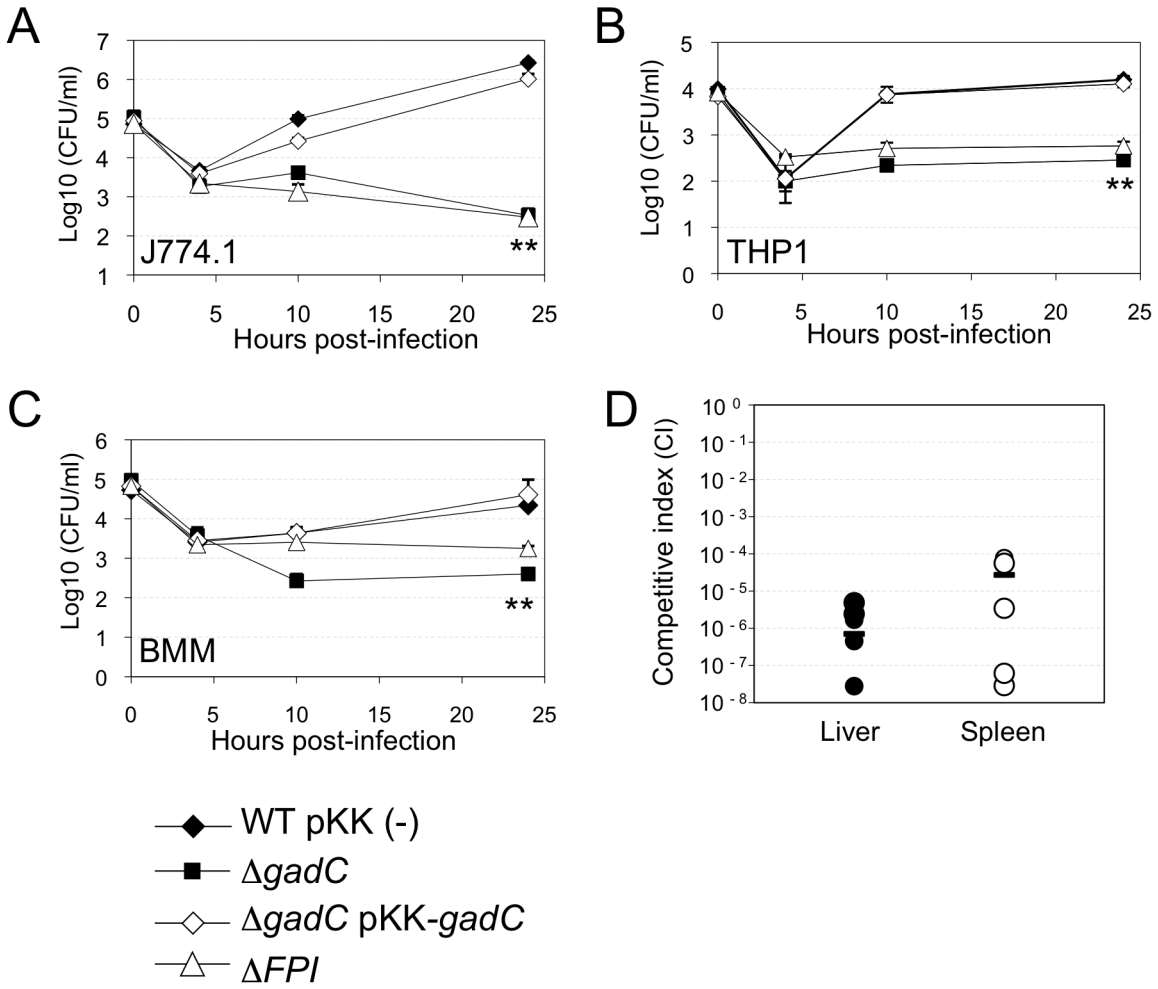

Figure 1. *gadC* inactivation affects intracellular survival and virulence. Intracellular replication of wild-type *F. novicida* (WT) carrying the empty plasmid pKK214 (WT/pKK(−)), of the *ΔgadC* mutant (Δ*gadC*) and complemented strain (Δ*gadC*/pKK-*gadC*), and of the Δ*FPI* mutant (Δ*FPI*), was monitored in J774.1 macrophage-like cells (**A**); in THP-1 human macrophages (**B**); and in bone marrow-derived macrophages (**C**), over a 24 h-period. Results are shown as the average of $\log_{10}$ cfu mL^{-1} ± standard deviation. Each experiment was performed in triplicate. **, $p<0.01$ (as determined by the Student's *t*-test). Competition assays (**D**). A group of five female BALB/c mice were infected i.p. with a 1:1 mixture of wild-type *F. novicida* and Δ*gadC* mutant strains (100 colony forming units (cfu) of each). The data represent the competitive index (CI) value for cfu of mutant/wild-type in the liver (L: black diamonds, left column) and spleen (S: black circles, right column) of each mouse, 48 h after infection. Bars represent the geometric mean CI value.
doi:10.1371/journal.ppat.1003893.g001

acquires reactive oxygen species. We therefore examined the ability of wild-type and Δ*gadC* mutant strains to survive under acid or oxidative stress conditions. For this, bacteria were exposed either to pH 5.5 or to 500 µM H_2O_2 (**Figure 2**). Under the pH condition tested, the viability of two strains was unaffected (**Figure 2A**). It should be noted that at the lower pH of 2.5, the viability of both wild-type and Δ*gadC* mutant was equally reduced (approximately 2 logs, not shown). In contrast, the Δ*gadC* mutant strain appeared to be significantly more sensitive to oxidative stress than the wild-type strain in TSB (**Figure 2B**). After 40 min of exposure, it showed a 10-fold decrease in the number of viable bacteria and an approximately 50-fold decrease after 60 min of exposure to H_2O_2. Remarkably, in CDM, the wild-type and Δ*gadC* mutant strains were equally sensitive to H_2O_2 in the absence of glutamate supplementation (**Figure 2C**). However, upon glutamate supplementation, the wild-type strain showed increased resistance to H_2O_2 whereas the Δ*gadC* strain was unaffected (**Figure 2D**).

GadC is involved in phagosomal escape

Confocal and electron microscopy analyses demonstrated that the Δ*gadC* mutant had lost the capacity to escape from the phagosomal compartment of infected macrophages.

Confocal microscopy. We used the differential solubilization process previously described [28] to follow the sub-cellular localization of the Δ*gadC* mutant in infected cells (**Figure 3A**). Briefly, the plasma membrane was selectively permeabilized with digitonin. This treatment allowed the detection of cytoplasmic bacteria and proteins. Subsequent treatment with saponin rendered intact phagosomes accessible to antibodies and allowed the detection of intra-phagosomal bacteria. Intracellular localization of the bacteria or LAMP-1 (used as a specific marker of phagosomes) was analyzed using specific antibodies and their co-localization was quantified with the Image J software (**Figure 3B**). Merging of LAMP-1 and bacteria was obtained at all three 3 time-point tested in cells infected with the Δ*gadC* or Δ*FPI* mutant strains. With both mutants, bacterial co-localization with LAMP-1

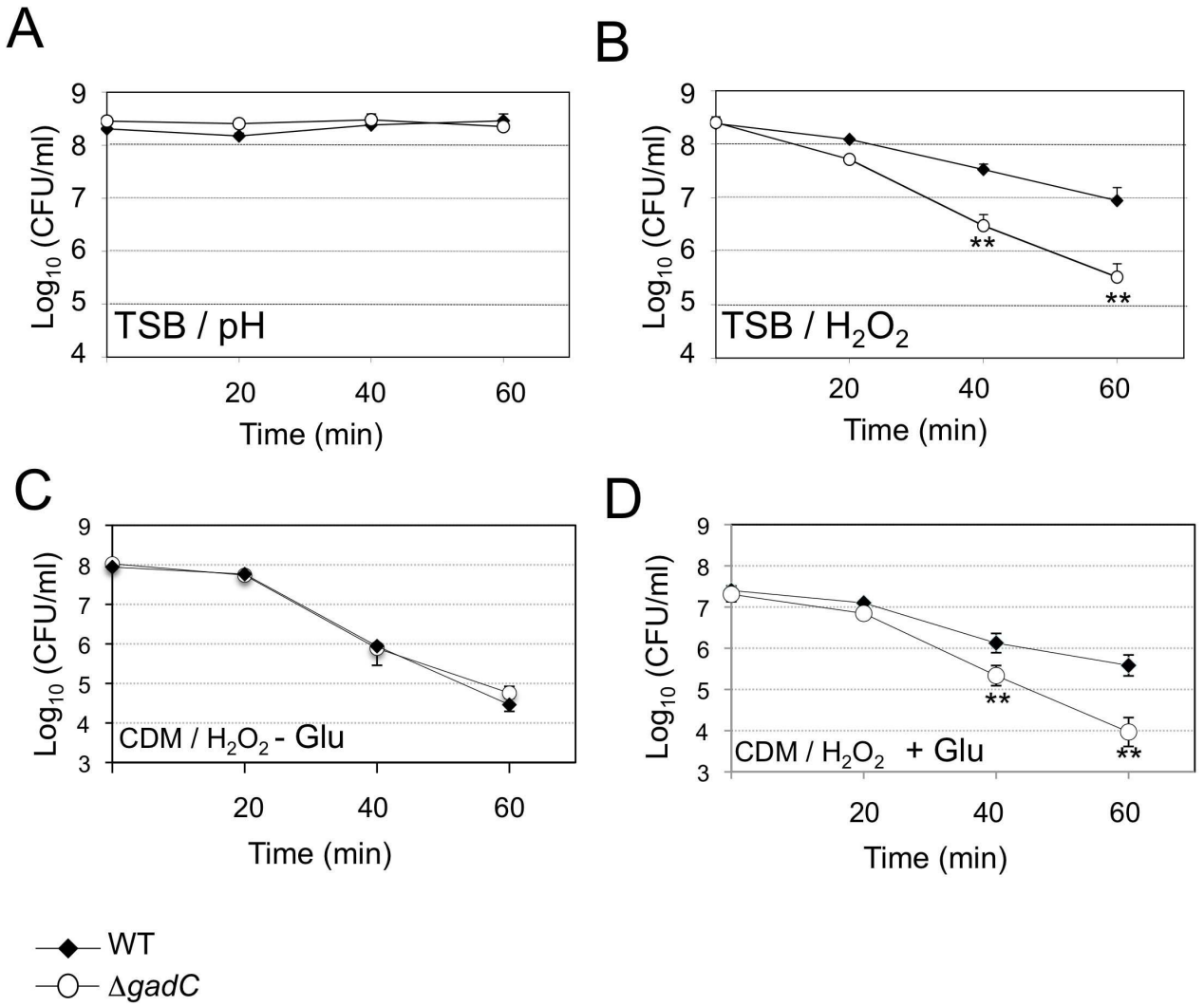

Figure 2. Stress sensitivity. Exponential phase bacteria, diluted in TSB medium, were subjected: (**A**) to acidic stress (pH 5.5), or (**B**) to oxidative stress (500 μM H_20_2). Exponential phase bacteria, diluted in chemically defined medium (CDM) (**C**), or CDM supplemented with 1 mM glutamate (**D**), were subjected to oxidative stress (500 μM H_20_2). The bacteria were plated on chocolate agar plates at different times and viable bacteria were monitored 2 days after. Data are the average *cfu* mL^{-1} for three points. Experiments were realized twice. **, $p<0.01$ (as determined by the Student's *t*-test).
doi:10.1371/journal.ppat.1003893.g002

was elevated (70% and 74%, with Δ*gadC* and Δ*FPI*; respectively) after 1 h and remained very high after 4 h (75% and 64% with Δ*gadC* and Δ*FPI*; respectively) and after 10 h (63% and 64% with Δ*gadC* and Δ*FPI*; respectively). In contrast, co-localization of the wild-type strain with LAMP-1 was only around 24% after 1 h and remained in the same range throughout the infection (20% and 22%, after 4 h and 10 h, respectively). These results strongly suggest that the Δ*gadC* mutant is still trapped in the phagosomal compartment after 10 h, as the Δ*FPI* mutant, whereas the wild-type strain has already escaped into the cytosol after 1 h.

Electron microscopy. To confirm this result, we performed thin section electron microscopy of J774.1 cells infected either with wild-type *F. novicida* or with the Δ*gadC* mutant (**Figure 3C**). As expected, significant bacterial replication was observed in the cytosol of most infected cells 10 h post-infection with wild-type *F. novicida* whereas bacterial multiplication was severely impaired in cells infected with the Δ*gadC* mutant. Furthermore, mutant bacteria surrounded by intact phagosomal membrane were still observed after 10 h of infection.

Bacterial death. We then determined whether the Δ*gadC* mutant bacteria, trapped in the phagosomal compartment of J774.1 macrophages, remained alive. For this, bacteria were subjected to an intracellular viability assay [29]. As illustrated in **Figure 3D** and quantified (**Figure 3E**), the majority of the replication-deficient Δ*gadC* mutant bacteria (>85%) were alive after 10 h of infection.

Infection of murine bone marrow derived macrophages (BMM) with wild-type *F. novicida* results in activation of the AIM2 inflammasome and pyroptosis [30,31,32], which can be monitored by real time incorporation of the membrane-impermeable dye propidium iodide [33]. Therefore, we compared the cell death kinetics of BMM infected either with the wild-type strain or with the Δ*gadC* mutant. As previously shown [33], infection with wild-type *F. novicida* triggered macrophage death after 6–8 h, while infection with the vacuolar mutant (Δ*FPI* mutant) had no effect on cellular viability during the time frame of the experiment. In agreement with its inability to escape from the vacuole and to replicate within host cell, the Δ*gadC* mutant behaved as a Δ*FPI* mutant and was unable to trigger host cell death (**Figure S3**).

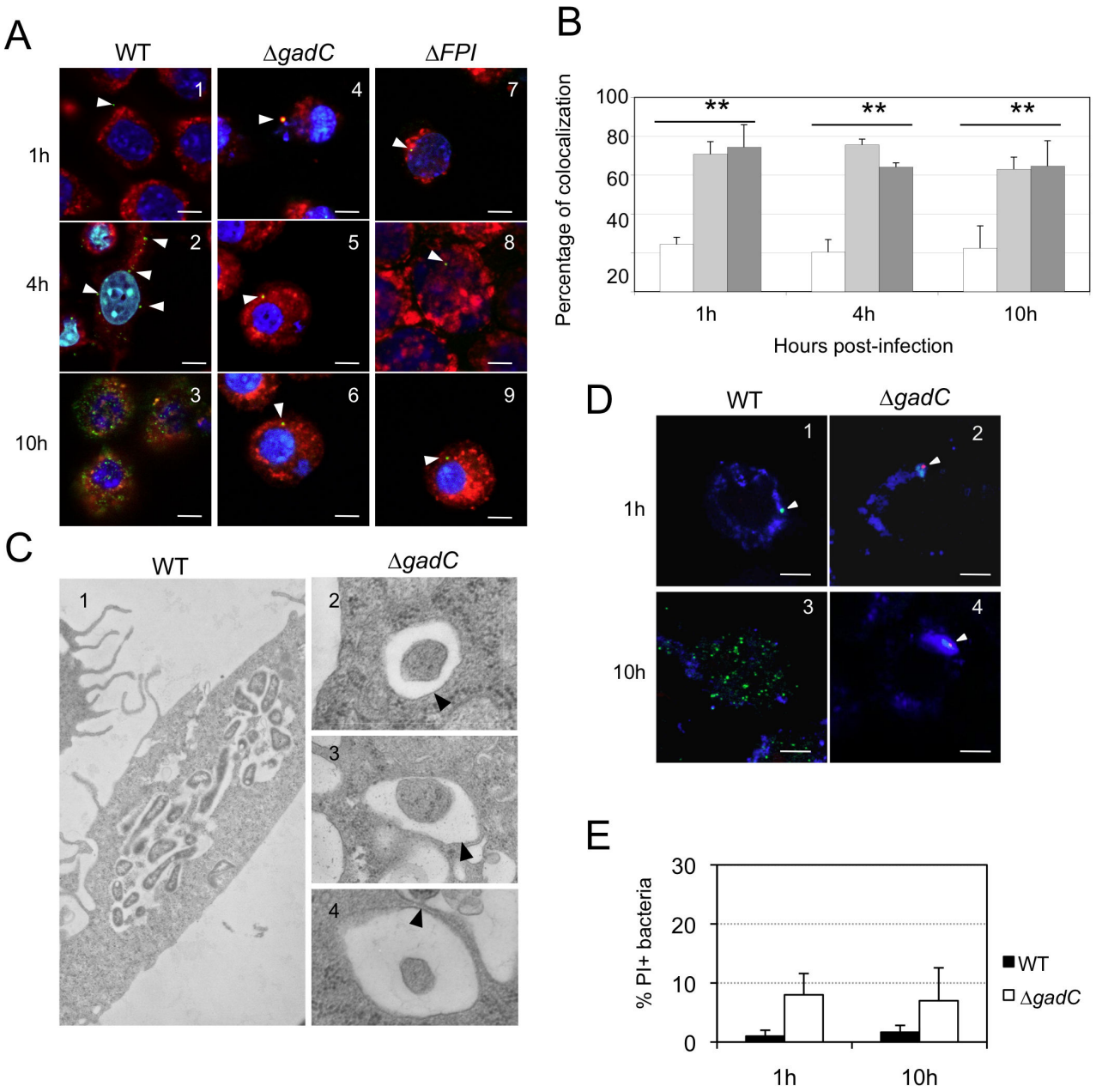

Figure 3. Subcellular localization of the Δ*gadC* mutant. (**A**) Co-localization of wild-type *F. novicida* (**1, 2, 3**), Δ*gadC* (**4, 5, 6**) or Δ*FPI* mutant strain (**7, 8, 9**) with LAMP-1 was monitored by confocal microscopy, in J774.1 macrophage cells. Co-localization was monitored at 1 h (**1, 4, 7**), 4 h (**2, 5, 8**) and 10 h (**3, 6, 9**). Anti-*Francisella* antibody was used at a final dilution of 1:500 and is shown in green. Anti-LAMP-1 antibody was used at a final dilution of 1:100 and is shown in red. White arrowheads point to individual bacteria. Cell nuclei were labeled with DAPI (in blue). The images are representative from triplicate coverslips in three independent experiments. Scale bars at the bottom right of each panel correspond to 10 μM. (**B**) Quantification of co-localization between bacteria and LAMP-1 was obtained with Image J software. The graph results from the analysis of 4 different fields for each time of infection, in three independent experiments. **, $p<0.01$ (as determined by the Student's *t*-test). White bars, *F. novicida* U112 (WT); light grey bars, Δ*gadC*; dark grey bars, Δ*FPI*. (**C**) Transmission electron micrographs of thin sections of J774.1 macrophages, infected by wild-type *F. novicida* and Δ*gadC* mutant strains. Infections were monitored over a 10 h-period. At 10 h, active cytosolic multiplication of wild-type *F. novicida* was observed in most of the infected cells (**1**) whereas the Δ*gadC* mutant remains trapped into spacious phagosomes (**2, 3, 4**). Black arrowheads point to intact phagosomal membrane. (**D**) To evaluate the viability of intracellular *Francisella*, labeling with the cell-impermeant nucleic acid dye propidium iodide (PI) was performed. Confocal images of J774.1 cells, infected with wild-type *F. novicida* (**1, 3**) or Δ*gadC* mutant (**2, 4**) strain; after 1 h (**1, 2**) and 10 h of infection (**3, 4**). Intact bacteria are labeled in green. Bacteria with compromised membranes are labeled with PI and appear in red (or a red spot). Phagosomes are labeled in blue. Scale bars at the bottom right of each panel correspond to 10 μM. (**E**) Quantification of the percentage of dead bacteria. At least 100 bacteria per experiment were scored for PI labeling at 1 h and 10 h post infection. Data are means ± standard deviation from three independent assays.

doi:10.1371/journal.ppat.1003893.g003

F. tularensis gadC encodes a genuine glutamate transporter

Earlier phylogenetic studies have distinguished ten distinct subfamilies within the APC family of transporters, inferring possible substrate specificities. Consensus signature motifs were defined for each of them [34]. Inspection of the *Francisella* GadC protein reveals a signature sequence of the Glutamate-GABA antiporter subfamily in its N-proximal portion (**Figure 4A**), prompting us to test functional complementation of an *E. coli gadC* mutant by the *Francisella gadC* orthologue.

Functional complementation (**Figure 4B**) was determined by comparing the acid resistance (at pH 2.5) of a *gadC*-inactivated strain of *E. coli* (EF491) to the same strain carrying a plasmid-borne *F. novicida gadC* gene (pCRT-*gadC*). As a positive control, we used the *E. coli gadC* mutant complemented with the wild-type *E. coli gadC* gene (EF547). IPTG-induced expression of the *Francisella gadC* allele in the *E. coli gadC* mutant strain restored acid resistance to wild-type level, indicating that the *Francisella* GadC protein displays the acid-resistance function of the *E. coli* GadC protein.

To further support the role of GadC in glutamate entry, we quantified the amounts of intracellular glutamate by HPLC analysis, in the wild-type and *ΔgadC* strains grown in CDM supplemented with 1.5 mM of glutamate (in the presence or in the absence of hydrogen peroxide). As shown in **Fig. 4C**, the concentration of intracellular glutamate was significantly lower in the Δ*gadC* mutant than in the wild-type strain, both in the absence (84% reduction in concentration) or in the presence (31% reduction) of H_2O_2. We also quantified the amount of glutamate in culture supernatants of the two strains in the presence of H_2O_2 (not shown). External glutamate present in the culture medium of the wild-type strain was 39% lower than that of the Δ*gadC* mutant.

Altogether these data are compatible with a reduced capacity of the Δ*gadC* mutant to take up external glutamate.

We then directly evaluated the impact of *gadC* inactivation on glutamate uptake by live *F. novicida*. For this, we compared the uptake of radiolabeled glutamate (^{14}C-Glu) by wild-type *F. novicida* to that of the Δ*gadC* mutant, over a broad range of glutamate concentrations (**Fig. 4D**). Incorporation of ^{14}C-Glu was significantly affected in the Δ*gadC* mutant (representing only approximately 50% of the wild-type values at each concentration tested), confirming that GadC is a genuine glutamate transporter. The fact that glutamate uptake was not totally abolished in the Δ*gadC* mutant suggests that other transporter(s) allow the entry of glutamate in this strain.

The *gadC* mutant shows impaired control of ROS production

We compared the amount of reactive oxygen species (ROS) in J774.1 cells infected either with wild-type *F. novicida*, Δ*gadC* or the Δ*FPI* strain, over a 60 min period. For this, we used the H_2DCF-DA assay (Sigma-Aldrich Co). H_2DCF-DA is a non-fluorescent cell-permeable compound that has been widely used for the detection of ROS [35]. Once inside the cell, this compound is first cleaved by endogenous esterases to H_2DCF. The de-esterified product becomes the highly fluorescent compound 2′,7′-dichloro-fluorescein (DCF) upon oxidation by ROS. The ROS content increased by 25% after 60 min in cells infected with wild-type *F. novicida* (**Figure 5**). A comparable increase was recorded with the *ΔFPI* mutant. However, in cells infected with the Δ*gadC* mutant, the ROS content was significantly higher than that recorded with the two other strains at each time point (25% higher at 15 min, and 55% higher after 60 min). These results suggest that the Δ*gadC* mutant is affected in its ability to neutralize the production of ROS in the phagosomal compartment. Alternatively, the Δ*gadC* mutant may trigger an increased production of ROS.

Impaired virulence of the *gadC* mutant is abrogated in NADPH oxidase KO mice

This result prompted us to evaluate the pathogenicity of the Δ*gadC* mutant in mice lacking a functional NADPH oxidase complex, both *in vitro* and *in vivo*.

In vitro. Intracellular replication of the Δ*gadC* mutant was monitored in bone marrow-derived macrophages from wild-type control mice or homozygotes gp91$^{phox-/-}$ in the same C57BL/6J background (designated WT and phox-KO BMMs, respectively) (**Figure 6A, 6B**). Multiplication of wild-type *F. novicida* and the Δ*gadC*/pKK*gadC*-complemented strain was similar at all time points tested in the two types of BMMs. In contrast, the Δ*gadC* mutant showed a significantly more severe intracellular multiplication defect in WT BMMs than in phox-KO BMMs. Indeed, the number of Δ*gadC* mutant bacteria was 10-fold lower than that of wild-type *F. novicida* already after 10 h in WT BMMs, and was 1,000-fold lower after 24 h (**Fig. 6A**). In BMM from phox-KO mice, multiplication of the mutant strain was 1/3 that of wild-type *F. novicida* after 10 h, and 100-fold higher than what was observed in WT macrophages after 24 h (**Figure 6B**). These results showed that multiplication of the Δ*gadC* mutant was mostly restored in BMMs having a defective NADPH oxidase.

In vivo. We also performed *in vivo* competition assays in these mice (**Figure 6C, 6D**), as described above for the BALB/c mice. The Competition Index (CI) calculated for both target organs was 10^{-4} in WT mice (**Figure 6C**). In contrast, the CI was 100-fold higher in phox-KO mice (10^{-2}, **Figure 6D**). This result comforts the data obtained in BMM cells and demonstrates that, in mice that are unable to produce ROS in the phagosome, the multiplication defect of the Δ*gadC* mutant is partially suppressed. However, the fact that the Δ*gadC* multiplication defect was not completely abolished suggests that oxidative stress may not be the only host restrictive factor.

Altogether, these *in vitro* and *in vivo* data obtained in phox-KO mice strongly suggest that GadC specifically contributes to the ROS defense of *Francisella* in the phagosomal compartment.

Impact of *gadC* inactivation in glutamate on metabolism

Intracellular glutamate plays a central role in a wide range of metabolic processes in bacteria. In order to evaluate the potential impact of the *gadC* inactivation on bacterial glutamate metabolism, we first quantitatively monitored the transcription of selected genes connecting glutamate utilization to either the TCA cycle or to glutathione biogenesis. This analysis was done for wild-type *F. novicida* and for the Δ*gadC* mutant strain, grown in broth with or without H_2O_2 (**Figure 7A**).

Expression of *FTN_0593* (*sucD*), *FTN_0127* (*gabD*) and *FTN_1532* (*gdhA*), was significantly decreased in the Δ*gadC* mutant under oxidative stress, whereas their expression was moderately increased in the wild-type strain. Expression of *FTN*_0277(gshA) and *FTN_0804* (*gshB*) was reduced in both strains, under oxidative stress. However, the decrease was significantly less important (app. 4-fold) in the Δ*gadC* mutant than in the wild-type strain. Expression of *FTN_1635* (*sucA*) was significantly decreased in both strains under oxidative stress. These data indicate that the absence of *gadC* affects the expression of several genes linked to glutamate metabolism under oxidative stress. The fact that expression of the *gadC* gene itself was significantly upregulated (approximately 10-fold) in the wild-type strain exposed to H_2O_2 stress (not shown) supports the importance of the GadC transporter in oxidative stress defense.

A

Signature	G-[LIV]-X-[LIVAST]-W-[LIVATM]-[RSKN]-[DKNQSH]- [AST]-[LIVM]-G-X(2)-[WFLIV]-[GA]-[FY]
Eco GadC	GVFAWVSNTLGPRWGF
Ftn GadC	GIYIWVKKAFGKRLGF

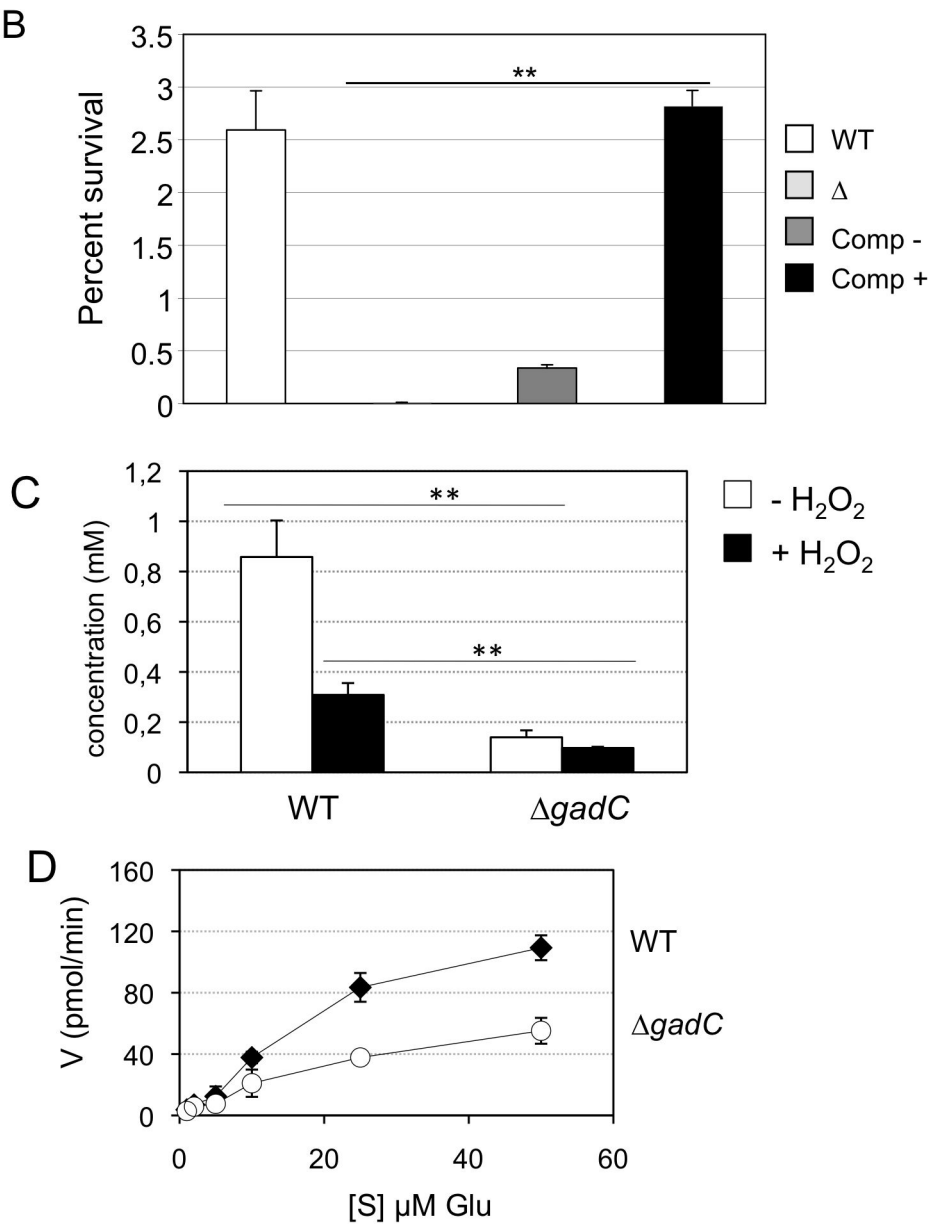

Figure 4. GadC is a glutamic acid transporter. (**A**) The signature sequence for the Glutamate/GABA subfamily of APC transporters is shown in the upper line. Middle line, sequence of the motif present in GadC of *E. coli*; lower line, sequence of the motif present in GadC of *Francisella* (in red the only residue diverging from the consensus). (**B**) Functional complementation of *E. coli gadC*. Acid resistance assays were performed on *E. coli* recombinant strains. Δ: *E. coli* strain bearing an inactivated *gadC* allele. WT: complemented strain bearing the wild-type *E. coli gadC* gene on plasmid pCF348 [49]. Comp −: complemented strain bearing the wild-type *Francisella gadC* gene carried on plasmid pCR2.1-Topo and Comp +: complemented strain bearing the wild-type *Francisella gadC* gene carried on plasmid pCR2.1-Topo and cultivated with IPTG . **$p<0.05$ as determined by the Student's *t*-test. (**C**) Intracellular glutamate detection and quantification was assayed on exponentially grown bacteria by HPLC analysis. Wild-type *F. novicida* and *ΔgadC* mutant strains were grown in CDM supplemented with 1.5 mM of glutamate, in the absence or presence of H_2O_2 (500 µM). **, $p<0.01$ (as determined by the Student's *t*-test). (**D**) Glutamate transport. Kinetics of ^{14}C-Glu uptake by wild-type *F. novicida* and Δ*gadC* mutant, at ^{14}C-Glu concentrations ranging from 1 µM to 50 µM. Bacteria grown to mid-exponential phase in CDM were tested. Uptake was measured after 5 min incubation with ^{14}C-Glu. Ordinate, pmol of glutamate taken up per min (per sample of app. 2.5×10^9 bacteria). Abscissa, final concentrations of glutamate tested.
doi:10.1371/journal.ppat.1003893.g004

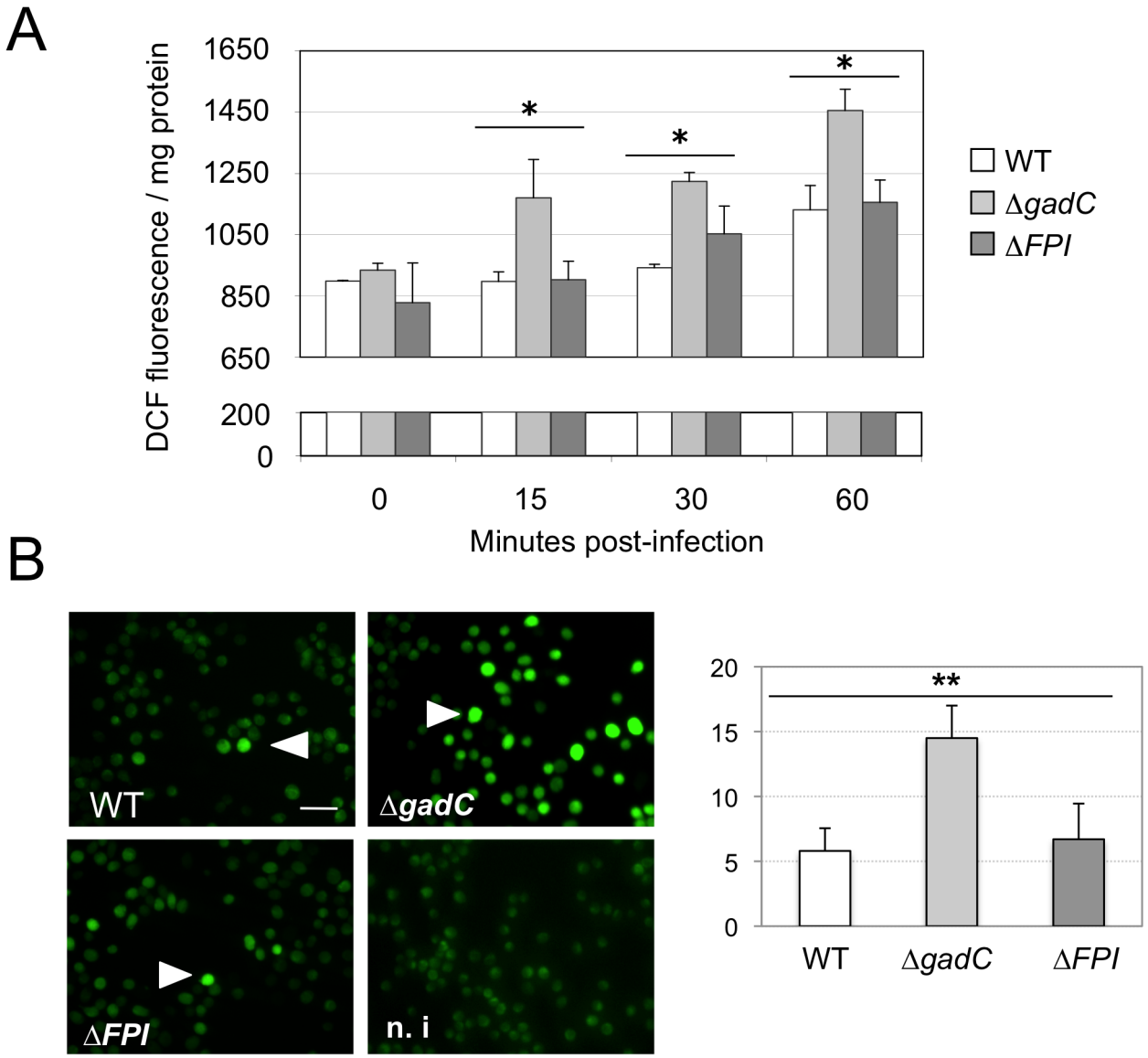

Figure 5. ROS dosage in infected J774.1 cells. (**A**) **ROS dosages.** Generation of ROS was measured by the H_2DCFDA assay in J774.1 cells infected with wild-type *F. novicida* (WT), the Δ*gadC* or the Δ*FPI* mutant strain. Results, normalized to the protein concentration in each well, are expressed per mg of total protein. The histogram is representative of three independent experiments. (**B**) **Fluorescence microscopy.** Left panel: DCFDA levels were also visualized using fluorescence microscopy. J774.1 cells were infected with wild-type (**1**), Δ*gadC* (**2**) or Δ*FPI* (**3**) bacteria. Non-infected J774.1 cells were used as negative control (**4**). White arrowheads indicate increased DCFDA levels. Scale bar is 50 μm. Images represent fluorescence after 1 h of DCFDA treatment. Typical fields were chosen for illustration. Right panel: Quantification of the percentage of fluorescent J774.1 cells. At least 500 cells per experiment were scored for DCFDA labeling after 1 h of DCFDA treatment. Data are means ± standard deviation from three independent assays.
doi:10.1371/journal.ppat.1003893.g005

Direct quantification of TCA cycle intermediates present in the cytoplasm of the wild-type and Δ*gadC* strains, by gas chromatography coupled with mass spectrometry (see Materials and methods for details), revealed that *gadC* inactivation significantly affected succinate, fumarate, and oxoglutarate contents (**Figure 7C**). Indeed, in the Δ*gadC* mutant, the concentrations of succinate and fumarate were reduced *ca.* 60% as compared to the wild-type strain, whereas oxoglutarate was below the detection threshold of the assay. The concentrations of the three molecules increased up to 40% in the wild-type strain exposed to oxidative stress, suggesting an activation of the TCA under this condition. The concentrations of succinate and fumarate were not significantly modified in the Δ*gadC* mutant upon oxidative stress and oxoglutarate production was still below detection. The concentration of citrate was similar in the wild-type and the Δ*gadC* mutant and did not vary upon oxidative stress, in any of the two strains. The intracellular concentrations of glutathione were also almost similar in the wild-type and Δ*gadC* mutant (**Figure 7B**). Remarkably, under oxidative stress, the intracellular concentration of glutathione increased in both strains but only reached 65% of the level of the Δ*gadC* mutant in the wild-type strain.

These observations prompted us to evaluate the impact of supplementation with different TCA cycle intermediates on survival of the Δ*gadC* mutant in response to H_2O_2 challenge.

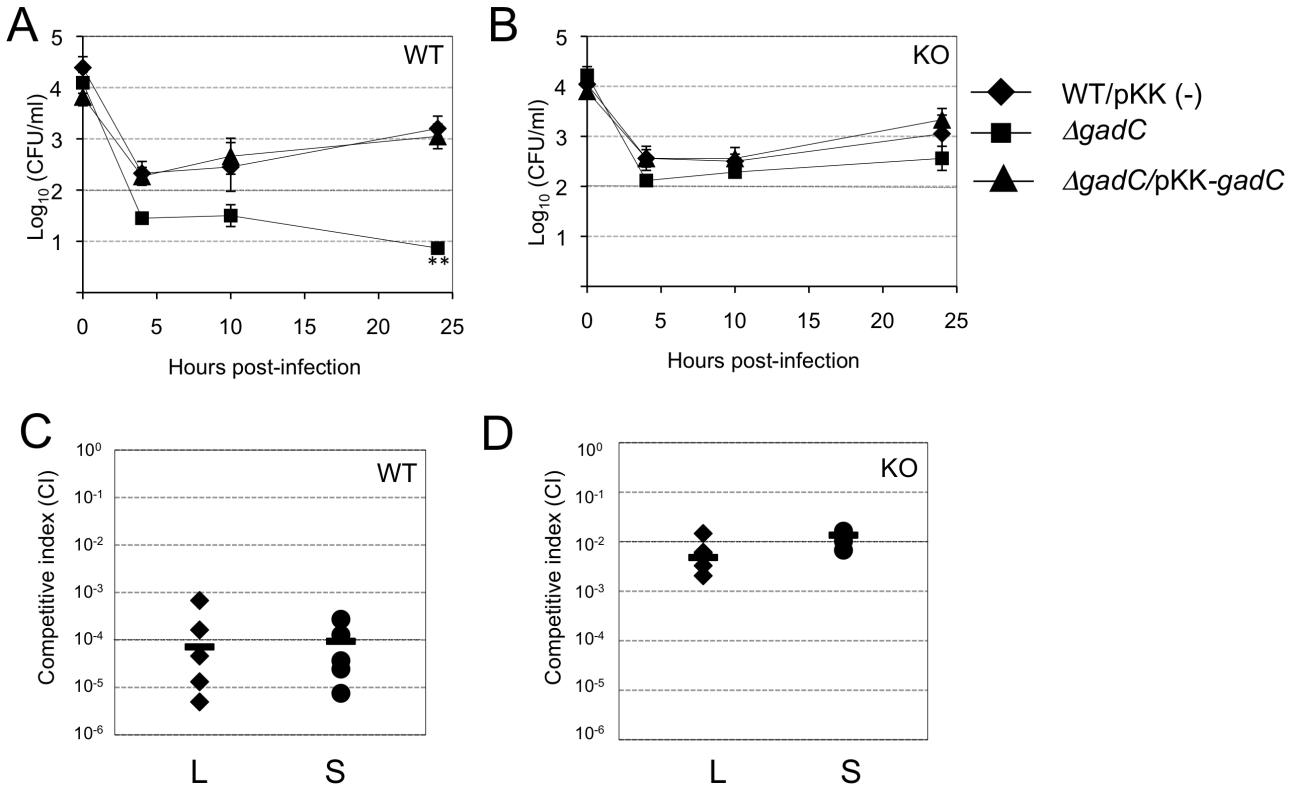

Figure 6. Intracellular survival and virulence in NADPH oxidase KO mice. (**A, B**) Intracellular replication of wild-type *F. novicida* (carrying the empty plasmid pKK214 (WT/pKK(−)), Δ*gadC* mutant and complemented strain (Δ*gadC*/pKK-*gadC*), and Δ*FPI* mutant (Δ*FPI*), was monitored in BMM from either (**A**) C57BL/6J control mice (WT) or (**B**) phox-KO mice (homozygotes gp91$^{phox-/-}$; KO), over a 24-h period. Results are shown as the average of $\log_{10}$ cfu mL^{-1} ± standard deviation. At all time points tested, the differences between the wild-type and Δ*gadC* mutant values were not statistically different ($p>0.1$, as determined by the Student's *t*-test). (**C, D**) Competition assays were performed by infecting intra-peritoneally: a group of five C57BL/6J control mice (WT, **C**); or a group of five phox-KO mice (KO, **D**), with a 1:1 mixture of wild-type *F. novicida* and Δ*gadC* mutant strains (100 cfu of each). The data represent the competitive index (CI) value for cfu of mutant/wild-type in the liver (L: black diamonds, left column) and spleen (S: black circles, right column) of each mouse, 48 h after infection. Bars represent the geometric mean CI value.
doi:10.1371/journal.ppat.1003893.g006

For this, exponential phase wild-type and *ΔgadC* mutant strains, diluted in CDM supplemented with glutamate, were subjected to oxidative stress, in the presence or absence of either fumarate, succinate or oxoglutarate (**Figure S5**). The sensitivity to H_2O_2 of the *ΔgadC* mutant was not modified neither by fumarate nor by oxoglutarate. In contrast, supplementation with succinate increased significantly the survival of the *ΔgadC* mutant, to nearly wild-type level.

Discussion

Intracellular pathogenic bacteria have adapted a variety of strategies and specific intracellular niches for survival and multiplication within their host [36]. Some reside in a vacuolar compartment whereas others have evolved to gain access to the host cytosol for multiplication. In mammalian host cells, *Francisella* intracellular replication occurs exclusively in the cytosolic compartment. We show here that inactivation of the GadC permease of *Francisella* prevents phagosomal escape, thus severely altering bacterial intracellular multiplication and virulence.

The data presented suggest that the GadC protein of *Francisella* is required to resist to the oxidative burst triggered by the NADPH oxidase in the phagosomal compartment of infected macrophages. We propose that GadC-mediated entry of glutamate contributes to fuel the tricarboxylic acid cycle and modulates the redox status of the bacterium. This work thus provides insights into the possible links between oxidative stress resistance, metabolism, and bacterial intracellular parasitism.

GadC is involved in oxidative stress defense and required for phagosomal escape

Inactivation of *gadC* in *F. novicida* led to a severe growth defect in all cell types tested and *in vivo* assays further demonstrated the importance of GadC in *Francisella* virulence. Confocal and electron microscopy analyses revealed that the severe intracellular growth defect of the mutant was due to its inability to escape from the phagosomal compartment of infected macrophages.

Interestingly, most of the mutant bacteria that remained trapped within the phagosome were still alive for at least 10 h post-infection, indicating that impaired escape was not due to bacterial death. Since the Δ*gadC* mutant showed increased susceptibility to oxidative stress in broth and failed to efficiently neutralize reactive oxygen species production in cells, it is likely that ROS may predominantly affect bacterial escape rather than survival.

F. tularensis produces enzymes that can metabolize and neutralize ROS, such as a superoxide dismutases (SodB, SodC), a catalase (KatG), a glutathione peroxidase and a peroxireductase [9,10]. Acid phosphatases have also been implicated in the resistance of intracellular *Francisella* to H_2O_2 generated in the phagosomal compartment by the NADPH oxidase ([37,38] and

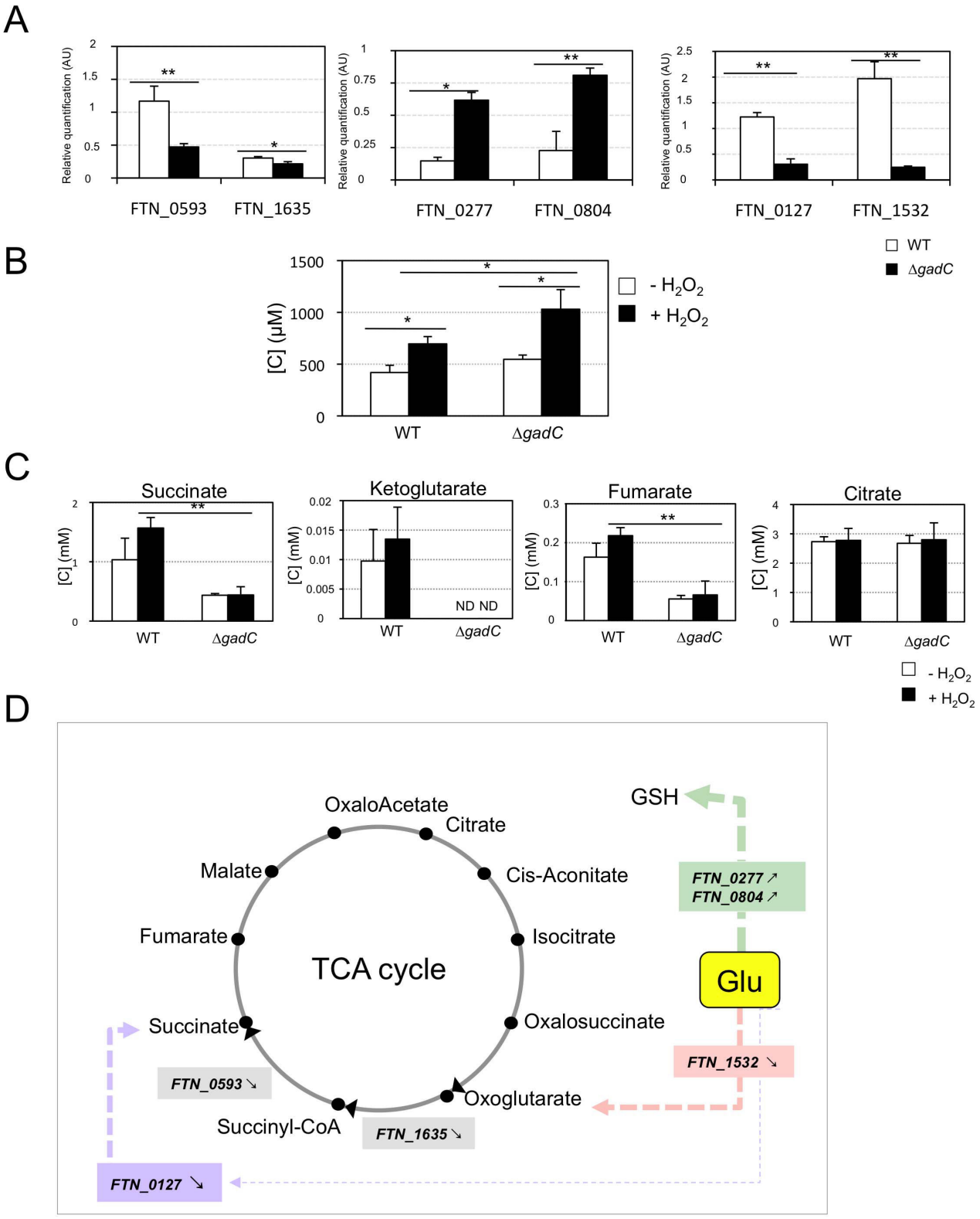

Figure 7. Glutamate transport and metabolism. (**A**) **qRT-PCR of metabolic genes ± H_2O_2.** Bacteria were grown in TSB, in the absence or in the presence of H_2O_2 (500 μM). qRT-PCR analyses were performed on selected genes, in wild-type *F. novicida* and in the Δ*gadC* mutant. For each gene, the data are represented as the ratios of the value recorded under H_2O_2 stress versus non-stress condition. *Left panel:* two genes encoding enzymes of the TCA cycle (*sucA*, *FTN_1635*; *sucD*, *FTN_0593*); m*iddle panel*: two genes encoding enzymes, converting glutamate (Glu) to glutathione (GSH) (*gshA*, *FTN_0277*; *gshB*, *FTN_0804*); r*ight panel:* two genes encoding enzymes, converting Glu to TCA cycle intermediates (*gdhA*, *FTN_1532*; *gabD*, *FTN_0127*). (**B**) **Dosage of glutathione.** The effect of oxidative stress on the cytoplasmic content of glutathione was evaluated in wild-type *F. novicida* and Δ*gadC* mutant strains. Bacteria were cultivated for 30 min, with or without H_2O_2 (500 μM), in CDM supplemented with glutamate

(1.5 mM). Reduced glutathione was quantified by HPLC analysis. Concentrations [C] are expressed in μM. *$p<0.05$ as determined by the Student's *t*-test. (**C**) **Dosage of TCA intermediates.** The effect of oxidative stress on the cytoplasmic contents of TCA cycle intermediates was monitored in wild-type *F. novicida* and Δ*gadC* mutant strains. Bacteria were cultivated for 30 min, with or without H_2O_2 (500 μM), in CDM supplemented with glutamate (1.5 mM). Succinate, fumarate, citrate and oxoglutarate, were quantified by gas chromatography coupled with mass spectrometry. Concentrations [C] are expressed in mM. *$p<0.05$, **$p<0.01$, as determined by the Student's *t*-test. (**D**) **Schematic representation of selected genes involved in glutamate metabolism.** The impact of *gadC* inactivation on the oxidative stress response of the target genes is indicated (↘ means the ratio (H_2O_2-treated/non-treated) is lower in the mutant strain than in the wild-type strain; ↗ the ratio (H_2O_2-treated/non-treated) is higher in the mutant strain than in the wild-type strain. In the absence of external glutamate (*e.g.* in standard chemically defined medium), the pool of glutamate present in the bacterial cytoplasm may be synthesized either from oxoglutarate, glutamine, GSH or even proline (according to KEGG metabolic pathways).
doi:10.1371/journal.ppat.1003893.g007

references therein). However, inactivation of the major phosphatase *acpA* in *F. tularensis* subsp. *tularensis*, had no impact on the activity of the NADPH oxidase in human neutrophils [5], thus confirming that other *Francisella* factors were involved in NADPH oxidase inhibition.

We show here that *Francisella* GadC is an important player specifically involved in oxidative stress defense. The existence of several paralogues of both the transporter GadC and the decarboxylase GadB in some bacterial species (for example in *L. monocytogenes*) might account for the fact that these have not yet been found to contribute to oxidative stress resistance and intracellular survival in standard genetic screens. Indeed, if functional paralogues exist, they must be simultaneously inactivated to observe a possible phenotypic defect. In addition, isofunctional antiporters with no significant amino acid sequence similarity to the GadC protein might exist in these bacteria.

The contribution of the GAD system to intracellular survival critically depends on the cellular compartment where bacterial survive and multiply. Indeed, bacteria residing in vacuolar compartments (such as *Salmonella*, *Mycobacteria*, *Legionella*, *Brucella and Chlamydia*) encounter different types of stresses (pH, oxidative, nutritional,…) than bacteria able to multiply in the host cell cytosol (such as *Francisella*, *Listeria*, *Shigella* and *Rickettsia*).

L-glutamate is very abundant in the intracellular compartment (reported concentrations vary between 2 and 20 mM) when compared to the extracellular compartment (app. 20 μM) [39]. Human macrophages have both the cystine/glutamate transporter and the Na-dependent high-affinity glutamate transporters (excitatory amino acid transporters, EAATs) that transport glutamate and aspartate. To maintain their intracellular pool of glutamate, macrophages may use either these transporters to import glutamate from the extracellular milieu or enzymatically convert cytosolic glutamine (via glutaminase) and aspartate (via aspartate transpeptidase) to glutamate. Glutamate might also be produced spontaneously intracellularly from pyroglutamate. Currently, nothing is known with respect to the content of glutamate in the phagosomal compartment. This might prove extremely difficult to establish, especially for pathogens such as *Francisella* or *Listeria* that reside only very transiently in this compartment.

A limited number of bacterial species have been shown to possess a GAD system [40]. These include *E. coli*, *Lactobacillus*, *L. monocytogenes* and *Shigella* species, in which the GAD system plays a major role in acid tolerance. It has been suggested that the GAD system is important for pathogenic microorganisms that, upon oral infection of mammalian hosts, need to survive the low pH of the stomach. However, some enteric pathogens like *Salmonella* do not possess a function GAD system and must thus rely on other anti-acidic pH strategies. Interestingly, the GAD system has been also found to contribute to oxidative stress defense in yeast and plant [41]. In bacteria, molecules such as the NADPH and NADH pools and glutathione (GSH), contribute to oxidative stress defense. Reduced GSH, present at mM concentrations, maintain a strong reducing environment in the cell. Specific enzymes are also dedicated to control the levels of reactive oxygen species (ROS).

Remarkably, the Δ*gadC* mutant was still outcompeted by wild-type bacteria in phox-KO mice. The different environments and the immune pressure, encountered by the bacterium during its systemic dissemination, are probably far more complex than in culture systems. *In vivo*, *Francisella* GadC is thus likely to contribute to other functions than combat ROS in the phagosomal compartment. It may, for instance, fulfill classical nutritional functions during bacterial cytosolic multiplication (in macrophages and/or in other infected non-phagocytic cells). Alternatively, GadC may be required during the bacterial blood stage multiplication and dissemination of the bacterium.

A link between oxidative stress and bacterial metabolism

In *E. coli*, GABA produced by the glutamate decarboxylase is metabolized via the GABA shunt pathway. This leads to the production of succinate via the consecutive action of two enzymes: a GABA/oxoglutarate amino-transferase (GabT) that removes the amino group from GABA to form succinic semialdehyde (SSA) and Glu; and a succinic semialdehyde dehydrogenase (GabD) that oxidises SSA to form succinate. Very recently, Karatzas and co-workers have shown [42] that *L. monocytogenes* also possessed functional GabT and GabD homologues that could provide a possible route for succinate biosynthesis in *L. monocytogenes*. The GABA shunt pathway, allowing the bypass of two enzymatic steps of the TCA (from oxoglutarate to succinate; **Figure 7 and S6**), is thought to play a role in glutamate metabolism, anaplerosis and antioxidant defense. However, its physiological role in pathogenesis is yet poorly understood. *Francisella* genomes possess a *gabD* orthologue but lack *gabT*. The GABA shunt pathway may therefore be non-functional in *Francisella*. Interestingly, the isogenic glutamate decarboxylase Δ*gadB* mutant (**Figure S4**) that we constructed, showed a much less severe intracellular multiplication defect than the Δ*gadC* mutant, and as well as no (or only a very mild) attenuation of virulence. If the glutamate imported via GadC would serve to produce GadB-mediated GABA, one would expect *gadB* inactivation to cause the same defect as *gadC* inactivation. As already mentioned in the Introduction, the *gadB* orthologue encodes a truncated protein in the subspecies *holarctica*. Altogether, these data support the notion that GadC and GadB of *Francisella* do not function in concert, unlike in several other bacterial species, and that GABA production plays a marginal role in *Francisella* pathogenesis. Further work will be required to understand the exact contribution of GadB in *Francisella* metabolism.

Our data indicate that GadC of *Francisella* encodes a genuine glutamate transporter involved in oxidative stress, unlike most other GadC orthologues described thus far. Glutamate can be converted in the bacterial cytoplasm into a number of compounds (**Figure 7**), such as glutamine, glutathione, GABA or the TCA cycle intermediate oxoglutarate. Oxoglutarate is known to be a potent anti-oxidant molecule that can be converted, in absence of

any enzymatic reaction, into succinate in the presence of H_2O_2. In addition, conversion of glutamate to oxoglutarate by the glutamate dehydrogenase GdhA increases the production of NADPH, which might also contribute to the anti-oxidant effect of glutamate acquisition.

Quantitative analyses of the intra-bacterial content of TCA cycle intermediates (**Figure 7B**) revealed a significant reduction of succinate and fumarate in the *gadC* mutant, as compared to wild-type *F. novicida*, and a striking decrease of oxoglutarate. These data support the notion that reduced entry of glutamate directly affects the production of these TCA cycle intermediates. In contrast, the amount of citrate remained unchanged in the mutant, suggesting refueling of the TCA cycle via other entry points (such as glycolysis or amino acid conversion).

Of note, mutants in genes *gdhA* (*FTN_1533*) and *gabD* (*FTN_0127*) were identified as required for replication in *D. melanogaster* S2 cells in a recent screen, supporting a role for these genes in intracellular bacterial survival [43]. The production and utilization of oxoglutarate by *Francisella* may thus constitute an efficient mean to modulate its cytoplasmic concentration of ROS.

In the absence of external glutamate, the pool of intracellular glutamate may be synthesized either from oxoglutarate, glutamine, GSH or even proline (according to KEGG metabolic pathways). Therefore, we evaluated the impact of *gadC* inactivation on the expression of genes involved in glutamate metabolism, under oxidative stress conditions. qRT-PCR analyses were performed in wild-type *F. novicida* and in the Δ*gadC* mutant, grown in chemically defined medium containing glutamate, in the absence or in the presence of H_2O_2 (**Figure 7A**). These assays revealed that *gadC* inactivation led to an important down-regulation of the genes involved the conversion of glutamate to oxoglutarate and succinate, upon oxidative stress (*FTN_1532* and *FTN_0127*, respectively). Conversely, *gadC* inactivation only moderately decreased the expression of *gshA* and *gshB*, the two genes involved in glutathione biosynthesis (*FTN_0277* and *FTN_0804*), upon oxidative stress whereas the expression of these genes was severely decreased in the wild-type strain.

These data are compatible with the notion that, under oxidative stress, the wild-type strain may favor the conversion of a fraction of its cytoplasmic pool of glutamate (neosynthesized and imported) to produce oxoglutarate and succinate rather than GSH. In contrast, when the cytosolic pool of glutamate is restricted to neosynthesized glutamate (*i.e.* in a *gadC* mutant or in a glutamate-depleted medium), the production of oxaloglutarate and succinate may be decreased to favor that of other molecules (including GSH).

In conclusion, we identified a glutamate transporter as a novel *Francisella* virulence attribute that suggests links between the oxidative stress response and the TCA cycle during the early stage of the bacterial intracellular life cycle. The importance of the TCA cycle in the homeostasis of reactive oxygen species has just started to be considered in pathogenic bacterial species [12,44,45,46]. The development of specific inhibitors of transport systems involved in intracellular adaptation might constitute interesting anti-bacterial therapeutic targets.

Materials and Methods

Ethics statement

All experimental procedures involving animals were conducted in accordance with guidelines established by the French and European regulations for the care and use of laboratory animals (Decree 87–848, 2001–464, 2001–486 and 2001–131 and European Directive 2010/63/UE) and approved by the INSERM Ethics Committee (Authorization Number: 75-906).

Bacterial strains, media, and chemicals

F. tularensis subsp. *novicida* (*F. novicida*) strain U112, its Δ*FPI* derivative, and all the mutant strains constructed in this work, were grown as described in **Supplementary Material**. *E. coli* strains (kindly provided by John Foster, University of South Alabama, USA) were grown as described in **Supplementary Material**. All bacterial strains, plasmids, and primers used in this study are listed in **Supplemental Table 1**.

Details of the construction and characterization of mutant and complemented strains; macrophage preparation and infections, are described in **Supplementary Material**. Quantitative (q)RT-PCR (real-time PCR) was performed with gene-specific primers (**Supplemental Table 1**), using an ABI PRISM 7700 and SYBR green PCR master mix (Applied Biosystems, Foster city, CA, USA).

Electron and confocal microscopy complete descriptions; real time cell death and phagosome permeabilization assays, are described in **Supplementary Material**.

Multiplication in macrophages

J774.1 macrophage-like cells (ATCC Number: TIB-67) were propagated in Dulbecco's Modified Eagle's Medium (DMEM) containing 10% fetal calf serum, whereas human monocyte-like cell line THP-1 (ATCC Number: TIB-202) and bone marrow-derived macrophages (BMM) from BALB/c were propagated in RPMI Medium 1640 containing 10% fetal calf serum, respectively. J774.1 and BMM were seeded at a concentration of $\sim 2\times10^5$ cells per well in 12-well cell tissue plates and monolayers were used 24 h after seeding. THP-1 were seeded at a concentration of $\sim 2\times10^5$ cells per well in 12-well cell tissue plates 48 h before infection, and supplemented with phorbol myristate acetate (PMA) to induce cell differentiation (200 ng/ml). J774.1, BMM and THP-1 were incubated for 60 min at 37°C with the bacterial suspensions (approximately multiplicities of infection 100) to allow the bacteria to enter. After washing (time zero of the kinetic analysis), the cells were incubated in fresh culture medium containing gentamicin (10 μg mL^{-1}) to kill extracellular bacteria. At several time-points, cells were washed three times in DMEM or RPMI, macrophages were lysed by addition of water and the titer of viable bacteria released from the cells was determined by spreading preparations on Chocolate agar plates. For each strain and time in an experiment, the assay was performed in triplicate. Each experiment was independently repeated at least three times and the data presented originate from one typical experiment.

Isolation of total RNA and reverse transcription

Bacteria were centrifuged for 2 min in a microcentrifuge at room temperature and the pellet was quickly re-suspended in Trizol solution (Invitrogen, Carlsbad, CA, USA). Samples were either processed immediately or frozen and stored at −80°C. Samples were treated with chloroform and the aqueous phase was used in the RNeasy Clean-up protocol (Qiagen, Valencia, CA, USA) with an on-column DNase digestion of 30 min [47].

RNA Reverse transcription (RT)-PCR experiments were carried out with 500 ng of RNA and 2 pmol of specific reverse primers. After denaturation at 65°C for 5 min, 6 μL of the mixture containing 4 μL of 5× first strand buffer and 2 μL of 0,1 M DTT were added. Samples were incubated 2 min at 42°C and, then, 1 μL of Superscript II RT (Thermo Scientific) was added. Samples were incubated for 50 min at 42°C, heated at 70°C for 15 min and chilled on ice. Samples were diluted with 180 μL of H_2O and stored at −20°C.

The following pair of primers was used to amplify the mRNA corresponding to the transcript of *FTN_0570* (p13/p14),

FTN_0571 (p15/p16), *FTN_1700* (p27/9p28), *FTN_1701* (p29/p30), *FTN_1702* (p31/p32), *FTN_1532* (p33/p34), *FTN_0127* (p35/p36), *FTN_0277* (p37/p38), *FTN_0804* (p39/p40), *FTN_0593* (p41/p42), *FTN_1434* (p43/p44) and *FTN_1635* (p45/p46) (**Supplemental Table 1**).

Quantitative real-time RT-PCR

Wild-type *F. novicida* and mutant strains were grown at 37°C from OD_{600} ~0.1. After 4 h of incubation, samples were harvested and RNA was isolated. For oxidative stress tests, samples were cultivated 30 min more with or without H_2O_2 (500 µM). The 25 µL reaction consisted of 5 µL of cDNA template, 12.5 µL of Fastart SYBR Green Master (Roche Diagnostics), 2 µL of 10 µM of each primer and 3.5 µL of water. qRT-PCR was performed according manufacturer's protocol on Applied Biosystems - ABI PRISM 7700 instrument (Applied Biosystems, Foster City, CA). To calculate the amount of gene-specific transcript, a standard curve was plotted for each primer set using a series of diluted genomic DNA from wild-type *F. novicida*. The amounts of each transcript were normalized to helicase rates (*FTN_1594*).

Oxidative and pH stress survival assays

Stationary-phase bacterial cultures were diluted at a final OD_{600} of 0.1 in TSB broth or CDM with or without glutamate (1.5 mM final). Exponential-phase bacterial cultures were diluted to a final concentration of 10^8 bacteria mL^{-1} and subjected to either 500 µM H_2O_2 or pH 5.5.

Oxidative stress response was also tested in CDM supplemented with glutamate, in the presence or absence of the TCA cycle intermediates: oxoglutarate, succinate or fumarate (1.5 mM final). The number of viable bacteria was determined by plating appropriate dilutions of bacterial cultures on Chocolate Polyvitex plates at the start of the experiment and after the indicated durations. Cultures (5 mL) were incubated at 37°C with rotation (100 rpm) and aliquots were removed at indicated times, serially diluted and plated immediately. Bacteria were enumerated after 48 h incubation at 37°C. Experiments were repeated independently at least twice and data represent the average of all experiments.

Confocal experiments

J774.1 cells were infected with wild-type *F. novicida*, *ΔgadC* or *ΔFPI* strains for 1 h, 4 h and 10 h at 37°C, and were washed in KHM (110 mM potassium acetate, 20 mM Hepes, 2 mM $MgCl_2$). Cells were incubated for 1 min with digitonin (50 µg/mL) to permeabilize membranes. Then cells were incubated for 15 min at 37°C with primary anti *F. novicida* mouse monoclonal antibody (1/500 final dilution, Immunoprecise). After washing, cells were incubated for 15 min at 37°C with secondary antibody (Ab) (Alexa Fluor 488-labeled GAM, 1/400 final dilution, Abcam) in the dark. After washing, cells were fixed with PFA 4% for 15 min at room temperature (RT) and incubated for 10 min at RT with 50 mM NH_4Cl to quench residual aldehydes. After washing with PBS, cells were incubated for 30 min at RT with primary anti-LAMP1 Ab (1/100 final dilution, Abcam) in a mix with PBS, 0.1% saponine and 5% goat serum. After washing with PBS, cells were incubated for 30 min at RT with secondary anti-rabbit Ab (alexa 546-labeled, 1/400 dilution, Abcam). DAPI was added (1/5,000 final dilution) for 1 min. After washing, the glass coverslips were mounted in Mowiol. Cells were examined using an X63 oil-immersion objective on a LeicaTSP SP5 confocal microscope. Co-localization tests were quantified by using Image J software; and mean numbers were calculated on more then 500 cells for each condition. Confocal microscopy analyses were performed at the Cell Imaging Facility (Faculté de Médecine Necker Enfants-Malades).

Electron microscopy

Infection of J774.1 cells was followed by thin section electron microscopy as previously described [48].

Determination of intracellular bacterial viability

To evaluate the viability of *F. tularensis*, labelings were adapted to use the cell-impermeant nucleic acid dye propidium iodide (PI). J774.1 macrophage-like cells were seeded at 5.10^5cells/ml on glass coverslips in 12-well bottom flat plates. Next day, cells were infected for 10 h with wild-type *F. novicida* or *ΔgadC* strain. After infection, cells were first permeabilized with digitonin for 1 min, washed three times with KHM and incubated for 12 min at 37°C with 2.6 µM PI (Life technologies, L7007) in KHM buffer to label compromised bacteria in permeabilized cells. Cells were washed three times with KHM and incubated for 15 min at 37°C with primary anti *F. novicida* mouse monoclonal antibody (1/500 final dilution). After washing, cells were incubated for 15 min at 37°C with secondary antibody (Ab) (Alexa Fluor 488-labeled GAM, 1/400 final dilution) in the dark. After washing, cells were fixed with PFA 4% for 15 min at room temperature (RT) and incubated for 10 min at RT with 50 mM NH_4Cl to quench residual aldehydes. After washing with PBS, cells were incubated for 30 min at RT with primary anti-LAMP1 Ab (1/100 final dilution) in a mix with PBS, 0.1% saponine and 5% goat serum. After washing with PBS, cells were incubated for 30 min at RT with secondary anti-rabbit Ab (alexa 405-labeled, 1/400 dilution). After washing, the glass coverslips were mounted in Mowiol. Cells were examined using an X63 oil-immersion objective on a LeicaTSP SP5 confocal microscope. Analysis of cell fluorescence was performed with Image J software (http://rsb.info.nih.gov/ij).

ROS detection assay

Intracellular reactive oxygen species (ROS) were detected by using the oxidation-sensitive fluorescent probe dye, 2′,7′-dichlorodihydrofluorescein diacetate (H_2DCF-DA) as recommended by the manufacturer (CM-H2DCF-DA, Molecular Probes, Eugene, OR). J774.1 cells were seeded at 5.10^4 cells/well. Cells were infected with bacteria for 15 min (MOI of 100:1), washed three times with PBS and incubated with H_2DCF-DA diluted in PBS (concentration). DCF fluorescence was measured with the Victor^2 D fluorometer (Perkin-Elmer, Norwal, CT) with the use of excitation and emission wavelengths of 480 nm and 525 nm, respectively. Values were normalized by protein concentration in each well (Bradford). Samples were tested in triplicates in three experiments.

Determination of ROS generation via fluorescent microscopy

J774.1 cells were seeded at 5.10^4 cells/well. Cells were infected with bacteria for 15 min (MOI of 1,000:1), washed three times with PBS and incubated with H_2DCF-DA diluted in PBS for 1 h (5 µM). Images of the cells were captured with an Olympus CKX41 microscope and treated with Image J software. Cell counts were performed over 10 images of approximately 50 cells.

Acid resistance assay

Acid resistance tests in *E. coli* were performed at pH 2.5 as described previously [49], by comparing the number of survival treated cells after 1 h of treatment over the number of cells at T0.

We compared survival of wild-type *E. coli* strain (WT) with *E. coliΔgadC* (Δ) and *E. coliΔgadC* complemented with the *F. novicida gadC* gene (PCR-amplified gene *FTN-0571* introduced into plasmid pCR2.1-Topo, in the correct orientation downstream of the p*lac* promoter) (Comp). Acid challenge was performed by diluting 1:100 the overnight (22 h) culture in LB, supplemented (Comp +) or not (Comp −) with 10^{-4} M final IPTG.

Glutamate assays

Glutamate detection and quantification was done by using HPLC analysis. Wild-type *F. novicida* and *ΔgadC* strains were tested in CDM supplemented with 1.5 mM of glutamate, with or without H_2O_2 (500 µM). For each condition, three independent cultures were prepared by overnight growth in CDM. The overnight cultures were diluted with 50 mL of fresh medium to OD_{600} of 0.05 and cultivated to an OD_{600} of app. 0.35. Bacteria were harvested by centrifugation at 4,000× *g* for 20 min, resuspended in 25 mL of pre-warmed appropriated medium and cultivated for 30 min. For extracellular glutamate dosage, 100 µL of each supernatant were resuspended with 400 µL of cold methanol and centrifuged at 12,000× *g* for 5 min. 20 µL of each preparation were derivatized with 80 µL of OPA. For intracellular dosage, each sample were resuspended in 600 µL of cold methanol. The bacterial suspensions were sonicated thrice for 30 sec at 4.0 output, 70% pulsed (Branson Sonifier 250). Lysates were then centrifuged at 3,300× *g* for 8 min, to remove debris.

Following steps were done with the standard procedure of Agilent using ZORBAX Eclipse AAA high as HPLC column. An amount equivalent to 2 µL of each sample was injected on a Zorbax Eclipse-AAA column, 5 µm, 150×4.6 mm (Agilent), at 40°C, with fluorescence detection. Aqueous mobile phase was 40 mM NaH_2PO_4, adjusted to pH 7.8 with NaOH, while organic mobile phase was acetonitrile/methanol/water (45/45/10 v/v/v). The separation was obtained at a flow rate of 2 mL min^{-1} with a gradient program that allowed for 2 min at 0% B followed by a 16-min step that raised eluent B to 60%. Then washing at 100% B and equilibration at 0% B was performed in a total analysis time of 38 min. To evaluate glutamate concentration, glutamate standard curve was made in parallel.

Glutathione assays

The procedure for the measurement of GSH was previously described [50]. Briefly, GSH were separated by HPLC, equipped with a Shimadzu Prominence solvent delivery system (Shimadzu Corp., Kyoto, Japan), using a reverse-phase C18 Kromasil (5 µm; 4.6×250 mm), obtained from AIT (Paris, Fr). The mobile phase for isocratic elution consisted of 25 mmol L^{-1} monobasic sodium phosphate, 0.3 mmol L^{-1} of the ion-pairing agent 1-octane sulfonic acid, 4% (v/v) acetonitrile, pH 2.7, adjusted with 85% phosphoric acid. The flow rate was 1 mL min^{-1}. Under these conditions, the separation of aminothiol was completed in 20 min. Deproteinated samples were injected directly onto the column using a Shimadzu autosampler (Shimadzu Corp.). Following HPLC separation, GSH was detected with a model 2465 electrochemical detector (Waters, MA, USA) equipped with a 2 mm Glassy carbon (GC) analytical cell and potential of +700 mV were applied.

Glutamate transport assays

Cells were grown in Chamberlain medium to mid-exponential phase and then harvested by centrifugation and washed twice with Chamberlain without amino acid. The cells were suspended at a final OD_{600} of 0.5 in the same medium containing 50 mg/ml of chloramphenicol. After 15 min of pre-incubation at 25°C, uptake was started by the addition of L-[U-^{14}C] glutamic acid (Perkin Elmer), at various concentrations (^{14}C-Glu ranging from 1 to 50 µM). The radiolabeled ^{14}C-Glu was at a specific activity of 9.25 GBq.mmol $^{-1}$. Samples (100 µL of bacterial suspension) were removed after 5 min and collected by vacuum filtration on membrane filters (Millipore type HA, 25 mm, 0.22 mm) and rapidly washed with Chamberlain without amino acid (2×5 mL). The filters were transferred to scintillation vials and counted in a Hidex 300 scintillation counter. The counts per minute (c.p.m.) were converted to picomoles of amino acid taken up per sample, using a standard derived by counting a known quantity of the same isotope under similar conditions.

Quantification of TCA cycle intermediates

Succinate, fumarate, citrate and oxoglutarate were quantified by gas chromatography coupled with mass spectrometry (GC/MS). Wild-type *F. novicida* and Δ*gadC* strains were grown as for glutamate quantification. Briefly, after an overnight preculture in CDM, three independent cultures of wild-type and Δ*gadC* mutant were cultivated in 50 mL CDM to an OD_{600} of app. 0.35. Bacteria were harvested by centrifugation at 4,000× g for 15 min, resuspended to the same OD_{600} in pre-warmed CDM supplemented with glutamate (1.5 mM) and cultivated for 30 min±500 µM H_2O_2.

Metabolite measurements were normalized by checking that each sample contained equal amounts of total proteins.

Protein dosage. After centrifugation at 4,000× g for 20 min, each sample was resuspended in 2 mL of ice-cold 5 mM Tris.HCl (pH8). The bacterial suspensions were sonicated thrice for 30 sec at 4.0 output, 70% pulsed (Branson Sonifier 25). Lysates (three per strain per condition) were then centrifuged at 3,300× *g* for 8 min, to remove debris. Protein concentration of the different samples was determined by the BCA assay (Pierce), following the manufacturer's recommendation. The values recorded for the wild-type and the *ΔgadC* mutant, in the absence or in the presence of H_2O_2, were not significantly different (1,000 mg mL^{-1}±10 mg mL^{-1}; *p* value≥0.5). The assay was repeated twice.

Metabolite measurements. After oxidative stress, bacterial samples were centrifugated at 4,000× g for 20 min, resuspended in 600 µl of cold methanol. The bacterial suspensions were sonicated thrice for 30 sec at 4.0 output, 70% pulsed (Branson Sonifier 250). Lysates were then centrifuged at 3,300× *g* for 8 min, to remove debris. Then, samples were purified through SPE column (Strata-X, 30 mg mL^{-1}, Phenomenex, California, USA). After elution, complete lyophilization and derivatization with methoxymation and syliation steps, 1 µl of each sample were injected on GC column coupled to detection mass. Analyses were performed on Shimadzu GC2/MS-2010 (Columbia, MD). Data represent the average of three independent cultures for each condition.

Virulence determination

Wild-type *F. novicida* and Δ*gadC* mutant strains were grown in TSB to exponential growth phase and diluted to the appropriate concentrations. 6 to 8-week-old female BALB/c mice (Janvier, Le Genest St Isle, France) were intra-peritoneally (i.p.) inoculated with 200 µl of bacterial suspension. The actual number of viable bacteria in the inoculum was determined by plating appropriate dilutions of bacterial cultures on Chocolate Polyvitex plates. For competitive infections, wild-type *F. novicida* and mutant bacteria were mixed in 1:1 ratio and a total of 100 bacteria were used for infection of each of five mice. After two days, mice were sacrificed. Homogenized spleen and liver tissue from the five mice in one experiment were mixed, diluted and spread on to chocolate agar plates. Kanamycin selection to distinguish wild-type and mutant

bacteria were performed. Competitive index (CI) [(mutant output/WT output)/(mutant input/WT input)]. Statistical analysis for CI experiments was as described in [51]. Macrophage experiments were analyzed by using the Student's *t*-test.

Supporting Information

Figure S1 The *gadC* region. (A) Schematic organization. The gene *gadC* (*FTN_0571*, grey arrow) is flanked, upstream (83 bp) by gene *FTN_0572* (transcribed on the opposite strand); and downstream, by gene *FTN_0570* (white arrows), separated by a 101 bp intergenic region. (**B**) **Transcriptional analysis.** We performed rapid amplification of cDNA ends (5′-RACE) to determine the 5′ end of the *gadC* mRNA. A broken arrow shows the transcription start of *gadC* (+1). Inspection of the sequence immediately upstream of the transcriptional start identified putative -10 and -35 promoter elements that share homology to the consensus site recognized by the major sigma factor σ^{70} [52]. The predicted σ^{70}-dependent -10 and -35 sequences are underlined. The predicted translation start codon of *gadC* is in bold italics. (**C**) **Quantitative real-time RT-PCR.** Quantification of *FTN_0570* expression in *F. novicida* strain U112 (WT) or *ΔgadC* mutant were performed in TSB at 37°C. qRT-PCRs were performed twice using independent samples (in triplicate).
(TIFF)

Figure S2 Growth kinetics in broth. Stationary-phase bacterial cultures of wild-type *F. novicida* and Δ*gadC* mutant strains were diluted to a final OD_{600} of 0.1, in 20 mL broth. Every hour, the OD_{600} of the culture was measured, during a 9 h-period. (**A**) CDM, chemically defined medium; (**B**) TSB, tryptic soy broth.
(TIFF)

Figure S3 Cell death. The cell death kinetics of infected BMM (from BALB/c mice) was followed by monitoring propidium iodide (PI) incorporation in real time. PI fluorescence was measured every 15 min on a microplate fluorimeter (Tecan Infinite 1000). BMM were infected with wild-type *F. novicida*, (WT), the Δ*gadC* mutant (Δ*gadC*), or the Δ*FPI* mutant (Δ*FPI*).
(TIFF)

Figure S4 The decarboxylase mutant Δ*gadB*. (**A**) Intracellular replication of wild-type *F. novicida* carrying the empty plasmid pKK214 (WT/pKK(−)), of the mutant Δ*gadB* and complemented strain (Δ*gadB*/pKK-*gadB*), and of the Δ*FPI* mutant (Δ*FPI*), was monitored in J774.1 macrophage-like cells over a 24 h-period. Results are shown as the average of $\log_{10}$ (cfu mL^{-1}) ± standard deviation. (**B**) Competition assays were performed by infecting a group of five female BALB/c mice by the i.p. route with a 1:1 mixture of wild-type bacteria and Δ*gadB* mutant strain (100 cfu of each). The data represent the competitive index (CI) value for cfu of mutant/wild-type in the liver (L: black diamonds, left column) and spleen (S: black circles, right column) of each mouse, 48 h after infection. Bars represent the geometric mean CI value.
(TIFF)

Figure S5 Oxidative stress response in the presence of the TCA cycle intermediates. Exponential phase bacteria, diluted in chemically defined medium supplemented with 1.5 mM glutamate were subjected to oxidative stress (500 µM H_20_2). *Upper panel*: in the presence or absence of fumarate (1.5 mM); *middle panel*: in the presence or absence of succinate (1.5 mM); *lower panel*: in the presence or absence of oxoglutarate (1.5 mM). The bacteria were plated on chocolate agar plates at different times and viable bacteria were monitored 2 days after. Data are the average cfu mL^{-1} for three points. Experiments were realized twice. **, $p<0.01$ (as determined by the Student's *t*-test).
(TIFF)

Figure S6 Fate of GadC-dependent glutamate entry into *Francisella*. External glutamate (Glu_E) is taken up by the GadC permease. Internal Glutamate (Glu_I) can be converted either to: i) glutamine by the glutamine synthase GlnA; ii) GABA by the glutamate decarboxylase GadD; ii) oxoglutarate (OG) by the glutamate dehydrogenase GdhA; or iii) glutathione (GSH) by the glutamate-cysteine ligase GshA and the glutathione synthetase GshB. Internal GABA may be either: i) translocated out of the cytoplasm, through GadC; or ii) converted to succinate (S), via the GABA shunt. The dotted green arrow indicates the alternative pathway leading (from Glu_I) to glutathione production (GSH, reduced form, GSSG, oxidized form). The dotted red arrows indicate the two possible pathways leading to the tricarboxylic acid (TCA) cycle: i) from glutamate to oxoglutarate, or ii) from GABA to succinate. OA, oxaloacetate; C, citrate; A, cis-aconitate; IC, isocitrate; OS, oxalosuccinate; S-CoA, succinyl-CoA; F, fumarate; M, malate. The two anti-oxidant pathways (GshA/GshB in green; GdhA in pink) lead to the production of glutathione (GSH) and oxoglutarate (OG) + NADPH, respectively. They allow the oxidoreduction reactions: 2 GSH + ROOH ↔ GSSG + ROH + H_2O; and NADPH + $2O_2$ ↔ $NADP^+$ + $2O_2^-$ + H^+), respectively.
(TIFF)

Text S1 Supporting text. This file includes one Table listing the strains, plasmids and primers used in this study (Table S1), Supplemental Experimental Procedures, and Supplemental References.
(DOCX)

Acknowledgments

We wish to thank the laboratory of Sebastian Amigorena (Institut Curie, Paris) for providing female p91 (phox) knockout mice (designated $p91^{phox-/-}$) and wild-type control mice (designated $p91^{phox+/+}$). We also thank Dr. JW Foster for providing the *E. coli* strains EF491 and EF547.

Author Contributions

Conceived and designed the experiments: ER TH KM MB AC. Performed the experiments: ER GG MR JD MD ID. Analyzed the data: ER KM TH MB AC. Wrote the paper: ER AC.

References

1. Sjostedt A, editor (2011) *Francisella tularensis* and tularemia: Fontiers Media SA.
2. Oyston PC, Sjostedt A, Titball RW (2004) Tularaemia: bioterrorism defence renews interest in *Francisella tularensis*. Nat Rev Microbiol 2: 967–978.
3. Keim P, Johansson A, Wagner DM (2007) Molecular epidemiolgy, evolution, and ecology of *Francisella*. Ann N Y Acad Sci 1105: 30–66.
4. Celli J, Zahrt TC (2013) Mechanisms of *Francisella tularensis* intracellular pathogenesis. Cold Spring Harb Perspect Med 3: a010314.
5. McCaffrey RL, Schwartz JT, Lindemann SR, Moreland JG, Buchan BW, et al. (2010) Multiple mechanisms of NADPH oxidase inhibition by type A and type B *Francisella tularensis*. J Leukoc Biol 88: 791–805.
6. Meibom KL, Charbit A (2010) The unraveling panoply of *Francisella tularensis* virulence attributes. Curr Opin Microbiol 13: 11–17.
7. Napier BA, Meyer L, Bina JE, Miller MA, Sjostedt A, et al. (2012) Link between intraphagosomal biotin and rapid phagosomal escape in *Francisella*. Proc Natl Acad Sci USA 109: 18084–18089.
8. Melillo AA, Bakshi CS, Melendez JA (2010) *Francisella tularensis* antioxidants harness reactive oxygen species to restrict macrophage signaling and cytokine production. J Biol Chem 285: 27553–27560.
9. Lindgren H, Shen H, Zingmark C, Golovliov I, Conlan W, et al. (2007) Resistance of *Francisella* strains against reactive nitrogen and oxygen species with special reference to the role of KatG. Infect Immun 75: 1303–1309.

10. Melillo AA, Mahawar M, Sellati TJ, Malik M, Metzger DW, et al. (2009) Identification of *Francisella tularensis* live vaccine strain CuZn superoxide dismutase as critical for resistance to extracellularly generated reactive oxygen species. J Bacteriol 191: 6447–6456.
11. Bakshi CS, Malik M, Regan K, Melendez JA, Metzger DW, et al. (2006) Superoxide dismutase B gene (*sodB*)-deficient mutants of *Francisella tularensis* demonstrate hypersensitivity to oxidative stress and attenuated virulence. J Bacteriol 188: 6443–6448.
12. Dieppedale J, Gesbert G, Ramond E, Chhuon C, Dubail I, et al. (2013) Possible links between stress defense and the tricarboxylic acid cycle in *Francisella* pathogenesis. Mol Cell Proteomics 12: 2278–2292.
13. Clemens DL, Lee BY, Horwitz MA (2004) Virulent and avirulent strains of *Francisella tularensis* prevent acidification and maturation of their phagosomes and escape into the cytoplasm in human macrophages. Infect Immun 72: 3204–3217.
14. Clemens DL, Lee BY, Horwitz MA (2009) *Francisella tularensis* phagosomal escape does not require acidification of the phagosome. Infect Immun 77: 1757–1773.
15. Santic M, Asare R, Skrobonja I, Jones S, Abu Kwaik Y (2008) Acquisition of the vacuolar ATPase proton pump and phagosome acidification are essential for escape of *Francisella tularensis* into the macrophage cytosol. Infect Immun 76: 2671–2677.
16. De Biase D, Pennacchietti E (2012) Glutamate decarboxylase-dependent acid resistance in orally acquired bacteria: function, distribution and biomedical implications of the *gadBC* operon. Mol Microbiol 86(4):770–86.
17. Foster JW (2004) *Escherichia coli* acid resistance: tales of an amateur acidophile. Nat Rev Microbiol 2: 898–907.
18. Karatzas KA, Brennan O, Heavin S, Morrissey J, O'Byrne CP (2010) Intracellular accumulation of high levels of gamma-aminobutyrate by *Listeria monocytogenes* 10403S in response to low pH: uncoupling of gamma-aminobutyrate synthesis from efflux in a chemically defined medium. Appl Environ Microbiol 76: 3529–3537.
19. Meibom KL, Charbit A (2010) *Francisella tularensis* metabolism and its relation to virulence. Front Microbiol 1: 140.
20. Gesbert G, Ramond E, Rigard M, Frapy E, Dupuis M, et al. (2013) Asparagine assimilation is critical for intracellular replication and dissemination of *Francisella*. Cell Microbiol [epub ahead of print].
21. Maier TM, Casey MS, Becker RH, Dorsey CW, Glass EM, et al. (2007) Identification of *Francisella tularensis* Himar1-based transposon mutants defective for replication in macrophages. Infect Immun 75: 5376–5389.
22. Weiss DS, Brotcke A, Henry T, Margolis JJ, Chan K, et al. (2007) *In vivo* negative selection screen identifies genes required for *Francisella* virulence. Proc Natl Acad Sci USA 104: 6037–6042.
23. Peng K, Monack DM (2010) Indoleamine 2,3-dioxygenase 1 is a lung-specific innate immune defense mechanism that inhibits growth of *Francisella tularensis* tryptophan auxotrophs. Infect Immun 78: 2723–2733.
24. Kraemer PS, Mitchell A, Pelletier MR, Gallagher LA, Wasnick M, et al. (2009) Genome-wide screen in *Francisella novicida* for genes required for pulmonary and systemic infection in mice. Infect Immun 77: 232–244.
25. Ma D, Lu P, Yan C, Fan C, Yin P, et al. (2012) Structure and mechanism of a glutamate-GABA antiporter. Nature 483: 632–636.
26. Lauriano CM, Barker JR, Nano FE, Arulanandam BP, Klose KE (2003) Allelic exchange in *Francisella tularensis* using PCR products. FEMS Microbiol Lett 229: 195–202.
27. Chamberlain RE (1965) Evaluation of Live Tularemia Vaccine Prepared in a Chemically Defined Medium. Appl Microbiol 13: 232–235.
28. Barel M, Meibom K, Charbit A (2010) Nucleolin, a shuttle protein promoting infection of human monocytes by *Francisella tularensis*. PLoS One 5: e14193.
29. Chong A, Wehrly T, Child R, Hansen B, Hwang S, et al. (2012) Cytosolic clearance of replication-deficient mutants reveals *Francisella tularensis* interactions with the autophagic pathway. Autophagy 8: 1342–1356.
30. Fernandes-Alnemri T, Yu JW, Juliana C, Solorzano L, Kang S, et al. (2010) The AIM2 inflammasome is critical for innate immunity to *Francisella tularensis*. Nat Immunol 11: 385–393.
31. Jones JW, Broz P, Monack DM (2011) Innate immune recognition of *Francisella tularensis*: activation of type-I interferons and the inflammasome. Front Microbiol 2: 16.
32. Rathinam VA, Jiang Z, Waggoner SN, Sharma S, Cole LE, et al. (2010) The AIM2 inflammasome is essential for host defense against cytosolic bacteria and DNA viruses. Nat Immunol 11: 395–402.
33. Pierini R, Juruj C, Perret M, Jones CL, Mangeot P, et al. (2012) AIM2/ASC triggers caspase-8-dependent apoptosis in Francisella-infected caspase-1-deficient macrophages. Cell Death Differ 19: 1709–1721.
34. Jack DL, Paulsen IT, Saier MH (2000) The amino acid/polyamine/organocation (APC) superfamily of transporters specific for amino acids, polyamines and organocations. Microbiology 146 (Pt 8): 1797–1814.
35. Takanashi T, Ogura Y, Taguchi H, Hashizoe M, Honda Y (1997) Fluorophotometric quantitation of oxidative stress in the retina in vivo. Invest Ophthalmol Vis Sci 38: 2721–2728.
36. Kwaik YA, Bumann D (2013) Microbial Quest for Food in vivo: ''Nutritional virulence'' as an emerging paradigm. Cell Microbiol 15: 882–890.
37. Mohapatra NP, Soni S, Reilly TJ, Liu J, Klose KE, et al. (2008) Combined deletion of four *Francisella novicida* acid phosphatases attenuates virulence and macrophage vacuolar escape. Infect Immun 76: 3690–3699.
38. Mohapatra NP, Soni S, Rajaram MV, Strandberg KL, Gunn JS (2013) Type A *Francisella tularensis* Acid Phosphatases Contribute to Pathogenesis. PLoS One 8: e56834.
39. Newsholme P, Procopio J, Lima MM, Pithon-Curi TC, Curi R (2003) Glutamine and glutamate–their central role in cell metabolism and function. Cell Biochem Funct 21: 1–9.
40. Feehily C, Karatzas KA (2012) Role of glutamate metabolism in bacterial responses towards acid and other stresses. J Appl Microbiol 114:11–24.
41. Cao J, Barbosa JM, Singh NK, Locy RD (2013) GABA shunt mediates thermotolerance in *Saccharomyces cerevisiae* by reducing reactive oxygen production. Yeast 30: 129–144.
42. Karatzas KA, Suur L, O'Byrne CP (2012) Characterization of the intracellular glutamate decarboxylase system: analysis of its function, transcription, and role in the acid resistance of various strains of *Listeria monocytogenes*. Appl Environ Microbiol 78: 3571–3579.
43. Asare R, Akimana C, Jones S, Abu Kwaik Y (2010) Molecular bases of proliferation of *Francisella tularensis* in arthropod vectors. Environ Microbiol 12: 2587–2612.
44. Mailloux RJ, Beriault R, Lemire J, Singh R, Chenier DR, et al. (2007) The tricarboxylic acid cycle, an ancient metabolic network with a novel twist. PLoS One 2: e690.
45. Eoh H, Rhee KY (2013) Multifunctional essentiality of succinate metabolism in adaptation to hypoxia in *Mycobacterium tuberculosis*. Proc Natl Acad Sci U S A 110: 6554–6559.
46. Richardson AR, Payne EC, Younger N, Karlinsey JE, Thomas VC, et al. (2011) Multiple targets of nitric oxide in the tricarboxylic acid cycle of Salmonella enterica serovar typhimurium. Cell Host Microbe 10: 33–43.
47. Thompson LJ, Merrell DS, Neilan BA, Mitchell H, Lee A, et al. (2003) Gene expression profiling of *Helicobacter pylori* reveals a growth-phase-dependent switch in virulence gene expression. Infect Immun 71: 2643–2655.
48. Alkhuder K, Meibom KL, Dubail I, Dupuis M, Charbit A (2009) Glutathione provides a source of cysteine essential for intracellular multiplication of *Francisella tularensis*. PLoS Pathog 5: e1000284.
49. Castanie-Cornet MP, Penfound TA, Smith D, Elliott JF, Foster JW (1999) Control of acid resistance in *Escherichia coli*. J Bacteriol 181: 3525–3535.
50. Rebrin I, Kamzalov S, Sohal RS (2003) Effects of age and caloric restriction on glutathione redox state in mice. Free Radic Biol Med 35: 626–635.
51. Brotcke A, Weiss DS, Kim CC, Chain P, Malfatti S, et al. (2006) Identification of MglA-regulated genes reveals novel virulence factors in *Francisella tularensis*. Infect Immun 74: 6642–6655.
52. Cowing DW, Bardwell JC, Craig EA, Woolford C, Hendrix RW, et al. (1985) Consensus sequence for *Escherichia coli* heat shock gene promoters. Proc Natl Acad Sci U S A 82: 2679–2683.

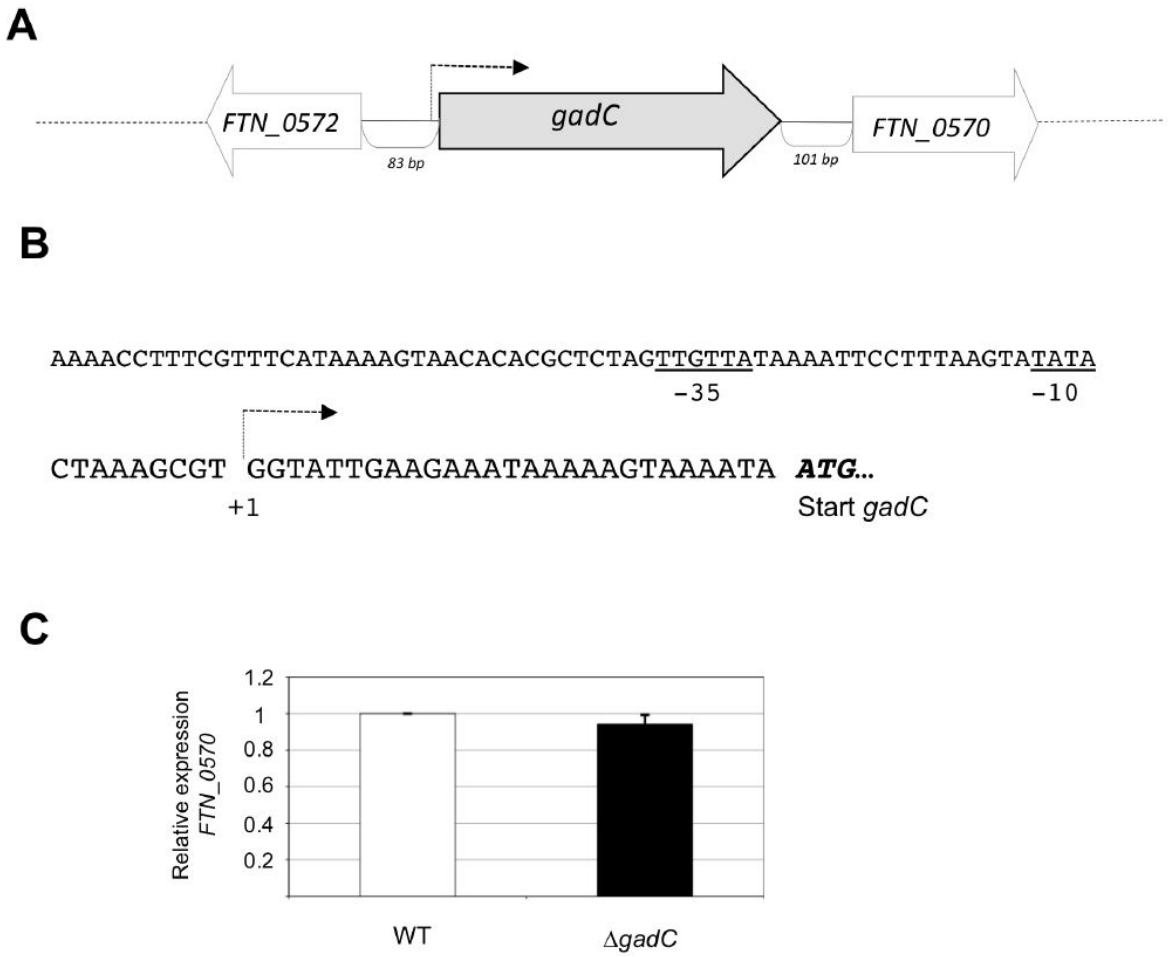

Figure S1

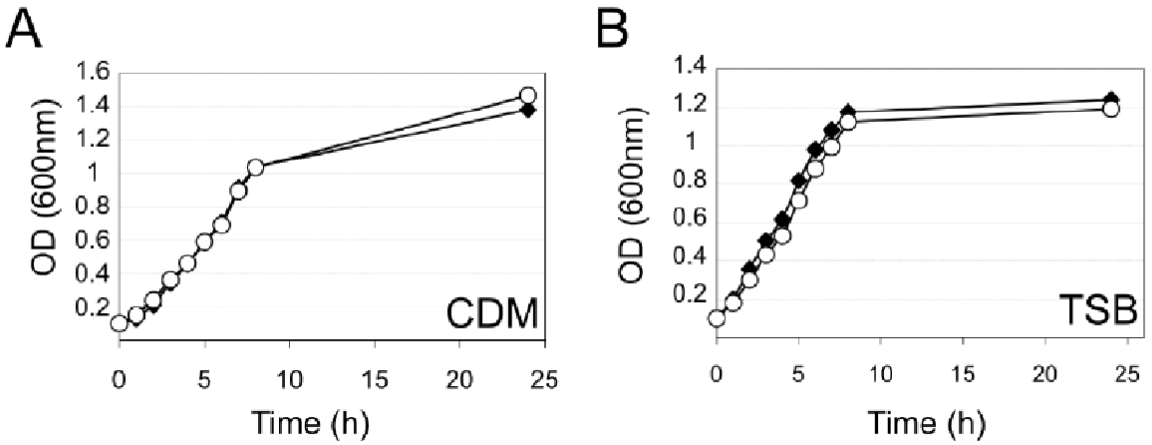

Figure S2

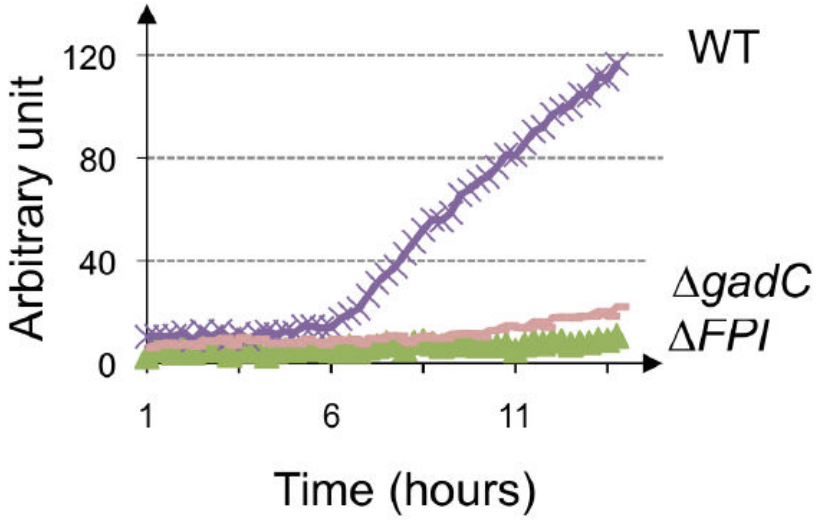

Figure S3

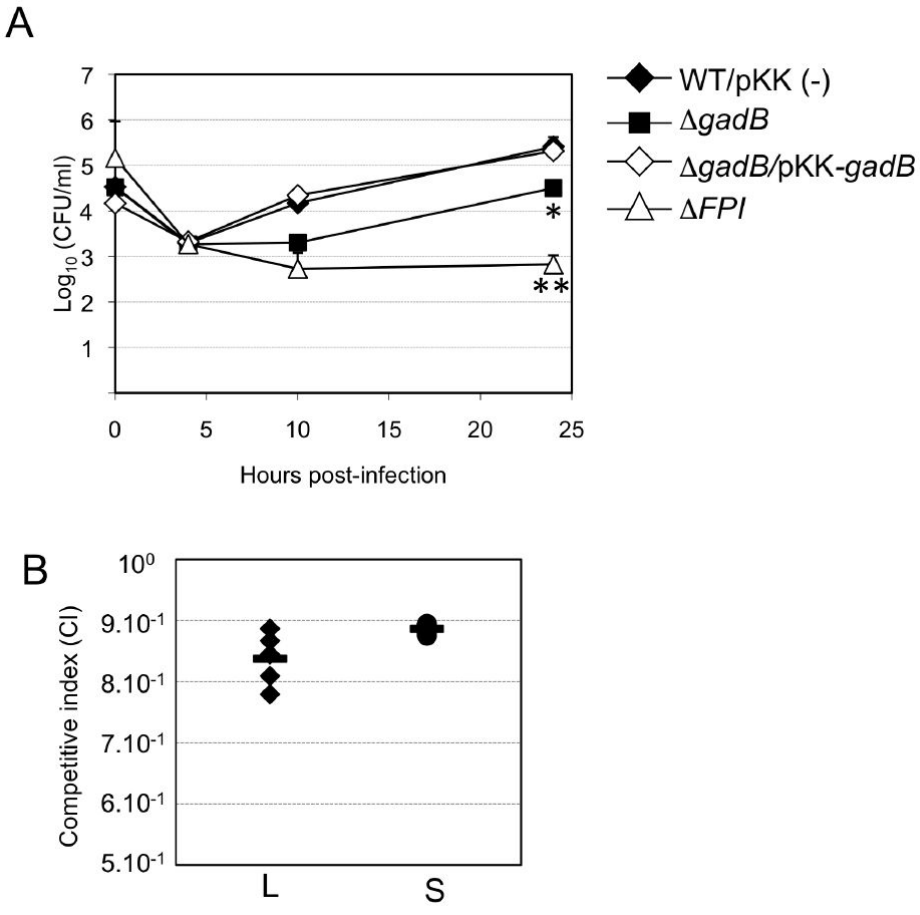

Figure S4

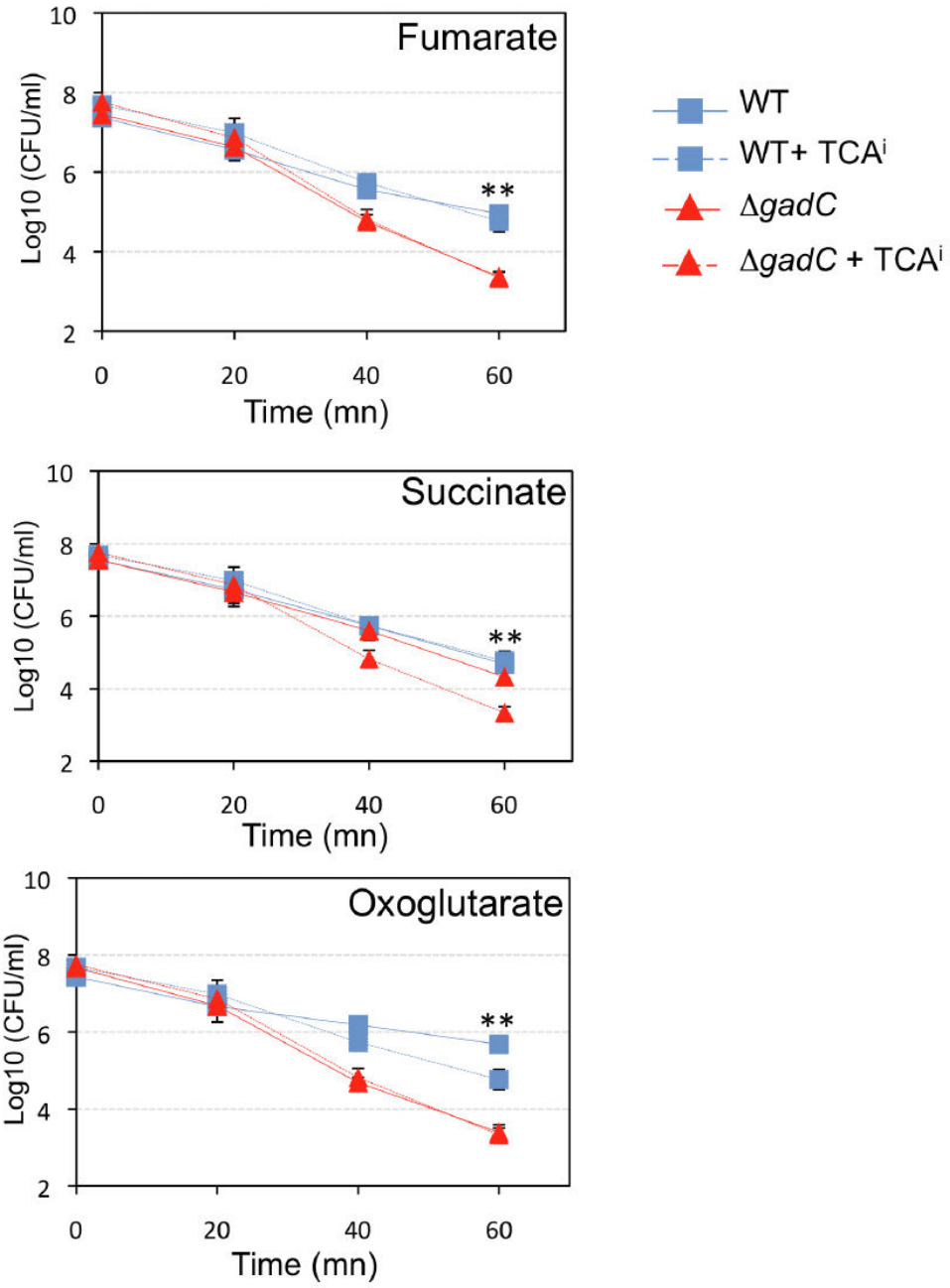
Fumarate
Succinate
Oxoglutarate
Log10 (CFU/ml)
Time (mn)
10
8
6
4
2
0
20
40
60
**
WT
WT+ TCA^{i}
ΔgadC
ΔgadC + TCA^{i}

Figure S5

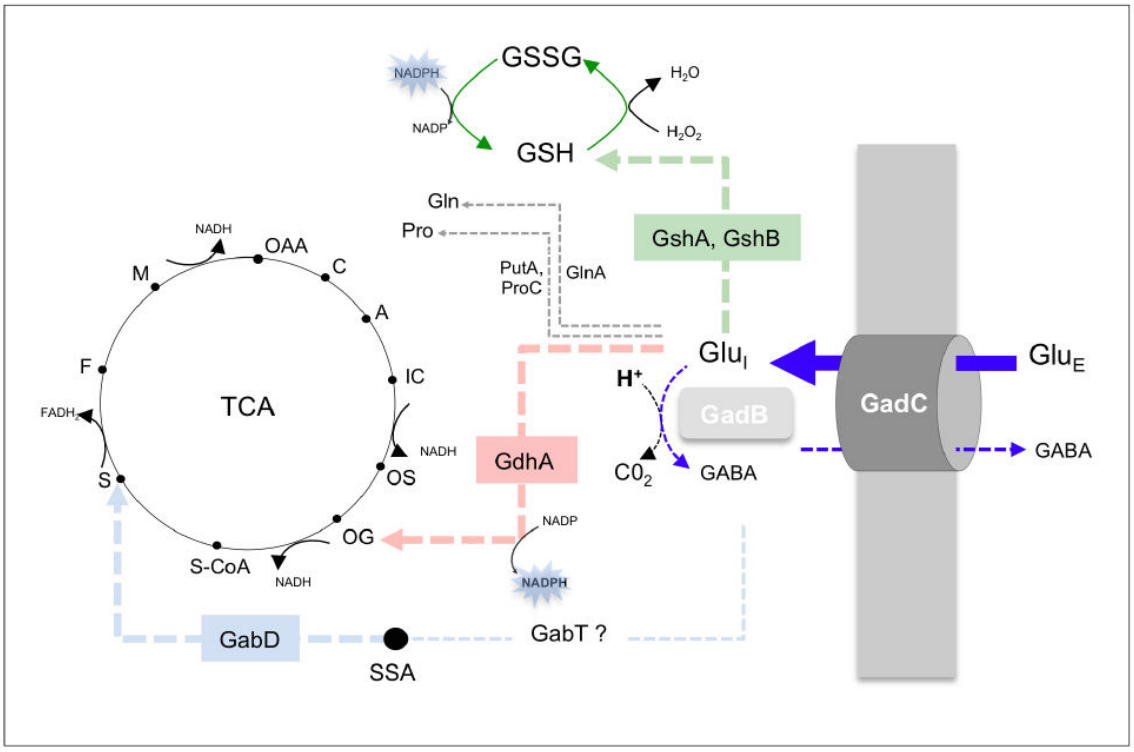

Figure S6

Table S1. Strains, plasmids and primers

Strain, plasmid, or primer	Primer code	Description or sequence (5′ → 3′)	Reference or source
E. coli strains			
E. coli DH5α		F– Φ80*lac*ZΔM15 Δ(*lac*ZYA-*arg*F) U169 *rec*A1 *end*A1 *hsd*R17 (rK–, mK+) *pho*A *sup*E44 λ– *thi*-1 *gyr*A96 *rel*A1	Laboratory strain collection
E. coli Top10		F– *mcr*A Δ(*mrr-hsd*RMS-*mcr*BC) Φ80*lac*ZΔM15 Δ*lac*X74 *rec*A1*ara*D139 Δ(*ara leu*) 7697 *gal*U *gal*K *rps*L (StrR) *end*A1 *nup*G	Laboratory strain collection
EF491		*E. coli* K12 *gadC*::pRR10 (Ap)	J.W. Foster (Castanie-Cornet et al., 1999)
EF547		*E. coli* K12 *gadC*::pRR10 (Ap)/pCF348 (*gadC*+ Tc^R)	J.W. Foster (Castanie-Cornet et al., 1999)
EF491 pCR.1TOPO-*FTN_0571*		*E. coli* K12 *gadC*::pRR10 (Ap) containing plasmid pCR.1TOPO-*FTN_0571*	This study

F. tularensis strains

U112	*F. tularensis* subsp. *novicida* U112	Laboratory strain collection
FTN (PKK214)	FTN containing empty plasmid PKK214	This study
FTNΔ*FTN_0571*	FTN with gene *FTN_0571* deleted	This study
FTNΔ*FTN_0571* (PKK214-*FTN_0571)*	FTN*ΔFTN_0571* containing PKK214-*FTN_0571*	This study
FTNΔ*FTN_1701*	FTN with gene *FTN_1701* deleted	This study
FTNΔ*FTN_1701* (PKK214-*FTN_1701)*	FTNΔ*FTN_1701* containing PKK214-*FTN_1701*	This study

Plasmids

pKK214	Derived from pKK202, promoter trap vector drives Cm^R Tet^R	Laboratory plasmid collection
pCR2.1TOPO	PCR cloning vector, Amp^R Km^R	Invitrogen

Primers

Pgro_F	1	TTG TAT GGA TTA GTC GAG CTA AA
npt_R	2	TCA GAA GAA CTC GTC AAG AAG G
FTN_0571upF	3	CAC ACC TTT ACC TAG TCT TTG C
FTN_0571upR	4	GAG CTT TTT AGC TCG ACT AAT CCA TAC AAC TTA AGC TAT CGA CAG CGA T
FTN_0571downF	5	CTA TCG CCT TCT TGA CGA GTT CTT CTG ACG ATA TGAA TGC TTA TTG TAG G
FTN_0571downR	6	GTC GAT ACT ATC AAA CCA GC
FTN_0571upF2 control	7	ACA TGG AGC TAT TTG TTT GA
FTN_0571downR2 control	8	TTA GTA CAG AAA ATA AAA CTG G
FTN_0571 5'race GSP1	9	CGA AGA ATC CAC AAA TAG ATG G
FTN_0571 5'race GSP2	10	ACT TTG TAA ACC CAC TGT AAC C
FTN_0571 compl forw	11	GAA TCC TTT AGA GTG TCA AAG CTT TT
FTN_0571 compl rev	12	CAT ACT ACT GAA ATT GTT GCG CC
FTN_0571 qRT forw	13	CAT ACT ACT GAA ATT GTT GCG CC
FTN_0571 qRT rev	14	CCT GAA ATT AGG AGG GCA CGA
FTN_0570 qRT forw	15	GGT GAT TAT ATA GCT CCA ATA TTA GCT GCA
FTN_0570 qRT rev	16	AAT ATA TAC TAA AAC TAT ACG CTT AAG CTT GGT G
FTN_0571up PCR TOPO	17	CGTTTCATAAAAGTAACACACGCTCTAG
FTN_0571down PCR TOPO	18	GAA TTC AAA GTG TTG ATA TTG TAA CAG TTT TAC

FTN_1701upF	19	TCA AGA GAT TGG TGC GGA T
FTN_1701upR	20	GAG CTT TTT AGC TCG ACT AAT CCA TAC AAT CAT CAA CTT CCG TTT GGC
FTN_1701downF	21	CTA TCG CCT TCT TGA CGA GTT CTT CTG ATG ATG ATT AGA GAT TTA GTT GCG G
FTN_1701downR	22	TGG CAC ATT AGT GAG ATT GCC
FTN_1701upF2 control	23	AGA GGA TAT CTT TGT TGC AGA AA
FTN_1701downR2 control	24	CAT AGC CCC CTT TGA CAT G
FTN_1701 compl forw	25	CCC GGG CTC ATG GCT TAG TAA TAG TTA TCC
FTN_1701 compl rev	26	GAA TTC AAC CTG ATC TGG TCC AGC
FTN_1700 qRT forw	27	GCA GGG ATT GCA ACT ATG GAT C
FTN_1700 qRT rev	28	ATA TCT AAC ATG ACC GAT ACC CAT ATT ACC
FTN_1701 qRT forw	29	TCG AAG CAA AAT TTA GCG ACG
FTN_1701 qRT rev	30	GTT TGC CAG GAT ATT T
FTN_1702 qRT forw	31	GCT GAT GAA GTC GCG ATG GTT GGC G
FTN_1702 qRT rev	32	CGG CAC CGT TTC AAC ATT TGC CGC
FTN_1532 qRT forw	33	AGG CTT CGA GCA AGT TTT CA
FTN_1532 qRT rev	34	ACC GCA CCA TAA CCT GTA GC
FTN_0127 qRT forw	35	AGC CAT TAG CTG AGG CAA AA
FTN_0127 qRT rev	36	TGC AAG TGC TGT GAG AGG AG
FTN_0277 qRT forw	37	CAA GTC CCG CAC AAA AAG AT
FTN_0277 qRT rev	38	CTT ATA CCC ACC GGC TCA AA
FTN_0804 qRT forw	39	CGC ATA CCT TGA TCA CCA GA
FTN_0804 qRT rev	40	CTG CAA GAT TGC CAC GAT TA
FTN_0593 qRT forw	41	CGT GGC GTA ACT CCT GGT AA
FTN_0593 qRT rev	42	TGA CCC GGC ATA ATA CCA AT
FTN_1434 qRT forw	43	TTG TTT GGT CAT GCG GTA GA
FTN_1434 qRT rev	44	TTT GCC ATC TTT GTT CCA CA
FTN_1635 qRT forw	45	GCT CAA TTT GGC GAT TTT GT
FTN_1635 qRT rev	46	TCG GCG TCA TTA CAA TCA AA

Supplemental Experimental procedures

Bacterial growth

F. novicida and its mutant derivatives were grown: i) in liquid, on Tryptic Soya broth (TSB, Becton, Dickinson and company) or Chamberlain chemically defined medium (CDM) and ii) in solid, on pre-made chocolate agar PolyViteX (BioMerieux SA Marcy l'Etoile, France) or chocolate plates prepared from GC medium base, IsoVitalex vitamins and haemoglobin (BD Biosciences, San Jose, CA, USA), at 37°C. *E. coli* was grown in LB (Luria-Bertani, Difco) at 37°C. Ampicillin was used at a final concentration of 100 μg mL^{-1} to select recombinant *E. coli* carrying pGEM and its derivatives. Kanamycin was used at a final concentration of 50 μg mL^{-1} and 20 μg mL^{-1} to select respectively recombinant *E. coli* and *Francisella* carrying pKK and its derivates. All bacterial strains, plasmids, and primers used in this study are listed in **Supplemental Table 1**.

Construction of a chromosomal Δ*gadC* deletion mutant

We have generated a chromosomal deletion of gene *FTN_0571* (*gadC*) in *F. novicida* strain U112 by allelic replacement of the wild-type region with a mutated region deleted of the entire *gadC* gene (from the ATG start codon till the TAA stop codon), substituted by the kanamycine resistance gene *npt* placed under the control of the P*gro* promoter. First, the two regions (app. 600 bp each) flanking gene *gadC* (designated *FTN_0571*up and *FTN_0571*down, respectively), and the *npt* gene (1,161 bp, amplified from plasmid pFNLTP16H3, (Maier et al., 2006), were amplified by PCR using the following pairs of primers: i) *FTN_0571*up, p3, p4; ii) *FTN_0571*down, p5, p6; iii) *npt*, p1, p2. The region

*FTN_0571*up-*npt*-*FTN_0571*down (*ca*. 2300 bp) was then amplified by triple overlap PCR, using the *FTN_0571*up, *FTN_0571*down and *npt* products. The resulting PCR product was gel purifed (using the QIAquick Gel extraction kit, QIAgen) and directly used to transform wild-type *F. novicida*. Chemical transformation was performed as described in (Ludu et al., 2008). Recombinant bacteria, resulting from allelic replacement of the wild-type region with the mutated *FTN_0571up*/*npt*/ *FTN_0571down* region, were selected on kanamycine-containing plates (20 μg mL^{-1}). The mutant strain, designated Δ*gadC,* was checked for loss of the wild-type *gadC* gene, using specific primers in PCR and qRT_PCR, by PCR sequencing (GATC Biotech) and Southern blot.

Functional complementation

The plasmid used for complementation of the Δ*gadC* mutant, pKK-*gadC*, was constructed by amplifying a 1,588 bp fragment (corresponding to the sequence 148 bp upstream of the *gadC* start codon and to 25 bp downstream of the stop codon) using primers *FTN_0571* compl forw and *FTN_0571* compl rev (**Supplemental Table 1**), followed by digestion with *Eco*RI and *Sma*I, and cloning into plasmid pKK214 (Kuoppa et al., 2001).

The plasmid used for complementation of the *ΔgadB* mutant, pKK-*gadB*, was constructed by amplifying a 1,638 bp fragment (corresponding to the sequence 159 bp upstream of the *gadC* start codon and to 133 bp downstream of the stop codon) using primers FTN_1701 compl forw and FTN_1701 compl rev (**Supplemental Table 1**), followed by digestion with *Eco*RI and *Sma*I, and cloning into plasmid pKK214 (Kuoppa et al., 2001). The plasmids pKK214, pKK214-*gadB* and pKK214-*gadC,* were introduced into wild-type *F. novicida* or into the Δ*gadB* and Δ*gadC* mutants by electroporation, as described previously (Dieppedale et al., 2011).

Multiplication in macrophages

J774.1 macrophage-like cells (ATCC Number: TIB67) were propagated in Dulbecco´s Modified Eagle's Medium (DMEM) containing 10% fetal calf serum, whereas human monocyte-like cell line THP-1 (ATCC Number: TIB202) and bone marrow-derived macrophages (BMM) from BALB/c were propagated in RPMI Medium 1640 containing 10% fetal calf serum, respectively. J774.1 and BMM were seeded at a concentration of ~2 x 10^5 cells per well in 12-well cell tissue plates and monolayers were used 24 h after seeding. THP-1 were seeded at a concentration of ~2 x 10^5 cells per well in 12-well cell tissue plates 48h before infection, and supplemented with phorbol myristate acetate (PMA) to induce cell differentiation (200 ng mL^{-1}). J774.1, BMM and THP-1 were incubated for 60 min at 37°C with the bacterial suspensions (approximate multiplicities of infection 100) to allow the bacteria to enter. After washing (time zero of the kinetic analysis), the cells were incubated in fresh culture medium containing gentamicin (10 µg mL^{-1}) to kill extracellular bacteria. At several time-points, cells were washed three times in DMEM or RPMI, macrophages were lysed by addition of water and the titer of viable bacteria released from the cells was determined by spreading preparations on Chocolate agar plates. For each strain and time in an experiment, the assay was performed in triplicate. Each experiment was independently repeated at least three times and the data presented originate from one typical experiment.

Real time cell death assay

The cell death kinetics was followed by monitoring propidium iodide incorporation in real time. Briefly, 5x10^4 BMM were seeded in 0.3 cm^2 wells of black 96 flat-bottom-well plate 24 hours before infection. Infection was performed as described above. One hour post-infection,

cells were washed three times and placed in CO2-independent medium (Gibco) supplemented with propidium iodide (5 µg mL^{-1}), 10% FCS, 10% M-CSF containing supernatant. Propidium iodide fluorescence was measured every 15 minutes on a micro plate fluorimeter (Tecan Infinite 1000).

References

Alkhuder, K., Meibom, K.L., Dubail, I., Dupuis, M., and Charbit, A. (2009). Glutathione provides a source of cysteine essential for intracellular multiplication of *Francisella tularensis*. PLoS Pathog *5*, e1000284.

Castanie-Cornet, M.P., Penfound, T.A., Smith, D., Elliott, J.F., and Foster, J.W. (1999). Control of acid resistance in *Escherichia coli*. J Bacteriol *181*, 3525-3535.

Dieppedale, J., Sobral, D., Dupuis, M., Dubail, I., Klimentova, J., Stulik, J., Postic, G., Frapy, E., Meibom, K.L., Barel, M., *et al*. (2011). Identification of a putative chaperone involved in stress resistance and virulence in *Francisella tularensis*. Infect Immun *79*, 1428-1439.

Kuoppa, K., Forsberg, A., and Norqvist, A. (2001). Construction of a reporter plasmid for screening in vivo promoter activity in *Francisella tularensis*. FEMS Microbiol Lett *205*, 77-81.

Ludu, J.S., de Bruin, O.M., Duplantis, B.N., Schmerk, C.L., Chou, A.Y., Elkins, K.L., and Nano, F.E. (2008). The Francisella pathogenicity island protein PdpD is required for full virulence and associates with homologues of the type VI secretion system. J Bacteriol *190*, 4584-4595.

Maier, T.M., Pechous, R., Casey, M., Zahrt, T.C., and Frank, D.W. (2006). In vivo Himar1-based transposon mutagenesis of *Francisella tularensis*. Appl Environ Microbiol *72*, 1878-1885.

Article n°2

Importance of host cell arginine import in ribosomal protein biogenesis and phagosomal escape of *Francisella*.

Elodie Ramond, Gael Gesbert, Ida Chiara Guerrera, Cerina Chhuon, Marion Dupuis, Mélanie Rigard, Thomas Henry, Monique Barel et Alain Charbit.

Je me suis ensuite intéressée à un second transporteur de la famille APC codé par le gène *FTN_0848* et appelée par la suite ArgP. Nous avons fait le choix d'étudier ce gène car il s'agit du paralogue le plus proche de la protéine GadC, avec une identité peptidique de 33.4%. De plus, le gène a*rgP* a été retrouvé dans plusieurs cribles génétiques (Ahlund et al., 2010; Moule et al., 2010; Peng et al., 2010; Su et al., 2007; Weiss et al., 2007), suggérant un rôle important de gène dans la virulence de *F. tularensis*.

Nous avons démontré que le gène *argP* code pour un importeur d'arginine à haute affinité. Cette protéine est essentielle pour l'échappement phagosomal de *F. tularensis* dans un modèle cellulaire macrophagique et permet sa réplication dans le cytosol. Le transporteur ArgP est aussi essentiel pour la virulence de la bactérie dans un modèle murin. D'autre part, nous avons mis en évidence l'importance de l'importation d'arginine par la bactérie dans la biogenèse des protéines ribosomales bactériennes par une analyse protéomique par spéctrométrie de masse à haute résolution. Les résultats obtenus suggèrent un lien fort entre la synthèse des protéines et le l'échappement phagosomal.

Importance of host cell arginine uptake in *Francisella* phagosomal escape and ribosomal proteins synthesis

Elodie Ramond[1,2], Gael Gesbert[1,2], Ida Chiara Guerrera[1,3], Cerina Chhuon[1,3], Marion Dupuis[1,2], Mélanie Rigard[4], Thomas Henry[4], Monique Barel[1,2], Alain Charbit[1,2]*

[1] Université Paris Descartes, Sorbonne Paris Cité, Bâtiment Leriche.

[2] INSERM U1151 - CNRS UMR 8253, Institut Necker-Enfants Malades, Team 11. Paris, France

[3] Plateforme Protéome Institut Necker, PPN, Structure Fédérative de Recherche SFR Necker, Université Paris Descartes, Paris 75015 France

[4] CIRI, Centre International de Recherche en Infectiologie, Lyon, France

Running title: Arginine uptake and phagosomal escape in *Francisella* pathogenesis

Keywords: arginine uptake; Intracellular pathogen; phagosomal escape; *Francisella*; ribosomal protein biogenesis

*Corresponding author: Alain Charbit; Bâtiment Leriche. 96 rue Didot 75993 Paris Cedex 14 - France

e-mail: alain.charbit@inserm.fr

Tel.: 33 1 – 72 60 65 11 — Fax: 33 1 - 72 60 65 13

Abbreviations	Definition
APC	Amino acid/polyamine/organocation
BMM	Bone marrow derived macrophages
CCF	Coumarin-cephalosporin-fluorescein
CDM	Chemically defined medium
CFU	Colony forming unit
CI	Competition index
DMEM	Dubelcco's modified eagle medium
E-AA	Essential amino acid
FCP	*Francisella*-containing phagosome
FDR	False discovery rate
FPI	*Francisella* pathogenicity Island
FRET	Fluorescence resonance energy transfer
iNOS	Inducible nitric oxyde synthase
KEGG	Kyoto encyclopedia of genes and genomes
L-NAME	L-N^G-Nitroarginine methyl ester
LAMP	Lysosomal associated membrane protein
LC-MS/MS	Liquid chromatography coupled to tandem mass spectrometry
LFQ	Label free quantification
LVS	Live vaccine strain
MOI	Multiplicity of infection
NE-AA	Non essential amino acid
NO	Nitric oxyde
OD	Optical density
qRT-PCR	Quantitative real-time polymerase chain reaction
TCA	Tricarboxylic acid
TSB	Triptic soy broth

SUMMARY

Upon entry into mammalian host cells, the pathogenic bacterium *Francisella* must import cell host arginine to multiply actively in the host cytoplasm. We identified an arginine transporter (hereafter designated ArgP) whose inactivation considerably delayed bacterial phagosomal escape and intracellular multiplication. Intra-macrophagic growth of the Δ*argP* mutant was fully restored upon supplementation of the growth medium with excess arginine, in both *F. tularensis* subsp *novicida* and *F. tularensis* subsp *holarctica* LVS, demonstrating the importance of arginine acquisition in these two subspecies. High-resolution mass spectrometry revealed that arginine limitation reduced the expression of essentially all the ribosomal proteins and concomitantly increased the expression of the major stress-related chaperones in the Δ*argP* mutant. In response to stresses such as nutritional limitation, repression of ribosomal protein synthesis has been observed in all kingdoms of life. Arginine availability may thus contribute to the sensing of the intracellular stage of the pathogen and to trigger phagosomal egress.

INTRODUCTION

Francisella tularensis is a Gram-negative coccobacillus responsible for the zoonotic disease tularemia. This pathogen is considered as one of the most virulent microorganisms and has been categorized as a Category A select agent by the USA Centers for Disease Control and Prevention (CDC). It is known to infect a broad range of animal species such as mammals including humans. *F. tularensis* is a facultative intracellular pathogen able to multiply in a variety of cell types but is thought to multiply in vivo preferentially in macrophages [1]. Upon entry into macrophages, *Francisella* escapes within one hour from *Francisella*-containing phagosome (FCP) to reach the cytosolic compartment where it multiplies actively [2]. To multiply efficiently in its cytosolic niche, *Francisella* needs to evade the immune responses of the host [3] and express dedicated virulence factors [4]. The bacteria must also adapt its metabolism to the nutrients available in the infected host [5] and has, therefore, developed sophisticated tools recently designated as "nutritional virulence" attributes [6,7].

Amino acids have been described as the essential nutrient source that *Francisella* has evolved to scavenge, by different means, during its intracellular life cycle [8]. For examples, activation of the host macro-autophagy degradation machinery [9], and exploitation of host polypeptides, such as glutathione [10], allow *Francisella* to obtain its essential amino acids. In addition, we recently demonstrated that *Francisella* possessed several amino acid transporters that were required to fulfill some of its metabolic requirements during different stages of its intracellular progression [11,12]. We showed, for example that AnsP-dependent asparagine uptake was critical for efficient bacterial multiplication in the cytosolic compartment of infected macrophages [12]. We also found that amino acid uptake was not restricted to a nutritional function and could participate to stress resistance. In particular, the

transporter GadC, a member of the amino acid/polyamine/organocation (APC) superfamily [13], promoted bacterial resistance to the oxidative stress generated in the phagosomal compartment by providing glutamate that was used to fuel the tricarboxylic acid (TCA) cycle [11].

A recent study revealed that *Salmonella* virulence depended on the simultaneous exploitation of numerous different host nutrients, including vitamins, carbohydrates and amino acids [14]. Comparisons of the predicted nutrient utilization and biosynthetic pathways of a series of other mammalian pathogens confirmed that most pathogens shared the capability to utilize multiple nitrogen and carbon sources. The recent literature suggests that *Francisella* also relies on multiple host-derived amino acid sources to multiply intracellularly [9,10,11,12].

Francisella genomes are predicted to encode eleven APC family members possibly involved in different amino acid uptake functions. Remarkably, only two of them *i.e. gadC* (*FTN_0571*) and *FTN_0848* (in *F. novicida*), were identified in at least four different genetic screens as potentially involved in bacterial virulence. FTN_0848 is the closest paralogue of GadC in *F. novicida* and shares 33.4% amino acid identity with GadC. In addition, the gene *FTN_0848* has been identified in multiple in vitro and in vivo screens, in both *F. novicida* and *F. tularensis* LVS [15,16,17,18,19,20], suggesting that it displays functions that could not be replaced by other *Francisella* transporter.

We demonstrate here that *argP* encodes a high affinity arginine transporter (hence designated ArgP for simplification). Arginine is an essential amino acid that can only be obtained by intracellular *Francisella* via import from the host. We show that ArgP-mediated arginine uptake is crucial for efficient phagosomal escape, highlighting for the first time the

importance of essential amino acids during early stage infection. The data presented further suggest that arginine limitation influences ribosomal protein synthesis.

EXPERIMENTAL PROCEDURES

Bacterial Strains, Media, and Chemicals

F. tularensis subsp. *novicida* (*F. novicida*) strain U112, its Δ*FPI* derivative, *F. tularensis* subsp. *holartica* strain LVS, its Δ*iglC* derivative, and all the mutant strains constructed in this work, were grown as described in **Supplementary Material**. All bacterial strains, plasmids, and primers used in this study are listed in **Table S2**.

Details of the construction and characterization of mutant and complemented strains; macrophage preparation and infections, are described in **Supplementary Material**. Quantitative (q)RT-PCR (real-time PCR) was performed with gene-specific primers (**Table S2**), using an ABI PRISM 7700 and SYBR green PCR master mix (Applied Biosystems, Foster city, CA, USA), are described in **Supplementary Material**.

Confocal and electron microscopy complete descriptions; real time cell death and phagosome permeabilisation assays, are described in **Supplementary Material**.

Stress survival assays

Oxidative stress. Exponential-phase bacterial cultures in TSB broth were diluted to a final concentration of 10^8 bacteria mL^{-1} and subjected to 500 μM H_2O_2. The number of viable bacteria was determined by plating appropriate dilutions of bacterial cultures on Chocolate Polyvitex plates at the start of the experiment and after the indicated durations. Cultures (10

mL) were incubated at 37°C with rotation (180 rpm) and aliquots were removed at indicated times, serially diluted and plated immediately.

pH stress. Bacteria were incubated for 2 h in CDM at pH 4, the presence of various arginine concentrations (2.3 mM, 0.46 mM and 0.23 mM). At 30 min intervals, bacteria were collected and numerated on TSB solid medium.

Bacteria were enumerated after 48 h incubation at 37°C. Each point represents the average of three different plates. Experiments were repeated independently twice.

Evaluation of nitrite levels

NO levels in supernatants were evaluated with Griess test. Briefly, J774.1 cells were seeded at 2.10^5cells/well in 96 microplates. Cells were infected at an MOI of 1000 for 1 h with WT or *ΔargP* strains versus non-infected cells, with DMEM without red phenol. 100 μl of each cell culture supernatant were reacted with equal volumes of Griess reagent (1% sulfanilamide, 0.1% naphthylenediamine dihydrochloride, 2.5% H_3PO_4) at room temperature (RT) for 10 min away from light. Sodium nitrite was used to generate a standard curve for NO_2^- production, and peak absorbance was measured at 540 nm (Biorad, iMark microplate absorbance reader). Levels present in cell medium of non-infected cells were subtracted from the values of experimental cultures.

L-NAME effect on ΔargP mutant

One day before infection, J774.1 cells were seeded at 2.10^5cells/well in 12-well cell tissue plates, supplemented with L-NAME (NG-nitro-L-arginine methyl ester hydrochloride) at the concentration of 1mM in DMEM. Cells were infected at an MOI 100 for 1 h. Bacteria were then counted after 1 h, 4 h, 10 h and 24 h of infection as described previously. L-NAME was present all along the infection.

Arginine transport assays

Cells were grown in Chamberlain medium to mid-exponential phase and then harvested by centrifugation and washed twice with Chamberlain without amino acid. The cells were suspended at a final OD_{600nm} of 0.5 in the same medium containing 50 μg mL^{-1} of chloramphenicol. After 15 min of pre-incubation at 25°C, uptake was started by the addition of L-[U-^{14}C] arginine (Perkin Elmer), at various concentrations (^{14}C-Arg ranging from 1 to 50 μM). The radiolabelled ^{14}C-Arg was at a specific activity of 9.25 GBq.mmol $^{-1}$. Samples (100 μL of bacterial suspension) were removed after 5 min and collected by vacuum filtration on membrane filters (Millipore type HA, 25 mm, 0.22 mm) and rapidly washed with Chamberlain without amino acid (2 x 5 mL). The filters were transferred to scintillation vials and counted in a Hidex 300 scintillation counter. The counts per minute (c.p.m.) were converted to picomoles of amino acid taken up per sample, using a standard derived by counting a known quantity of the same isotope under similar conditions.

Virulence Determination

All experimental procedures involving animals were conducted in accordance with guidelines established by the French and European regulations for the care and use of laboratory animals (Decree 87–848, 2001–464, 2001–486 and 2001–131 and European Directive 2010/63/UE) and approved by the INSERM Ethics Committee (Authorization Number: 75-906).

Wild-type *F. novicida* and Δ*argP* mutant strains were grown in TSB to exponential growth phase and diluted to the appropriate concentrations. 6 to 8-week-old female BALB/c mice (Janvier, Le Genest St Isle, France) were intraperitoneally (i.p.) inoculated with 200 µl of

bacterial suspension. The actual number of viable bacteria in the inoculum was determined by plating dilutions of the bacterial suspension on chocolate plates. For competitive infections, wild-type *F. novicida* and mutant bacteria were mixed in 1:1 ratio and a total of 100 bacteria were used for infection of each of five mice. After two days, mice were sacrificed. Homogenized spleen and liver tissue from the five mice in one experiment were mixed, diluted and spread on to chocolate agar plates. Kanamycin selection to distinguish wild-type and mutant bacteria was performed. Competitive index (CI) [(mutant output/WT output)/(mutant input/WT input)]. Statistical analysis for CI experiments was as described in [21]. Macrophage experiments were analyzed by using the Student's unpaired t test.

MS/MS Protein Identification and Quantification

WT and Δ*argP* mutant strains were grown overnight in CDM_{min}. The next day, bacteria were resuspended at an OD_{600} of 0.1 in CDM_{min} or in CDM containing arginine at the concentration of 0.43 mM and cultivated for 1 h or 2 h. The cells (50 mL) were harvested by centrifugation at 3,000 x *g* for 20 min and resuspended in 2 mL of 5 mM Tris-HCl pH 8. The bacterial suspensions were sonicated three times for 30 s at 4.0 output, 70% pulsed (Branson Sonifier 250). Lysates were centrifuged once again at 8,000 x *g* for 6 min and supernatant were collected.

For label-free, relative quantitative analysis, 50 μg protein from each of the eight samples (WT and Δ*argP*, at 1 h and 2 h of growth, at 2.3 mM or 0.46 mM arginine) were precipitated in 80%, acetone and digested with 1 μg sequencing grade trypsin (Promega). Following an overnight digestion at 37°C samples were vacuum dried, and resuspended in 100 μL of 10% acetonitrile, 0.1% formic acid, for LC-MS/MS.

For each run, 5 μL were injected in a nanoRSLC-Q Exactive PLUS (Dionex RSLC Ultimate 3000, Thermo Scientific, Waltham, MA, USA). Peptides were separated on a reversed-phase

211 liquid chromatographic column (Pepmap C18, Dionex). Chromatography solvents were (A)
212 0.1% formic acid in water, and (B) 80% acetonitrile, 0.08% formic acid. Peptides were eluted
213 from the column with the following gradient 5% to 40% B (120 min), 40% to 80% (10
214 minutes). At 131 min, the gradient returned to 5% to re-equilibrate the column for 30 minutes
215 before the next injection. Two blanks, one short 40 min-step gradient and one 60 min-linear
216 gradient, were run between triplicates to prevent sample carryover. Peptides eluting from the
217 column were analyzed by data dependent MS/MS, using top-10 acquisition method. Briefly,
218 the instrument settings were as follows: resolution was set to 70,000 for MS scans and 17,500
219 for the data dependent MS/MS scans in order to increase speed. The MS AGC target was set
220 to 3.10^6 counts, while MS/MS AGC target was set to 5.10^4. The MS scan range was from 400
221 to 2000 m/z. MS and MS/MS scans were recorded in profile mode. Dynamic exclusion was
222 set to 20 sec duration. Three replicates of each sample were analyzed by nanoLC/MS/MS.
223
224 *Data Processing Following LC-MS/MS acquisition*
225 The MS files were processed with the MaxQuant software version 1.4.1.2 and searched with
226 Andromeda search engine against the NCBI *F. tularensis* subsp. *novicida* database (release
227 28-04-2014, 1719 entries). To search parent mass and fragment ions, we set an initial mass
228 deviation of 4.5 ppm and 0.5 Da respectively. The minimum peptide length was set to 7
229 aminoacids and strict specificity for trypsin cleavage was required, allowing up to two missed
230 cleavage sites. Carbamidomethylation (Cys) was set as fixed modification, whereas oxidation
231 (Met) and N-term acetylation were set as variable modifications. The false discovery rates
232 (FDRs) at the protein and peptide level were set to 1%. Scores were calculated in MaxQuant
233 as described previously (Cox J., Mann M., 2008). The reverse and common contaminants hits
234 were removed from MaxQuant output. Proteins were quantified according to the MaxQuant

label-free algorithm using LFQ intensities [22,23]; protein quantification was obtained using at least 2 peptides per protein.

Statistical and bioinformatic analysis, including heatmaps, profile plots and clustering, were performed with Perseus software (version 1.4.1.3) freely available at www.perseus-framework.org. For statistical comparison, we set eight groups, each containing triplicates, we then filtered the data to keep only proteins with at least 12 valid values out of 24. Next, the data were imputed to fill missing data points by creating a Gaussian distribution of random numbers with a standard deviation of 33% relative to the standard deviation of the measured values and 1.8 standard deviation downshift of the mean to simulate the distribution of low signal values. We performed an ANOVA test, with a permutation based testing correction that was controlled by using a false discovery rate threshold of 0.01, 250 randomizations. Hierarchical clustering of proteins that survived the test was performed in Perseus on logarithmised LFQ intensities after z-score normalization of the data, using Euclidean distances.

RESULTS

A new member of the APC superfamily of transporter - The protein ArgP (FTN_0848) is highly conserved in all the *F. tularensis* subspecies and shares more than 99% identity with its orthologues in *F. tularensis* subsp. *tularensis* (FTT_0968c), *F. tularensis* subsp. *holarctica* (FTL_1233) and *F. tularensis* subsp. *mediasiatica* (FTM_0980). Secondary structure prediction (using the program HMM™ available at the internet site www.cbs.dtu.dk) indicates that the protein ArgP comprizes 12 transmembrane helixes (not shown). The closest homologue in other bacterial species is the protein Lpg1917 of *Legionella pneumophila*

(47.9% identity), an APC member of unknown function, also predicted to comprize 12 transmembrane helixes (http://www.membranetransport.org/ protein.php?pOID =lpne1&pSynonym=lpg1917). High-resolution three-dimensional X-ray structures of several members of the APC superfamily have been published [24,25,26,27,28,29,30]. ArgP shares only limited homology with these APC members, including the arginine/agmatine antiporter AdiC of *E. coli* (26% amino acid sequence identity; [24]).

To investigate the function of gene *argP*, we constructed a chromosomal deletion in *F. novicida* (*FTN_0848*) by allelic replacement [31]. We checked that the deletion of *argP* did not have any polar effect on the expression of the flanking genes by qRT_PCR (**Fig. S1**). This was further confirmed by functional complementation (see below). The mutant showed wild-type growth kinetics when grown in broth, in chemically defined [32] or rich medium (**Fig. S2A, B**).

ArgP is involved in bacterial multiplication and virulence - We monitored bacterial multiplication in J774.1 macrophage-like cells and bone marrow-derived macrophages (BMM) from BALB/c mice (**Figure 1A, B**). Cells were incubated either with wild-type *F. novicida*, Δ*argP* mutant, Δ*argP*-complemented strain or Δ*FPI* strain, for 1 h with a multiplicity of infection (MOI) of 100. In both cells types, the Δ*argP* and Δ*FPI* mutant strains showed a significant growth defect. At 10 h of infection, a 17-fold and 11-fold reduction of intracellular bacteria were recorded in J774.1 and BMM, respectively as compared to wild-type *F. novicida*; and at 24 h, a 50-fold and 112-fold reduction, respectively. Introduction of the complementing plasmid (pKK-214-*argP*) restored bacteria multiplication to wild-type levels, confirming the unique role of *argP* gene inactivation in the intracellular multiplication defect observed.

We then evaluated the impact of *argP* deletion on bacterial virulence in BALB/c mice. For

this, we performed a competition assay by injecting simultaneously WT and Δ*argP* mutant strain (100 bacteria of each) in 7 week-old females. Two days after infection, mice were sacrificed, liver and spleen were collected and serial dilutions were plated on chocolate agar plates with or without kanamycin. The competition index (CI) recorded (**Fig. 1C**) was very low in both target organs (10^{-6} in liver and 10^{-5} in spleen), demonstrating that *argP* plays an essential role in *F. novicida* virulence.

ArgP is the major arginine transporter of F. novicida - *Francisella* is auxotroph for several amino acids due to inactive or incomplete biosynthetic pathways [33,34,35] and must therefore obtain these essential amino acids (E-AA) from the external medium via dedicated transporters. These include arginine, cysteine, histidine, lysine and methionine. *Francisella* has also the capacity to import amino acids that it is able to synthetize *i.e.* the non essential amino acids (NE-AA, alanine, asparagine, glutamic acid, glutamine, glycine, phenylalanine and tryptophan) and can thus relies either on biosynthesis or uptake to constitute its cytoplasmic pools.

To identify which amino acid was imported by FTN_0848 (ArgP), we hypothesized that an excess of amino acid could be sufficient to bypass the specific defect of this transporter. Therefore, we first evaluated whether supplementation with an excess of each of these two different pools would restore multiplication of the Δ*argP* mutant in J774.1 macrophages (**Fig. 2**). Supplementation with a pool of NE-AA did not alleviate the growth defect of the Δ*argP* mutant (**Fig. 2A**). In contrast, wild-type growth was restored by supplementation with a pool of E-AA (**Fig. 2B**). The same experiment was then performed by individually supplementing the cell culture medium with each of the E-AA. Only supplementation with arginine could reverse the multiplication defect of the Δ*argP* mutant in J774.1 (**Fig. 2C**). The fact that the Δ*argP* mutant did not display any growth defect in CDM (**Fig. S2**) is likely due to the

310 elevated concentration of arginine in the synthetic medium (2.3 mM as compared to 0.4 mM
311 in standard DMEM).
312 We also measured bacterial growth in CDM_{min} supplemented with reduced arginine
313 concentrations (0.46 mM and 0.23 mM). At 0.23 mM arginine, growth of wild-type *F.*
314 *novicida* and Δ*argP* mutant was almost abolished (**Fig. S2C, D**). At 0.46 mM arginine,
315 growth of the wild-type strain was not affected (as compared to that in 2.3 mM arginine),
316 during the first five hours, whereas that of the Δ*argP* mutant was slightly delayed. However,
317 both strains reached approximately the same final OD_{600} after 8 h of growth.
318 To directly demonstrate the role of ArgP in arginine uptake, we measured ^{14}C-Arg
319 incorporation in wild-type *F. novicida* and compared it to that in Δ*argP* mutant (**Fig. 2D**).
320 Bacteria grown to mid-exponential phase in CDM were tested. Uptake was measured after 5
321 min incubation with ^{14}C-Arg. Remarkably, incorporation of ^{14}C-Arg was completely
322 abrogated in the Δ*argP* mutant, at all the arginine concentrations tested (1 to 50 μM),
323 confirming that ArgP is a genuine high affinity arginine transporter (with an apparent Km in
324 the10 μM range).
325
326 *ArgP is involved for phagosomal escape* - We followed the subcellular localization of the
327 Δ*argP* mutant in infected cells by confocal microscopy. Intracellular localization of bacteria
328 or LAMP-1 (used as a specific marker of phagosomes) was analyzed using specific antibodies
329 and their co-localization was monitored at 3 time-points (1 h, 4 h and 10 h post-infection; **Fig.**
330 **3A**). Quantification of each co-localization was performed with the Image J software (**Fig.**
331 **3B**). In cells infected with wild-type *F. novicida*, co-localization of bacteria with LAMP-1
332 was only 8% at 1 h and remained in the same range throughout the infection, showing that
333 most bacteria escape the phagosome rapidly. In contrast, the Δ*FPI* mutant strain showed high
334 co-localization with LAMP-1 throughout the infection (87 % at 1 h, 90 % at 4 h and 91 % at

10 h). In this assay, the Δ*argP* strain showed a severe delayed phagosomal escape. Indeed, at 4 h, 85 % LAMP-1 co-localization was still observed. Partial phagosomal escape was detected only at 10 h of infection (with less that 55 % bacteria still associated with LAMP-1). Taken together, these results demonstrate that *argP* gene is necessary for the bacteria to reach cytosol.

We next tested the ability of the Δ*argP* mutant to induce vacuolar membrane rupture in macrophages by using a CCF4 assay, as previously described [36]. Briefly, after 2 h of infection with wild-type *F. novicida*, Δ*argP* or Δ*FPI* strains, cells were loaded for 1 h with CCF4, a fluorescence resonance energy transfer (FRET) probe which is retained in the cytosol following the action of host esterases. *F. novicida* naturally secretes β-lactamase, a molecule able to cleave the CCF4 substrate. Once CCF4 is lysed, emission spectrum turns from 535 nm (green) to 450 nm (blue) (see Experimental procedures). Wild-type *F. novicida* and Δ*argP* strains showed the same amount of cleaved CCF4 whereas there was no FRET signal for Δ*FPI* strain (**Fig. 3C**).

These data suggest that, although still confined in the phagosomal compartment after 3 h infection (as revealed by confocal microscopy), the Δ*argP* mutant is able to partially breach the phagosomal membrane, thus leading to the release of β-lactamase in the host cytosol.

Finally, to rule out a possible cytotoxicity of the Δ*argP* mutant, cell death kinetics were performed in infected bone marrow-derived macrophages (BMM) [11]. As expected, delayed cell death was observed (measured by propidium iodide incorporation) in BMM infected with wild-type *F. novicida* (**Fig. 3D**) as a result of normal intracellular bacterial multiplication whereas the Δ*FPI* has no effect on BMM death. The Δ*argP* mutant reached an intermediate level of cell death (*i.e.* approximately 1/3 that of the WT, after 16 h of infection. These results demonstrate that the intracellular multiplication defect of the Δ*argP* mutant could not be attributed to increased cytotoxicity.

Impact of argP inactivation on the bacterial proteome - In order to get further insights into the importance of arginine uptake in *Francisella* metabolism, we used high-resolution mass spectrometry to quantitatively compare the proteomes of wild-type *F. novicida* and Δ*argP* mutant bacteria, under arginine-replete or arginine-limiting conditions. For this, bacteria were grown in chemically defined medium, containing either 2.3 mM ($CDM_{100\%}$) or 0.46 mM ($CDM_{20\%}$) arginine. The samples analyzed corresponded to 1 h and 2 h of growth (**Fig. S2**).

In total, 1,180 different proteins (out of 1,719 proteins predicted to be encoded by the *F. novicida* genome) were identified across the 24 samples analyzed (*i.e.* 8 samples, each in triplicate, see Experimental procedures). We kept only the proteins detected in more than 12 of 24 samples (*i.e.* 911 proteins with reliable quantification values across samples). ANOVA test identified 685 proteins significantly different between the 8 groups (*i.e.* changed in at least one condition versus the others). These groups are represented in the heat-map (**Fig. 4**). Remarkably, the vertical clustering revealed that: i) the protein expression profiles of the wild-type strain and of the Δ*argP* mutant were different; ii) the arginine concentration had only minor impact on the expression profiles of the two strains. The proteins whose expression varied between the wild-type strain and the Δ*argP* mutant, could be divided in two categories, those that were down-regulated in the Δ*argP* mutant and those that were up-regulated.

Down-regulated proteins. One hundred and four proteins were down-regulated in the Δ*argP* mutant, only in arginine-limiting conditions ($CDM_{20\%}$; T**able S1**). Strikingly, approximately 30% of these proteins were ribosomal proteins, including 14 Small subunit proteins (S-proteins) and 16 Large subunit proteins (L-proteins). One hundred proteins were down-regulated in the Δ*argP* in both growth conditions ($CDM_{20\%}$ and $CDM_{100\%}$; **Table S1**). This

385 subgroup included all the remaining ribosomal proteins, except S14. Thus, expression of all
386 (but one) of the ribosomal proteins appeared to be down-regulated in the Δ*argP* mutant as
387 compared to wild-type (**Table 1A**). The other proteins within the two subgroups belonged to a
388 variety of functional categories, including proteins predicted to be associated with ribosomal
389 activity (*e.g.* EF-Tu, SRP). Remarkably, the ratio of protein expression in $CDM_{20\%}$ as
390 compared to that in standard CDM ($CDM_{20\%}/CDM_{100\%}$) was significantly inferior to 1 for the
391 vast majority of ribosomal proteins in the Δ*argP* mutant, whereas it remained generally close
392 or equal to 1 in the wild-type (**Table S1**). The decreased ribosomal protein expression, in the
393 Δ*argP* mutant in $CDM_{20\%}$, was observed independently of ribosomal subunit, protein size or
394 arginine content.
395 ***Up-regulated proteins.*** Sixty-seven proteins were up-regulated in the Δ*argP* mutant, only in
396 arginine-limiting medium (**Table S1**). These included notably the major predicted stress-
397 related proteins such as, Usp, Hsp 90, Hsp20, DnaK, DnaJ, GrpE, GroEL and ClpB (**Table**
398 **1B**). Ninety-two proteins were up-regulated in the Δ*argP* mutant, in both growth conditions
399 (**Table S1**), including the RNA chaperone Hfq and several proteins of the FPI. The ratios of
400 protein expression $CDM_{20\%}/CDM_{100\%}$ were significantly superior to 1 for almost all the stress-
401 related proteins in the Δ*argP* mutant, whereas they remained close or equal to 1 in the wild-
402 type (**Table S1**).
403
404 *Role of ArgP in stress defense* - Upon entry into cells, *Francisella* resides transiently in a
405 phagosomal compartment that transiently acidifies and acquires reactive oxygen species. We
406 therefore first examined the ability of wild-type and Δ*argP* mutant strains to survive under
407 acid or oxidative stress conditions. Bacteria were exposed either to pH 4 (**Fig. S3A)** or to 500
408 μM H_2O_2 (**Fig. S3B**). Under the pH condition tested, the viability of two strains was
409 unaffected in standard CDM (containing 2.3 mM arginine), as well as in CDM containing

410 limiting concentrations of arginine (0.46 mM or 0.23 mM). The Δ*argP* mutant was also as
411 sensitive as wild-type *F. novicida* after 1 h of H_2O_2 challenge. Thus, the arginine transporter
412 ArgP is not involved in acid or oxidative stress resistance, at least in the conditions tested,
413 confirming the peculiar properties of the APC family members in *Francisella*.

414 We next evaluated a possible contribution of ArgP in the control of reactive nitrogen species
415 production by infected macrophages (**Fig. S4**). The amount of NO, generated in infected
416 J774.1 macrophages, was quantified using the Griess test (**Fig. S4A**). After 1 h, 24 h and 48 h
417 of infection, we found no difference of NO production between cells infected either by wild-
418 type *F. novicida* or Δ*argP* mutant strain. We also tested whether reducing the amount of NO
419 by infected macrophages would impact the intracellular behavior of the Δ*argP* mutant either
420 by chemically inactivating iNOS synthase (using the irreversible inhibitor L-N^G-Nitroarginine
421 methyl ester) or by using iNOS-KO BMM. We did not observe any restoration of
422 multiplication of Δ*argP* mutant in any of two conditions (**Fig. S4B, C**). Altogether, these
423 assays suggest that ArgP is not involved in the control of NO production in infected
424 macrophages.

425

426 *Cytosolic ΔargP mutant bacteria are captured by the autophagic pathway* - Celli and
427 co-workers have recently demonstrated [37] that *Francisella* mutants unable to multiply in
428 the host cytosol (independently of the type of genetic alteration responsible for this defect)
429 were captured and processed by the classical LC3-dependent autophagic pathway. This
430 prompted us to evaluate the physiological status of cytosolic Δ*argP* mutant bacteria by
431 determining their capture by the classical autophagy pathway. J774.1 cells were infected with
432 wild-type *F. novicida* or Δ*argP* mutant over a 1 h, 4 h and 10 h period. LC3 recruitment to *F.*
433 *tularensis* was measured by examining colocalization of bacteria with LC3.
434 Interestingly, at 1 h, there was no -or very low- colocalization (**Fig. 5A, B).** In contrast, 80%

colocalization was recorded with Δ*argP* mutant at 4 h, and 91 % at 10 h. For wild-type *F. novicida*, colocalization between bacteria and LC3 remained very low throughout the assay (13 % at 10 h) whereas with the Δ*ansP* mutant [12], used as a cytosolic non-replicating control, 90% colocalization was already recorded at 1 h and remained very high at 10 h. Transmission electron microscopy analyses of J774-infected macrophages at 10 h post infection revealed individual replication-deficient bacteria within double-membrane structures resembling autophagosomes (**Fig. 5C**), consistent with the observations made by fluorescence microscopy. Hence, Δ*argP* replication-deficient bacteria are captured within vacuoles displaying autophagic features, suggesting that they were metabolically inactive. It is thus likely that a rapid phagosomal escape is critical for maintaining sufficient metabolic activity.

F. tularensis LVS also relies on ArgP for its intracellular survival - In order to evaluate whether the properties of ArgP in the subspecies *novicida* could be extended to other subspecies, we also constructed a chromosomal deletion mutant in *F. tularensis* LVS (Δ*FTL_1233*) and evaluated the impact of the mutation in synthetic medium as well as in J774.1 macrophages. As for *F. novicida* Δ*argP* mutant, *F. tularensis* LVS Δ*argP* showed a severe multiplication defect in J774.1 macrophages after 24 h of infection (more than a 500-fold) as compared to wild-type LVS strain (in standard DMEM; **Fig. S5A**). The growth defect was abolished in the complemented strain.

Notably, in standard CDM, the LVS Δ*argP* mutant showed a significant multiplication defect (**Fig. S5B**). However, this defect was partially compensated upon supplementation with a ten-fold excess arginine (23 mM) and wild-type growth was restored upon supplementation with a twenty-fold excess arginine (46 mM). As in CDM, supplementation of the cell culture medium with 23 mM arginine partially restored intracellular multiplication of the Δ*argP* mutant in J774.1; and 46 mM arginine restored wild-type multiplication. Altogether, these

results fully confirmed the importance of the transporter ArgP in *F. tularensis* intracellular multiplication.

DISCUSSION

Arginine is an essential modulator of the cellular immune response during infection, notably via the generation of nitrogen reactive species in macrophages, for the elimination of invading bacterial and parasitic pathogens ([38,39] and references therein). Arginine has also been shown to be important for the pathogen itself [40]. In this study, we show that inactivation of the transporter ArgP severely impairs *Francisella* phagosomal escape, revealing that intracellular bacteria must import arginine to access to their cytoplasmic replicative niche. By using high-resolution mass spectrometry, we found that arginine limitation affected in particular ribosomal protein biogenesis in the Δ*argP* mutant. These data suggest possible links between ribosomal proteins synthesis and phagosomal escape.

Importance of arginine uptake in bacterial phagosomal escape - Macrophages are able to synthesize their own arginine [41] and to import it via constitutive and inducible cationic amino acid transporters (CAT-1 or SLC7A1 and CAT-2, or SLC7A2, respectively) [42]. Macrophages may either use arginine to produce potentially harmful nitrogen reactive species (NO, via NO synthases) or convert it to ornithine and urea via type 1 arginase (**Figure S6A**). In spite of its apparent simplicity, the balance between the two processes is often quite complex. For example, it has been shown recently that two intracellular bacterial pathogens, *Mycobacterium bovis* and *Listeria monocytogenes*, induced early expression of iNOS, delayed expression of Arg1 upon infection of primary macrophages and boosted arginine

485 import for NO synthesis [40]. However, at a later stage of infection, macrophages re-import
486 citrulline (initially expelled during the production of NO) to regenerate their intracellular pool
487 of arginine via the action of the arginosuccinate synthase Ass1, thus maintaining sufficient
488 NO production to control bacterial multiplication (**Fig. S6A**). *Salmonella typhimurium* has
489 also been shown to reduce the production of the host iNOS through induction of the type 2
490 arginase, in the spleen of infected mice [43] and to induce arginine uptake through enhanced
491 expression of the genes encoding the cationic amino acids transporters CAT1 and CAT2 [38].
492 However, these transporters are recruited preferentially to the *Salmonella*-containing vacuole
493 (SCV), thus, fueling arginine into the SCV and supporting bacterial growth of in this
494 compartment. Of note, a recent study demonstrated that, in C57BL/6 mice, the major arginine
495 transporter CAT-2 was non-functional [39] due to a deletion in the promoter region of the
496 corresponding gene. As a consequence, the intracellular arginine concentration in
497 macrophages from C57BL/6 mice is significantly lower than that in macrophages from
498 BALB/c mice. Of note, the kinetics of intracellular multiplication of wild-type *F. novicida* in
499 bone marrow-derived macrophages (BMM) from C57BL/6 mice was comparable to that in
500 BMM from BALB/c mice (data not shown), suggesting that the intracellular concentration of
501 arginine in these cells is sufficient to promote bacterial growth.
502 As recalled earlier, *Francisella* is auxotroph for arginine and therefore can only obtain this
503 amino acid from its environment. The fact that ArgP inactivation severely impaired
504 phagosomal escape implies that arginine utilization is required at this early stage of the
505 intracellular life cycle of the pathogen. Intra-macrophagic growth of the Δ*argP* mutant was
506 fully restored upon supplementation of the growth medium with excess arginine, in both *F.*
507 *tularensis* subsp *novicida* and *F. tularensis* subsp *holarctica* LVS, demonstrating the
508 importance of arginine acquisition in these two subspecies.
509

Arginine uptake is critical for protein synthesis – Our study represents the most comprehensive proteomic analysis of *Fancisella*. We could cover 68% of *Francisella* predicted gene products, marking a real improvement from the best coverage published so far. Further, state-of-the-art mass spectrometry was used to obtain high quality identification and quantification data for the majority of the proteins expressed in the bacterium, enabling us to gain insights on the global changes of different cellular processes.

In *Francisella*, the metabolic pathways leading to -or coming from- arginine are predicted to be inactive (**Fig. S6B**), suggesting that arginine could be mainly involved in protein synthesis. Strikingly, our proteomic analyses of wild-type and Δ*argP* mutant bacteria grown under arginine limiting conditions, revealed that the expression of essentially all the ribosomal proteins was down-regulated in the Δ*argP* mutant as compared to wild-type. In contrast, the proteins that were up-regulated in the Δ*argP* mutant included all the major stress-related chaperones (such as for examples, DnaK, GroEL, and ClpB) indicating that arginine limitation is sensed as a stress in the Δ*argP* mutant. Remarkably, most of the stress proteins identified have been shown to be under the control of the alternative sigma factor σ32 [44,45,46], suggesting a possible link between ribosome biogenesis and stress response in *Francisella*. Of interest, the existence of a stress response pathway mediated by the bacterial ribosome has been already evoked in *E. coli* and *Bacillus subtilis* [47,48] and repression of ribosomal protein synthesis in response to stresses, such as nutritional limitation, has been observed in all kingdoms of life ([49] and references therein). Yet, the regulatory pathways controlling ribosomal protein syntheses are complex and not fully elucidated [50]. The concept of a ‘‘ribosome code’’ that influences translation, initially proposed by Komili *et al.* [51], has been recently supported by a number of studies in different eukaryotic models.

The phagosome into which *Francisella* transiently resides is a dynamic entity whose size shrinks progressively until bacterial escape. The concentration of available nutrients is thus likely to vary considerably during the short lifespan of this compartment. It is reasonable to assume that the arginine concentration available to *Francisella* also decreases progressively in the phagosome during its maturation. This, in turn, should lead to a reduction of the bacterial arginine cytoplasmic pool itself. It is tempting to propose that intracellular *Francisella* may respond to variations of arginine availability in the phagosome (and consequently in its own cytoplasm) by regulating its ribosomal protein biogenesis (**Fig. 6**). The links between this process and phagosomal membrane disruption remain to be elucidated.

Unlike other cytosolic pathogens, as *L. monocytogenes* that is equipped with the pore-forming listeriolysin O to disrupt the phagosomal membrane [52], *Francisella* genomes do not encode any cytolysin-like molecule. Instead, several enzymatic activites (*e.g.* phosphatases [53]) as well as metabolic or stress resistance functions (*e.g.* biotin biogenesis, oxidative stress [11,54]) have been shown to contribute -directly or indirectly- to escape. This study reveals that ArgP-dependent arginine acquisition constitutes a novel player in phagosomal egress.

Acknowledgements – We thank Dr A. Sjöstedt for providing the *Francisella* strains U112 and LVS. This study was funded by INSERM, CNRS and Université Paris Descartes Paris V. Elodie Ramond was funded by a fellowship from the "Région Ile de France" and Gael Gesbert by a fellowship from the Délégation Générale à l'Armement (DGA).

555

556 ## REFERENCES

557 1. Sjostedt A, editor (2011) *Francisella tularensis* and tularemia: *Fontiers Media SA*.

558 2. Celli J, Zahrt TC (2013) Mechanisms of *Francisella tularensis* intracellular pathogenesis.
559 *Cold Spring Harb Perspect Med* 3: a010314.

560 3. Jones CL, Napier BA, Sampson TR, Llewellyn AC, Schroeder MR, et al. (2012)
561 Subversion of Host Recognition and Defense Systems by *Francisella* spp. *Microbiol*
562 *Mol Biol Rev* 76: 383-404.

563 4. Ramond E, Gesbert G, Barel M, Charbit A (2012) Proteins involved in *Francisella*
564 *tularensis* survival and replication inside macrophages. *Future Microbiol* 7: 1255-
565 1268.

566 5. Meibom KL, Charbit A (2010) The unraveling panoply of *Francisella tularensis* virulence
567 attributes. *Curr Opin Microbiol* 13: 11-17.

568 6. Abu Kwaik Y, Bumann D (2013) Microbial quest for food in vivo: 'nutritional virulence' as
569 an emerging paradigm. *Cell Microbiol* 15: 882-890.

570 7. Santic M, Abu Kwaik Y (2013) Nutritional virulence of *Francisella tularensis*. *Front Cell*
571 *Infect Microbiol* 3: 112.

572 8. Raghunathan A, Shin S, Daefler S (2010) Systems approach to investigating host-pathogen
573 interactions in infections with the biothreat agent *Francisella*. Constraints-based
574 model of *Francisella tularensis*. *BMC Syst Biol* 4: 118.

575 9. Steele S, Brunton J, Ziehr B, Taft-Benz S, Moorman N, et al. (2013) *Francisella tularensis*
576 Harvests Nutrients Derived via ATG5-Independent Autophagy to Support
577 Intracellular Growth. *PLoS Pathog* 9: e1003562.

578 10. Alkhuder K, Meibom KL, Dubail I, Dupuis M, Charbit A (2009) Glutathione provides a
579 source of cysteine essential for intracellular multiplication of *Francisella tularensis*.
580 *PLoS Pathog* 5: e1000284.
581 11. Ramond E, Gesbert G, Rigard M, Dairou J, Dupuis M, et al. (2014) Glutamate utilization
582 couples oxidative stress defense and the tricarboxylic acid cycle in *Francisella*
583 phagosomal escape. *PLoS Pathog* 10: e1003893.
584 12. Gesbert G, Ramond E, Rigard M, Frapy E, Dupuis M, et al. (2014) Asparagine
585 assimilation is critical for intracellular replication and dissemination of *Francisella*.
586 *Cell Microbiol* 16: 434-449.
587 13. Wong FH, Chen JS, Reddy V, Day JL, Shlykov MA, et al. (2012) The amino acid-
588 polyamine-organocation superfamily. *J Mol Microbiol Biotechnol* 22: 105-113.
589 14. Steeb B, Claudi B, Burton NA, Tienz P, Schmidt A, et al. (2013) Parallel exploitation of
590 diverse host nutrients enhances *Salmonella* virulence. *PLoS Pathog* 9: e1003301.
591 15. Weiss DS, Brotcke A, Henry T, Margolis JJ, Chan K, et al. (2007) In vivo negative
592 selection screen identifies genes required for *Francisella* virulence. *Proc Natl Acad*
593 *Sci U S A* 104: 6037-6042.
594 16. Peng K, Monack DM (2010) Indoleamine 2,3-dioxygenase 1 is a lung-specific innate
595 immune defense mechanism that inhibits growth of *Francisella tularensis* tryptophan
596 auxotrophs. *Infect Immun* 78: 2723-2733.
597 17. Su J, Yang J, Zhao D, Kawula TH, Banas JA, et al. (2007) Genome-wide identification of
598 *Francisella tularensis* virulence determinants. *Infect Immun* 75: 3089-3101.
599 18. Ahlund MK, Ryden P, Sjostedt A, Stoven S (2010) Directed screen of *Francisella*
600 novicida virulence determinants using Drosophila melanogaster. *Infect Immun* 78:
601 3118-3128.

602 19. Moule MG, Monack DM, Schneider DS (2010) Reciprocal analysis of *Francisella*
603 novicida infections of a *Drosophila melanogaster* model reveal host-pathogen
604 conflicts mediated by reactive oxygen and imd-regulated innate immune response.
605 *PLoS Pathog* 6: e1001065.
606 20. Llewellyn AC, Jones CL, Napier BA, Bina JE, Weiss DS (2011) Macrophage replication
607 screen identifies a novel *Francisella* hydroperoxide resistance protein involved in
608 virulence. *PLoS One* 6: e24201.
609 21. Brotcke A, Weiss DS, Kim CC, Chain P, Malfatti S, et al. (2006) Identification of MglA-
610 regulated genes reveals novel virulence factors in *Francisella tularensis*. *Infect Immun*
611 74: 6642-6655.
612 22. Luber CA, Cox J, Lauterbach H, Fancke B, Selbach M, et al. (2010) Quantitative
613 proteomics reveals subset-specific viral recognition in dendritic cells. *Immunity* 32:
614 279-289.
615 23. Cox J, Mann M (2008) MaxQuant enables high peptide identification rates, individualized
616 p.p.b.-range mass accuracies and proteome-wide protein quantification. *Nat*
617 *Biotechnol* 26: 1367-1372.
618 24. Gao X, Lu F, Zhou L, Dang S, Sun L, et al. (2009) Structure and mechanism of an amino
619 acid antiporter. *Science* 324: 1565-1568.
620 25. Shaffer PL, Goehring A, Shankaranarayanan A, Gouaux E (2009) Structure and
621 mechanism of a Na+-independent amino acid transporter. Science 325: 1010-1014.
622 26. Singh SK, Yamashita A, Gouaux E (2007) Antidepressant binding site in a bacterial
623 homologue of neurotransmitter transporters. *Nature* 448: 952-956.
624 27. Weyand S, Shimamura T, Yajima S, Suzuki S, Mirza O, et al. (2008) Structure and
625 molecular mechanism of a nucleobase-cation-symport-1 family transporter. *Science*
626 322: 709-713.

627 28. Perez C, Koshy C, Yildiz O, Ziegler C (2012) Alternating-access mechanism in
628 conformationally asymmetric trimers of the betaine transporter BetP. *Nature* 490: 126-
629 130.
630 29. Schulze S, Koster S, Geldmacher U, Terwisscha van Scheltinga AC, Kuhlbrandt W
631 (2010) Structural basis of Na(+)-independent and cooperative substrate/product
632 antiport in CaiT. *Nature* 467: 233-236.
633 30. Watanabe A, Choe S, Chaptal V, Rosenberg JM, Wright EM, et al. (2010) The
634 mechanism of sodium and substrate release from the binding pocket of vSGLT.
635 *Nature* 468: 988-991.
636 31. Lauriano CM, Barker JR, Nano FE, Arulanandam BP, Klose KE (2003) Allelic exchange
637 in *Francisella tularensis* using PCR products. FEMS Microbiol Lett 229: 195-202.
638 32. Chamberlain RE (1965) Evaluation of Live Tularemia Vaccine Prepared in a Chemically
639 Defined Medium. *Appl Microbiol* 13: 232-235.
640 33. Larsson P, Oyston PC, Chain P, Chu MC, Duffield M, et al. (2005) The complete genome
641 sequence of *Francisella tularensis*, the causative agent of tularemia. *Nat Genet* 37:
642 153-159.
643 34. Larsson P, Elfsmark D, Svensson K, Wikstrom P, Forsman M, et al. (2009) Molecular
644 evolutionary consequences of niche restriction in *Francisella tularensis*, a facultative
645 intracellular pathogen. *PLoS Pathog* 5: e1000472.
646 35. Meibom KL, Charbit A (2010) *Francisella tularensis* metabolism and its relation to
647 virulence. *Front Microbiol* 1: 140.
648 36. Nothelfer K, Dias Rodrigues C, Bobard A, Phalipon A, Enninga J (2011) Monitoring
649 *Shigella flexneri* vacuolar escape by flow cytometry. *Virulence* 2: 54-57.

650 37. Chong A, Wehrly TD, Child R, Hansen B, Hwang S, et al. (2012) Cytosolic clearance of
651 replication-deficient mutants reveals *Francisella tularensis* interactions with the
652 autophagic pathway. *Autophagy* 8: 1342-1356.
653 38. Das P, Lahiri A, Chakravortty D (2010) Modulation of the arginase pathway in the
654 context of microbial pathogenesis: a metabolic enzyme moonlighting as an immune
655 modulator. *PLoS Pathog* 6: e1000899.
656 39. Sans-Fons MG, Yeramian A, Pereira-Lopes S, Santamaria-Babi LF, Modolell M, et al.
657 (2013) Arginine transport is impaired in C57Bl/6 mouse macrophages as a result of a
658 deletion in the promoter of Slc7a2 (CAT2), and susceptibility to Leishmania infection
659 is reduced. *J Infect Dis* 207: 1684-1693.
660 40. Qualls JE, Subramanian C, Rafi W, Smith AM, Balouzian L, et al. (2012) Sustained
661 generation of nitric oxide and control of mycobacterial infection requires
662 argininosuccinate synthase 1. *Cell Host Microbe* 12: 313-323.
663 41. Morris SM, Jr. (2007) Arginine metabolism: boundaries of our knowledge. *J Nutr* 137:
664 1602S-1609S.
665 42. Closs EI, Boissel JP, Habermeier A, Rotmann A (2006) Structure and function of cationic
666 amino acid transporters (CATs). J Membr Biol 213: 67-77.
667 43. Lahiri A, Das P, Chakravortty D (2008) Arginase modulates *Salmonella* induced nitric
668 oxide production in RAW264.7 macrophages and is required for *Salmonella*
669 pathogenesis in mice model of infection. *Microbes Infect* 10: 1166-1174.
670 44. Meibom KL, Dubail I, Dupuis M, Barel M, Lenco J, et al. (2008) The heat-shock protein
671 ClpB of *Francisella tularensis* is involved in stress tolerance and is required for
672 multiplication in target organs of infected mice. *Mol Microbiol* 67: 1384-1401.

673 45. Meibom KL, Forslund AL, Kuoppa K, Alkhuder K, Dubail I, et al. (2009) Hfq, a novel
674 pleiotropic regulator of virulence-associated genes in *Francisella tularensis*. *Infect*
675 *Immun* 77: 1866-1880.
676 46. Grall N, Livny J, Waldor M, Barel M, Charbit A, et al. (2009) Pivotal role of the
677 *Francisella tularensis* heat-shock sigma factor RpoH. *Microbiology* 155: 2560-2572.
678 47. Jin DJ, Cagliero C, Zhou YN (2012) Growth rate regulation in *Escherichia coli*. *FEMS*
679 *Microbiol Rev* 36: 269-287.
680 48. Zhang S, Scott JM, Haldenwang WG (2001) Loss of ribosomal protein L11 blocks stress
681 activation of the *Bacillus subtilis* transcription factor sigma(B). *J Bacteriol* 183: 2316-
682 2321.
683 49. Conrad M, Schothorst J, Kankipati HN, Van Zeebroeck G, Rubio-Texeira M, et al. (2014)
684 Nutrient sensing and signaling in the yeast *Saccharomyces cerevisiae*. *FEMS*
685 *Microbiol Rev* 38: 254-299.
686 50. Henras AK, Soudet J, Gerus M, Lebaron S, Caizergues-Ferrer M, et al. (2008) The post-
687 transcriptional steps of eukaryotic ribosome biogenesis. *Cell Mol Life Sci* 65: 2334-
688 2359.
689 51. Komili S, Farny NG, Roth FP, Silver PA (2007) Functional specificity among ribosomal
690 proteins regulates gene expression. *Cell* 131: 557-571.
691 52. Kayal S, Charbit A (2006) Listeriolysin O: a key protein of *Listeria monocytogenes* with
692 multiple functions. *FEMS Microbiol Rev* 30: 514-529.
693 53. Mohapatra NP, Soni S, Rajaram MV, Strandberg KL, Gunn JS (2013) Type A *Francisella*
694 *tularensis* Acid Phosphatases Contribute to Pathogenesis. *PLoS One* 8: e56834.
695 54. Napier BA, Meyer L, Bina JE, Miller MA, Sjostedt A, et al. (2012) Link between
696 intraphagosomal biotin and rapid phagosomal escape in *Francisella*. *Proc Natl Acad*
697 *Sci U S A* 109: 18084-18089.
698

LEGENDS TO FIGURES AND TABLES

Fig. 1. *In vitro* and *in vivo* properties of a *Francisella* Δ*argP* mutant.

Intracellular replication of wild-type *F. novicida* (WT) carrying the empty plasmid pKK214 (WT pKK (-)), of the Δ*argP* mutant (Δ*argP*) and complemented strain (Δ*argP* pKK-*argP*), and of the Δ*FPI* mutant (Δ*FPI*), was monitored in J774.1 murine macrophage-like cells (**A**) and in murine bone marrow-derived macrophages (BMDM, **B**) over a 24 h-period. Results are shown as the averages of $\log_{10}$ (CFU/ml) ± standard deviations. Experiences were realized twice. ** P<0.01 as determined by Student's t test.

(C) Virulence. Group of five BALB/c mice were infected intraperitoneally with 100 CFU of wild-type *F. novicida* and 100 CFU of Δ*argP* mutant strain.

Bacterial burden was realized in liver and spleen of mice. The data represent the competitive index (CI) value (in ordinate) for CFU of mutant/wild-type of each mouse, 48 h after infection divided by CFU of mutant/wild-type in the inoculum. Bars represent the geometric mean CI value.

Fig. 2. Arginine is required for mutant multiplication in macrophages

Amino acid supplementation. J774.1 cells were infected with wild-type *F. novicida* (WT) or Δ*argP* mutant for 24 h, in medium supplemented (+ AA) or not, with a pool of essential E-AA amino acids (**A**) or NE-AA (**B**) each at a final concentration of 1.5 mM.

(C) Arginine supplementation. J774.1 cells were infected with wild-type *F. novicida* (WT), or Δ*argP* mutant for 24 h with medium, supplemented (+AA) or not, with arginine 1.5 mM (+ Arg).

(D) Arginine transport assay. Kinetics of uptake of ^{14}C radiolabeled arginine by wild-type

F. novicida (WT, open circles) and Δ*argP* mutant (ΔargP, closed triangles), at substrate concentrations ranging from 1 to 50 μM. Ordinate, picomoles (pmol) of arginine taken up per minute (per sample of app. $2.5x10^9$ bacteria). Abcissa, final concentration of arginine tested.

Fig. 3. Subcellular localization of the Δ*argP* mutant.

(A) Confocal microscopy. J774 cells were incubated for 1 h with wild-type *F. novicida* (WT), Δ*argP* or Δ*FPI* strains and their colocalization with the phagosomal marker LAMP1 was observed by confocal microscopy. The phagosomes of J774 cells were labeled with anti-LAMP1 antibody (1/100 final dilution). Cell nuclei were labeled with DAPI. Bacteria were labeled with primary mouse monoclonal antibody anti-*F. novicida* (1/500 final dilution). (A) The color images represent wild-type *F. novicida* (WT), Δ*argP*, Δ*FPI*, strains (green); phagosomes (red); and nuclei (blue); cytosolic bacteria appear in green (white arrowheads). Scale bars at the bottom right of each panel correspond to 10 μM.

(B) Quantification of bacteria/phagosome colocalization at 1 h, 4 h and 10 h for wild-type *F. novicida* (WT), Δ*argP* and Δ*FPI* strains. **P < 0.01 (as determined by Student's t-test).

(C) CCF4. The cytosol of bone marrow-derived infected macrophages was loaded with CCF4, as described previously [36]. Wild-type *F. novicida* naturally expresses a β-lactamase able to cleave the CCF4. Bacterial escape into the host cytosol is thus associated with a shift of the CCF4 probe, upon excitation at 405 nm to a shift of fluorescence from green (535 nm) to blue (450 nm). After infection (at a multiplicity of infection of 100) with wild-type *F. novicida* (WT), Δ*argP* mutant and Δ*FPI* mutant, 43.5 %, 50.5% and 0.56% of Pacific blue-positive cells were recorded, respectively.

(D) Cell death. The cell death kinetics of infected BMM (from BALB/c mice) was followed by monitoring propidium iodide (PI) incorporation in real time. PI fluorescence was measured every 15 min on a microplate fluorimeter (Tecan Infinite 1000). Wild-type *F. novicida* (WT),

748 Δ*argP* and Δ*FPI* mutant strains.

749

750 **Fig. 4. Hierarchical clustering and heatmap.**

751 Data were obtained by proteomic analyses of wild-type *F. novicida* and Δ*argP* mutant strains
752 grown in chemically defined medium (CDM) containing two different concentrations of
753 arginine (2.3 mM or 0.46 mM). Samples were collected at 1 h or 2 h of growth. The map
754 corresponds to the data collected at 2 h. The standard deviation of the distribution of the
755 protein intensity logarithm was constant across samples (0.61<SD<0.63). The analysis was
756 performed on 685 proteins differentially expressed in at least one condition (test ANOVA,
757 FDR=1%).
758 Four interesting protein clusters are represented as profile plots to the right of the figure. The
759 ribosomal proteins were highlighted in blue (mostly present in cluster 643). The stress related
760 proteins are highlighted in red (all comprised within cluster 644). For a detailed list of
761 proteins see **Table S1.**

762

763 **Fig. 5. Cytosolic Δ*argP* mutant bacteria are LC3-positive.**

764 **(A) Confocal microscopy.** J774.1 cells were incubated for 1 h with wild-type *F. novicida*
765 (WT), Δ*argP* or Δ*FPI* strains and their colocalization with the autophagy marker LC3 was
766 observed by confocal microscopy.
767 (**B) Quantification** at 1 h, 4 h and 10 h for WT, Δ*argP* and Δ*FPI* strains. **P < 0.01 (as
768 determined by Student's t-test).
769 (**C) Electron microscopy.** Thin section electron microscopy of J774 cells infected with *F.*
770 *novicida* Δ*ansP* mutant strain at 10 h. The two left panels show individual bacteria
771 surrounded by multilamellar structures; the right panel, an intact phagosome.

772

Fig. 6. Hypothetical model for arginine sensing in the phagosome.

Francisella responds to variations of arginine availability in the phagosomal environment by regulating ribosomal protein biogenesis. In wild-type *Francisella* (WT, upper panel), import of arginine mediated by the transporter ArgP, promotes ribosomal protein synthesis (R), a pre-requisite for efficient protein (P) syntheses, a pre-requisite for membrane disruption and cytosolic escape. In the absence of ArgP (lower panel), ribososomal protein synthesis is down-regulated (R↘), impairing thus protein syntheses (P↘), leading to impaired bacterial escape.

Table 1. Selected proteins identified by mass spectrometry under limiting arginine condiditions

(**A**) **Ribosomal proteins.** The expression of almost all the ribosomal proteins was reduced in the Δ*argP* mutant upon arginine limitation (ratio $CDM_{20\%}$ / $CDM_{100\%}$ <1) whereas their expression did not vary (or marginally) in the wild-type strain. The genes of the predicted ribosomal operons are shaded in dark grey.

(**B**) **Stress-related proteins.** Stress-related proteins were up-regulated in the Δ*argP* mutant (ratio $CDM_{20\%}$ / $CDM_{100\%}$ >1) whereas their expression did not vary (or marginally) in the wild-type strain. Remarkably, a putative σ32-dependent promoter precedes all the genes in this list.

Location in the text of each figure and table

Figure 1: In Results, on page 13

Figure 2: n Results, on page 14

Figure 3: In Results, on, on page 15

Figure 4: In Results, on page 18

Figure 5: In Results, on page 19

Figure 6: In Discussion, on page 23

Table 1: In Results, on page 17

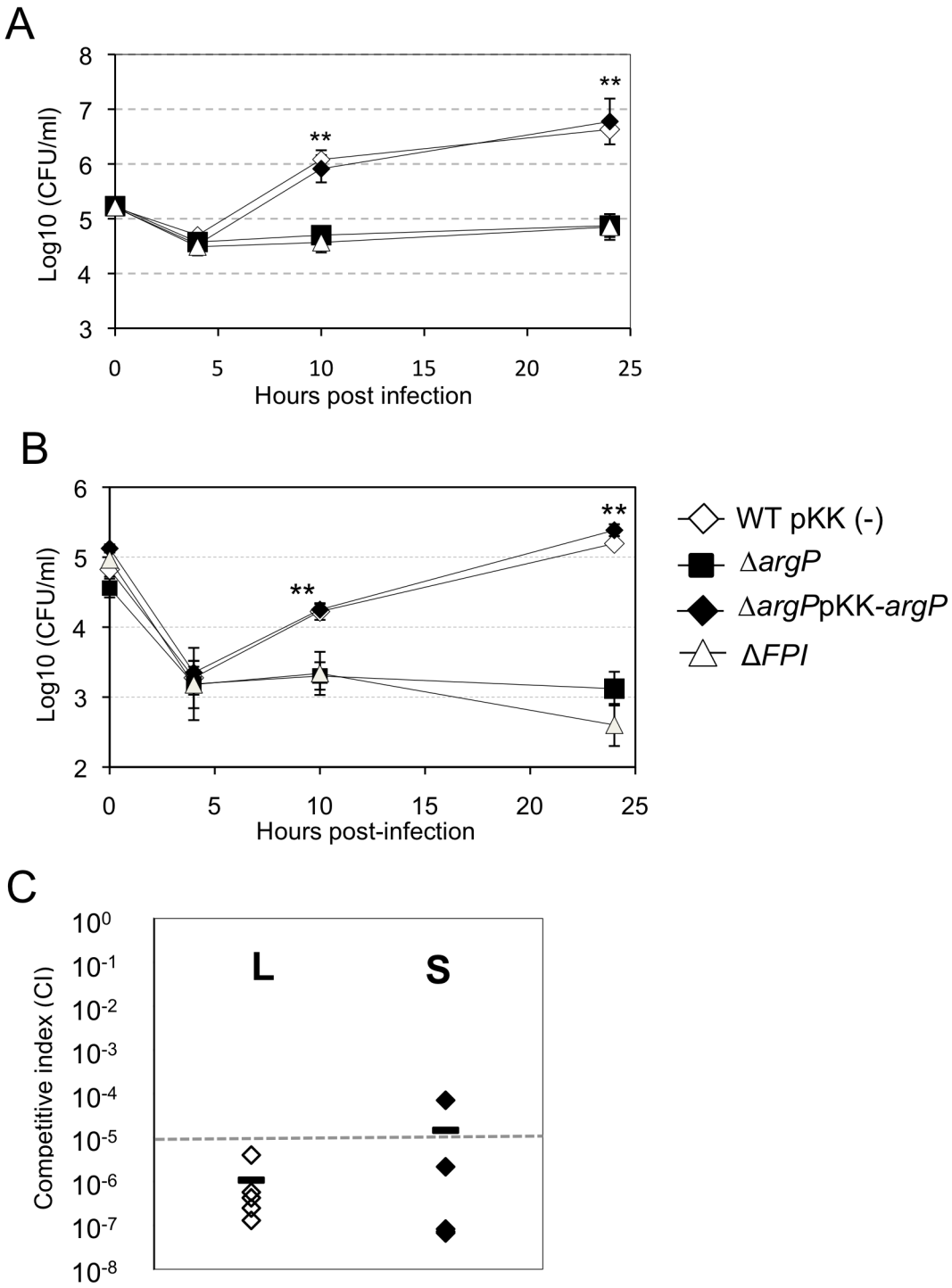

Fig. 1 Ramond *et al.*

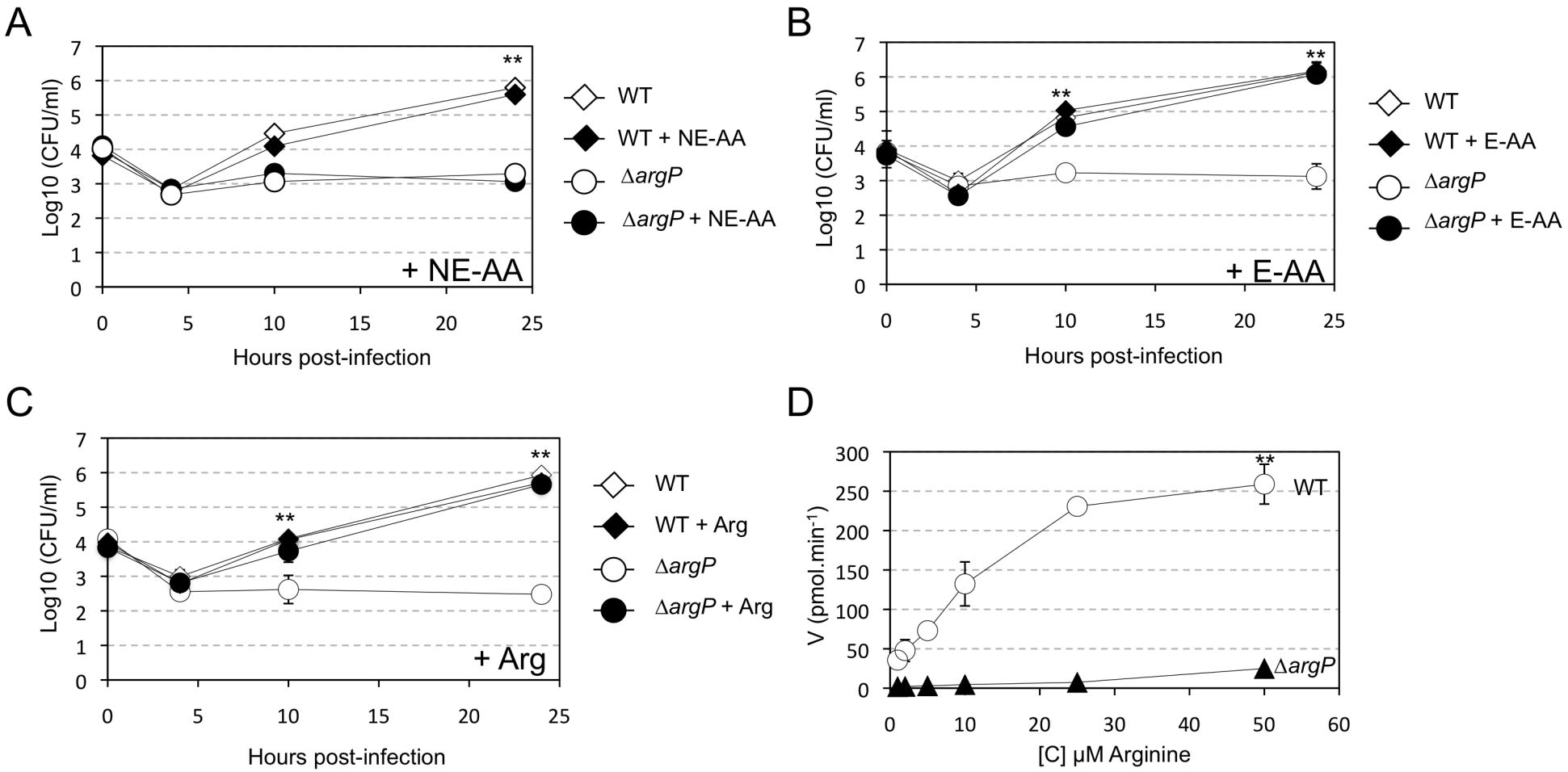

Fig. 2 Ramond *et al.*

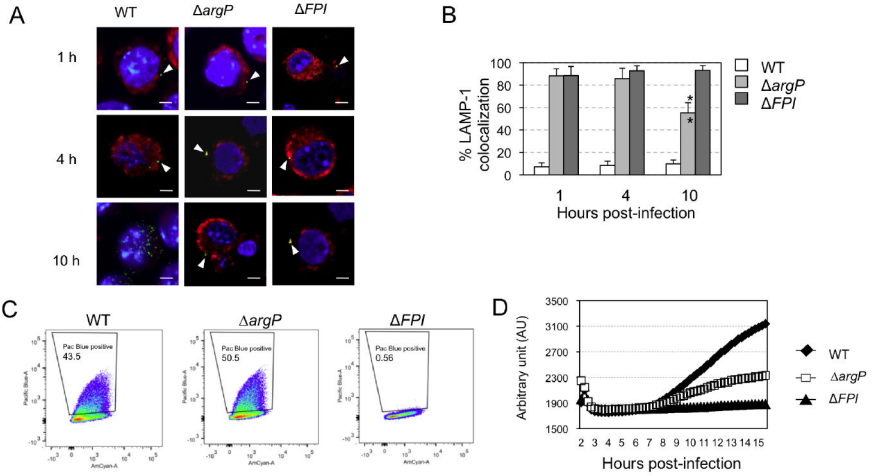

Fig. 3 Ramond *et al.*

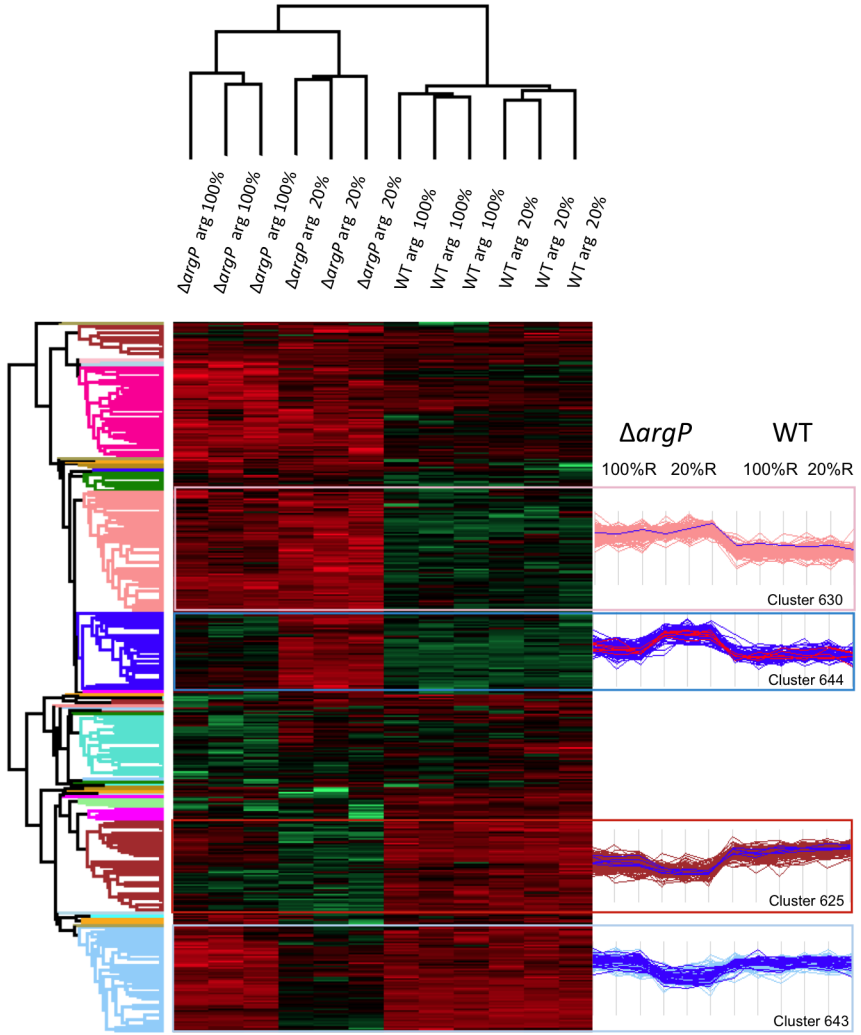

Fig. 4 Ramond *et al.*

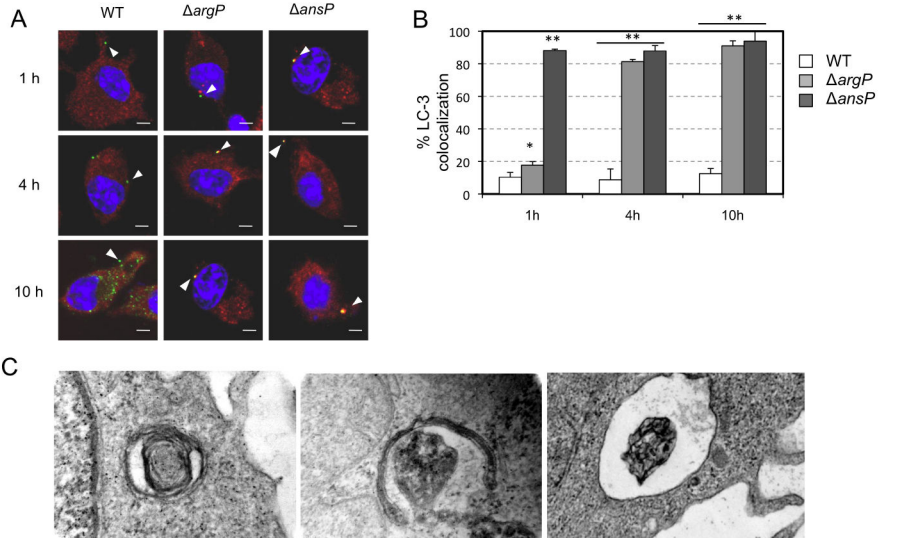

Fig. 5 Ramond *et al.*

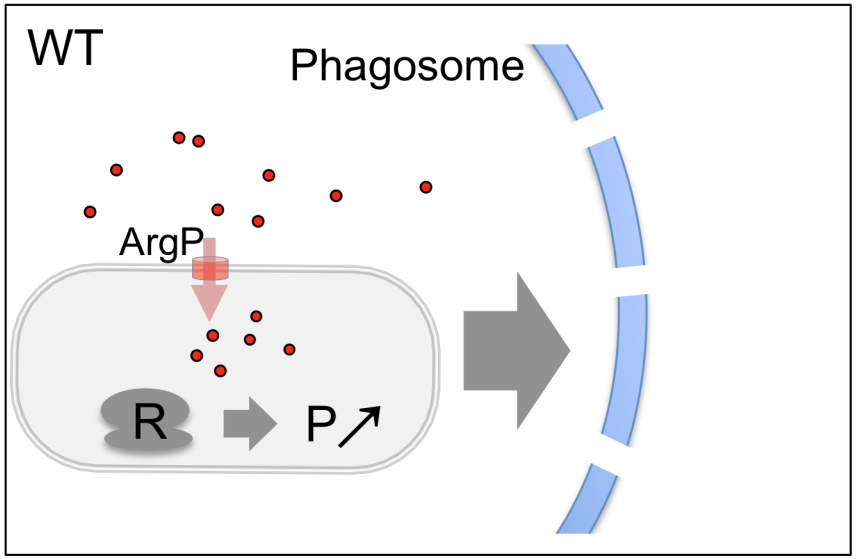

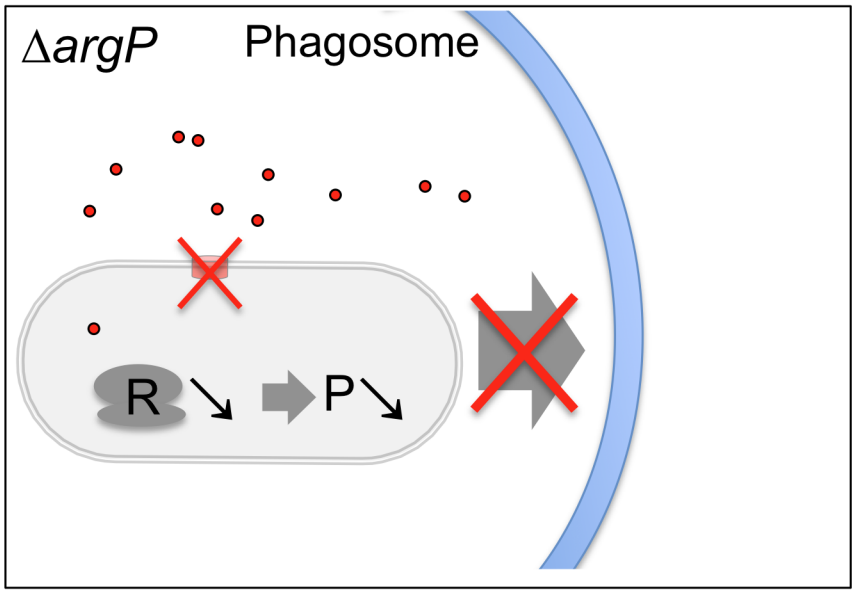

Fig. 6 Ramond *et al.*

Gene number	Gene name	Gene product	WT 20% / WT 100%	Δ*argP* 20% / Δ*argP* 100%	%Arg
FTN_0159	*rpsA*	30S ribosomal protein S1	1.00	0.77	3.8
FTN_0227	*rpsB*	30S ribosomal protein S2	0.99	0.91	3.3
FTN_0235	*rpsL*	30S ribosomal protein S12	1.01	0.78	5.8
FTN_0236	*rpsG*	30S ribosomal protein S7	1.03	0.79	10.2
FTN_0238	*rpsJ*	30S ribosomal protein S10	1.07	0.71	7.6
FTN_0239	*rplC*	50S ribosomal protein L3	1.07	0.79	4.8
FTN_0240	*rpLD*	50S ribosomal protein L4	1.08	0.97	3.4
FTN_0241	*rplW*	50S ribosomal protein L23	1.05	0.78	6.1
FTN_0242	*rplB*	50S ribosomal protein L2	1.04	0.84	10.2
FTN_0243	*rpsS*	30S ribosomal protein S19	1.01	0.74	5.4
FTN_0245	*rpsC*	30S ribosomal protein S3	0.99	0.78	7.2
FTN_0246	*rplP*	50S ribosomal protein L16	1.06	0.78	12.4
FTN_0247	*rpmC*	50S ribosomal protein L29	0.99	0.67	7.6
FTN_0248	*rpsQ*	30S ribosomal protein S17	0.98	0.91	6
FTN_0249	*rplN*	50S ribosomal protein L14	1.04	0.72	9
FTN_0250	*rplX*	50S ribosomal protein L24	0.99	0.68	5.7
FTN_0251	*rplE*	50S ribosomal protein L5	1.06	0.91	6.7
FTN_0252	*rpsL*	30S ribosomal protein S14	0.90	1.19	7
FTN_0253	*rpsH*	30S ribosomal protein S8	1.05	0.90	5.3
FTN_0254	*rplF*	50S ribosomal protein L6	1.07	0.80	3.9
FTN_0255	*rplR*	50S ribosomal protein L18	1.06	0.72	10.3
FTN_0256	*rpsE*	30S ribosomal protein S5	1.03	0.92	4.8
FTN_0257	*rpmD*	50S ribosomal protein L30	0.90	0.70	6.6
FTN_0258	*rplO*	50S ribosomal protein L15	0.99	0.77	5.6
FTN_0261	*rpsM*	30S ribosomal protein S13	1.08	0.71	13.6
FTN_0262	*rpsK*	30S ribosomal protein S11	0.84	0.68	8.5
FTN_0263	*rpsD*	30S ribosomal protein S4	1.06	0.75	9.2
FTN_0265	*rplQ*	50S ribosomal protein L17	0.99	0.84	11
FTN_0278	*rpmE*	50S ribosomal protein L31	1.14	1.21	3.9
FTN_0332	*rpmG*	50S ribosomal protein L33	0.98	0.53	2.8
FTN_0333	*rpmB*	50S ribosomal protein L28	0.74	0.65	9.9
FTN_0358	*rimO*	S12 methylthiotransferase	0.96	1.07	3.4
FTN_0608	*rpsO*	30S ribosomal protein S15	1.01	0.91	11.4
FTN_0675	*rplU*	50S ribosomal protein L21	0.98	0.75	6.7
FTN_0676	*rpmA*	50S ribosomal protein L27	1.02	0.83	11.4
FTN_0916	*rpsU*	30S ribosomal protein S21	1.02	0.85	18.5
FTN_0949	*rplI*	50S ribosomal protein L9	1.06	0.85	2.6
FTN_0951	*rpsF*	30S ribosomal protein S6	0.96	1.02	6.3
FTN_1007	*rplY*	50S ribosomal protein L25	0.87	0.87	3.3
FTN_1188	*rplT*	50S ribosomal protein L20	0.98	0.69	11.9
FTN_1288	*rplM*	50S ribosomal protein L13	1.02	0.87	5.3
FTN_1289	*rpsI*	30S ribosomal protein S9	1.01	0.85	12.4
FTN_1335	*rpmF*	50S ribosomal protein L32	0.93	0.89	6.3
FTN_1559	*rplS*	50S ribosomal protein L19	1.02	0.78	10.4
FTN_1562	*rpsP*	30S ribosomal protein S16	0.99	0.64	6
FTN_1569	*rplL*	50S ribosomal protein L7/L12	0.91	0.78	0.8
FTN_1570	*rplJ*	50S ribosomal protein L10	1.07	0.88	5.8
FTN_1571	*rplA*	50S ribosomal protein L1	1.03	0.98	3.9
FTN_1572	*rplK*	50S ribosomal protein L11	1.05	0.99	2.8

Table 1A. Ribosomal proteins

Gene number	Gene name	Gene number	WT 20% / WT 100%	Δ*argP* 20% / Δ*argP* 100%	% Arg
FTN_0266	*htpG*	chaperone protein HSP90	0.99	1.24	3
FTN_1283	*dnaJ*	chaperone protein DnaJ	0.80	0.90	5.8
FTN_1285	*grpE*	heat shock protein GrpE	1.06	1.21	4.1
FTN_1522	-	DnaJ-type HSP40	1.05	1.27	4.2
FTN_1538	*groEL*	chaperonin GroEL	1.00	1.36	3.5
FTN_1539	*groES*	co-chaperonin GroES	1.05	1.69	5.3
FTN_1743	*clpB*	chaperone ClpB	1.00	1.33	5.1

Table 1B. Stress proteins

SUPPORTING INFORMATION

Supplemental Information includes six Figures, two Tables, Supplemental Experimental Procedures, and Supplemental References.

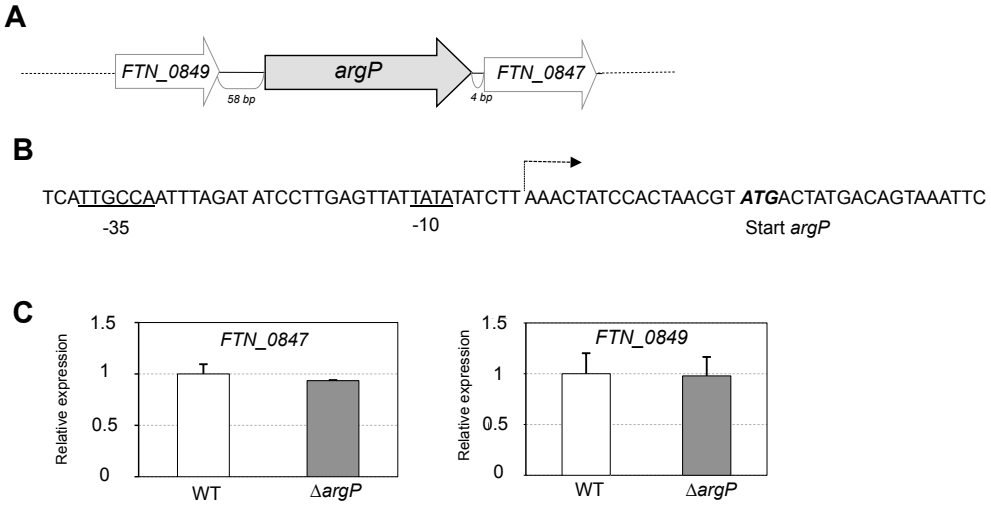

Figure S1. Sequence analysis of *argP* region

(A) Schematic organization of the region. The gene *argP* (*FTN_0848*) encoding ArgP APC superfamily transporter is colored in grey. It is flanked, upstream (58 bp) by gene *FTN_0849* and downstream (4 bp) by gene *FTN_0847*, both are transcribed on the same strand.

(B) Transcriptional analysis. We realized rapid amplification of cDNA ends (5' race) to determine the 5'end of the *argP* mRNA. A broken arrow shows the transcription start of *argP* (+1). Inspection of the sequence immediately upstream of the transcriptional start identified putative -10 and -35 promoter elements that share homology to the consensus site recognized by the major sigma factor σ^{70}. The predicted σ^{70}-dependent -10 and -35 sequences are underlined. The predicted translation start codon of *argP* is in bold italics.

(C) Quantitative real-time RT-PCR. Quantification of *FTN_0847* and *FTN_0849* expression in wild-strain *F. novicida* and Δ*argP* mutant, were performed in TSB at 37°C. Analyses were performed twice using independent samples (in triplicates).

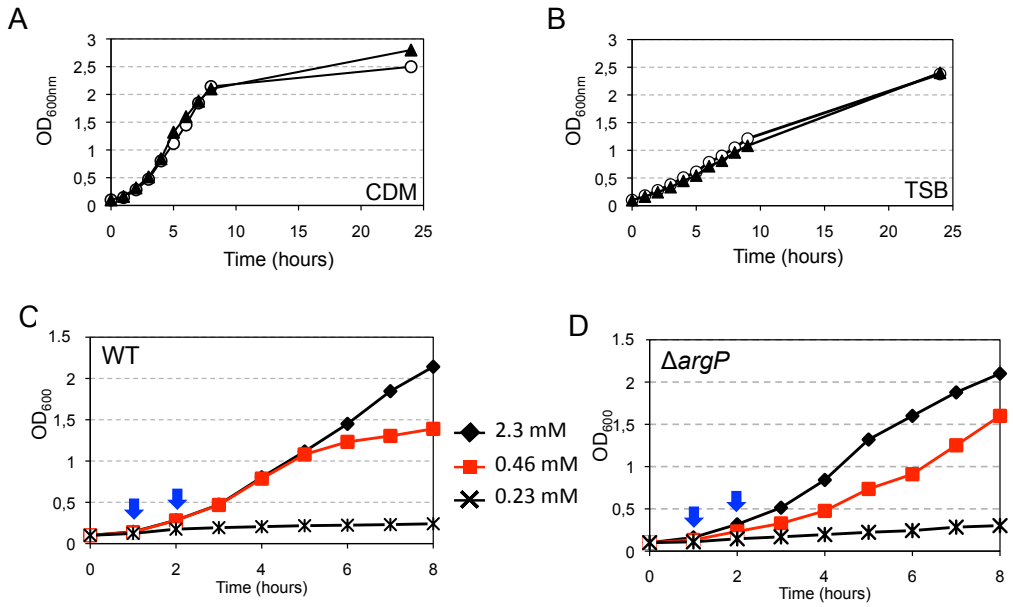

Figure S2. Bacterial growth in broth

Bacterial growth was monitored at $OD600_{nm}$ over a 24 h-period, **(A)** in standard Chemically defined medium (CDM); **(B)** in Tryptic soya broth (TSB).

Effect of different arginine concentrations on wild-type *F. novicida* (**C**) and Δ*argP* mutant strain (**D**) growth was monitored over a 5 h-period. Growth was evaluated in CDM with 2.3 mM arginine, 0.46 mM arginine and 0.23 mM arginine. The blue arrows indicate the time points taken for the Mass spectrometry analyses.

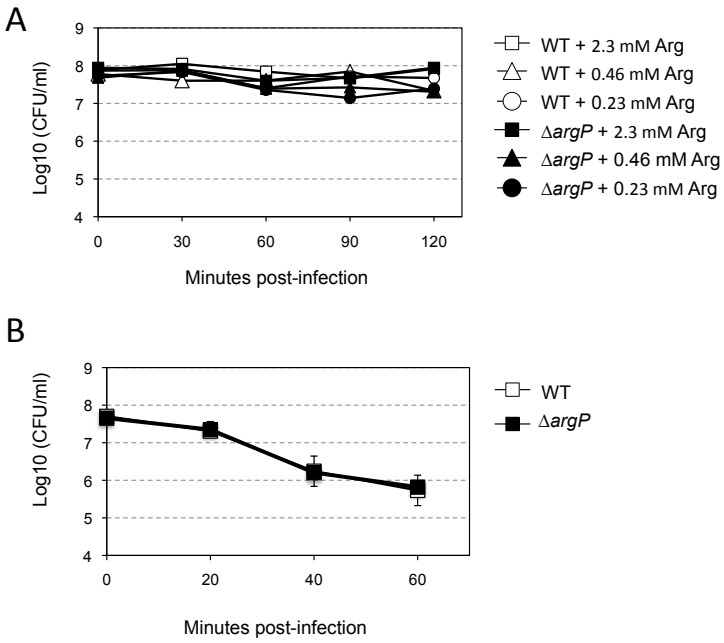

33

34 **Figure S3. Sensitivity to pH and oxidative stresses**

35 **(A) pH stress**. Bacteria were incubated for 2 h in CDM at pH 4, the presence of
36 various concentrations of arginine. *i.e*. 2.3 mM (corresponding to the arginine
37 concentration present in standard CDM), 0.46 mM and 0.23 mM, respectively. At 30
38 min intervals, bacteria were collected and numerated on TSB solid medium.

39 (**B**) **Oxidative stress.** Exponential phase bacteria, diluted in TSB medium were
40 subjected to oxidative stress (500 μM H_20_2). The bacteria were plated on chocolate
41 agar plates at different times and viable bacteria were monitored 2 days after. Data are
42 the average c.f.u mL^{-1} for three points. Experiments were realized twice.

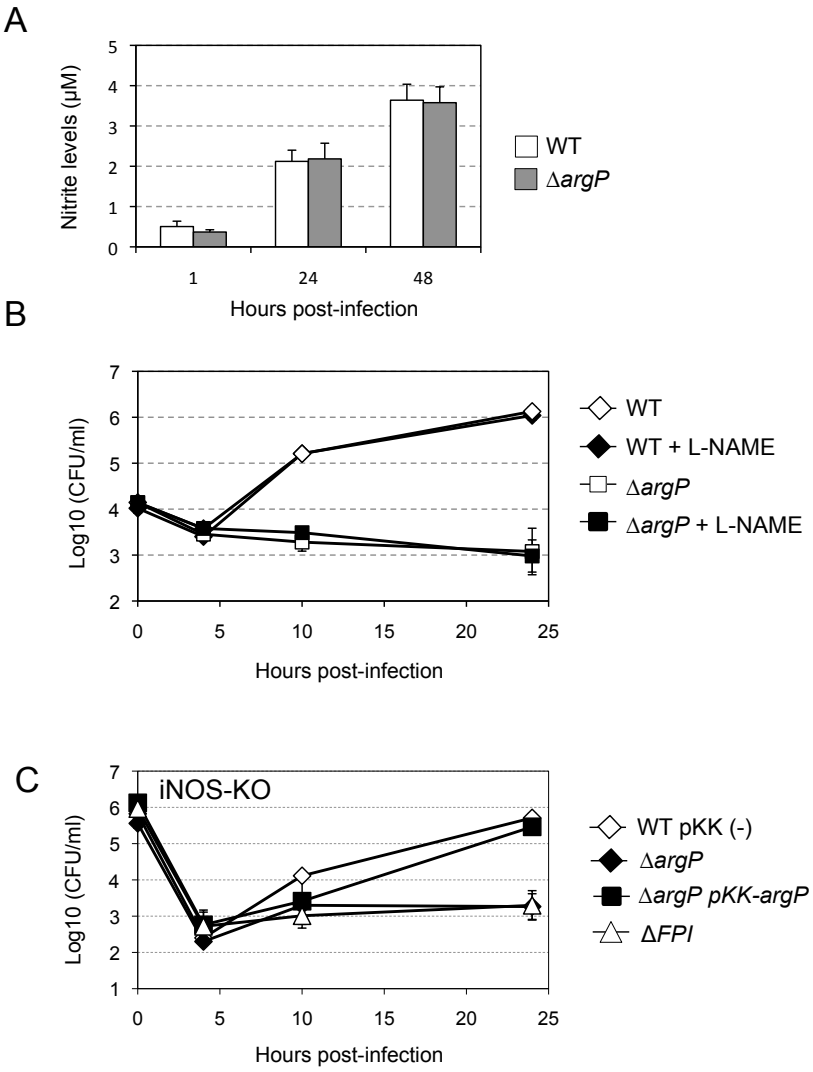

43

44 **Figure S4. Susceptibility to NO**

45 **(A) Nitrite levels.** Nitric oxide amount was determined by the Griess test in J774.1
46 cells infected with Wild-type *F. novicida* and Δ*argP* mutant for 1 h. Supernatants
47 were analyzed after 1 h, 24 h and 48 h of infection. Data were normalized with non-
48 infected cells nitrites amount. They are expressed as means ± standard deviations for
49 three determinations. Experience was realized twice.

50 (**B**) **Intracellular multiplication in the presence of the arginine analog L-NAME.**
51 J774.1 cells were treated with 1 mM iNOS inhibitor L-NAME before and all along

52 the infection with Wild-type *F. novicida* and Δ*argP* mutant. At several time-points,
53 cells were washed and lysed by the addition of demineralized water. For each strain
54 and time in an experiment, the assay was performed in triplicate. Each experiment
55 was independently repeated twice and the data presented originate from one typical
56 experiment.
57 (**C**) **Intracellular multiplication in iNOS-KO BMM.** Representative intracellular
58 multiplication of wild-type *F. novicida* (WT) carrying the empty plasmid pKK214
59 (WT pKK (-)), of the Δ*argP* mutant (Δ*argP*) and complemented strain (Δ*argP* pKK-
60 *argP*), and of the Δ*FPI* mutant (Δ*FPI*), in iNOS-deficient BMMs over a 24 h period.
61 Results are shown as the average of $\log_{10}$ (CFU/ml) ± standard deviations.
62 Experiences were realized twice.
63

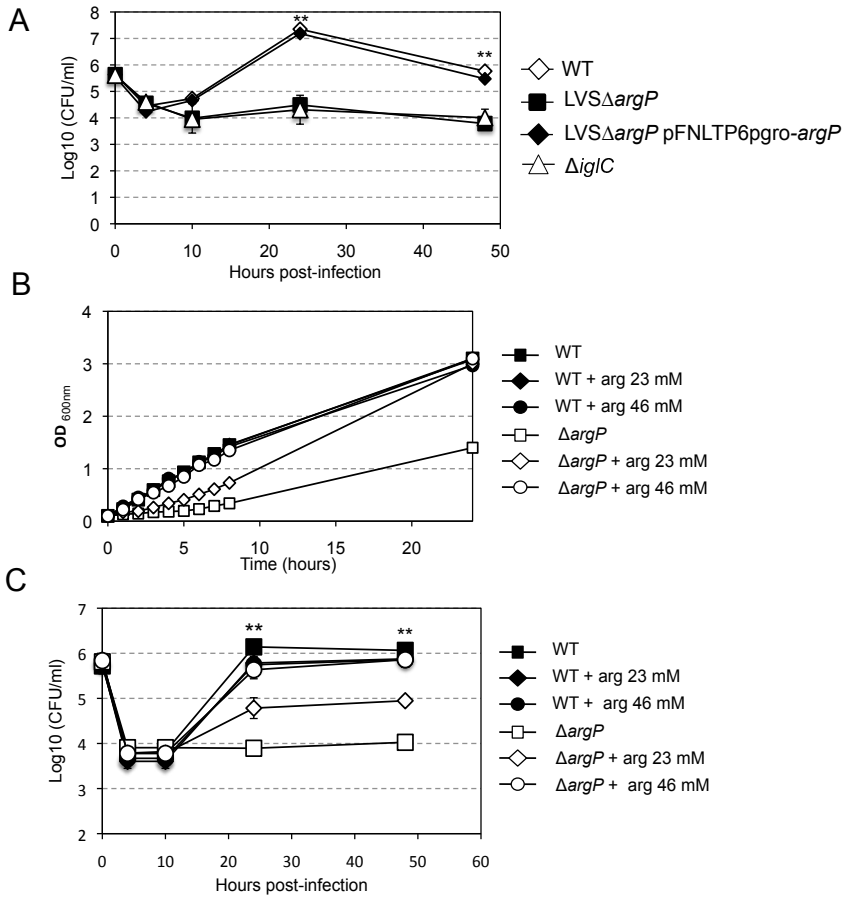

Figure S5. Critical role of ArgP in *F. tularensis* LVS

(A) Intracellular replication in J774.1 cells. The LVSΔ*argP* mutant showed a severe intracellular replication defect in J774.1 cells, in standard DMEM. Wild-type intracellular multiplication was restored in the complemented strain. Each experiment was performed in triplicate. **P < 0.01 (as determined by Student's t -test).

(B) Growth in synthetic medium. Growth of wild-type LVS and LVSΔ*argP* mutant was studied in CDM supplemented with various concentrations of arginine. In standard CDM, LVSΔ*argP* mutant showed a strong growth defect. This defect was partially alleviated upon supplementation with 23 mM arginine and wild-type growth was restored upon supplementation with 46 mM arginine Experiments were repeated twice. The figure represents a typical experiment.

(C) Arginine supplementation restores LVSΔ*argP* intracellular multiplication. Standard DMEM was supplemented with either 26 mM or 43 mM arginine. At 43 mM arginine, the multiplication of LVSΔ*argP* was restored to wild-type levels in J774.1 cells. Each experiment was performed in triplicate. **P < 0.01 (as determined by Student's t -test).

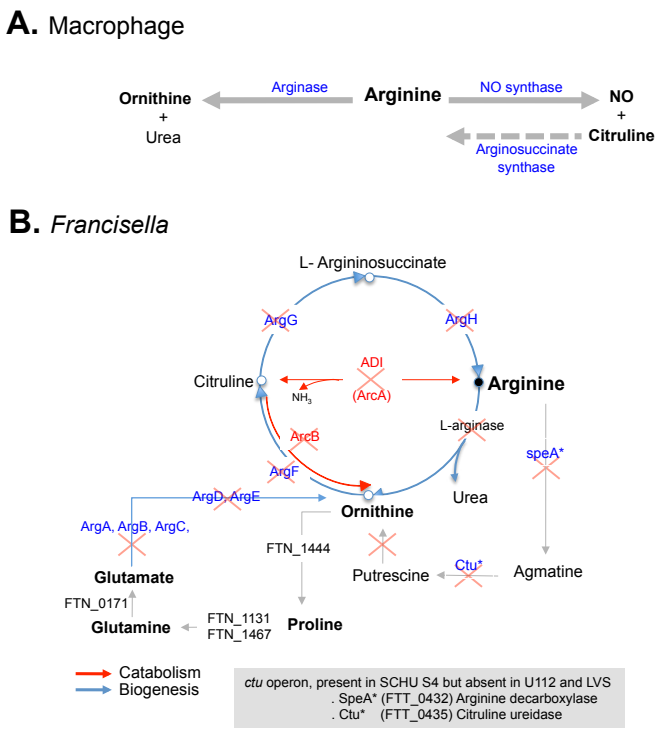

Figure S6. Arginine metabolic pathways

(**A**) Overview of mammalian arginine metabolism. Arginase and NOS use arginine as a common substrate and compete with each other for this substrate.

(**B**) In *F. novicida*, all the genes for the biosynthesis or degradation of arginine are inactive or altered (according to KEGG metabolic pathways; symbolized by a red cross). Grey arrows symbolize the predicted enzymatic reactions.

Table S1 (see attached xls file)

Table S2. Strains, plasmids and primers

Strain, plasmid, or primer	Primer code	Description or sequence (5' → 3')	Reference or source
E. coli strains			
E. coli Top10		F– *mcr*A Δ(*mrr-hsd*RMS-*mcr*BC) Φ80*lac*ZΔM15 Δ*lac*X74 *rec*A1*ara*D139 Δ(*ara leu*) 7697 *gal*U *gal*K *rps*L (StrR) *end*A1 *nup*G	Laboratory strain collection
F. tularensis strains			
U112		*F. tularensis* subsp. *novicida* U112	Laboratory strain collection
FTN (PKK214)		FTN containing empty plasmid PKK214	This study
FTNΔ*FTN_0848*		FTN with gene *FTN_0848* deleted	This study
FTNΔ*FTN_0848* (PKK214-*FTN_0848)*		FTNΔ*FTN_0848* containing PKK214-*FTN_0848*	This study
LVS		*F. tularensis* ssp *holarctica* strain LVS	A. Sjostedt
LVSΔ*FTL_1233*		Chromosomal deletion of *FTL_1233*	This work
LVS Δ*FTL_1233* (pFNLTP6p*gro-FTL_1233*)		LVSΔ*FTN_1233* containing complementing plasmid pFNLTP6 p*gro-FTL_1233*	This work
LVSΔiglC		Chromosomal deletion of *iglC*	A. Sjostedt
Plasmids			
pGEM		*E. Coli* cloning vector, Amp^R	Promega
pGEM-*FTL_1233* up/down		pGEM containing the indel; Amp^R	This work
pKK214		Derived from pKK202, promoter trap vector drives Cm^R Tet^R	(Kuoppa et al., 2001)
pKK214-*FTN_0848*		pKK214 containing the gene *FTN_0848*	This work
pMP812		*sacB* suicide vector, Kan^R	(LoVullo et al., 2009)
pMP812-*FTL_1233* up/down		pMP812 containing the indel; Kan^R	This work
pFNLTP6 p*gro*		*E. coli / F. tularensis shuttle vector; Kan^R Amp^R* Expression of the kanamycine resistance *npt* gene under p*gro* promoter control	(Maier et al., 2006)
pFNLTP6 p*gro-FTL_1233*		pFNLTP6 p*gro* containing the gene *FTL_1233*	This work
Primers			
Pgro_F	1	TTG TAT GGA TTA GTC GAG CTA AA	
npt_R	2	TCA GAA GAA CTC GTC AAG AAG G	
FTN_0848upF	3	CCC AAG TGC AGA AAA ATG TGA G	
FTN_0848upR	4	GAG CTT TTT AGC TCG ACT AAT CCA TAC AAC ATA CGT TAG TGG ATA GTT TAA G	
FTN_0848downF	5		
FTN_0848downR	6		
FTN_0848upF2 control	7	AGG TAT AAA CTA TGC AAG TAT C	
FTN_0848downR2 control	8	TTT TTG AAG AGA TCT TTG AG	
FTN_0848 5'race GSP1	9	TCA AAA TAC TTG GAA ACC AGA TAA G	
FTN_0848 5'race GSP2	10	TAT CCA TTG GAA CCA TAC AGC	
FTN_0848 compl forw	11	CCC GGG ATC AAG ATA GAT TAA TCA TCA AAG TGG	
FTN_0848 compl rev	12	GAA TTC AAC AAG AGT TAG AAA AAG TAT TAA TGA TT	
FTN_0847 qRT forw	15	CTC TCA AAA TTG TAC GGT TGA TAA ATC G	
FTN_0847 qRT rev	16	CAG TAT AAC CGA CAC TTA TAC CGA TAA CTT C	
FTN_0848 qRT forw	13	CTT CCA TCT ACA GCC ACT TCA GGA	
FTN_0848 qRT rev	14	GCA GTA TAT GTC GTA GTC ATC TCT GCA	
FTN_0849 qRT forw	17	CTG TTA TTG ATC TAG ATG AAG AAA AAC TTG G	
FTN_0849 qRT rev	18	ATT TGA TGT CAC AGC TAT TAT CAT ATC AGT ATC	
FTL_1233 upF NotI	19	ATG TAG CGG CCG CCC TTT CCG AAA AAAG C	
FTL_1233 upR	20	ACA AAT TAT CTG GTG GGA CAA AGC CGT T	
FTL_1233 doF	21	TTC CAT CTA CAG CCA CTT CAG GAA CGG CT	
FTL_1233 doR BamHI	22	CCA TAG GAT CCG CAG TAT TAG CGG CAT A	

Supplemental Experimental procedures

Bacterial growth

F. novicida and its mutant derivatives were grown: i) in liquid, in Tryptic Soya broth (Becton, Dickinson and company) or Chamberlain chemically defined medium and ii) in solid, on pre-made chocolate agar PolyViteX (BioMerieux SA Marcy l'Etoile, France) or chocolate plates prepared from GC medium base, IsoVitalex vitamins and haemoglobin (BD Biosciences, San Jose, CA, USA), at 37°C. *E. coli* was grown in LB (Luria-Bertani, Difco) at 37°C. Ampicillin was used at a final concentration of 100 μg mL^{-1} to select recombinant *E. coli* carrying pGEM and its derivatives. Kanamycin was used at a final concentration of 50 μg mL^{-1} and 15 μg mL^{-1} to select respectively recombinant *E. coli* and *Francisella* carrying pKK and its derivates.

All bacterial strains, plasmids, and primers used in this study are listed in **Table S1**.

Construction of chromosomal Δ*argP* deletion mutants

In *F. novicida*. We have generated a chromosomal deletion of gene *FTN_0848* (*argP*) in *F. novicida* strain U112 by allelic replacement of the wild-type region with a mutated region deleted of the entire *argP* gene (from the ATG start codon till the TAA stop codon), substituted by the kanamycine resistance gene *npt* placed under the control of the P*gro* promoter. First, the two regions (app. 500 bp each) flanking gene *argP* (designated *FTN_0848*up and *FTN_0848*down, respectively), and the *npt* gene (1,161 bp, amplified from plasmid pFNLTP16H3 (Maier et al., 2006), were amplified by PCR using the following pairs of primers: i) *FTN_0848*up, p3, p4; ii) *FTN_0848*down, p5, p6; iii) *npt*, p1, p2. The region *FTN_0848*up-*npt*-

*FTN_0848*down (*ca.* 2300 bp) was then amplified by triple overlap PCR, using the *FTN_0848*up, *FTN_0848*down and *npt* products. The resulting PCR product was gel purified (using the QIAquick Gel extraction kit, QIAgen) and directly used to transform wild-type *F. novicida*. Chemical transformation was performed as described previously (Ludu et al., 2008). Recombinant bacteria, resulting from allelic replacement of the wild-type region with the mutated *FTN_0848up/npt/ FTN_0848down* region, were selected on kanamycine-containing plates (15 µg mL^{-1}). The mutant strain, designated Δa*rgP,* was checked for loss of the wild-type *argP* gene, using specific primers in PCR and qRT-PCR, by PCR sequencing (GATC Biotech) and Southern blot.

In *F. tularensis* LVS. We generated a chromosomal deletion of the orthologous gene *FTL_1233* in *F. tularensis* LVS, by using the counter-selectable plasmid pMP812 (LoVullo et al., 2009). The recombinant plasmid pMP812-Δ*FTL_1645* was constructed by overlap PCR. Primers p15/p16 amplified the 994 bp region upstream of position + 1 of the *FTL_1645* coding sequence, and primers p17/p18 amplified the 1,012 bp region immediately downstream of the *FTL_1645* stop codon (Table S1). Primers p16/p17 have an overlapping sequence of 23 nucleotides, resulting in complete deletion of the *FTL_1233* coding sequence after cross-over PCR. PCR reactions with primers p15/p16 and p17/p18 were performed with exTaq polymerase (Fermentas). The products were purified using the QIAquick PCR purification kit (QIAgen, CA). 200 ng of each was used as a template for PCR with primers p15/p18 and treated with 30 cycles of PCR (94°C for 30 s, 54°C for 30 s and 72°C for 120 s). The gel-purified 1,996 bp fragment was digested with *BamH*I and *Not*I (New England Biolabs) and cloned into *BamH*I–*Not*I digested pMP812 (LoVullo et al., 2009). The plasmid is introduced into *F. tularensis* LVS by electroporation. *F. tularensi*s LVS

was grown to OD 600 0.3–0.6 in Schaedler-K13 broth; bacteria were collected and washed twice with 0.5 M sucrose. Bacteria were suspended in 0.6 mL of 0.5 M sucrose and 200 µL were used immediately for electroporation in a 0.2 cm cuvette (2.5 kV, 25 mF, 600 W). After electroporation, bacteria were mixed with 1 ml of Schaedler-K3 broth and incubated at 37°C for 6 h before selection on chocolate agar (Bio-Rad, Hercules, CA, USA) with 5 µg mL^{-1} kanamycine concentration. Colonies appeared after 3 days of incubation at 37°C and were subsequently passed once on plates with selection, followed by a passage in liquid medium without selection (to allow recombination to occur). Next, bacteria were passed once on agar plates containing 5% sucrose. Isolated colonies were checked for loss of the wild-type *FTL_1233* gene by size analysis of the fragment obtained after PCR using primers combination p15/p18, p33/p18 and p15/p34. One colony harbouring a *FTL_1645* deletion, as determined by PCR analysis, was used for further studies. Genomic DNA was isolated and used as the template in a PCR with primers p33/p34. The PCR product was directly sequenced using primers p33/p34 to verify the complete deletion of the *FTL_1233* gene.

Functional complementation

The plasmid used for complementation of the Δ*argP* mutant, pKK-*argP*, was constructed by amplifying a 1,612 bp fragment (corresponding to the sequence 92 bp upstream of the *argP* start codon and to 40 bp downstream of the stop codon) using primers *FTN_0848* compl forw and *FTN_0848* compl rev (**Table S2**), followed by digestion with *Eco*RI and *Sma*I, and cloning into plasmid pKK214 (Kuoppa et al., 2001).

The plasmids pKK214 and pKK214-*argP,* were introduced into wild-type *F. novicida*

by electroporation, as described previously (Dieppedale et al., 2011).

Multiplication in macrophages

J774.1 macrophage-like cells (ATCC® Number: TIB67™) were propagated in Dulbecco´s Modified Eagle's Medium (DMEM) containing 10% fetal calf serum. Bone marrow-derived macrophages (BMM) from BALB/c mice, iNOS-KO mice, C57Bl/6j mice and IRAP-KO C57Bl/6j mice, were differentiated in RPMI 1640 Medium containing 10% fetal calf serum and 10% L-CSF. Bone marrow-derived dendritic cells (BM-DC) from C57Bl/6j mice and IRAP-KO C57Bl/6j mice were differentiated in Iscove's modified Dulbecco's medium supplemented with 10% fetal calf serum and 3% GM-CSF. J774.1, BMM and BM-DC, were seeded at a concentration of ~2 x 10^5 cells per well in 12-well cell tissue plates and monolayers were used 24 h after seeding. All cell types were incubated for 60 min at 37°C with the bacterial suspensions (at MOI of 100) to allow the bacteria to enter. After washing (time zero of the kinetic analysis), the cells were incubated in fresh culture medium containing gentamicin (10 μg mL^{-1}) to kill extracellular bacteria. At several time-points, cells were washed three times in DMEM, RPMI or Iscove's modified Dulbecco's medium depending on the kind of phagocytic cells. Cells were lysed by addition of demineralized water and the titer of viable bacteria released from the cells was determined by spreading serial dilutions on Chocolate agar plates. For each strain and time in an experiment, the assay was performed in triplicate. Each experiment was independently repeated at least twice and the data presented originate from one typical experiment.

Confocal experiments

J774.1 macrophage-like cells were seeded at 5.10^5 cells per well on glass coverslips in 12-well bottom flat plates. Next day, cells were infected at a MOI of 1,000 with wild-type *F. novicida*, Δ*argP* or Δ*FPI* strains for 1 h, 4 h and 10 h at 37°C. For each time point, cells were fixed with paraformaldehyde (4%) for 15 min, quenching was realized with NH_4Cl for 10 min and cells were permeabilized and blocked with 0.1% saponine, 5% goat serum in PBS for 10 min. All antibodies were diluted in the same mix and all steps are separated by PBS washing. Monolayers were then incubated with anti *F. tularensis* ssp *novicida* mouse monoclonal antibody (Creative diagnostics) diluted 1:500 and anti LAMP-1 rabbit monoclonal antibody (Abcam), diluted 1:250, for 30 min at room temperature (RT) followed with donkey anti-mouse Alexa Fluor 488 (Abcam) and donkey anti-rabbit Alexa fluor 546 (Abcam), both diluted 1:400, for 30 min. Monolayers were then incubated 1 min in DAPI diluted 1:1000 in PBS. Coverslips were washed in PBS and in demineralized water and then mounted in Mowiol.

Cells were examined using an X63 oil-immersion objective on a LeicaTSP SP5 confocal microscope. Co-localization tests were performed by using Image J software; and mean numbers were calculated on more than 500 cells for each condition. Confocal microscopy analyses were performed at the Cell Imaging Facility (Faculté de Médecine Necker Enfants-Malades).

Electron microscopy

J774 cells were infected with wild-type *F. novicida* and mutant Δ*ansP* bacteria. Samples for electron microscopy were prepared using the thin-sectioning procedure as previously described (Alkhuder et al., 2009).

Vacuolar rupture assay

Quantification of vacuolar escape by flow cytometry using the β -lactamase-CCF4 assay (Life technologies) was performed following manufacturer's instructions. Briefly, macrophages were infected in non-Tc treated plates with Wild-type *F. novicida*, Δ*argP* mutant or Δ*FPI* mutant with a MOI of 10. At 2 h post-infection (PI) , macrophages were incubated with CCF4 for 1 h at RT in the presence of 2.5 mM probenicid (Sigma). Cells were collected by gentle scraping, washed once, resuspended in PBS containing 2.5 mM probenicid and propidium iodide at 5 ug mL^{-1} and directly analysed by flow cytometry on a canto 2 cytometer (BD Bioscience). Propidium iodide negative cells were considered for the quantification of cells containing cytosolic *F. novicida* using excitation at 405 nm and detection at 450 nm (cleaved CCF4) or 535 nm (intact CCF4).

Real time cell death assay

Cell death was quantified in real time by monitoring propidium iodide incorporation. Briefly, 5.10^4 BMM were seeded in 0.3 cm^2 wells of black 96-flat-bottom-well plate and infected with Wild-type *F. novicida*, Δ*argP* mutant or Δ*FPI* mutant with an MOI of 100. Two hours post-infection, cells were washed and incubated in CO_2-independent medium (Gibco) containing 5 ug mL^{-1} propidium iodide, MCSF, 10% FCS and 2 mM glutamine. The 96 wells plate was immediately transferred to a microplate fluorimeter (Tecan infinite M1000) prewarmed at 37°C. Propidium iodide fluorescence was measured every 15 min over a 15 h-period.

Isolation of total RNA and reverse transcription

Bacteria were centrifuged for 2 min at RT and the pellet was quickly resuspended in Trizol solution (Invitrogen, Carlsbad, CA, USA). Samples were either processed immediately or frozen and stored at -80°C. Samples were treated with chloroform and the aqueous phase was used in the RNeasy Clean-up protocol (Qiagen, Valencia, CA, USA) with an on-column DNase digestion of 30 min (Thomson et al., 2008).

RNA Reverse transcription (RT)-PCR experiments were carried out with 500 ng of RNA and 2 pmol of specific reverse primers. After denaturation at 65°C for 5 min, 6 μL of the mixture containing 4 μL of 5X first strand buffer and 2 μL of 0.1 M DTT were added. Samples were incubated for 2 min at 42°C, then 1 μL of Superscript II RT (Thermo Scientific) was added. Samples were incubated for 50 min at 42°C, heated at 70°C for 15 min and chilled on ice. Samples were diluted with 180 μL of H_2O and stored at –20°C.

The following pair of primers was used to amplify the mRNA corresponding to the transcript of *FTN_0847* (p15/p16), *FTN_0848* (p13/p14), *FTN_0849* (p15/p16) (**Table S1**).

Quantitative real-time RT-PCR

The 25 μL reaction consisted of 5 μL of cDNA template, 12.5 μL of Fastart SYBR Green Master (Roche Diagnostics), 2 μL of each primer (at 10 μM) and 3.5 μL water. qRT-PCR was performed according manufacturer's protocol on Applied Biosystems - ABI PRISM 7700 instrument (Applied Biosystems, Foster City, CA). To calculate the amount of gene-specific transcript, a standard curve was plotted for each primer set using a series of diluted genomic DNA from wild-type *F. novicida*. The amounts of each transcript were normalized to helicase rates (*FTN_1594*).

References

Alkhuder, K., K. L. Meibom, I. Dubail, M. Dupuis & A. Charbit, (2009) Glutathione provides a source of cysteine essential for intracellular multiplication of *Francisella tularensis*. *PLoS Pathog* **5**: e1000284.

Dieppedale, J., D. Sobral, M. Dupuis, I. Dubail, J. Klimentova, J. Stulik, G. Postic, E. Frapy, K. L. Meibom, M. Barel & A. Charbit, (2011) Identification of a putative chaperone involved in stress resistance and virulence in *Francisella tularensis*. *Infect Immun* **79**: 1428-1439.

Kuoppa, K., A. Forsberg & A. Norqvist, (2001) Construction of a reporter plasmid for screening in vivo promoter activity in *Francisella tularensis*. *FEMS Microbiol Lett* **205**: 77-81.

LoVullo, E. D., C. R. Molins-Schneekloth, H. P. Schweizer & M. S. Pavelka, Jr., (2009) Single-copy chromosomal integration systems for *Francisella tularensis*. *Microbiology* **155**: 1152-1163.

Ludu, J. S., O. M. de Bruin, B. N. Duplantis, C. L. Schmerk, A. Y. Chou, K. L. Elkins & F. E. Nano, (2008) The *Francisella* pathogenicity island protein PdpD is required for full virulence and associates with homologues of the type VI secretion system. *J Bacteriol* **190**: 4584-4595.

Maier, T. M., R. Pechous, M. Casey, T. C. Zahrt & D. W. Frank, (2006) In vivo Himar1-based transposon mutagenesis of *Francisella tularensis*. *Appl Environ Microbiol* **72**: 1878-1885.

Thomson, N. R., D. J. Clayton, D. Windhorst, G. Vernikos, S. Davidson, C. Churcher, M. A. Quail, M. Stevens, M. A. Jones, M. Watson, A. Barron, A. Layton, D. Pickard, R. A. Kingsley, A. Bignell, L. Clark, B. Harris, D. Ormond, Z. Abdellah, K. Brooks, I. Cherevach, T. Chillingworth, J. Woodward, H.

296 Norberczak, A. Lord, C. Arrowsmith, K. Jagels, S. Moule, K. Mungall, M.
297 Sanders, S. Whitehead, J. A. Chabalgoity, D. Maskell, T. Humphrey, M.
298 Roberts, P. A. Barrow, G. Dougan & J. Parkhill, (2008) Comparative genome
299 analysis of *Salmonella Enteritidis* PT4 and *Salmonella Gallinarum* 287/91
300 provides insights into evolutionary and host adaptation pathways. *Genome Res*
301 **18**: 1624-1637.
302
303

II Discussion et perspectives

L'ensemble des travaux réalisés au cours de cette thèse a permis de mettre en évidence le rôle essentiel de deux transporteurs d'acides aminés de la sous-famille APC dans la virulence de *F. tularensis*. L'adaptation nutritionnelle de *F. tularensis* au compartiment extrêmement pauvre en nutriments que constitue le phagosome, apparaît comme un élément clef de son cycle intracellulaire. De plus, les résultats obtenus soulignent la contribution des acides aminés à la réponse au(x) stress. Les données disponibles sur le contenu du phagosome sont à ce jour encore très limitées. Cependant il est généralement admis que le phagosome contribue à l'élimination des pathogènes par la cellule hôte, en limitant notamment l'accès aux acides aminés. Les résultats très récents obtenus dans notre laboratoire indiquent que *F. tularensis* a développé un réseau de transporteurs spécifiques lui permettant d'importer les acides aminés dont elle a besoin, et ce, dès son entrée dans la cellule hôte.

De nombreux cribles génétiques, réalisés sur *F. tularensis,* ont conduit à l'identification de gènes du métabolisme et en particulier des transporteurs d'acides aminés, suggérant un lien direct entre nutrition et virulence bactérienne. Une sous-famille est particulièrement bien représentée : la sous-famille APC (amino acid-polyamine-organocation). En effet, elle présente 11 protéines dont 8 sont retrouvées dans plusieurs cribles génétiques. Au cours d'une première étude nous nous sommes intéressés à l'une d'entre elle, une protéine que nous avons nommé GadC et qui a été retrouvée comme impliquée dans la multiplication intracellulaire de *F. tularensis* ssp *holarctica* LVS (Maier et al., 2007) et dans la virulence de *F. tularensis* ssp *novicida* (Kraemer et al., 2009; Peng et al., 2010; Weiss et al., 2007). Pour mieux comprendre son implication dans la pathogénicité de *F. tularensis*, nous avons réalisé un mutant dans la sous-espèce *novicida* (Δ*gadC*) où nous avons délété le gène d'intérêt (*FTN_0571*) que nous avons remplacé par une cassette kanamycine afin de faciliter nos travaux de recherche. Ce mutant Δ*gadC* montre un sévère défaut de multiplication intracellulaire dans des macrophages murins de lignée tumorale (J774.1) et des macrophages de moelle osseuse (défaut de 3 log) mais aussi un sévère défaut de virulence dans un modèle murin (défaut de 5 log), confirmant les résultats des cribles génétiques. Les outils de microscopie confocale et microscopie électronique nous ont permis de mettre en évidence l'implication de GadC dans l'échappement phagosomal.

La protéine GadC de *F. tularensis* présente une identité d'environ 25% avec la protéine GadC d'*E. coli* qui est impliquée dans la résistance au stress acide (Castanie-Cornet et al., 1999). Cette protéine importe une molécule de glutamate et exporte simultanément une molécule de GABA (Ma et al., 2012). Dans la bactérie, le glutamate est métabolisé en GABA grâce à la glutamate décarboxylase GadB en utilisant par la même occasion un proton, ce qui permet la détoxification de l'espace interne de la bactérie. De façon très intéressante, nous montrons que la protéine GadC de la bactérie *F. tularensis* importe du glutamate mais qu'elle ne joue aucun rôle dans la résistance à ce type de stress, en revanche, elle permet la résistance de la bactérie au stress oxydant. De plus, nous montrons de façon assez inattendue une implication extrêmement limitée de la glutamate décarboxylase GadB (*FTN_1701*) dans la virulence de *F. tularensis* (défaut de virulence inférieur à un log dans un modèle murin). Ces données suggèrent que ce fonctionnement en tandem de GadC et GadB est inexistant chez *F. tularensis* et elles proposent surtout une adaptation nutritionnelle de ce transporteur chez *F. tularensis*. Par ces travaux nous montrons aussi un nouveau système de détoxification des ERO chez la bactérie *F. tularensis*. Ce type de système a été mis en évidence jusqu'à maintenant seulement chez les levures et les plantes. Nous confirmons l'implication de GadC dans la résistance au stress oxydant grâce à l'utilisation d'un modèle murin C57BL/6J $gp91^{phox-/-}$. Il s'agit d'un modèle qui comprend des NADPH oxydase non fonctionnelles puisqu'il manque la sous-unité $gp91^{phox}$. Elles sont par conséquent incapables de générer des ERO dans les cellules phagocytaires. On assiste à un rétablissement total de la multiplication intracellulaire du mutant Δ*gadC* dans des macrophages issus de moelle osseuse. Nous assistons aussi à un rétablissement significatif de la virulence de ce mutant.
Cette protéine s'ajoute aux systèmes de détoxification des ERO déjà identifiés qui sont la catalase KatG, les superoxydes dismutases SodB et SodC (H. Lindgren et al., 2007; A. A. Melillo et al., 2010; A. A. Melillo et al., 2009), une glutathion peroxydase, une peroxydase (Sugano et al., 2007) et une protéine découverte cette année qui s'assimilerait aussi à une peroxydase, codée par le gène *FTN_1133* (Meireles Dde et al., 2014).

Le pool cytosolique du macrophage présente une concentration importante en glutamate qui varie de 2 à 20mM, cela s'explique par la présence de plusieurs systèmes d'acquisition tels que des transporteurs de glutamate à haute affinité Na+ dépendants. Il a aussi la possibilité de transformer la glutamine (via la glutaminase) ou l'aspartate (via l'aspartate transpeptidase) en glutamate (Newsholme et al., 2003). Rien n'est encore connu concernant le pool phagosomal de glutamate. On peut supposer qu'il contient aussi du glutamate puisque la cellule possède

un transporteur capable d'importer de la cystine et d'exporter du glutamate. Lorsque ce transporteur est compris dans une vacuole, on peut imaginer qu'il va diriger ces flux dans le sens inverse permettant ainsi l'entrée de glutamate dans le phagosome (cf figure 22).

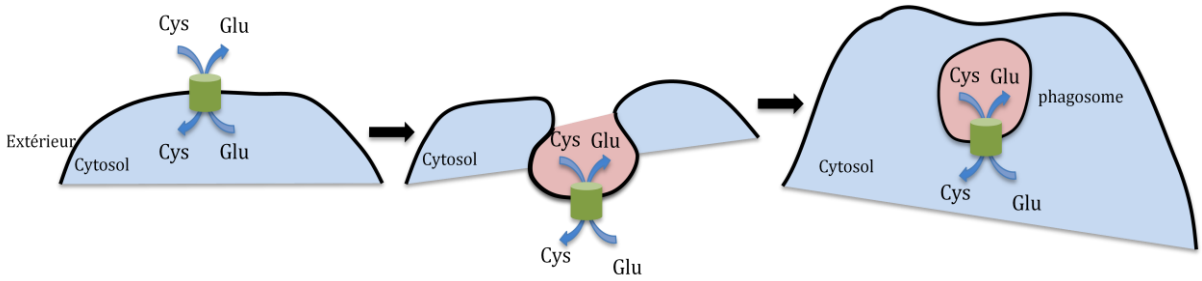

Figure 22 ***Hypothèse de l'import de glutamate dans la vacuole phagosomale lors de l'internalisation de F. tularensis.***

Dans la seconde partie de ce travail, nous mettons en évidence le lien fort qui existe entre la résistance au stress oxydant apportée par GadC et le fonctionnement du Cycle de Krebs. Plusieurs voies d'adressage du glutamate vers le Cycle de Krebs sont connues. L'une met en jeu la glutamate déshydrogénase (*gdhA* ou *FTN_1532*, voie n°1 sur la figure 23), l'autre voie, appelée GABA shunt, met en jeu la glutamate décarboxylase (*gadB* ou *FTN_1701*, voie n°2 sur la figure 23), la GABA transaminase qui est inexistante dans toutes les sous-espèces de *F. tularensis* et la succinate semialdéhyde déshydrogénase (*gabD* ou *FTN_0127*) qui existe seulement chez la ssp *novicida* (cf. figure 23). Notre hypothèse est donc que le glutamate qui rentre grâce au transporteur GadC est directement métabolisé en 2-oxoglutarate. En effet cette réaction produit par la même occasion du NADPH, une molécule essentielle dans la détoxification des ERO.

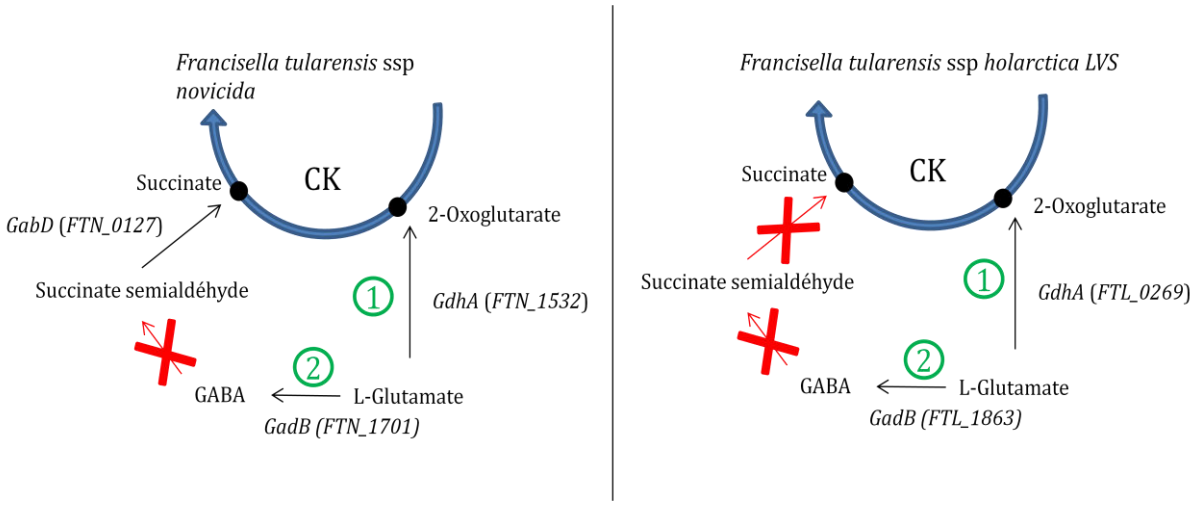

Figure 23 ***Métabolisme du glutamate chez F. tularensis***

Au-delà d'une adaptation métabolique, ces données soulignent la mise en place d'un autre système de détoxification des ERO par la bactérie et le détournement de l'utilisation d'un acide aminé non essentiel comme le glutamate à des fins non nutritionnelles.
Enfin ces résultats suggèrent un autre rôle concernant le devenir du glutamate. En effet, il est généralement admis que le glutamate est métabolisé en glutathion pour prendre en charge les ERO et que ce système joue un rôle majeur dans la résistance au stress oxydant. Ici nous démontrons la prise en charge du glutamate vers le cycle de Krebs (via l'oxoglutarate).

Il serait aussi intéressant d'évaluer l'effet de la délétion du gène *gadC* (*FTL_1583*) chez *F. tularensis* ssp *holarctica* afin de savoir si nous pouvons extrapoler ce phénotype à d'autres sous-espèces de *F. tularensis*. Il serait également intéressant d'étudier l'importance du système de détoxification GadC par rapport aux autres systèmes déjà mis en évidence chez *F. tularensis* ssp *novicida,* par exemple en regardant la sensibilité respective de chaque mutant (Δ*gadC*, Δ*katG*, Δ*sodB*…) dans un milieu de culture supplémenté en péroxyde d'hydrogène ou en comparant leur multiplication intracellulaire respective et leur virulence respective. Le système de détoxification impliquant GadC semble être un système « fort » dans le sens où le mutant délété pour le gène *gadC* présente l'une des virulences les plus atténuées.
Par la suite, il serait également intéressant d'évaluer l'activité des enzymes intervenant dans ces régulations, en particulier la glutamate déshydrogénase (GdhA) qui métabolise le glutamate en 2-oxoglutarate et l'oxoglutarate déshydrogénase (OGDH) qui métabolise l'oxoglutarate en succinyl-CoA.

Notre laboratoire s'intéresse désormais à l'importance du Cycle de Krebs dans la virulence de *F. tularensis* et en particulier à la partie du cycle qui comprend l'OGDH. Ce complexe OGDH est composé de trois sous-unités : *FTN_1635* qui code pour la sous-unité E1, *FTN_1634* pour la sous-unité E2 et *FTN_1492* pour la sous-unité E3. Cette troisième sous-unité joue aussi un rôle dans le complexe de la pyruvate déshydrogénase. Dans un précédent travail réalisé par Jennifer Dieppedale au laboratoire, il a été montré un lien indirect entre la résistance au stress oxydant et l'activité des sous-unités E1 et E2 de l'OGDH. Aux vues de ces résultats, nous avons voulu connaître la réelle implication de l'OGDH dans la virulence de *F. tularensis*. C'est pourquoi, nous avons réalisé un mutant délété pour le gène codant pour la sous-unité E1 et donc présentant théoriquement un complexe inactif. Ce mutant est actuellement en cours de caractérisation.

La deuxième étude qui constitue mon travail de thèse met en évidence l'implication d'un second transporteur de la sous-famille APC dans la multiplication intracellulaire et la virulence des bactéries *F. tularensis*, dans les ssp *novicida* et *holarctica* : le transporteur ArgP. Chez la souche *novicida*, nous démontrons, grâce à des techniques de supplémentation d'acides aminés en concentration supra-physiologique mais aussi par des techniques de transport d'acide aminé radiomarqué qu'il est nécessaire dans l'import d'arginine. Il est à noter que l'arginine est un acide aminé essentiel pour la bactérie *F. tularensis*. Les résultats que nous avons obtenus établissent le rôle fondamental joué par ArgP dans l'échappement phagosomal de la bactérie, permettant par la suite la multiplication cytosolique.

Nous nous sommes posés la question de l'importance de l'arginine pour *F. tularensis* dans le compartiment phagosomal. En effet, l'arginine apparaît dans la littérature scientifique comme un acide aminé clé dans la réponse bactéricide (Das et al., 2010) et en particulier pour la production de dérivés nitrés. En effet, grâce à la NO synthase, le macrophage métabolise son arginine en citrulline et oxyde nitrique (cf figure 24).

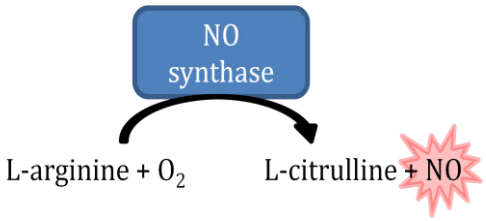

Figure 24 ***Schéma de la production d'oxyde nitrique par la cellule phagocytaire***

Nos trois hypothèses de départ quant au rôle du transporteur ArgP étaient : i) la bactérie importe l'arginine de façon à limiter sa disponibilité pour la NO synthase et donc limiter la production de dérivés nitrés ; ii) la bactérie s'en sert comme outil pour détoxifier l'espace phagosomal des protons générés par les vATPases (cf figure 25) ; iii) l'arginine importé par ArgP joue un rôle dans le Cycle de l'Urée. Nos résultats expérimentaux indiquent que les deux premières hypothèses sont à écarter. D'autre part, le fait que quasiment toutes les enzymes inclues dans le cycle de l'urée sont inexistantes chez toutes les sous-espèces de *F. tularensis* (database KEGG) suggèrent que la troisième hypothèse n'est pas valable non plus.

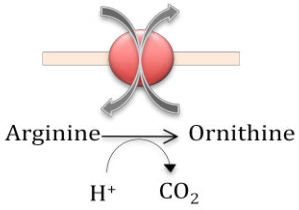

Figure 25 ***Schéma de la détoxification des protons mettant en jeu l'arginine par F. tularensis***

Comme cité précédemment, l'arginine est un acide aminé essentiel pour *F. tularensis*. Une étude bio-informatique du pool protéique de cette bactérie nous a permis de mettre en évidence un pourcentage élevé de molécules d'arginine chez la majorité des protéines ribosomales. Nous avons donc émis l'hypothèse que le défaut de sortie de *F. tularensis* s'expliquait par un défaut particulier de synthèse de ce type de protéine. Nous avons donc réalisé une étude protéomique à large échelle grâce à la spectrométrie de masse à haute résolution en comparant les pools protéiques d'une souche sauvage et d'une souche mutante Δ*argP* dans un milieu de culture contenant une concentration normale d'arginine et dans un milieu de culture contenant 20% de l'arginine total (de façon à mimer la concentration d'arginine dans le phagosome). Nos résultats montrent la sous-expression de 104 protéines chez le mutant en condition limitée en arginine, avec parmi elles, 29 des 30 protéines ribosomales identifiées. Ainsi nous confirmons notre hypothèse de départ en mettant en évidence la modification significative de la production des protéines ribosomales riches en arginine. D'autre part le fait que les protéines ribosomales moins riches en arginine soit aussi affectées suggèrent qu'il existe peut être une régulation globale, voire un système senseur des conditions nutritionnelles extérieures, qui affecterait la production globale de protéines.

A l'inverse et de façon surprenante, on assiste à la surexpression de 67 protéines chez le mutant aussi en condition restreinte en arginine avec notamment parmi elles des protéines chaperonnes (DnaK, GroeEL et ClpB). Ces données indiquent que le défaut d'import d'arginine génère un stress nutritionnel chez le mutant. Ainsi l'import d'arginine est le garant d'une synthèse protéique optimale permettant la sortie du phagosome.

Comme le montrent nos données actuelles, le mutant Δ*argP* est capable de lyser la membrane phagosomale (expérience impliquant le CCF4). En se basant sur les résultats obtenus en spectrométrie de masse, on peut supposer que la lyse de la membrane phagosomale n'est pas dépendante d'une protéine néosynthétisée mais plutôt d'une protéine déjà produite avant même l'entrée dans la cellule. Cette étape de l'échappement phagosomal est extrêmement peu documentée, c'est pourquoi il est difficile d'imaginer les mécanismes mis en jeu dans cette situation.

Ces résultats démontrent donc la nécessité pour *F. tularensis* de posséder un transporteur d'arginine hautement spécifique pendant la phase phagosomale pour s'adapter aux concentrations extrêmement faibles de cet acide aminé. Il serait intéressant de savoir si les concentrations en arginine dans le cytosol sont suffisantes pour permettre la multiplication du

mutant Δ*argP*. Pour cela, on pourrait réaliser des expériences de micro-injection du mutant dans le cytosol de la cellule hôte et évaluer par la suite sa multiplication cytosolique (Goetz et al., 2001).

Enfin, il pourrait être intéressant d'effectuer une analyse systématique de tous les membres de la famille APC, par construction d'une série de mutants simples (ou multiples) de chacun des transporteurs de cette sous-famille et d'évaluer leur comportement dans la cellule phagocytaire (notamment en microscopie confocale). Par ailleurs, nous nous sommes plaçés jusqu'ici dans un contexte exclusivement cellulaire. *F. tularensis* ssp *novicida* étant une souche retrouvée aussi dans l'environnement (eau, cadavres, etc...) ; il pourrait être aussi intéressant d'évaluer les comportements des mutants Δ*gadC* et Δ*argP* dans ce type de contexte.

D'un point de vue plus général, les résultats récents obtenus dans notre laboratoire (cf articles n°1, n°2 et annexes) démontrent l'importance du Cycle de Krebs dans la virulence de *F. tularensis*. Comme décrit dans l'étude bibliographique, on distingue deux autres voies de métabolisme impliquant la dégradation des lipides mais surtout celle des sucres. Il serait intéressant de comparer l'importance du métabolisme des acides aminés avec celui des sucres et de comprendre dans quelle circonstance *F. tularensis* va utiliser préférentiellement l'une ou l'autre source de carbone.

III Conclusion

F. tularensis constitue un objet d'étude de plus en plus utilisé pour comprendre les stratégies d'infection des bactéries à multiplication intracellulaire facultative et pour comprendre les réponses immunitaires de la cellule phagocytaire. L'importance du métabolisme des acides aminés dans la virulence de *F. tularensis* a été mis en évidence par notre laboratoire. Ces travaux de thèse démontrent que *F. tularensis* a développé des systèmes d'acquisition des acides aminés à la fois comme mécanisme de résistance aux stress générés dans le phagosome mais aussi comme senseur de la disponibilité en acides aminés extérieurs.

Annexes

Sont présentés en annexes des travaux auxquels j'ai participé durant ma thèse.

Les deux premiers articles correspondent à deux études menées par Gaël Gesbert sur les transporteurs de la famille MFS (transporteurs secondaires). Ils correspondent à l'étude d'un transporteur d'asparagine et un transporteur d'isoleucine essentiels à la multiplication de la bactérie *F. tularensis* ssp *novicida* dans le cytosol des macrophages infectés.

D'autre part, j'ai participé à un projet mené par Jennifer Dieppedale et qui porte sur l'étude d'une protéine chaperon, MoxR, impliquée dans plusieurs fonctions métaboliques majeures de la bactérie.

Enfin, j'ai participé à la rédaction d'une revue portant sur les protéines impliquées dans la virulence et la réplication de *Francisella* à l'intérieur des macrophages.

Cellular Microbiology (2014) **16**(3), 434–449
doi:10.1111/cmi.12227
First published online 8 November 2013

Asparagine assimilation is critical for intracellular replication and dissemination of *Francisella*

Gael Gesbert,[1,2] Elodie Ramond,[1,2] Mélanie Rigard,[3,4] Eric Frapy,[1,2] Marion Dupuis,[1,2] Iharilalao Dubail,[1,2] Monique Barel,[1,2] Thomas Henry,[3,4] Karin Meibom[1,2] and Alain Charbit[1,2]*

[1]*Université Paris Descartes, Sorbonne Paris Cité, Bâtiment Leriche, 96 rue Didot 75993, Paris, Cedex 14, France.*
[2]*INSERM, U1002, Unité de Pathogénie des Infections Systémiques, Paris, France.*
[3]*Université de Lyon, Lyon, France.*
[4]*Bacterial Pathogenesis and Innate Immunity Laboratory, INSERM U851 'Immunity, Infection and Vaccination', Lyon, France.*

Summary

In order to develop a successful infectious cycle, intracellular bacterial pathogens must be able to adapt their metabolism to optimally utilize the nutrients available in the cellular compartments and tissues where they reside. *Francisella tularensis*, the agent of the zoonotic disease tularaemia, is a highly infectious bacterium for a large number of animal species. This bacterium replicates in its mammalian hosts mainly in the cytosol of infected macrophages. We report here the identification of a novel amino acid transporter of the major facilitator superfamily of secondary transporters that is required for bacterial intracellular multiplication and systemic dissemination. We show that inactivation of this transporter does not affect phagosomal escape but prevents multiplication in the cytosol of all cell types tested. Remarkably, the intracellular growth defect of the mutant was fully and specifically reversed by addition of asparagine or asparagine-containing dipeptides as well as by simultaneous addition of aspartic acid and ammonium. Importantly, bacterial virulence was also restored *in vivo*, in the mouse model, by asparagine supplementation. This work unravels thus, for the first time, the importance of asparagine for cytosolic multiplication of *Francisella*. Amino acid transporters are likely to constitute underappreciated players in bacterial intracellular parasitism.

Received 11 September, 2013; revised 10 October, 2013; accepted 11 October, 2013. *For correspondence. E-mail alain.charbit@inserm.fr; Tel. (+33) 1 72 60 65 11; Fax (+33) 1 72 60 65 13.

Introduction

Francisella tularensis is a Gram-negative bacterium causing the zoonotic disease tularaemia in a large number of wildlife animal species and has one of the broadest host range than any other known zoonotic disease-causing organism (Sjöstedt, 2011). Rodents, lagomorphs and amoeaba are thought to be the main reservoirs for human contamination (Keim *et al.*, 2007). This highly infectious pathogen can be transmitted to humans in numerous ways, including direct contact with sick animals, inhalation, ingestion of contaminated water or food or by insect bites. Four different subspecies (subsp.) of *F. tularensis* that differ in virulence and geographic distribution exist, designated subsp. *tularensis, holarctica*, *novicida* and *mediasiatica* respectively. *F. tularensis* subsp. *tularensis* is the most virulent subspecies causing a severe disease in humans (Sjöstedt, 2007) and is considered a potential bioterrorism agent (Oyston *et al.*, 2004). *F. tularensis* subsp. *novicida* (or *F. novicida*) is considered non-pathogenic for humans but is fully virulent for mice and is widely used as a model to study highly virulent subspecies.

Francisella is able to survive and to replicate inside a variety of mammalian host cells and in particular, macrophages (Hall *et al.*, 2008). Its virulence is tightly linked to its ability to escape rapidly from the phagosome into the host cytosol (Santic *et al.*, 2008) where it can replicate actively (Chong and Celli, 2010).

Several recent studies, mainly based on the characterization of nucleic acid and amino acid auxotrophic mutants, support the importance of metabolism in *Francisella* pathogenesis. For example, utilization of uracil has been shown to be required for inhibition of the neutrophil respiratory burst and intra-macrophage survival (Schulert *et al.*, 2009). Uracil auxotroph mutants of *F. tularensis* LVS showed impaired phagosomal escape and severe multiplication defects in monocyte-derived macrophages. The mutant bacteria that could reach the cytosol were unable to replicate but still triggered the secretion of IL-8 and IL-1β. Remarkably, in J774 and

HepG2 cells, these uracil auxotrophs appeared to multiply normally, implying that the defects in the pyrimidine biosynthetic pathway affect *Francisella* virulence in a cell type-specific manner. More recently, Peng and Monack showed that tryptophan auxotrophs of *F. novicida* were severely affected in intracellular multiplication and were attenuated in the mouse model (Peng and Monack, 2010).

Additional metabolic pathways have been shown to contribute to *Francisella* pathogenesis, including gluconeogenesis and glycolysis (Meibom and Charbit, 2010a) as well as biotin biosynthesis (Napier *et al*., 2012).

The identification of bacterial attributes specifically required for cytosolic replication by *Francisella* in the host cytosol may prove technically complex and time-consuming (Celli and Zahrt, 2013). Remarkably, two genome-scale screens, reported in human macrophages and Drosophila-derived cells (Asare and Abu Kwaik, 2010; Asare *et al*., 2010), identified more than 90 mutants that showed deficient phagosomal escape. These included genes encoding proteins with a broad variety of predicted functions. To date the best functionally characterized genes include: (i) purine biosynthetic genes (Pechous *et al*., 2006; 2008), (ii) the γ-glutamyl transpeptidase gene *ggt* (Alkhuder *et al*., 2009) and (iii) several genes of still unknown biological function, such as *dipA* (Wehrly *et al*., 2009; Chong *et al*., 2012), *FTT0989* (Brotcke *et al*., 2006) and *ripA* (Fuller *et al*., 2008; Mortensen *et al*., 2012).

Earlier genome-scale genetic screens, aimed at identifying specific *Francisella* intracellular survival attributes, have also repeatedly identified genes encoding membrane proteins. These included notably putative amino acid transporters (Pechous *et al*., 2009; Meibom and Charbit, 2010b), highlighting the potential critical role of such nutrient acquisition systems in intracellular adaptation of *Francisella*. However, there is currently no functional or structural information available on any of these hypothetical transporters.

The *Francisella* genomes encode numerous predicted transport systems, the majority of which are secondary carriers (Meibom and Charbit, 2010a). Secondary transporters encompass several major families, including the major facilitator superfamily (MFS), involved in various functions including drug efflux, sugar and amino acid uptake (Reddy *et al*., 2012). Of particular interest, in the pathogenic intracellular bacterium *Legionella pneumophila* (Sauer *et al*., 2005), a MFS threonine transporter, designated PhtA (for Phagosomal transporter A), was shown to be required for intraphagosomal growth and differentiation. Phylogenetic analyses revealed that the *Legionella* genomes encode numerous Pht paralogues (Sauer *et al*., 2005). Importantly, Pht family members were also found in other bacterial species (Chen *et al*., 2008) but exclusively among intracellular pathogenic bacteria.

Remarkably, *Francisella*, which resides only transiently in a phagosomal compartment and multiplies exclusively in the cytosol of infected cells, also encodes several putative Pht orthologues (four to six, depending on the e value threshold chosen for the blast analysis; Sauer *et al*., 2005; Chen *et al*., 2008). Recently, a study aimed at developing anti-*Francisella* vaccines (Marohn *et al*., 2012), showed that inactivation of several of these putative transporters had altered intracellular replication kinetics and attenuation of virulence in mice in *F. tularensis* LVS (including the orthologue of *ansP* in *F. tularensis* LVS, see below). However, none of them has been functionally characterized yet and their substrate specificity is currently unknown.

In the present work, we addressed the functional role of one of these transporters, hereafter designated AnsP, which has been repeatedly identified by earlier genetic screens, in different *Francisella* subspecies and using a variety of different screening procedures. We demonstrate that the MFS transporter AnsP is required for bacterial multiplication in the cytosolic compartment of infected macrophages and for systemic dissemination in the mouse.

Results

AnsP, a member of the major facilitator superfamily of secondary transporters

The region of gene *ansP* (Fig. S1) is highly conserved in all the *Francisella* genomes sequenced thus far and the AnsP protein of *F. novicida* (FTN_1586, 437 amino acids in length) shares more than 99% identity with its orthologues in *F. tularensis* subsp. *holartica* (FTL_1645), *mediasiatica* (FTM_0191) and *tularensis* (FTT_0129) (Fig. S2). In contrast, the homologues of the *Francisella* AnsP protein in other bacterial species do not exceed 28% amino acid identity. Indeed, the closest homologue in *L. pneumophila* (PhtE) shares only 26.7% amino acid identity, suggesting that the *Francisella* AnsP proteins displays properties specific to *Francisellae* species. Secondary structure prediction predicts that, like all MFS family members, AnsP comprises 12 transmembrane helixes (not shown).

Remarkably, the *ansP* gene was found among the genes required for replication of *F. novicida* (*FTN_1586*) in RAW264.7 macrophages (Llewellyn *et al*., 2011) as well as involved in replication in both U937 macrophages and drosophila S2 cells (Asare and Abu Kwaik, 2010). The orthologue of *ansP* in *F. tularensis* subsp. *tularensis* Schu S4 (*FTT_0129*) has also been found to be required

for normal bacterial replication in the hepatocytic human cell line HepG2 (Qin and Mann, 2006). These screening results imply that the transporter AnsP has specific properties that are not compensated by any other putative transporter encoded by the *Francisella* genome in cells as well as *in vivo*. In this respect, it is worth mentioning that the other predicted Pht family members of *Francisella* share less than 27% amino acid identity with AnsP (and in most cases, also between each other).

Role of AnsP in Francisella *intracellular survival*

We constructed a chromosomal deletion of the *ansP* gene in *F. novicida* (*FTN_1586*) by allelic replacement (Lauriano *et al*., 2003). We first evaluated the possible impact of the mutation *in vitro* (using different media and growth conditions) and then followed the capacity of the mutant to infect and multiply in different cell types as well as *in vivo*, in the mouse model.

AnsP is not required for growth in broth

Inactivation of *ansP* had no impact on bacterial growth in broth and did not prevent acquisition of any of the essential amino acid present in Chemically defined minimal medium (CDM_{min}; Fig. S3). We used Biolog Phenotypic Microarray GNII plates to test possible metabolic defects of the Δ*ansP* mutant. The respiration pattern obtained with the Δ*ansP* and wild-type strains were identical, indicating that the mutation had not led to a defect in the utilization of any of the 96 carbon sources tested (Fig. S4).

AnsP is essential for intracellular bacterial multiplication

Quantitative RT-PCR analysis demonstrated that inactivation of the *ansP* gene (in a Δ*ansP* deletion strain, see below) had no impact on the transcription of the two flanking genes *FTN_1585* and *FTN_1587* (Fig. S1). To further confirm that inactivation of the *ansP* gene had no polar effect on downstream gene expression, we complemented the Δ*ansP* mutant strain with a plasmid-encoded copy of the wild-type *ansP* gene under p*gro* promoter control (see *Experimental procedures* for details).

We examined the ability of wild-type *F. novicida* (WT), Δ*ansP* and Δ*ansP*-complemented strains to survive and multiply in: (i) murine macrophage-like J774 cells, (ii) primary murine bone marrow-derived macrophages (BMM) and (iii) human hepatocytic HepG-2 cells (Fig. 1). Remarkably, the Δ*ansP* mutant showed a severe growth defect in all cell types tested. In J774 cells, the Δ*ansP* mutant showed a 10-fold reduction of intracellular bacteria after 10 h, and almost a 100-fold reduction after 24 h, as compared to wild-type *F. novicida* (Fig. 1A). In

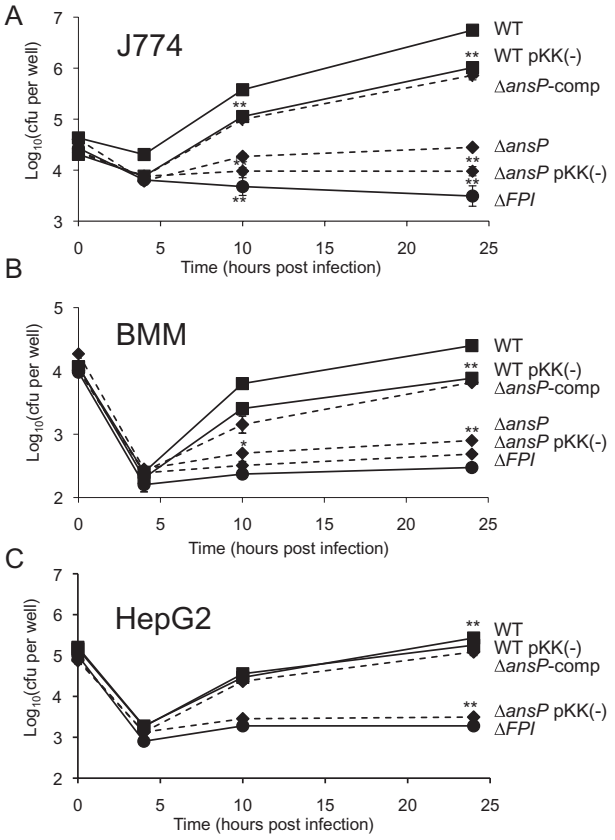

Fig. 1. The Δ*ansP* mutant is defective for intracellular replication. The Δ*ansP* mutant failed to replicate in J774 murine macrophage-like cells (A), murine bone marrow-derived macrophages (BMM) (B) and human hepatocytic cell line HepG2 (C). In all cell types, constitutive expression of the wild-type gene *ansP* (carried on *pKK*-p*gro-ansP*) restored normal intracellular replication. WT, wild-type *F. novicida*; WT *pKK(–)*, WT carrying pKK214; Δ*ansP*, WT deleted from gene *ansP*; *ΔansP pKK(–)*, Δ*ansP* strain carrying pKK214; Δ*ansP*-comp, Δ*ansP* carrying pKK214-p*gro-ansP*; and Δ*FPI*, wild-type *F. novicida* deleted of the entire FPI. Intracellular replication was monitored by enumerating colony-forming units (cfu) on chocolate agar plates. Each experiment was performed in triplicate. $^{*}P < 0.05$; $^{**}P < 0.01$ (as determined by Student's *t*-test).

BMM, the Δ*ansP* mutant showed an eightfold reduction of intracellular bacteria after 10 h, and a 16-fold reduction after 24 h (Fig. 1B). Finally, in HepG-2 cells, the Δ*ansP* mutant showed a 10-fold reduction of intracellular bacteria after 10 h, and a 70-fold reduction after 24 h (Fig. 1C).

In all cell types tested, the intracellular growth defect of Δ*ansP* mutant was similar to that observed with a deletion of the entire *Francisella* pathogenicity island [the Δ*FPI* mutant (Weiss *et al*., 2007)]. Introduction of the complementing plasmid (pKK214-p*gro-ansP*) restored bacterial viability to same level as in the wild-type parent, confirming the specific involvement of gene *ansP* in intracellular survival.

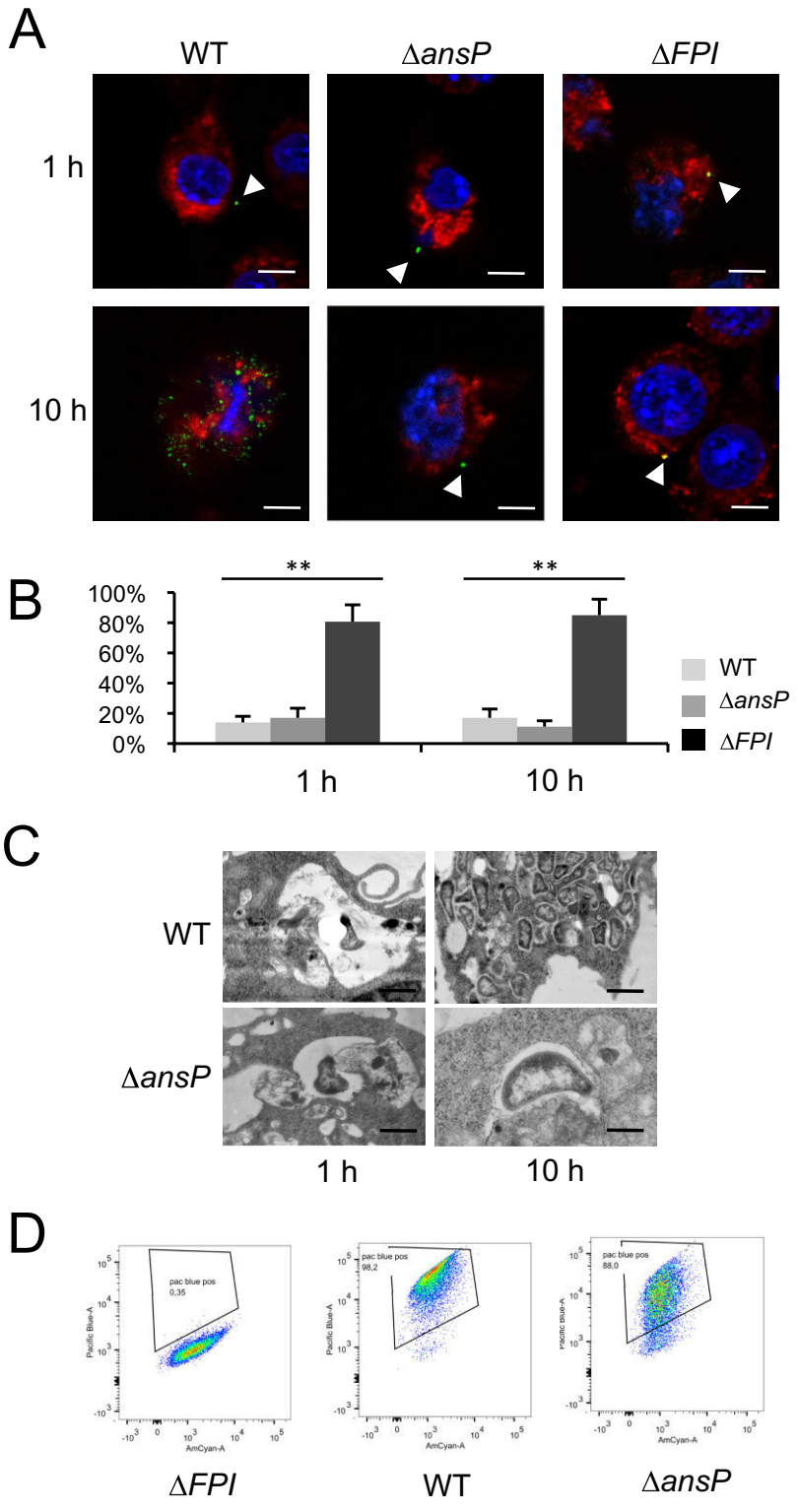

Fig. 2. Subcellular localization of the Δ*ansP* mutant.
A and B. Confocal microscopy. J774 cells were incubated for 1 h with wild-type *F. novicida*, Δ*ansP* or Δ*FPI* strains and their colocalization with the phagosomal marker LAMP1 was observed by confocal microscopy. The phagosomes of J774 cells were labelled with anti-LAMP1 antibody (1/100 final dilution). Cell nuclei were labelled with DAPI. Bacteria were labelled with primary mouse monoclonal antibody anti-*F. novicida* (1/500 final dilution). (A) The colour images represent wild-type *F. novicida* (WT), Δ*ansP*, Δ*FPI*, strains (green); phagosomes (red); and nuclei (blue). Scale bars at the bottom right of each panel correspond to 10 μM. (B) Quantification of bacteria/phagosome colocalization at 1 h, 4 h and 10 h for WT, Δ*ansP* and Δ*FPI* strains. $^{**}P < 0.01$ (as determined by Student's *t*-test).
C. Electron microscopy. J774 cells were incubated for 1 h or 24 h with wild-type *F. novicida* (WT) or Δ*ansP* mutant strains and replication was observed by transmission electronic microscopy (× 20 000 for WT and Δ*ansP* at 1 h, × 27 000 for Δ*ansP* at 24 h and × 14 000 for WT at 24 h). After 10 h, active intracellular multiplication is observed in J774 macrophages infected with WT. In contrast, no multiplication is visible in most of the macrophages infected with the Δ*ansP* mutant. The scale bars at the bottom right of the two left panels correspond to 400 nm (1 h); and to 600 nm (WT) and 200 nm (Δ*ansP*), respectively, for the two right panels (10 h).
D. CCF4. The cytosol of bone marrow-derived infected macrophages was loaded with CCF4. Upon cleavage by cytosolic β-lactamase, the CCF4 FRET is lost leading upon excitation at 405 nm to a shift of fluorescence from green (535 nm) to blue (450 nm). *F. novicida* naturally express a β-lactamase able to cleave the CCF4. *F. novicida* escape into the host cytosol is thus associated with a shift of the CCF4 probe from green to blue. Upon infection (at a multiplicity of infection of 100) with wild-type *F. novicida* (WT) and Δ*ansP* mutant, 98% and 88% of Pacific blue-positive cells were recorded respectively. In contrast, less than 1% of the cells were positive when infected with the Δ*FPI* mutant.

Subcellular localization of the ΔansP mutant in infected macrophages

We used the differential solubilization process previously described (Barel *et al.*, 2010) to follow the subcellular localization of the Δ*ansP* mutant in infected cells (Fig. 2A and B). Briefly, the plasma membrane was selectively permeabilized with digitonin. This treatment allowed the detection of cytoplasmic bacteria and proteins. Subsequent treatment with saponin rendered intact

phagosomes accessible to antibodies and allowed detection of intra-phagosomal bacteria. Intracellular localization of the bacteria or LAMP-1 (used as a specific marker of phagosomes) was analysed using specific antibodies and their colocalization was monitored at two time points (1 h and 10 h post-infection; Fig. 2A). Quantification of each colocalization was performed with the Image J software (Fig. 2B).

With both wild-type *F. novicida* and the Δ*ansP* mutant, colocalization with LAMP-1 was only around 15% after 1 h and remained in the same range throughout the infection. In contrast, for the *ΔFPI* mutant strain, 80% of bacteria colocalized with LAMP-1 after 1 h and colocalization remained very high after 10 h (85%). These results strongly suggest that the capacity of the *ΔansP* mutant to escape rapidly from the phagosomal compartment is unaffected.

To confirm these results, we performed thin section electron microscopy of J774 cells infected either with wild-type *F. novicida* or with the *ΔansP* mutant (Fig. 2C). Significant bacterial replication was observed in the cytosol of most infected cells 10 h post-infection with wild-type *F. novicida*. In contrast, bacterial multiplication was severely impaired in cells infected with the *ΔansP* mutant.

Finally, to quantify phagosomal permeabilization following *F. novicida* infection, we used the CCF4/β-lactamase technique originally described by Enninga and collaborators (Nothelfer *et al*., 2011), which we recently adapted to *F. novicida* (Juruj *et al*., 2013). Briefly, macrophages were loaded with CCF4, a fluorescence resonance energy transfer (FRET) probe retained within the host cytosol following the action of host cytosolic esterases. When cleaved by β-lactamase, the CCF4 FRET is lost leading upon excitation at 405 nm to a shift of fluorescence from green (535 nm) to blue (450 nm). *F. novicida* naturally express a β-lactamase able to cleave the CCF4 substrate (Broms *et al*., 2012). The phagosome permeabilization or *F. novicida* escape into the host cytosol is thus associated with a shift of the CCF4 probe from green to blue. Using this sensitive assay, we could not detect any differences in term of phagosomal permeabilization/vacuolar escape at 1 h post-infection (PI) in BMM between wild-type *F. novicida* and the Δ*ansP* mutant (Fig. 2D). As expected (Juruj *et al*., 2013), we did not detect phagosomal permeabilization using a Δ*FPI* mutant.

This result confirms thus that the Δ*ansP* mutant has normally access to the host cytosol but fails to multiply normally within this compartment.

Nutritional requirement of the ΔansP mutant

Since AnsP belongs to a family of putative amino acid transporters, we hypothesized that the intracellular multiplication defect of the Δ*ansP* mutant might be alleviated by amino acid supplementation (Fig. 3). Therefore, we first compared the kinetics of multiplication of the Δ*ansP* mutant in J774 macrophages, in the presence or absence of casamino acids in the cell culture medium (Fig. 3A). Addition of 0.5% casamino acids restored multiplication of the Δ*ansP* mutant to the wild-type level.

This result suggested that AnsP might be an amino acid transporter whose function can be bypassed by other amino acids or peptide permeases.

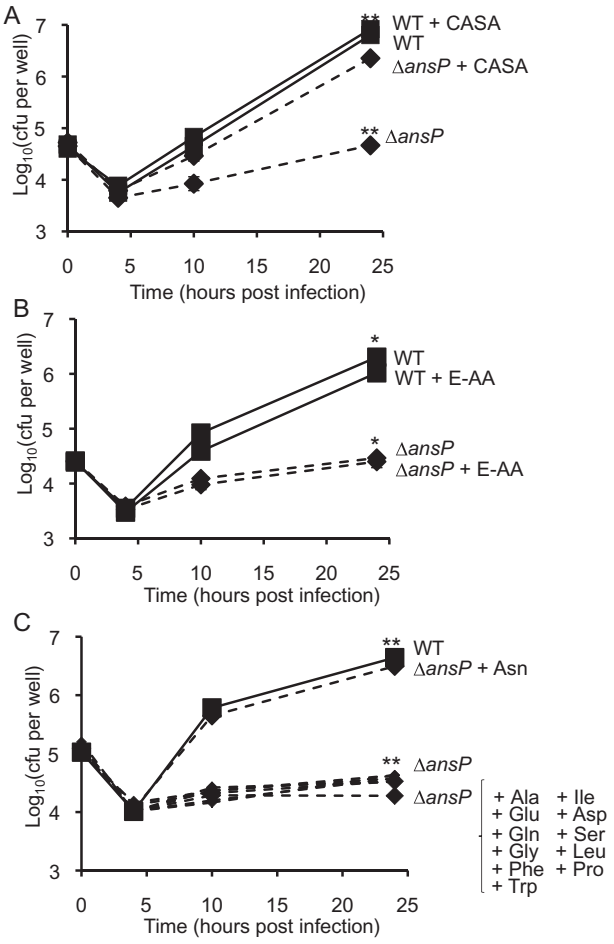

Fig. 3. Amino acid supplementation. Intracellular multiplication of the Δ*ansP* mutant was partially rescued by addition of casamino acids (CASA) and fully rescued by the addition of non-essential amino acids (NE-AA). In contrast, the addition of essential amino acids fails to restore growth. (A) J774 cells supplemented with CASA (5 g l^{-1} final concentration); (B) J774 cells supplemented with a pool of essential amino acid (E-AA); (C) J774 cells supplemented individually either with the useful but non-essential amino acid (UNE-AA) isoleucine (Ile), aspartic acid (Asp), serine (Ser), leucine (Leu), proline (Pro); or with the non-essential amino acid (NE-AA) alanine (Ala), asparagine (Asn), glutamic acid (Glu), glutamine (Gln), glycine (Gly), phenylalanine (Phe), tryptophane (Trp), each at 3 mM final concentration. E-AA pool: equimolecular mixture of arginine, histidine, lysine, methionine, tyrosine, cysteine, each at 3 mM final concentration). Intracellular replication was monitored by enumerating colony-forming units (cfu) on chocolate agar plates. Each experiment was performed in triplicate.

We then reasoned that the substrate of AnsP could be deduced by further identifying the amino acid(s) responsible for this supplementation. For this, we tested the capacity of pools of amino acids to restore wild-type intracellular multiplication of the Δ*ansP* mutant in J774 macrophages. Supplementation with a pool of six amino acids essential for growth in CDM did not improve intracellular multiplication of the Δ*ansP* mutant (Fig. 3B). In contrast, a pool of seven amino acids (alanine, glutamate, glutamine, glycine, phenylalanine, tryptophane and asparagine), non-essential for growth in CDM (and, thus, not present in the CDM), restored wild-type intracellular multiplication to the Δ*ansP* mutant (not shown).

As mentioned above, the Δ*asnP* mutant was able to grow like wild-type *F. novicida* in CDM_{min} (Fig. S3). This implies that: (i) the AnsP protein is not required for the capture of the amino acid present in the CDM_{min}, and (ii) that the amino acid(s) that is (are) not required for growth of the Δ*asnP* mutant in CDM, become(s) essential for growth in cells. Finally, each of the remaining amino acids (i.e. from the non-essential and useful but non-essential pools) was tested individually (Fig. 3C). These assays demonstrated that only asparagine was capable of supplementing the defect of the Δ*ansP* mutant.

AnsP is an asparagine transporter required for intracellular multiplication

The multiplication defect of the Δ*ansP* mutant was specifically and totally restored by asparagine supplementation whereas the intracellular defect of the Δ*FPI* mutant (Weiss *et al*., 2007) was not improved by asparagine supplementation (Fig. 4A).

To further assess the specificity of the AnsP transporter, we tested whether the growth defect suppression by free asparagine was dose-dependent (Fig. 4B). Supplementation with asparagine at a final concentration of 0.03 mM failed to completely restore bacterial multiplication in infected J774 cells (the initial DMEM cell culture medium is devoid of asparagine). Indeed, after 24 h, growth of the Δ*ansP* mutant was improved 10-fold as compared to growth without asparagine, but was still 15-fold lower than that of the parental strain. Supplementation with 0.3 mM asparagine, significantly improved intracellular multiplication of the mutant but this was still fivefold lower than that of the wild-type strain after 24 h. In contrast, addition of 3 mM asparagine restored wild-type multiplication levels.

The fact that the Δ*ansP* mutant showed no apparent defect in phagosomal escape prompted us to test the impact of supplementation with asparagine (3 mM) at later times during the infection of J774 macrophages. Therefore, we supplemented the Δ*ansp* mutant with asparagine after 1 h or after 4 h of infection (*i.e.* when the mutant bacteria are in the cytosolic compartment but fail to multiply normally). Remarkably, in both conditions, multiplication of the Δ*ansP* mutant was restored to wild-type levels already at 10 h and remained similar to the wild-type strain after 24 h (Fig. 4C).

These results thus confirmed that the multiplication defect of the Δ*ansP* mutant is due to an asparagine

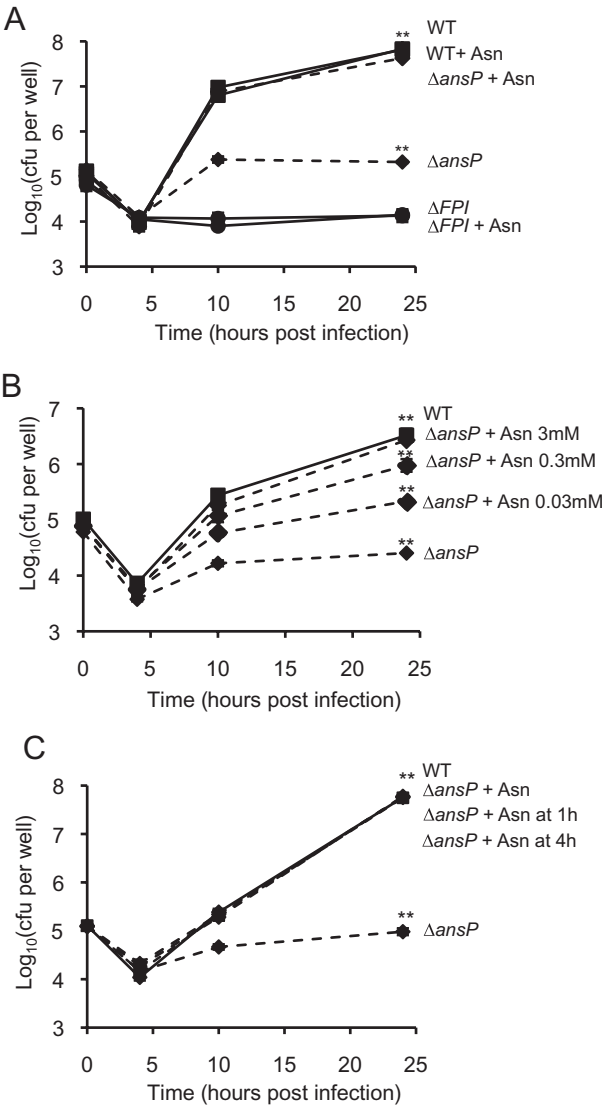

Fig. 4. Intracellular multiplication of the mutant Δ*ansP* is fully and specifically rescued by addition of asparagine.
A. When DMEM was supplemented with 3 mM asparagine (Asn), intracellular growth of the Δ*ansP* mutant was identical to that of wild-type U112. In contrast, asparagine supplementation had no effect on the Δ*FPI* mutant (Δ*FPI*).
B. When DMEM was supplemented with 0.03 mM or 0.3 mM Asn, growth of the Δ*ansP* mutants was only partially restored.
C. When DMEM was supplemented with 3 mM asparagine (Asn), after 1 h of infection, intracellular growth of the Δ*ansP* mutant was restored to wild-type levels, at 10 h and 24 h. The same complete restoration of multiplication of the Δ*ansP* mutant was observed when DMEM was supplemented with asn, after 4 h of infection.
$^{**}P < 0.01$ (as determined by Student's *t*-test).

uptake defect when the bacteria are present in the cytosolic compartment of infected cells.

We then tested whether the addition of aspartic acid and/or a source of ammonium (NH_4Cl) would also restore intracellular growth of the mutant. In order to avoid a possible inhibitory effect on phagosomal escape, NH_4Cl was added only 4 h after infection. Strikingly, only the simultaneous addition of both aspartic acid (3 mM) and NH_4Cl (1 mM) restored wild-type intracellular multiplication to the Δ*ansP* mutant (Fig. 5A), implying either that aspartic acid and ammonium serve as substrates for the production of asparagine or, conversely, that asparagine serves as a source of aspartic acid and ammonium.

Finally, to test whether asparagine-containing dipeptides could also bypass AnsP function, we followed the kinetics of intracellular multiplication of the Δ*ansP* mutant in J774 macrophages supplemented with either Leu–Asn or Leu–Gly dipeptides (3 mM). The asparagine-containing peptide restored wild-type multiplication of the mutant, but the Leu–Gly peptides did not (Fig. 5B). This assay confirmed thus the specific asparagine requirement of the Δ*ansP* mutant for intracellular growth. As additional controls, we tested two dipeptides containing either glutamate (Glu–Gly) or aspartic acid (Asp–Gly). None of them compensated the multiplication defect of the Δ*ansP* mutant (Fig. 5C).

We also constructed a chromosomal deletion mutant (Δ*FTL_1645*) in *F. tularensis* LVS and evaluated its impact on intracellular growth. Similar to our findings with *F. novicida*, the *F. tularensis* LVSΔ*FTL_1645* mutant had a defect in intracellular multiplication in macrophages (Fig. S5). In J774 cells, the Δ*ansP* mutant of LVS showed a fourfold reduction of intracellular bacteria after 24 h, and an 11-fold reduction after 48 h, as compared to the parental LVS strain. Remarkably, as in *F. novicida*, upon supplementation of the culture media with asparagine (3 mM), the Δ*FTL_1645* mutant multiplied with wild-type kinetics. These results strongly support the conserved role of AnsP among *Francisella* species.

AnsP transports both aspartic acid and asparagine

Since asparagine is the amide derivative of aspartic acid, we reasoned that AnsP might also be involved in the transport of aspartic acid. We therefore first compared the uptake of radiolabelled aspartic acid (^{14}C-Asp) by wild-type *F. novicida* to that of the Δ*ansP* mutant. The wild-type strain incorporated ^{14}C-Asp more rapidly than the Δ*ansP* mutant, at 10 μM ^{14}C-Asp (Fig. 6A). However, aspartic acid incorporation was only partially affected in the Δ*ansP* mutant, at all time points tested. This prompted us to evaluate the impact of *ansP* inactivation in a broad range of aspartic acid concentrations (Fig. 6B). At all the concentrations tested, aspartic acid incorporation was only partially affected in the Δ*ansP* mutant (approximately 60% of the wild-type values) and the apparent Km of aspartic acid transport was similar in both strains (approximately 20 μM). These data strongly suggested the presence of additional aspartic acid transporter(s) in the Δ*ansP* mutant.

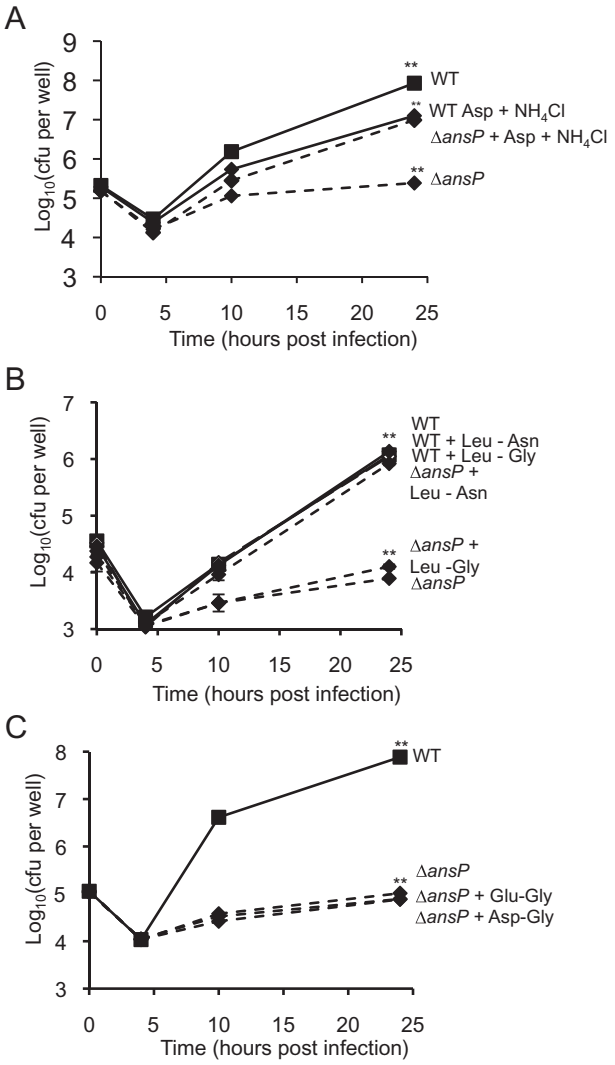

Fig. 5. Intracellular multiplication is restored by simultaneous addition of aspartic acid + ammonium or an asparagine-containing dipeptide.
A. The simultaneous addition of aspartic acid and NH_4Cl restored wild-type intracellular multiplication of the Δ*ansP* mutant at all time points; whereas the separate supplementation with either aspartic acid (see Fig. 3C) or NH_4Cl (not shown) had no effect.
B and C. (B) Supplementation with the asparagine-containing dipeptide leucine–asparagine (Leu–Asn) also fully restored intracellular growth of Δ*ansP*. In contrast, supplementation with the dipeptides leucine-glycine (Leu–Gly), glutamate-glycine (Glu–Gly), or aspartic acid-glycine (Asp–Gly) (C) had no effect.

We then measured ^{14}C-Asp incorporation in wild-type *F. novicida* and in the Δ*ansP* mutant, in the presence

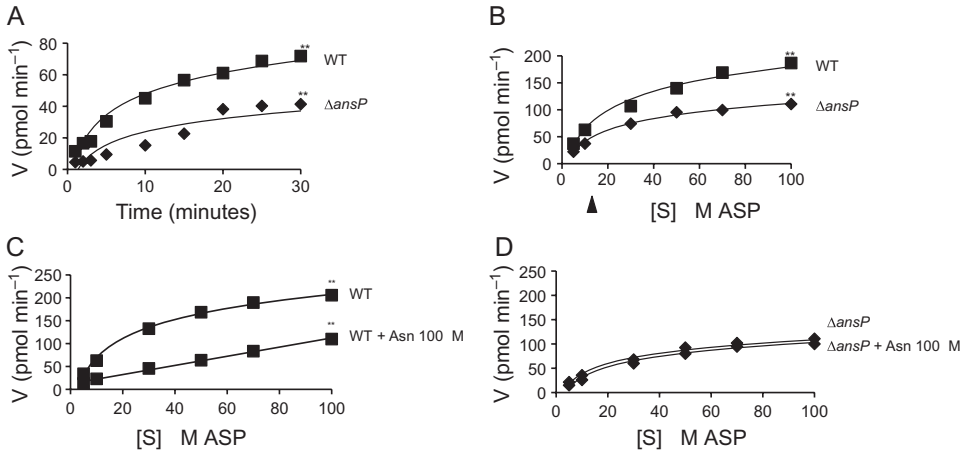

Fig. 6. Transport assays.
A. Uptake of 10 μM ^{14}C-Asp by wild-type *F. novicida* and Δ*ansP* mutant, over at 10 min period.
B. Kinetics of ^{14}C-Asp uptake by wild-type *F. novicida* and Δ*ansP* mutant at ^{14}C-Asp concentrations ranging from 1 to 100 μM. The apparent Km of ^{14}C-Asp transport for both strains (app. 20 μM) is indicated below the *x*-axis by an arrow.
C and D. (C) ^{14}C-Asp uptake by wild-type *F. novicida* or (D) Δ*ansP* mutant, in the presence of either 100 μM of competing asparagine.

of increasing concentrations of competing asparagine (Fig. 6C and D). Fully supporting our first results, addition of asparagine reduced the incorporation of ^{14}C-Asp, at all the concentrations tested in the wild-type strain. The uptake of ^{14}C-Asp was not abrogated (40% to 60% reduction were recorded, with 100 μM cold asparagine), most likely due to the presence of additional aspartic acid transporter(s) in the strain. Interestingly, addition of asparagine had no effect on the incorporation of ^{14}C-Asp in the Δ*ansP* mutant, strongly suggesting that the additional aspartic acid transporters do not mediate asparagine transport in the conditions tested. Altogether, these assays strongly suggest that AnsP is involved in the transport of both asparagine and aspartic acid; and that *Francisella* possesses additional aspartic acid transporter(s).

Contribution of AnsP to Francisella *virulence*

To determine if the AnsP protein played a role for the ability of *Francisella* to cause disease, we performed *in vivo* competition assays in 6- to 8-week-old BALB/c mice. Groups of five mice were inoculated by the intraperitoneal (i.p.) route with a 1:1 mixture of the wild-type *F. novicida* and Δ*ansP* mutant strains. Multiplication in the liver and spleen was monitored at day 2 (Fig. 7). The competition index (CI), calculated in both target organs, was very low ($2–5 \times 10^{-4}$), demonstrating that gene *ansP* is critical for virulence of *F. novicida* in the mouse model (Fig. 7).

Strikingly, upon treatment of the mice with asparagine (3 i.p. injections with 0.5 ml of a 0.5 mM solution of asparagine; see *Experimental procedures*), the CI in both organs raised approximately 1000-fold, in both liver and spleen. This experiment demonstrated that asparagine supplementation *in vivo* also restored virulence of the Δ*ansP* mutant.

Discussion

In order to survive and multiply within their hosts, intracellular bacterial pathogens must evade host innate immune surveillance pathways (Jones *et al*., 2012). They must also cope with a nutrient-restricted environment and have therefore evolved uptake systems adapted to the nutrient resources available in the host cell compartment

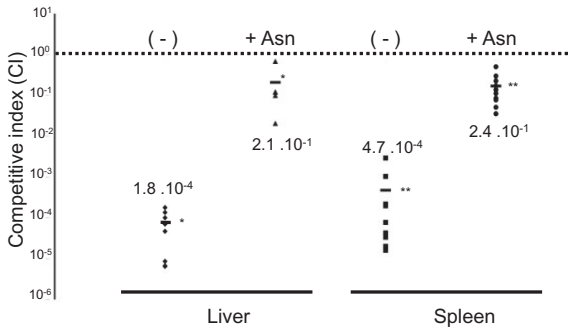

Fig. 7. *In vivo* dissemination. Groups of five female BALB/c mice were infected intraperitoneally (i.p.) with a 1:1 mixture of wild-type *F. novicida* and Δ*ansP* mutant strain (100 cfu of each). + Asn. Mice were injected i.p. three times with 0.5 ml of a 0.5 mM solution of asparagine: 1 day before infection, and twice after infection (after 6 h and 12 h). (–) non-pretreated mice. The data represent the competitive index (CI) value (in ordinate) for cfu of mutant/wild-type in the liver (left part) and spleen (right part) of each mouse, 48 h after infection divided by cfu of mutant/wild-type in the inoculum. Bars represent the geometric mean CI value.

where they reside (Abu Kwaik and Bumann, 2013; Zhang and Rubin, 2013). We report here the identification of a novel amino acid transporter that is required for intracellular multiplication and virulence of the facultative intracellular pathogen *Francisella*. We show that inactivation of this transporter does not affect phagosomal escape but prevents bacterial multiplication in the host cytosol. Importantly, this work unravels for the first time the critical role of asparagine acquisition in the virulence of this pathogen.

The host cytosol, initially considered as a safe and nutrient-replete haven (Ray *et al*., 2009), is now recognized as a potentially life-threatening and nutrient-deprived environment for invading bacteria. Intracellular bacterial pathogens have therefore learned to adapt their metabolism and are equipped with efficient uptake systems, to capture limiting nutrients (amino acids, carbohydrates, ions, . . .) from the host. Furthermore, intracellular bacterial have also developed a variety of strategies to modulate the nutritional content of the host cell compartment where they reside.

To fulfil their needs in amino acids, intracellular bacteria may take advantage of natural degradative pathways, such as proteasomal degradation and autophagy, like *Legionella* and *Anaplasma*, respectively (Price *et al*., 2011; Niu *et al*., 2012), to access to plentiful sources of amino acids. Indeed, *L. pneumophila*, which resides in a vacuolar compartment that evades lysosomal fusion and is remodelled by the endoplasmic reticulum, injects the eukaryotic-like F box protein effector AnkB into the infected host cells (Al-Quadan *et al*., 2012). After lipidation by the host farnesylation machinery, AnkB anchors to the vacuolar membrane and serves then as a platform for the assembly of Lys48-linked poly-ubiquitinated proteins. Their degradation by the host proteasome generates elevated levels of amino acids, which can be imported into the vacuole (Price *et al*., 2011). The obligate intracellular bacterium *Anaplasma phagocytophilum*, which replicates inside a membrane-bound vacuole that resembles an early autophagosome but that does not fuse to lysosomes (Niu *et al*., 2008), was recently shown to actively induce autophagy, by secreting the effector Ats-1. After translocation to the cytoplasm of infected cells, a portion of Ats-1 interacts with the host autophagosome initiation complex. Ats-1 autophagosomes are then recruited to the vacuole containing bacteria. Upon fusion of the two outer membranes, the autophagic content is released in the resulting vacuolar compartment (Niu *et al*., 2012).

Of note, *F. tularensis* has been reported to induce the formation of a multi-membranous, autophagosome-like structure in primary murine macrophages, by Celli and co-workers (Checroun *et al*., 2006), initially suggesting that the bacterium might use autophagosome as an alternative intracellular survival niche. However, more recent studies have shown that only replication-deficient and chloramphenicol-treated *F. tularensis* were degraded via canonical autophagy (Chong *et al*., 2012), implying that wild-type *F. tularensis* avoids classical autophagy. Of particular interest, Steel *et al*. very recently reported (Steele *et al*., 2013) that *F. tularensis* induced autophagy in infected mouse embryonic fibroblasts and primary human monocytes. The authors showed that *F. tularensis* not only survived autophagy, but required autophagy for optimal intracellular growth. *F. tularensis* was shown to be able to import amino acids derived from host proteins. Furthermore, impaired intracellular growth upon autophagy inhibition could be rescued by supplying excess non-essential amino acids or pyruvate. Remarkably, *F. tularensis* intracellular replication was not affected in ATG5–/– macrophages or ATG5–/– MEF cells, indicating that the canonical autophagy pathway was not involved. Altogether, these data suggest that *F. tularensis* induces an ATG5-independent autophagy process in infected cells to obtain carbon and energy sources to support their intracellular replication.

Supporting the notion that *Legionella* and *Anaplasma* use these natural degradative pathways to acquire host nutrients for their growth, inhibition of these pathways (proteasomal degradation and autophagy respectively) block bacterial multiplication. Remarkably, in both cases, the resulting growth defects can be totally bypassed upon supplementation with excess amino acids (Price *et al*., 2011; Niu *et al*., 2012).

Alternatively, intracellular bacteria may also stop growing to restrict their need as much as possible upon amino acid starvation (*Chlamydia*); or be self-sufficient and constitutively produce all their amino acids (*Mycobacterium tuberculosis*) (Zhang and Rubin, 2013). In the case of *Francisella*, we have previously shown that the bacterium used the cysteine-containing tripeptide glutathione (GSH) as a source of cysteine, to replicate in infected cells (Alkhuder *et al*., 2009), thus suggesting that *Francisella* has evolved by exploiting the natural abundance of GSH in the host cytosol to compensate its natural auxotrophy for cysteine. We have also recently shown that *Francisella* infection simultaneously up-regulated the surface expression of the eukaryotic amino acid transporter SLC1A5 and the downregulation of SLC7A5, in infected monocytes (Barel *et al*., 2012). Since both SLC7A5 and SLC1A5 work in concert to equilibrate the cytoplasmic amino acid pool (Fuchs and Bode, 2005), the differential effect of *Francisella* infection on their expression could be profitable to the bacterium for increasing the intracellular concentration of essential amino acids. These two examples suggest that *Francisella* is capable of triggering optimal intracellular nutrient growth conditions as well as taking advantage of abundant nutrients already present.

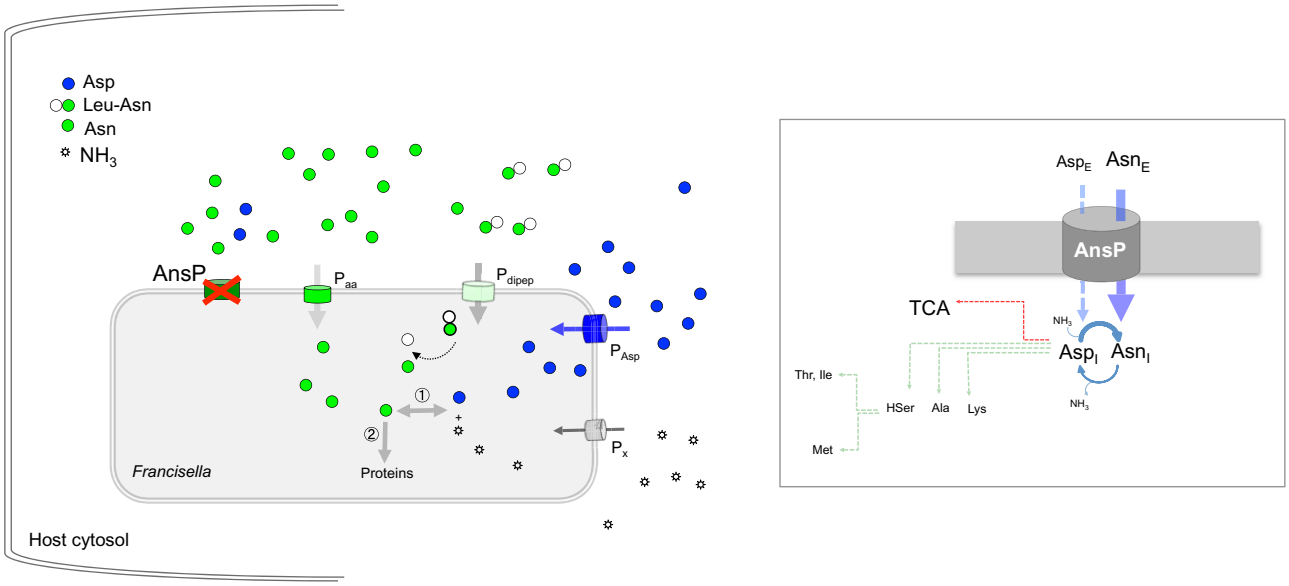

Fig. 8. Model of asparagine uptake by intracellular *Francisella*. Intracellular asparagine is transported by AnsP (dark green) in the absence of asparagine in the culture medium. In the absence of AnsP, the alternative amino acid permease P_{aa} (bright green) allows asparagine entry, when it is present at high concentration (in the mM range) in the culture medium. P_{dipep} (pale green). The dipeptide amino acid permease allows asparagine-containing dipeptides entry. P_{aa} (blue). The amino acid permease allowing aspartic acid entry. P (grey). The permease allowing ammonium entry. ① above the dotted grey arrow: Asparagine may either serve as a source of aspartic acid + ammonium (by the action of asparaginases) or be generated from aspartic acid + ammonium (by the action of asparagine synthases). ② above the dotted grey arrow: Asparagine is used as building block for protein synthesis. To the right. Upon entry into the bacterium via AnsP, asparagine can be metabolized into aspartic acid; which in turn can be transformed into a variety of important metabolites via different enzymatic pathways.

The capacity of the host cell to adapt its metabolism for starving the invading bacteria of essential nutrients has led to the now widely accepted paradigm of 'nutritional immunity' (Weinberg, 1975). In turn, the terms 'nutritional virulence' have been very recently proposed to designate the specific virulence properties of intracellular pathogens (Abu Kwaik, 2013; Abu Kwaik and Bumann, 2013). We found here that inactivation of the *ansP* gene (*FTN_1586*) severely impaired *Francisella* intracellular multiplication in all cell types studied and successfully identified asparagine as the unique amino acid residue able to restore normal intracellular multiplication of the Δ*ansP* mutant. Altogether, these data presented support the following model that is depicted in Fig. 8: AnsP is an asparagine transporter whose function is, not required in broth, but essential inside host cells. Remarkably, in infected cells, the absence of AnsP can be bypassed by alternative (probably less efficient) amino acid transporters (P_{aa}) when the level of asparagine is high; and/or by peptide transporters (P_{dipep}) (Meibom and Charbit, 2010a) supplying asparagine-containing peptides. The fact that asparagine supplementation of the Δ*ansP* mutant, even after 1 h or 4 h of infection, completely alleviated the growth defect, establishes that asparagine is specifically required for bacterial multiplication in the cytosolic compartment of the host. We found that AnsP was also involved in aspartic acid transport. Remarkably, intracellular growth of the Δ*ansP* mutant was only restored when both aspartic acid and ammonium were added, strongly suggesting that it is primarily the role of asparagine transporter that is critical for bacterial cytosolic multiplication.

Amino acids represent the major sources of carbon and energy for *Legionella* and *Francisella*. Both species have lost several of their amino acid biosynthetic pathways [arginine, serine, valine, threonine, methionine, cysteine, for *Legionella* (Ristroph *et al.*, 1981)]; arginine, histidine, lysine, tyrosine, methionine, cysteine, for *Francisella* (Larsson *et al.*, 2005). Hence, they both rely on the host to obtain these essential amino acids for their intracellular multiplication. However, mammalian cells are auxotrophic for several of these amino acids (Young, 1994). Their intracellular concentration is thus likely to be particularly critical for multiplication of these pathogens.

Asparagine is a non-essential amino acid for *Francisella* as well as for mammalian cells. Its physiological intracellular concentration is estimated in the μM range in mammalian cells (Rinehart and Canellakis, 1985; Wang *et al.*, 1998). The severe intracellular growth defect of the *ansP* mutant suggests that this concentration of asparagine is limiting for the multiplication of *Francisella* in infected cells, in the absence of the AnsP transporter. *In vivo*, the mammalian asparagine synthase (ASNS) enzyme catalyses the conversion of L-aspartic acid and

L-glutamine into L-asparagine and L-glutamate. However, although ubiquitously expressed, the levels of ASNS expression in adult animals may vary considerably among tissues (Balasubramanian *et al*., 2013). Thus, *Francisella* must cope with variable pools of asparagine during *in vivo* dissemination.

Our data indicate that AnsP also transports aspartic acid, an amino acid at the crossroad of numerous important metabolic pathways, including the biogenesis of several amino acids (asparagine, methionine, threonine, isoleucine, alanine and lysine) and which can also serve as a precursor for pyrimidine biogenesis. The intracellular multiplication defect of the Δ*ansP* mutant might thus be the consequence of the reduced capacity of the mutant to acquire both aspartic acid and asparagine.

Of note, *in silico* analysis of the predicted proteome of *F. novicida* revealed a broad heterogeneity in asparagine residues content per protein (ranging from 17.6% to less than 1% per coding sequence), with an average of 5.9% (i.e. close to 1/20). This rules out the possibility that asparagine acquisition might be needed due to an over-representation of this amino acid residue in *Francisella* proteins.

AnsP belongs to the Phagosomal transporter (Pht) subclass of MFS that is exclusively found among intracellular pathogenic bacteria. As recalled in the Introduction, *L. pneumophila* encodes the PhtA threonine transporter (Sauer *et al*., 2005) that is required for intra-phagosomal bacterial growth and differentiation. Threonine is an essential amino acid for *Legionella* that is likely to be present in limiting concentration in the host (human cells are notably auxotroph for threonine). The growth defect of *phtA* mutant could be abrogated by supplementation with excess threonine or threonine-containing peptide, supporting the notion that the *Legionella*-containing phagosomes indeed do not contain sufficient peptides or threonine to bypass the *phtA* defect.

Our study confirms that, at least some, Pht members are involved in amino acid uptake but indicates that these transporters are not restricted to bacteria residing exclusively in a phagosomal compartment. This subfamily of MFS transporter might therefore be renamed ICAATs (for Intra Cellular Amino Acid Transporters). The present study unravels for the first time the role of an MFS transporter as a key player in *Francisella* intracellular nutrition, further strengthening the link between nutrition and virulence for intracellular pathogens. It is likely that a number of other *Francisella* MFS members are specifically involved in acquisition of other limiting intracellular substrates, still to be discovered. More generally, it is reasonable to assume that transporter family members contribute to the intracellular nutrition of many (if not all) intracellular bacteria and could thus constitute attractive targets for the rational design of molecules to manage spread of these pathogens.

Experimental procedures

Bacterial strains and plasmids

Francisella tularensis subsp. *tularensis* strain U112 (kindly provided by A. Sjöstedt) and its derivatives were grown: (i) in liquid, on Schaedler broth (BioMérieux, Marcy l'Etoile, France), Tryptic Soya broth supplemented with cysteine (Becton, Dickinson and company) or Chamberlain chemically defined medium (Chamberlain, 1965), and (ii) in solid, on pre-made chocolate agar PolyViteX (BioMerieux SA Marcy l'Etoile, France) or chocolate plates prepared from GC medium base, IsoVitalex vitamins and haemoglobin (BD Biosciences, San Jose, CA, USA), at 37°C. *Escherichia coli* was grown in LB (Luria–Bertani, Difco) at 37°C. Ampicillin was used at a final concentration of 100 μg ml^{-1} to select recombinant *E. coli* carrying pGEM and its derivatives. All bacterial strains, plasmids and primers used in this study are listed in Table S1.

Metabolic profiling was tested, using Biolog Phenotypic Microarray GNII plates. A positive respiration pattern (visualized by the appearance of a dark colour in the well) reflects the capacity of the bacterium to utilize the carbon sources tested. Each plate contained 96 different carbon sources, each present in non-limiting amounts. The assay was performed according to the Biolog guidelines (available at the internet site http://www.biolog.com).

Bioinformatic analyses

Secondary structure predictions were performed using the program HMM™ available at the internet site http://www.cbs.dtu.dk).

Construction of a chromosomal deletion mutants

ΔansP. We generated a chromosomal deletion of gene *ansP* in wild-type *F. novicida* strain U112 (Δ*FTN_1586*), by allelic replacement of the wild-type region with a mutated region deleted of the entire gene (from the start codon to the TAA stop codon), substituted by the kanamycin (Kan) resistance gene *npt* placed under the control of the p*gro* promoter. First, the two regions (*c*. 600 bp each) flanking gene *ansP* (designated *FTN_1586*up and *FTN_1586*down respectively), and the *npt* gene [1161 bp, amplified from plasmid pFNLTP16H3 (Maier *et al*., 2006)] were amplified by PCR using the following pairs of primers: (i) *FTN_1586*up, p3/p4; *FTN_1586*down, p5/p6, (ii) *npt*, p1/p2. The region *FTN_1586*up-*npt* (*c*. 1700 bp) was then amplified by overlap PCR, using the *FTN_1586*-up and *npt* products, and cloned into pGEM–T easy vector to yield plasmid pGEM *FTN_1586-up/npt*. The fragment *FTN_1586-down* was finally digested with PstI and SalI (New England Biolabs) and subcloned into the corresponding sites of plasmid pGEM-*FTN_1586up-npt* (immediately downstream of the *npt* gene) to yield plasmid pGEM-*FTN_1586up-npt-FTN_1586down*. This plasmid was used as a template for the amplification of a 2260 bp fragment comprising *FTN_1586up-npt-FTN_1586down*, using primers p9/p10. This PCR product was gel purified (using the QIAquick Gel extraction

kit, QIAgen) and directly used to transform wild-type U112. Recombinant bacteria, resulting from allelic replacement of the wild-type region with the mutated *FTN_1586up/npt/FTN_1586down* region, were selected on Kan-containing plates (10 μg ml^{-1}). The mutant strain, designated Δ*ansP* was checked for loss of the wild-type *ansP* gene, using specific primers, and by PCR sequencing (GATC Biotech).

ΔFTL_1645. We also generated a chromosomal deletion of the orthologous gene *FTL_1645* in *F. tularensis* subsp. *holarctica* strain LVS. For this, we used the counter selectable plasmid pMP812 (LoVullo *et al*., 2009). The recombinant plasmid pMP812-Δ*FTL_1645* was constructed by overlap PCR. Primers p15/p16 amplified the 994 bp region upstream of position +1 of the *FTL_1645* coding sequence, and primers p17/p18 amplified the 1012 bp region immediately downstream of the *FTL_1645* stop codon (Table S1). Primers p16/p17 have an overlapping sequence of 23 nucleotides, resulting in complete deletion of the *FTL_1645* coding sequence after cross-over PCR. PCR reactions with primers p15/p16 and p17/p18 were performed with exTaq polymerase (Fermentas). The products were purified using the QIAquick PCR purification kit (QIAgen, CA). 200 μM of each was used as a template for PCR with primers p15/p18 and treated with 30 cycles of PCR (94°C for 30 s, 54°C for 30 s and 72°C for 120 s). The gel-purified 1996 bp fragment was digested with BamHI and NotI (New England Biolabs) and cloned into BamHI–NotI digested pMP812 (LoVullo *et al*., 2009). The plasmid is introduced into *F. tularensis* LVS by electroporation. *F. tularensis* LVS was grown to OD_{600} 0.3–0.6 in Schaedler-K3 broth; bacteria were collected and washed twice with 0.5 M sucrose. Bacteria were suspended in 0.6 ml of 0.5 M sucrose and 200 μl was used immediately for electroporation in a 0.2 cm cuvette (2.5 kV, 25 mF, 600 W). After electroporation, bacteria were mixed with 1 ml of Schaedler-K3 broth and incubated at 37°C for 6 h before selection on chocolate agar (Bio-Rad, Hercules, CA, USA) and 5 μg ml^{-1} Kan. Colonies appeared after 3 days of incubation at 37°C and were subsequently passed once on plates with selection, followed by a passage in liquid medium without selection (to allow recombination to occur). Next, bacteria were passed once on agar plates containing 5% sucrose. Isolated colonies were checked for loss of the wild-type *FTL_1645* gene by size analysis of the fragment obtained after PCR using primers combination p15/p18, p33/p18 and p15/p34. One colony harbouring a *FTL_1645* deletion, as determined by PCR analysis, was used for further studies. Genomic DNA was isolated and used as the template in a PCR with primers p33/p34. The PCR product was directly sequenced using primers p33/p34 to verify the complete deletion of the *FTL_1645* gene.

Functional complementation

The plasmid used for complementation of the Δ*ansP* mutant, pKK214-p*gro-ansP*, was constructed by overlap PCR. Primers p13/p14 amplified the wild-type *ansP* gene (1454 bp), and the primers p11/p12 amplified the 333 bp of the p*gro* promoter. Primers p12/p13 have an overlapping sequence of 20 nucleotides. PCR reactions with primer pairs p11/p12 and p13/p14, were performed with exTaq polymerase (Fermentas), and the products were purified using the QIAquick PCR purification kit (QIAgen, CA). 200 μM of each amplification product was used as a template for PCR with primers p11/p13 and treated with 30 cycles of PCR (94°C for 30 s, 54°C for 30 s and 72°C for 120 s). The gel-purified 1787 bp fragment was digested with SmaI and PstI (New England Biolabs) and cloned into SmaI–PstI-digested pKK214. The plasmids pKK214 (empty plasmid) and pKK214-p*gro-ansP* (complementing plasmid) were introduced into U112 and the Δ*ansP* mutant by electroporation.

Growth kinetics in broth

Stationary-phase bacterial cultures of wild-type U112 and U112Δ*ansP* mutant strains were diluted at a final OD_{600} of 0.1 in tryptic soya broth (TSB). Every hour, the OD_{600} of the culture wads measured, during a 9 h period.

Transport assays

Cells were grown in Chamberlain medium to mid-exponential phase and then harvested by centrifugation and washed twice with Chamberlain without amino acid. The cells were suspended at a final OD_{600} of 0.5 in the same medium containing 50 μg ml^{-1} of chloramphenicol. After 15 min of pre-incubation at 25°C, uptake was started by the addition of L-[U-^{14}C] aspartic acid (Perkin Elmer), at various concentrations (^{14}C-Asp ranging from 1 to 100 μM); with or without competitor asparagine, at various concentrations (Asn ranging from 10 μM to 1 mM). The radiolabelled ^{14}C-Asp was at a specific activity of 7.4 GBq mmol^{-1}. Samples (100 μl of bacterial suspension) were removed at regular intervals and collected by vacuum filtration on membrane filters (Millipore type HA, 25 mm, 0.22 μm) and rapidly washed with Chamberlain without amino acid (2 × 5 ml). At the end of each experiment, the filters were transferred to scintillation vials and counted in a Hidex 300 scintillation counter. The counts per minute (cpm) were converted to picomoles of amino acid taken up per sample, using a standard derived by counting a known quantity of the same isotope under similar conditions.

Multiplication in macrophages

J774 (ATCC TIB67), BMM (ATCC TIB-202) and HepG-2 (ATCC HB 8065) cells were propagated in Dulbecco's modified Eagle's medium (DMEM) containing 10% fetal calf serum. Cells were seeded at a concentration of 2 × 10^5 cells per well in 12-well cells tissue plates, and monolayers were used at 24 h after seeding. J774, BMM and HepG2 macrophages monolayers were incubated for 60 min at 37°C with the bacterial suspensions (multiplicity of infection of 100) to allow the bacteria to enter. After washing (time zero of the kinetic analysis), the cells were incubated in fresh culture medium containing gentamicin (10 μg ml^{-1}) to kill extracellular bacteria.

At several time points, cells were washed three times in DMEM, macrophages were lysed by addition of water and the titre of viable bacteria released from the cells was determined by spreading preparations on chocolate agar plates. For each strain and time in an experiment, the assay was performed in triplicate. Each experiment was independently repeated at least three times, and the data presented originate from one typical experiment. For Δ*ansP* suppression experiments, amino acids or peptides were added to 3 mM at the time of infection and maintained throughout the infection.

Electron microscopy

J774 cells were infected with wild-type *F. novicida* and mutant Δ*ansP* bacteria. Samples for electron microscopy were prepared using the thin-sectioning procedure as previously described (Alkhuder *et al*., 2009).

Confocal experiments

J774 cells were infected with wild-type *F. novicida*, Δ*ansP* or Δ*FPI*, strains for 1 h, 4 h and 10 h at 37°C, and were washed in KHM (110 mM potassium acetate, 20 mM Hepes, 2 mM $MgCl_2$). Cells were incubated for 1 min with digitonin (50 μg ml^{-1}) to permeabilize membranes. Then cells were incubated for 15 min at 37°C with primary anti-*F. novicida* mouse monoclonal antibody (1/500 final dilution). After washing, cells were incubated for 15 min at 37°C with secondary antibody (Ab) (Alexa Fluor 488-labelled GAM, 1/400 final dilution) in the dark. After washing, cells were fixed with PFA 4% for 15 min at room temperature (RT) and incubated for 10 min at RT with 50 mM NH_4Cl to quench residual aldehydes. After washing with PBS, cells were incubated for 30 min at RT with primary anti-LAMP1 Ab (1/100 final dilution) in a mix with PBS, 0.1% saponine and 5% goat serum. After washing with PBS, cells were incubated for 30 min at RT with secondary anti-rabbit Ab (Alexa 546-labelled, 1/400 dilution). DAPI was added (1/5000 final dilution) for 1 min. After washing, the glass coverslips were mounted in Mowiol. Cells were examined using an X63 oil-immersion objective on a LeicaTSP SP5 confocal microscope. Colocalization tests were performed by using Image J software; and mean numbers were calculated on more than 500 cells for each condition. Confocal microscopy analyses were performed at the Cell Imaging Facility (Faculté de Médecine Necker Enfants-Malades).

Phagosome permeabilization assay

Quantification of phagosome permeabilization/vacuolar escape using the β-lactamase-CCF4 assay (Life technologies) was performed following manufacturer's instructions. Briefly, macrophages were infected as previously described for 1 h, washed and incubated in CCF4 for 1 h at room temperature in the presence of 2.5 mM probenicid (Sigma). Cells were collected by gentle scraping and analysed by flow cytometry on a canto 2 cytometer (BD Bioscience) without any fixation step. Propidium iodide-negative cells were considered for the quantification of cells containing cytosolic *F. novicida* using excitation at 405 nm and detection at 450 nm (cleaved CCF4) or 535 nm (intact CCF4).

Mice infections

All experimental procedures involving animals were conducted in accordance with guidelines established by the French and European regulations for the care and use of laboratory animals (Décrets 87-848, 2001-464, 2001-486 and 2001-131 and European Directive 2010/63/UE) and approved by the INSERM Ethics Committee (Authorization Number: 75-906).

Wild-type *F. novicida* and mutant strains were grown in TSB to exponential growth phase and diluted to the appropriate concentrations. Six- to 8-week-old female BALB/c mice (Janvier, Le Genest St Isle, France) were intraperitoneally (i.p.) inoculated with 200 μl of bacterial suspension. The actual number of viable bacteria in the inoculum was determined by plating dilutions of the bacterial suspension on chocolate plates. For competitive infections, wild-type *F. novicida* and mutant bacteria were mixed in 1:1 ratio and a total of 100 bacteria were used for infection of each of five mice. After 2 days, mice were sacrificed. Homogenized spleen and liver tissue from the five mice in one experiment were mixed, diluted and spread on to chocolate agar plates. Kanamycin selection to distinguish wild-type and mutant bacteria were performed. For Δ*ansP* supplementation experiments, asparagine was injected i.p. into mice (500 μl of a 0.5 mM solution) 14 h before infection and during infection, at days 1 and 2.

Acknowledgements

We thank Dr A. Sjöstedt for providing the strain LVS. These studies were supported by INSERM, CNRS and Université Paris Descartes Paris Cité Sorbonne. Gael Gesbert was funded by a fellowship from the 'Délégation Générale à l'Armement' (DGA) and Elodie Ramond by a fellowship from the 'Région Ile de France'.

References

Abu Kwaik, Y. (2013) Targeting nutrient retrieval by *Francisella tularensis*. *Front Cell Infect Microbiol* **3:** 1–2.

Abu Kwaik, Y., and Bumann, D. (2013) Microbial quest for food *in vivo*: 'nutritional virulence' as an emerging paradigm. *Cell Microbiol* **15:** 882–890.

Al-Quadan, T., Price, C.T., and Abu Kwaik, Y. (2012) Exploitation of evolutionarily conserved amoeba and mammalian processes by *Legionella*. *Trends Microbiol* **20:** 299–306.

Alkhuder, K., Meibom, K.L., Dubail, I., Dupuis, M., and Charbit, A. (2009) Glutathione provides a source of cysteine essential for intracellular multiplication of *Francisella tularensis*. *PLoS Pathog* **5:** e1000284.

Asare, R., and Abu Kwaik, Y. (2010) Molecular complexity orchestrates modulation of phagosome biogenesis and escape to the cytosol of macrophages by *Francisella tularensis*. *Environ Microbiol* **12:** 2559–2586.

Asare, R., Akimana, C., Jones, S., and Abu Kwaik, Y. (2010) Molecular bases of proliferation of *Francisella tularensis* in arthropod vectors. *Environ Microbiol* **12:** 2587–2612.

Balasubramanian, M.N., Butterworth, E.A., and Kilberg, M.S. (2013) Asparagine synthetase: regulation by cell stress and involvement in tumor biology. *Am J Physiol Endocrinol Metab* **304:** E789–E799.

Barel, M., Meibom, K., and Charbit, A. (2010) Nucleolin, a shuttle protein promoting infection of human monocytes by *Francisella tularensis*. *PLoS ONE* **5:** e14193.

Barel, M., Meibom, K., Dubail, I., Botella, J., and Charbit, A. (2012) *Francisella tularensis* regulates the expression of the amino acid transporter SLC1A5 in infected THP-1 human monocytes. *Cell Microbiol* **14:** 1769–1783.

Broms, J.E., Meyer, L., Sun, K., Lavander, M., and Sjöstedt, A. (2012) Unique substrates secreted by the type VI secretion system of *Francisella tularensis* during intramacrophage infection. *PLoS ONE* **7:** e50473.

Brotcke, A., Weiss, D.S., Kim, C.C., Chain, P., Malfatti, S., Garcia, E., and Monack, D.M. (2006) Identification

of MglA-regulated genes reveals novel virulence factors in *Francisella tularensis*. *Infect Immun* **74:** 6642–6655.

Celli, J., and Zahrt, T.C. (2013) Mechanisms of *Francisella tularensis* intracellular pathogenesis. *Cold Spring Harb Perspect Med* **3:** a010314.

Chamberlain, R.E. (1965) Evaluation of live tularemia vaccine prepared in a chemically defined medium. *Appl Microbiol* **13:** 232–235.

Checroun, C., Wehrly, T.D., Fischer, E.R., Hayes, S.F., and Celli, J. (2006) Autophagy-mediated reentry of *Francisella tularensis* into the endocytic compartment after cytoplasmic replication. *Proc Natl Acad Sci USA* **103:** 14578–14583.

Chen, D.E., Podell, S., Sauer, J.D., Swanson, M.S., and Saier, M.H., Jr (2008) The phagosomal nutrient transporter (Pht) family. *Microbiology* **154:** 42–53.

Chong, A., and Celli, J. (2010) The *Francisella* intracellular life cycle: toward molecular mechanisms of intracellular survival and proliferation. *Front Microbiol* **1:** 1–12.

Chong, A., Wehrly, T.D., Child, R., Hansen, B., Hwang, S., Virgin, H.W., and Celli, J. (2012) Cytosolic clearance of replication-deficient mutants reveals *Francisella tularensis* interactions with the autophagic pathway. *Autophagy* **8:** 1342–1356.

Fuchs, B.C., and Bode, B.P. (2005) Amino acid transporters ASCT2 and LAT1 in cancer: partners in crime? *Semin Cancer Biol* **15:** 254–266.

Fuller, J.R., Craven, R.R., Hall, J.D., Kijek, T.M., Taft-Benz, S., and Kawula, T.H. (2008) RipA, a cytoplasmic membrane protein conserved among *Francisella* species, is required for intracellular survival. *Infect Immun* **76:** 4934–4943.

Hall, J.D., Woolard, M.D., Gunn, B.M., Craven, R.R., Taft-Benz, S., Frelinger, J.A., and Kawula, T.H. (2008) Infected-host-cell repertoire and cellular response in the lung following inhalation of *Francisella tularensis* Schu S4, LVS, or U112. *Infect Immun* **76:** 5843–5852.

Jones, C.L., Napier, B.A., Sampson, T.R., Llewellyn, A.C., Schroeder, M.R., and Weiss, D.S. (2012) Subversion of host recognition and defense systems by *Francisella* spp. *Microbiol Mol Biol Rev* **76:** 383–404.

Juruj, C., Lelogeais, V., Pierini, R., Perret, M., Py, B.F., Jamilloux, Y., *et al*. (2013) Caspase-1 activity affects AIM2 speck formation/stability through a negative feedback loop. *Front Cell Infect Microbiol* **3:** 1–11.

Keim, P., Johansson, A., and Wagner, D.M. (2007) Molecular epidemiology, evolution, and ecology of *Francisella*. *Ann N Y Acad Sci* **1105:** 30–66.

Larsson, P., Oyston, P.C., Chain, P., Chu, M.C., Duffield, M., Fuxelius, H.H., *et al*. (2005) The complete genome sequence of *Francisella tularensis*, the causative agent of tularemia. *Nat Genet* **37:** 153–159.

Lauriano, C.M., Barker, J.R., Nano, F.E., Arulanandam, B.P., and Klose, K.E. (2003) Allelic exchange in *Francisella tularensis* using PCR products. *FEMS Microbiol Lett* **229:** 195–202.

Llewellyn, A.C., Jones, C.L., Napier, B.A., Bina, J.E., and Weiss, D.S. (2011) Macrophage replication screen identifies a novel *Francisella* hydroperoxide resistance protein involved in virulence. *PLoS ONE* **6:** e24201.

LoVullo, E.D., Molins-Schneekloth, C.R., Schweizer, H.P., and Pavelka, M.S., Jr (2009) Single-copy chromosomal integration systems for *Francisella tularensis*. *Microbiology* **155:** 1152–1163.

Maier, T.M., Pechous, R., Casey, M., Zahrt, T.C., and Frank, D.W. (2006) *In vivo* Himar1-based transposon mutagenesis of *Francisella tularensis*. *Appl Environ Microbiol* **72:** 1878–1885.

Marohn, M.E., Santiago, A.E., Shirey, K.A., Lipsky, M., Vogel, S.N., and Barry, E.M. (2012) Members of the *Francisella tularensis* phagosomal transporter subfamily of major facilitator superfamily transporters are critical for pathogenesis. *Infect Immun* **80:** 2390–2401.

Meibom, K.L., and Charbit, A. (2010a) *Francisella tularensis* metabolism and its relation to virulence. *Front Microbiol* **1:** 1–13.

Meibom, K.L., and Charbit, A. (2010b) The unraveling panoply of *Francisella tularensis* virulence attributes. *Curr Opin Microbiol* **13:** 11–17.

Mortensen, B.L., Fuller, J.R., Taft-Benz, S., Collins, E.J., and Kawula, T.H. (2012) *Francisella tularensis* RipA protein topology and identification of functional domains. *J Bacteriol* **194:** 1474–1484.

Napier, B.A., Meyer, L., Bina, J.E., Miller, M.A., Sjöstedt, A., and Weiss, D.S. (2012) Link between intraphagosomal biotin and rapid phagosomal escape in *Francisella*. *Proc Natl Acad Sci USA* **109:** 18084–18089.

Niu, H., Yamaguchi, M., and Rikihisa, Y. (2008) Subversion of cellular autophagy by *Anaplasma phagocytophilum*. *Cell Microbiol* **10:** 593–605.

Niu, H., Xiong, Q., Yamamoto, A., Hayashi-Nishino, M., and Rikihisa, Y. (2012) Autophagosomes induced by a bacterial Beclin 1 binding protein facilitate obligatory intracellular infection. *Proc Natl Acad Sci USA* **109:** 20800–20807.

Nothelfer, K., Dias Rodrigues, C., Bobard, A., Phalipon, A., and Enninga, J. (2011) Monitoring *Shigella flexneri* vacuolar escape by flow cytometry. *Virulence* **2:** 54–57.

Oyston, P.C., Sjöstedt, A., and Titball, R.W. (2004) Tularaemia: bioterrorism defence renews interest in *Francisella tularensis*. *Nat Rev Microbiol* **2:** 967–978.

Pechous, R., Celli, J., Penoske, R., Hayes, S.F., Frank, D.W., and Zahrt, T.C. (2006) Construction and characterization of an attenuated purine auxotroph in a *Francisella tularensis* live vaccine strain. *Infect Immun* **74:** 4452–4461.

Pechous, R.D., McCarthy, T.R., Mohapatra, N.P., Soni, S., Penoske, R.M., Salzman, N.H., *et al*. (2008) A *Francisella tularensis* Schu S4 purine auxotroph is highly attenuated in mice but offers limited protection against homologous intranasal challenge. *PLoS ONE* **3:** e2487.

Pechous, R.D., McCarthy, T.R., and Zahrt, T.C. (2009) Working toward the future: insights into *Francisella tularensis* pathogenesis and vaccine development. *Microbiol Mol Biol Rev* **73:** 684–711.

Peng, K., and Monack, D.M. (2010) Indoleamine 2,3-dioxygenase 1 is a lung-specific innate immune defense mechanism that inhibits growth of *Francisella tularensis* tryptophan auxotrophs. *Infect Immun* **78:** 2723–2733.

Price, C.T., Al-Quadan, T., Santic, M., Rosenshine, I., and Abu Kwaik, Y. (2011) Host proteasomal degradation generates amino acids essential for intracellular bacterial growth. *Science* **334:** 1553–1557.

Qin, A., and Mann, B.J. (2006) Identification of transposon insertion mutants of *Francisella tularensis tularensis* strain Schu S4 deficient in intracellular replication in the hepatic cell line HepG2. *BMC Microbiol* **6:** 69.

Ray, K., Marteyn, B., Sansonetti, P.J., and Tang, C.M. (2009) Life on the inside: the intracellular lifestyle of cytosolic bacteria. *Nat Rev Microbiol* **7:** 333–340.

Reddy, V.S., Shlykov, M.A., Castillo, R., Sun, E.I., and Saier, M.H., Jr (2012) The major facilitator superfamily (MFS) revisited. *FEBS J* **279:** 2022–2035.

Rinehart, C.A., Jr, and Canellakis, E.S. (1985) Induction of ornithine decarboxylase activity by insulin and growth factors is mediated by amino acids. *Proc Natl Acad Sci USA* **82:** 4365–4368.

Ristroph, J.D., Hedlund, K.W., and Gowda, S. (1981) Chemically defined medium for *Legionella pneumophila* growth. *J Clin Microbiol* **13:** 115–119.

Santic, M., Asare, R., Skrobonja, I., Jones, S., and Abu Kwaik, Y. (2008) Acquisition of the vacuolar ATPase proton pump and phagosome acidification are essential for escape of *Francisella tularensis* into the macrophage cytosol. *Infect Immun* **76:** 2671–2677.

Sauer, J.D., Bachman, M.A., and Swanson, M.S. (2005) The phagosomal transporter A couples threonine acquisition to differentiation and replication of *Legionella pneumophila* in macrophages. *Proc Natl Acad Sci USA* **102:** 9924–9929.

Schulert, G.S., McCaffrey, R.L., Buchan, B.W., Lindemann, S.R., Hollenback, C., Jones, B.D., and Allen, L. (2009) *Francisella tularensis* genes required for inhibition of the neutrophil respiratory burst and intramacrophage growth identified by random transposon mutagenesis of strain LVS. *Infect Immun* **77:** 1324–1336.

Sjöstedt, A. (2007) Tularemia: history, epidemiology, pathogen physiology, and clinical manifestations. *Ann N Y Acad Sci* **1105:** 1–29.

Sjöstedt, A. (2011) Special topic on *Francisella tularensis* and tularemia. *Front Microbiol* **2:** 86. doi:10.3389/fmicb.2011.00086.

Steele, S., Brunton, J., Ziehr, B., Taft-Benz, S., Moorman, N., and Kawula, T. (2013) *Francisella tularensis* harvests nutrients derived via ATG5-independent autophagy to support intracellular growth. *PLoS Pathog* **9:** e1003562.

Wang, J.Y., Li, J., Patel, A.R., Summers, S., Li, L., and Bass, B.L. (1998) Synergistic induction of ornithine decarboxylase by asparagine and gut peptides in intestinal crypt cells. *Am J Physiol* **274:** C1476–C1484.

Wehrly, T.D., Chong, A., Virtaneva, K., Sturdevant, D.E., Child, R., Edwards, J.A., *et al*. (2009) Intracellular biology and virulence determinants of *Francisella tularensis* revealed by transcriptional profiling inside macrophages. *Cell Microbiol* **11:** 1128–1150.

Weinberg, E.D. (1975) Nutritional immunity. Host's attempt to withhold iron from microbial invaders. *JAMA* **231:** 39–41.

Weiss, D.S., Brotcke, A., Henry, T., Margolis, J.J., Chan, K., and Monack, D.M. (2007) *In vivo* negative selection screen identifies genes required for *Francisella* virulence. *Proc Natl Acad Sci USA* **104:** 6037–6042.

Young, V.R. (1994) Adult amino acid requirements: the case for a major revision in current recommendations. *J Nutr* **124:** 1517S–1523S.

Zhang, Y.J., and Rubin, E.J. (2013) Feast or famine: the host–pathogen battle over amino acids. *Cell Microbiol* **15:** 1079–1087.

Supporting information

Additional Supporting Information may be found in the online version of this article at the publisher's web-site:

Supplemental Experimental procedures

Fig. S1. The gene *ansP* of *F. novicida*.

A. Schematic organization of the *ansP* region. The *ansP* gene of *F. novicida* is flanked by two genes in the same orientation (*FTN_1587*, upstream; and *FTN_1585*, downstream), separated by intergenic regions (69 bp and 56 bp respectively).

B. RACE PCR. The transcription start of *ansP*, determined by RACE PCR, is shown. The putative σ^{70}-dependent −10 and −35 sequences are in red. The translation start codon of *ansP* and the preceding putative Shine–Dalgarno sequence (SD) are in italics and underlined.

C. Quantitative real-time RT-PCR. Quantification of *FTN_1585* and *FTN_1587* expression in wild-type *F. novicida* (WT) or Δ*ansP* mutant were performed in TSB at 37°C. qRT-PCRs were performed twice using independent samples (in triplicate).

Fig. S2. The AnsP protein is highly conserved among *Francisella* subspecies. Left panel. Multiple amino acid sequence alignments (CLUSTAL 2.1) of FTN_1586 (AnsP) with its orthologues in *F. tularensis* subsp. *holarctica* (FTL_1645), *F. tularensis* subsp. *mediasiatica* (FTM_0191) and *F. tularensis* subsp. *tularensis* (FTT_0129). In the KEGG database, two of the four proteins have slightly different sizes due to different predicted start codons. Right panel. In LVS, the predicted protein FTL_1645 is 403 aa in length (i.e. 30 aa shorter than in *F. novicida* FTN_1586). In Schu S4, the predicted protein FTT_0121 is 422 aa in length (i.e. 15 aa shorter than *F. novicida* FTN_1586). However, a careful inspection of the proximal and upstream portions of the four gene sequences, revealed the presence of a single base difference at codon 16 (*F. novicida* nomenclature) leading to a TCG to TTG codon modification (changing serine16 in FTN_1586 to leucine, in the proteins from three other subspecies). The four proteins are thus likely to encode a 437 aa protein, except FTL_1645 that is four amino acid shorter at its C-terminus.

Fig. S3. Growth in CDM.

A. Setting up of a modified chemically defined medium (CDM_{min}). We re-evaluated systematically the actual amino acid requirement of *F. novicida* U112 in chemically defined medium (CDM) (Chamberlain, 1965). Bacterial growth was assayed in CDM devoid of each individual amino acid (left column, CDM amino acid). This led us to redefine three classes of amino acids (right column, amino acid types). Essential amino acids (E-AAs): means, if absent, no growth. Useful non-essential (UNE-AAs): means, if absent growth impaired but not abolished. Non-essential (NE-AAs): means U112 is prototroph for all these amino acids (threonine, valine, asparagine, alanine, glutamic acid, glutamine, glycine, phenylalanine, tryptophane). Confirming earlier reports, the E-AAs were: arginine, histidine, lysine, methionine, tyrosine, cysteine. CDM_{min} contains all the amino acids required for optimal growth of U112. It corresponds to classical Chamberlain medium (CDM) without threonine and valine.

B. Growth of WT and *ΔansP* strains in CDM_{min} at 37°C.

Fig. S4. Biolog GN II plate assay. The list of substrates that *Francisella* actually metabolizes is shown to the right of the figure. ++, dark blue staining; +, pale blue staining.

Fig. S5. Intracellular multiplication defect of the mutant Δ*ansP* in LVS is fully rescued by addition of asparagine. The intracellular multiplication of the Δ*FTL_1645* mutant was impaired in J774 macrophages as compared to wild-type LVS (> 10-fold reduction of bacterial counts after 48 h). When DMEM was supplemented with 3 mM asparagine (+ asn), intracellular growth of the Δ*FTL_1645* mutant was identical to that of wild-type LVS (+/– asn).

Table S1. Strains, plasmids and primers used in this study.

This paper is available on line at http://www.mcponline.org

Possible Links Between Stress Defense and the Tricarboxylic Acid (TCA) Cycle in *Francisella* Pathogenesis*[S]

Jennifer Dieppedale‡§, Gael Gesbert‡§, Elodie Ramond‡§**, Cerina Chhuon‡¶, Iharilalao Dubail‡§, Marion Dupuis‡§, Ida Chiara Guerrera‡¶, and Alain Charbit‡§‖**

Francisella tularensis **is a highly infectious bacterium causing the zoonotic disease tularemia.** ***In vivo*****, this facultative intracellular bacterium survives and replicates mainly in the cytoplasm of infected cells. We have recently identified a genetic locus, designated** ***moxR*** **that is important for stress resistance and intramacrophage survival of** ***F. tularensis*****. In the present work, we used tandem affinity purification coupled to mass spectrometry to identify** ***in vivo*** **interacting partners of three proteins encoded by this locus: the MoxR-like ATPase (FTL_0200), and two proteins containing motifs predicted to be involved in protein–protein interactions, bearing von Willebrand A (FTL_0201) and tetratricopeptide (FTL_0205) motifs. The three proteins were designated here for simplification, MoxR, VWA1, and TPR1, respectively. MoxR interacted with 31 proteins, including various enzymes. VWA1 interacted with fewer proteins, but these included the E2 component of 2-oxoglutarate dehydrogenase and TPR1. The protein TPR1 interacted with one hundred proteins, including the E1 and E2 subunits of both oxoglutarate and pyruvate dehydrogenase enzyme complexes, and their common E3 subunit. Remarkably, chromosomal deletion of either** ***moxR*** **or** ***tpr1*** **impaired pyruvate dehydrogenase and oxoglutarate dehydrogenase activities, supporting the hypothesis of a functional role for the interaction of MoxR and TPR1 with these complexes. Altogether, this work highlights possible links between stress resistance and metabolism in** ***F. tularensis*** **virulence.** ***Molecular & Cellular Proteomics 12: 10.1074/mcp.M112.024794, 2278–2292, 2013.***

Francisella tularensis is responsible for the disease tularamia in a large number of animal species. This highly infectious bacterial pathogen can be transmitted to humans in numerous ways (1, 2, 3), including direct contact with sick animals, inhalation, ingestion of contaminated water or food, or by bites from ticks, mosquitoes, or flies. Four different subspecies (subsp.) of *F. tularensis* that differ in virulence and geographic distribution exist, designated subsp. *tularensis* (type A), subsp. *holarctica* (type B), subsp. *Novicida*, and subsp. *mediasiatica*, respectively. *F. tularensis* subsp. *tularensis* is the most virulent subspecies causing a severe disease in humans, whereas *F. tularensis* subsp. *holarctica* causes a similar disease but of less severity (4). Because of its high infectivity and lethality, *F. tularensis* is considered a potential bioterrorism agent (5).

F. tularensis is able to survive and to replicate in the cytoplasm of a variety of infected cells, including macrophages. To resist this stressful environment, the bacterium must have developed stress resistance mechanisms, most of which are not yet well characterized. We recently reported the identification of a novel genetic locus that is important for stress resistance and intracellular survival of *F. tularensis* (6). This locus was designated *moxR* because the first gene *FTL_0200*, encodes a protein belonging to the AAA+ ATPase of the MoxR family ((7) and references therein). The data obtained in that first study had led us to suggest that the *F. tularensis* MoxR-like protein might constitute, in combination with other proteins of the locus, a chaperone complex contributing to *F. tularensis* pathogenesis.

To further validate this hypothesis and expand our initial observations, we here decided to perform tandem affinity purification (TAP),[1] using a dual affinity tag approach coupled to mass spectroscopy analyses (8), to identify proteins inter-

From the ‡Université Paris Descartes, Sorbonne Paris Cité, Bâtiment Leriche. 96 rue Didot 75993 Paris Cedex 14 – France; §INSERM, U1002, Unité de Pathogénie des Infections Systémiques, Paris, France; ¶Plateau Protéome Necker, PPN, IFR94, Université Paris-Descartes, Faculté de Médecine René Descartes, Paris 75015 France

Received October 9, 2012, and in revised form, May 1, 2013

Published, MCP Papers in Press, May 13, 2013, DOI 10.1074/mcp.M112.024794

[1] The abbreviations used are: ACC, acetyl-CoA carboxylase; BACTH, bacterial two-hybrid; BCA, bicinchoninic acid; BMM, bone marrow derived macrophages; CBP, calmodulin binding protein; CDS, coding sequence; CFU, colony forming unit; CID, collision-induced dissociation; DSP, dithiobis(succinimidyl propionate); DTNB, 3–3′dithio-bis(6-nitrobenzoic acid); IPTG, isopropyl-beta-D-1- thiogalactopyranoside; KEGG, Kyoto encyclopedia of genes and genomes; LTQ, linear trap quadrupole; LVS, live vaccine strain; OAA, oxaloacetate; OGDH, 2-oxoglutarate dehydrogenase; PDH, pyruvate dehydrogenase; RP, reversed-phase; RPMI, Roswell park memorial institute medium; RSLC, rapid separation liquid chromatography; TAP, tandem affinity purification; TCA, tricarboxylic acid; TPP, thiamine pyrophosphate; TPR, tetratricopeptide; VWA, Von Willebrand type A factor.

acting *in vivo* with three proteins encoded by the proximal portion of the *moxR* locus. For this, we chose as baits: the MoxR-like protein (FTL_0200) and two proteins bearing distinct motifs possibly involved in protein–protein interactions, FTL_0201 (Von Willebrand Factor Type A domain, or VWA) and FTL_0205 (tetratrichopeptide repeat or TPR). The three proteins were designated here for simplification, MoxR, VWA1, and TPR1; and the corresponding genes *moxR*, *vwa1*, and *tpr1*, respectively.

VWA domains are present in all three kingdoms of life. They consist of a β-sheet sandwiched by multiple α helices. Frequently, VWA domain-containing proteins function in multiprotein complexes (9). TPR typically contain 34 amino acids. Many three-dimensional structures of TPR domains have been solved, revealing amphipathic helical structures (10). TPR-containing proteins are also found in all kingdoms of life. They can be involved in a variety of functions, and generally mediate protein–protein interactions. In the past few years, several TPR-related proteins have been shown to be involved in virulence mechanisms in pathogenic bacteria ((11) and references therein).

Our proteomic approach allowed us to identify a series of protein interactants for each of the three *moxR*-encoded proteins. Remarkably, the protein TPR1 interacted with all the subunits of the pyruvate dehydrogenase (PDH) and 2-oxoglutarate dehydrogenase (OGDH) complexes. Furthermore, inactivation of *tpr1* also severely impaired the activities of these two enzymes. Inactivation of *tpr1* affected bacterial resistance to several stresses (and in particular oxidative stress), intramacrophagic bacterial multiplication and bacterial virulence in the mouse model. Functional implications and possible relationship between bacterial metabolism, stress defense, and bacterial virulence are discussed.

EXPERIMENTAL PROCEDURES

Bacterial Strains and Plasmids—*Francisella tularensis* LVS was grown on premade chocolate agar (BioMerieux SA Marcy l'Etoile, France), chocolate plates prepared from GC medium base, IsoVitalex vitamins, and hemoglobin (BD Biosciences, San Jose, CA, USA), or in Schaedler + vitamin K3 broth (Schaedler-K3, BioMerieux) at 37 °C. All bacterial strains, plasmids, and primers used in this study are listed in supplemental Table S1.

Construction of a Chromosomal LVSΔtpr1 Deletion Mutant—The *F. tularensis* LVSΔ*tpr1* deletion mutant was constructed using the same procedure as described previously (6). Briefly, we used the ≪ suicide ≫ plasmid pPV an *E. coli*-F. tularensis shuttle vector (12), which possesses a *sacB* counter-selective gene, chloramphenicol and ampicillin selective genes, an *E. coli* replication origin (*ori pUC19*), and a transfer origin for conjugation (*oriT* RP4). The upstream and downstream regions of *tpr1* gene were amplified by overlapping PCR, and the resulting fragment was subcloned in the XbaI and SalI restriction sites of the plasmid pPV, yielding recombinant pPV-Δ*tpr1*. This plasmid was introduced in LVS by conjugation (6) and the chromosomal Δ*tpr1* deletion mutant was obtained by the classical two-step allelic replacement procedure (12).

Functional Complementation—Plasmids pFNLTP6p*gro-tpr1* and pFNLTP6p*gro-tpr1-FTL_0206* (here designated p6*gro-tpr1* and p6*gro-tpr1-FTL_0206*) were used for complementation of LVSΔ*tpr1*. Plasmid p6*gro-tpr1* was constructed by amplifying a 761 base pair (bp) fragment comprising the sequence 16 bp upstream of the *tpr1* start codon to 11 bp downstream of the stop codon. The primers used were Compl-*FTL_0205*-FW and Compl-*FTL_0205*-RV (supplemental Table S1). The plasmid p6*gro-tpr1-FTL_0206*, was constructed by amplifying a 2508 bp fragment (corresponding to the sequence 100 bp upstream of the *tpr1* start codon and to 39 bp downstream of the stop codon of the *FTL_0206* gene) using primers Compl-*FTL_205/206*-FW EcoRI and Compl-*FTL_205/206*-RV BamHI (supplemental Table S1), followed by digestion with EcoRI and BamHI, and cloning into plasmid pFNLTP6p*gro* (p6*gro*) (13). The amplified product was digested with BamHI and EcoRI and cloned into the corresponding sites of plasmid p6*gro*.

The plasmids p6*gro* (plasmid without insert), p6*gro-tpr1*and p6*gro-tpr1-FTL_0206* (the complementing plasmids) were introduced into LVS or LVSΔ*tpr1* mutant strain by electroporation, as described previously (6).

Construction of Strains Expressing TAP-tagged Proteins—The *moxR, vwa1* and *tpr1* genes were amplified from genomic DNA of LVS, using the appropriate pairs of primers (supplemental Table S1). The amplified fragments were cloned into the expression vector p6*gro*, resulting in the following plasmids: p6*gro-moxR,* p6*gro-vwa1,* p6*gro-tpr1*. The tandem affinity purification tag (TAPtag) sequence was amplified from plasmid pEB304 (8, 14), using primers 7 or 8, and 9 (supplemental Table S1). This TAP tag sequence (composed of the sequence of protein A, a TEV protease cleavage site, and the calmodulin binding domain) was fused in frame, in the NotI or XhoI restriction sites, after the last codon of each coding sequence) to the C-terminal end of each gene (in p6*gro* recombinant plasmids). The resulting plasmids were finally introduced in the LVS strain by electroporation, yielding the recombinant strains LVS/p6*gro-moxR-TAP*, LVS/p6*gro-vwa1-TAP*, and LVS/p6*gro-tpr1-TAP*, respectively. The tagged proteins were designated MoxR-TAP, VWA1-TAP, and TPR1-TAP, respectively. The p6*gro-moxR-TAP* plasmid was also introduced in the mutant strain LVSΔ*tpr1* to verify the activity of protein TPR1-TAP by functional complementation.

Purification of TAP-tagged Proteins from F. tularensis LVS—*F. tularensis* cells of logarithmic phase (2 liters of culture at an OD_{600} of 0.5–0.7) were harvested (3000 × *g* for 20 min) and resuspended in 20 ml of a solubilization buffer consisting of 100 mM HEPES/KOH, pH 7.4, 100 mM KCl, 8% glycerol and complete protease inhibitor mixture, Roche (one tablet for 50 ml of buffer). Then, cells were harvested (3000 × *g* for 30 min) and resuspended in 10 ml of solubilization buffer. The cross-linker dithiobis(succinimidyl propionate) (DSP) (G-Biosciences) was added at a concentration of 20 mg/ml for 5 min on ice, and the cross-link reaction was stopped by addition of 1 mM Tris/HCl pH 7.4 (15). The bacterial suspension was sonicated 20 times for 30 s at 4.0 output, 70% pulsed (Branson Sonifier 250). After centrifugation of cell debris (16,000 × *g* for 30 min), 0.1% Nonidet P-40 was added to the protein lysate. Then, the protein extracts were incubated for 2 h at 4 °C, with 0.5 ml of Sepharose-IgG beads (GE Healthcare), previously washed with binding buffer (100 mM HEPES/KOH, pH 7.4, 100 mM KCl, 8% glycerol, 0.1% Nonidet P-40). The column was washed three times with binding buffer. The bound proteins were recovered by addition of 1 ml (four times with 250 μl) of 100 mM glycine-HCl at pH 3, supplemented with 100 mM KCl. The eluate was added to three volumes of Calmodulin binding buffer (binding buffer supplemented with 4 mM $CaCl_2$) and the pH was readjusted to 7 by addition of KOH before binding to the calmodulin beads. Then, this protein eluate was incubated at 4 °C for 1 h with 0.5 ml of Sepharose-calmodulin beads (GE Healthcare), previously washed with calmodulin binding buffer. After, the column was washed three times with this same buffer and the protein complex was eluted with 1 ml (five times with 200 μl) of 20 mM Tris/HCl pH 8,

containing 50 mM NaCl, 5 mM EGTA. Purified proteins were washed with PBS 1X and concentrated, using microcons 10,000 MWCO (Amicon, Millipore). Proteins were quantified with BCA assay kit (Pierce, Thermo Scientific).

Western Blot Analysis—The TAP-tagged proteins were detected by Western blot using ECL™ Western blot Detection Reagents (GE Healthcare) and anti-TAPtag antibodies (Genscript), according to the manufacturer's recommendations. The primary rabbit anti-TAPtag antibody was used at a final dilution of 1:1000 in PBS Tween 0.05%, 5% milk (PBS-TM), and incubated for 1 h. The secondary anti-rabbit antibody was used at a final dilution of 1:2000 in PBS-TM and incubated for 1 h.

Bacterial Two-Hybrid (BACTH) Complementation Assays—The LVS genes were amplified from genomic DNA, using the appropriate pairs of primers (supplemental Table S1). These genes were fused in-frame to the DNA sequences encoding the T18 or T25 domains of *Bordetella pertussis* adenylate cyclase. The gene *moxR* was cloned into pKT25 vector (C-terminal fusion to T25 domain), and the gene *tpr1* was cloned into pKT25 and pKNT25 vectors (yielding C-terminal and N-terminal fusions to T25, respectively) (16). The genes *FTL_1783, FTL_0309, FTL_0310, FTL_0311*, and *FTL_0295,* were cloned into pUT18C vector (C-terminal fusion to T18 domain). The different pairs of recombinant plasmids (pKT25-x/pUT18C-y or pKNT25-x/pUT18C-y) were used to cotransform *E. coli* strain BTH101.

The transformants were selected onto LB plates containing 40 μg/ml X-Gal, 0.5 mM IPTG, 50 μg/ml Kanamycin and 100 μg/ml Ampicillin, and incubated at 30 °C for 24 to 36 h. As negative control, BTH101 cells were co-transformed with empty pUT18C vector and pKT25 vector containing either *moxR* gene or *tpr1* gene (or pKNT25 vector containing *tpr1* gene). Each BACTH assay was performed twice.

Enzymatic Assays—LVS, LVSΔ*moxR*, and LVSΔ*tpr1* strains were grown until exponential phase (OD_{600} of 0.5–0.7). The cells (15 ml) were harvested by centrifugation at 3000 $\times$ *g* for 20 min and resuspended in 2 ml of 5 mM Tris-HCl pH 8. The bacterial suspensions were sonicated four times for 30 s at 4.0 output, 70% pulsed (Branson Sonifier 250). Oxoglutarate and pyruvate dehydrogenase activities were assayed by measuring the reduction of NAD^+ at 340 nm upon the addition of 0.5 mM NAD^+, 200 μM TPP, 40 μM CoASH, 3 mM $MgCl_2$, 9 mM L-cysteine and either 16 mM oxoglutarate (α-ketoglutarate) or 16 mM pyruvate to 20 μg ml^{-1} *F. tularensis* cell lysate, as described in (17, 18). Protein concentration was estimated with BCA assay kit (Pierce, Thermo Scientific). Assays were performed in a final volume of 1 ml.

Assays for the carboxyltransferase subunit of acetyl-CoA carboxylase were performed at 412 nm in the reverse direction in which malonyl-CoA reacts with biocytin to form acetyl-CoA and carboxybiotin. The production of acetyl-CoA was coupled to citrate synthase, which produced citrate and coenzyme A. The amount of coenzyme A formed was detected using 5,5-dithiobis(2-nitrobenzoic acid) (DTNB), as described in (19).

The assay buffer consisted of 100 mM potassium phosphate (pH 7.6) with 0.1% Tween 20. Final concentrations of reagents in the assay were as follows: 200 mM malonyl-CoA, 12 mM biocytin, 10 mM oxaloacetate, 200 mM DTNB, 104 nM citrate synthase, and 50 μg of total protein. The assay was realized in a final volume of 100 μl in 96-well plates, with a classic plate reader (Multiskan RC, ThermoLabsystems).

Catalase activity assay was realized using the Amplite™ Fluorimetric Catalase Assay Kit (AAT Bioquest Inc® CA, USA). The assay was performed according to manufacturer's recommendation. Briefly, the samples (50 μl containing 0.04 μg of total proteins) were incubated with 50 μl of H_2O_2-containing assay buffer, at room temperature for 30 min. Then, the catalase assay mixture (containing Amplite™ Red substrate and Horseradish peroxidase) was added and the incubation pursued for another 30 min. Therefore, the reduction in fluorescence intensity is proportional to catalase activity. The fluorescence of the final mixture was then determined on a BioRad iMark™ absorbance microplate reader at 576 nm.

Growth Kinetics in Broth and Stress Survival Assays—Stationary-phase bacterial cultures of LVS/p6*gro*), LVSΔ*tpr1*/p6*gro* and LVSΔ*tpr1*/p6*gro-tpr1*) mutant strains were diluted at a final OD_{600} of 0.1 in Schaedler-K3 broth. Exponential-phase bacterial cultures were diluted to a final concentration of 10^8 bacteria/ml and subjected to the following stress conditions: 10% ethanol, 0.03% H_2O_2, pH 4.0, 50 °C or 0.05% SDS The number of viable bacteria was determined by plating appropriate dilutions of bacterial cultures on Chocolate Polyvitex plates at the start of the experiment and after the indicated durations. For experiments at 50 °C, aliquots of 0.25 ml in a 1.5 ml tube were placed at 50 °C statically and at the indicated times, the tubes were placed on ice, serially diluted, and plated. For experiments with ethanol, H_2O_2, pH 4.0 or 0.05% SDS, cultures (5 ml) were incubated at 37 °C with rotation (100 r.p.m.) and aliquots were removed at indicated times, serially diluted and plated immediately. Bacteria were enumerated after 72 h incubation at 37 °C. Experiments were repeated independently at least twice and data represent the average of all experiments.

Multiplication in Macrophages—Intracellular multiplication assays were performed essentially as previously described (6). THP1 (ATCC Number: TIB-202™) cells were propagated in RPMI containing 5% fetal calf serum. Cells were seeded at a concentration of $\sim 2 \times 10^5$ cells per well in 12-well cell tissue plates and monolayers were used 48 h after seeding. THP-1 cells were differentiated by treatment, with 200 ng ml^{-1} phorbol myristate acetate (PMA). THP1 macrophage monolayers were incubated for 60 min at 37 °C with the bacterial suspensions (multiplicities of infection 100) to allow the bacteria to enter. After washing (time zero of the kinetic analysis), the cells were incubated in fresh culture medium containing gentamicin (10 μg ml^{-1}) to kill extracellular bacteria. At several time-points, cells were washed three times in RPMI, macrophages were lysed by addition of water and the titer of viable bacteria released from the cells was determined by spreading preparations on Chocolate agar plates. For each strain and time in an experiment, the assay was performed in triplicate. Each experiment was independently repeated at least three times and the data presented originate from one typical experiment.

Mice Virulence Assay—All animal experiments were carried out in accordance to the European guidelines and following the recommendations of the INSERM guidelines for laboratory animal husbandry. LVS/p6*gro*, LVSΔ*tpr1*/p6*gro* and LVSΔ*tpr1*/p6*gro-tpr1-FTL_0206* strains were grown in Schaedler-K3 containing kanamycin to exponential growth phase and diluted to the appropriate concentration. six to 8 weeks old female BALB/c mice (Janvier, Le Genest-St-Isle, France) were injected each day subcutaneously with kanamycin (50 μl of 12 mg ml^{-1} solution) 1 day before and every day during the infection. Mice were intraperitoneally inoculated with 200 μl of bacterial suspension (corresponding to $\sim$250 CFU). The actual number of viable bacteria in the inoculum was determined by plating dilutions of the bacterial suspension on chocolate plates. After 4 days, the mice were sacrificed. Homogenized spleen and liver tissue from the five mice were diluted and spread onto chocolate agar plates supplemented with kanamycin and the number of viable bacteria per organ determined.

Identification of Proteins by Mass Spectrometry—Protein samples were run on SDS-PAGE gels and silver stained (20). Gel lanes were excised and subjected to tryptic digestion with sequencing grade modified Trypsin (Promega), as described previously (15). Nano-LC-MS/MS analysis of in-gel digested samples was performed on an

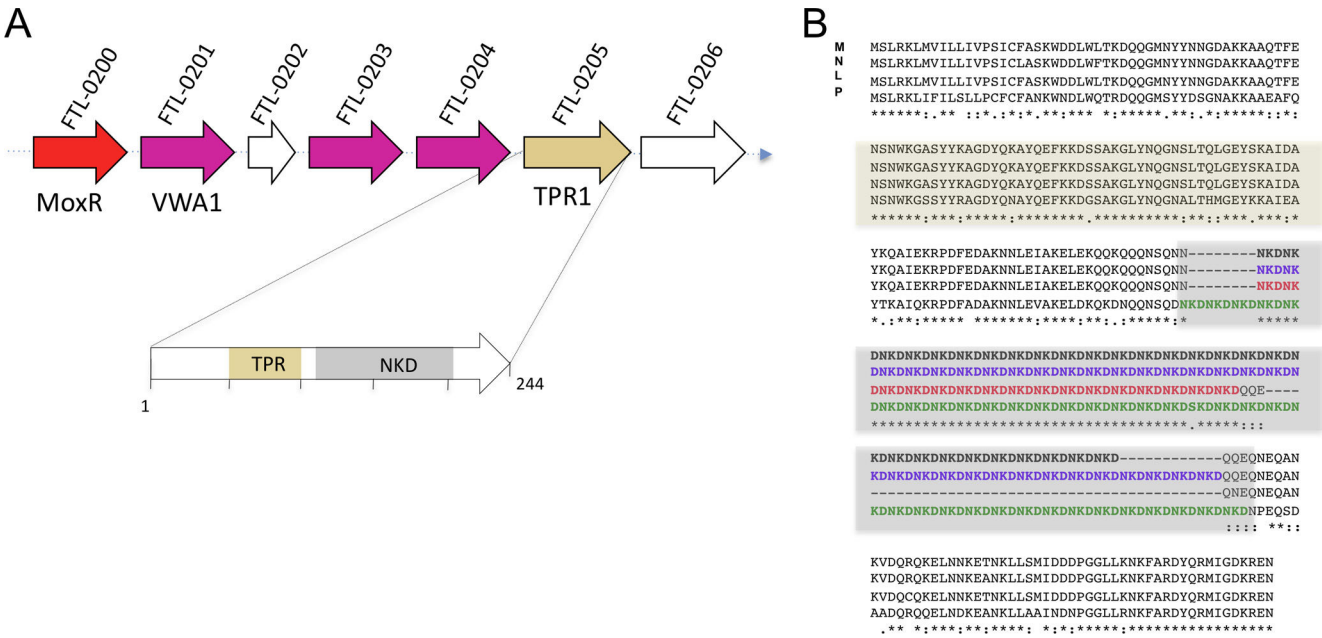

FIG. 1. **Sequence analysis of protein TPR1.** *A*, Upper line. Schematic organization of the proximal region of the *moxR* locus (genes *FTL_0200-FTL_0206*). Gene *moxR* (*FTL_0200*), encoding the MoxR protein is colored in red. The three genes encoding proteins containing VWA motifs are in magenta. Gene *vwa1* (*FTL_0201*) encodes the VWA1 protein. Gene *tpr1* (*FTL_0205*), encoding the protein TPR1 (containing the TPR motif), is in beige. Lower line. Schematic representation of the regions of the tetratricopeptide repeats (TPR, residues 31–130 (e value 5.7 e-15) and of the NKD repeats (region of residues 138 - 186). *B*, ClustalW 2.1 multiple sequence alignments of selected orthologues of TPR1. M, *F. tularensis* susp. *mediasiatica;* N, *F. tularensis* susp. *novicida;* L, *F. tularensis* susp. *holarctica;* P, *F. philomiragia.* The orthologues of TPR1 contain variable numbers of NKD repeats: 28 in *F. tularensis* susp. *mediasiatica* (in bold black, FTM_1557); 32 in *F. tularensis* susp. *novicida* (in bold blue, FTN_0209); and 36 in *F. philomiragia* (in bold green, Fphi_0623), respectively.

Ultimate 3000 Rapid Separation Liquid Chromatography (RSLC) system (Dionex) coupled to LTQ-Orbitrap Velos mass spectrometer (Thermo Scientific). Extracted peptides were dissolved in 0.1% (v/v) trifluoroacetic acid, 10% acetonitrile, and preconcentrated on a 75 μm i.d. reversed-phase (RP) trapping column and separated with an aqueous-organic gradient (solution "A": 0.1% (v/v) formic acid in 5% (v/v) acetonitrile; solution "B": 0.085% (v/v) formic acid in 80% (v/v) acetonitrile; flow rate 400 nL/min) on a 75 μm i.d. RP column (Acclaim PepMap RSLC 75 μm $\times$ 15 cm, 2 μm, 100Å, Dionex). Elution gradient settings for standard protein samples were: 3 min at 0% B, 10 min from 0% B to 10% B, 7 min from 10% B to 20% B, 7 min from 20% B to 40% B, 4 min from 40% B to 50% B, 0.5 min from 50% B to 90% B, 5 min at 90% B, 0.5 min from 90% B to 0% B, 5 min at 0%. MS instrument settings were as follows: spray voltage 1.8 kV; capillary temperature 250 °C; FT full MS target 1,000,000 (maximum injection time 500 ms); IT MSn target 5000 (maximum injection time 100 ms). 2 FTMS full scan were averaged (resolution 30,000 for LTQ-Orbitrap velos; positive polarity; centroid data; scan range 400 to 2000 *m/z*) and the 20 most intense signals were subjected to MS/MS in the collision-induced dissociation (CID) cell (resolution 15,000; centroid data) with dynamic exclusion (repeat count 1; exclusion list size 500; repeat/exclusion duration 12 s; exclusion mass width $\pm$ 10 ppm), preview mode for FTMS master scans, charge state screening, monoisotopic precursor selection and charge state rejection (charge state 1 and 4+) enabled. Activation type was CID with default settings.

LC-MS/MS data were extracted and raw files from the analysis of bands from each independent experiment were merged. For data analysis, peak lists were generated by Proteome Discoverer v1.2 (Thermo Scientific) and searched against all the concatenated sequences of all the subspecies of *F. tularensis* (14,148 sequences; available online on http://www.uniprot.org/taxonomy/?query = complete%3Ayes+content%3Afrancisella+tularensis&sort = score) from UniProtKB/Swiss-Prot complete proteome database (release 2011_01; 524,420 sequences) using the Mascot search engine (version 2.2.07; Matrix Science).

Default parameters used were: fixed modification (Carbamidomethyl (C)), and variable modification (Oxidation (M)) were allowed as well as one missed cleavage. Enzyme was trypsin, monoisotopic peptide mass tolerance was $\pm$ 5 ppm (after linear recalibration), fragment mass tolerance was $\pm$ 0.5 Da, false discovery rate was lower than 2%. Only proteins identified with at least two unique peptides and with the ion score higher than 25 were retained.

RESULTS

In Silico Analyses—We have recently identified a genetic locus, conserved among *Francisella* genomes, that comprises ten consecutive genes in the same orientation (*FTL_0200* to *FTL_0209*, in *F. tularensis* LVS). Deletion of gene *moxR* (*FTL_0200*) led to a mutant bacterium with increased vulnerability to various stress conditions and a growth defect in infected macrophages (6). Remarkably, the proximal part of the *moxR* operon, which is conserved in the genomes of several other pathogenic bacterial species, encodes proteins containing either tetratricopeptide repetition (TPR) or von Willebrand type A (VWA) motifs (Fig. 1). Confirming the peculiar characteristics of this genetic region, we identified only a limited number of proteins bearing either TPR or VWA motifs in the *F. tularensis* genomes currently available in the Kyoto Encyclopedia of Genes and Genomes (KEGG) database, us-

ing the Superfamily prediction program (available at http://supfam.cs.bris.ac.uk). Indeed, FTL_0201 (here designated VWA1), FTL_0203 and FTL_0204, were the only three proteins predicted to contain VWA-like motifs; and four proteins, including FTL_0205 (here designated TPR1), were predicted to contain TPR motifs with significant hits.

We identified a multiple 9 bp repeat in the middle part of gene *tpr1* (*FTL_0205*), accounting for the presence of a NKD tripeptide repeat in the central part of the TPR1 protein (Fig. 1). The presence of 25 regions of 9 bp repeats (designated SSTR9 for short sequence tandem repeat with 9 nucleotides) had been previously reported in the genome of *F. tularensis* SCHU S4 (21). Twelve of these repeats were identified within predicted open reading frames, one of which corresponds to the ortholog of *tpr1*. Multiple amino acid sequence alignments reveals that the number of repetitions of the NKD motif varies among the different TPR1 protein homologs *i.e.* 32 repeats in *F. tularensis* subsp. *novicida* and 36 repeats in *Francisella philomiragia* ortholog (as compared with 16 repeats in TPR1 of LVS) **(**Fig. 1*A*). Hence, the protein TPR1 contains both a TPR motif in its proximal part and a NKD repeat region in its central part, suggesting unique structural properties for this protein (Fig. 1*B*).

In *F. tularensis* subsp. *tularensis* SCHU S4, a careful re-examination of the gene designated *FTT_0294,* which corresponds to the two distinct genes *FTL_0204* and *FTL_0205* in LVS*,* revealed it was erroneously annotated as a pseudogene in the KEGG database. In fact, the DNA sequence of *FTT_0294* encompasses two consecutive coding sequences with a 10 bp overlap (supplemental Fig. S1*A*). The proximal part of *FTT_0294* encodes a protein sharing 99.7% identity with FTL_0204 and the distal part of *FTT_0294*, a protein sharing 84.1% identity with FTL_0205 (TPR1) (supplemental Fig. S1*B*).

Identification of In Vivo Interaction Partners—Tandem affinity purification (TAP) was used to identify proteins interacting *in vivo* with proteins of the *moxR* locus, using a dual affinity tag coupled to mass spectrometry (8). We focused in the present work on MoxR, and on one protein for each type of protein–protein interaction motif. Our working hypothesis was that the interactomes of these baits would lead to the identification of other *moxR*-encoded proteins. VWA1 was chosen as a prototypic VWA-bearing motif protein because gene *vwa1* was the only gene (of the three genes encoding VWA-bearing proteins), to be significantly up-regulated upon infection of macrophages (22). We thus considered that it was the most relevant candidate to identify interacting partners possibly involved in *Francisella* intracellular survival and virulence. TPR1 was chosen because it was the only protein of the *moxR* locus to bear a TPR motif and the only TPR protein encoded by the *Francisella* genome that also carried a NKD tripeptide repeat.

The three TAP-tagged proteins constructed were designated MoxR-TAP, VWA1-TAP and TPR1-TAP, respectively (see Experimental procedures for details). The corresponding recombinant genes were expressed under the control of the p*gro* promoter in the pFNLTP6p*gro* expression vector (Fig. 2*A***)**. The resulting plasmids were introduced in the *F. tularensis* LVS strain and expression of the tagged-proteins was verified by Western blot, using anti-tag antibody (15) on bacterial lysates. As shown in Fig. 2*B*, a band with the expected molecular weight (MW) was detected for the three recombinant proteins. An additional lower MW was also detected for MoxR-TAP, likely to correspond to a C-terminal proteolytic degradation product.

The three recombinant proteins were used individually as baits and their interacting LVS proteins were purified using a two-step elution procedure (15). In most cases, several bands were specifically eluted by this procedure (Fig. 2*C*). In each case, the MS-MS data obtained for each band were combined and analyzed to compact results in a single table for simplification.

Experiments were performed in biological replicates. One-dimensional SDS-PAGE protein profiles and MS-MS protein identifications obtained for each experiment were always compared with verify reproducibility. Results issued from triplicate experiments for MoxR-TAP and VWA1-TAP and duplicate experiments for TPR1-TAP are summarized in Tables I*A–C*. In each table, we chose as a threshold, the protein partners identified with at least two unique peptides and identified in at least two independent experiments.

Thirty-one different proteins interacting with MoxR-TAP were identified (Table I*A*), including MoxR-TAP itself. The most highly represented protein was FTL_1714 (or GroEL). The other proteins identified encompassed various predicted biological activities (ranging from ribosomal proteins to hypothetical proteins). Eight proteins appeared to interact with VWA1-TAP, including VWA1-TAP itself (Table I*B*). The two most highly represented proteins (peptide number >10) were FTL_1714 (GroEL) and FTL-1783 (or SucB), the E2 component of the 2-oxoglutarate dehydrogenase (OGDH) complex. Remarkably, TPR1 was also identified as a binding partner of VWA1-TAP. Finally, one hundred proteins interacting with TPR1-TAP were identified. These proteins belonged to various functional categories (Table 1*C*). TPR1-TAP itself was among the most highly represented proteins. The other highly represented proteins (18 proteins with >10 unique peptides) included notably the E1 components of OGDH and pyruvate dehydrogenase (PDH). The E2 components of the two complexes were also detected (FTL_1783, OGDH E2; and FTL_0310, PDH E2) as well as the E3 component common to both complexes (FTL_0311, PDH/OGDH E3). Only one protein, FTL_0207, encoded by the *moxR* locus was identified among the interactants of TPR1-TAP. In addition, the two subunits of the acetyl-CoA carboxyl transferase (ACC-α and ACC-β) were identified (12 peptides each).

BACTH Analyses—The bacterial two-hybrids (BACTH) system was used to confirm several of the interacting partners

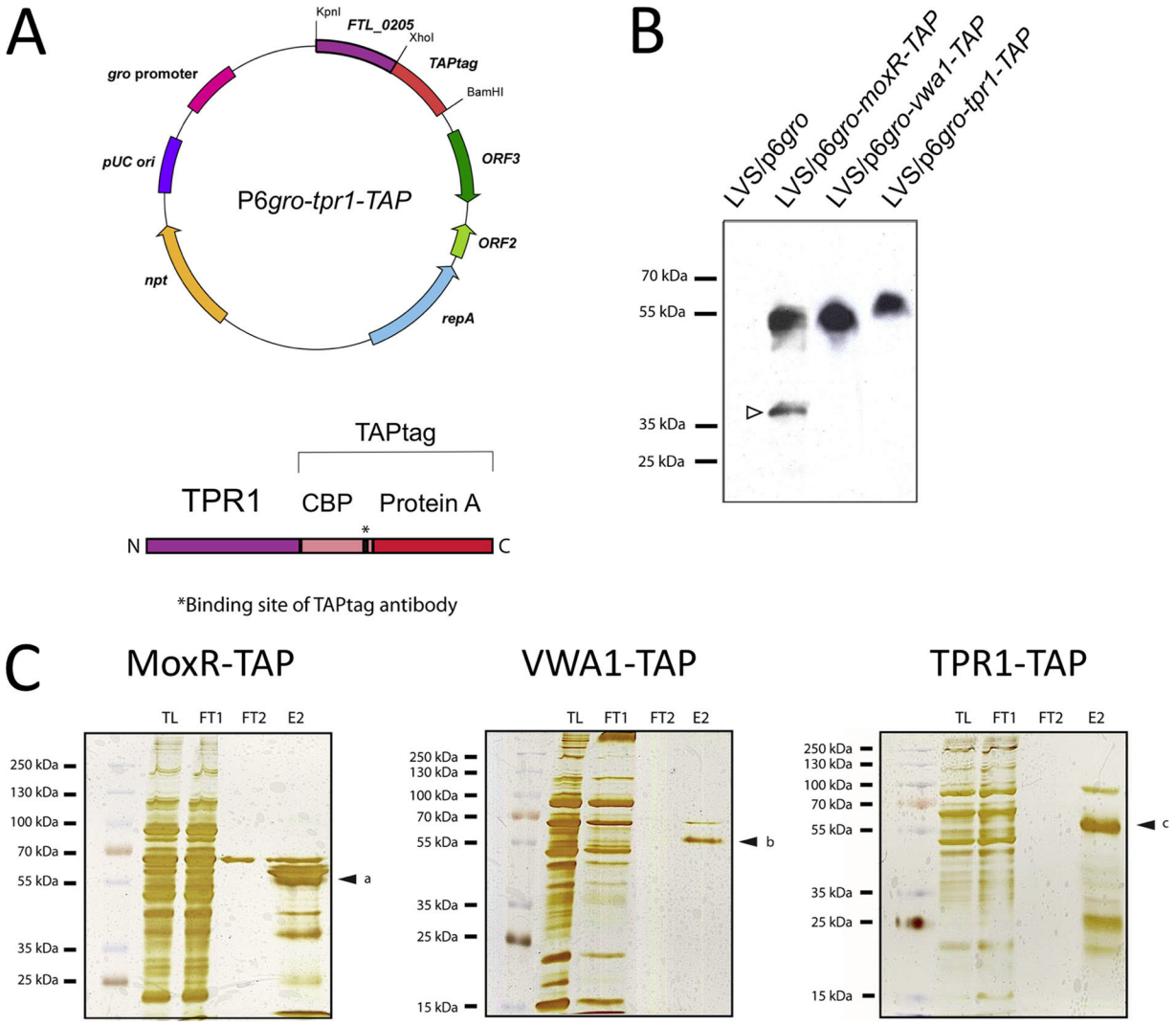

FIG. 2. **Construction of MoxR, VWA1 and TPR1 tagged proteins.** *A*, Constructions. *Left* panel, the 5.1 kb p6*gro*-derived recombinant plasmid carrying the fusion gene *tpr1-Tap* under the control of the p*gro* promoter. *Right* panel, schematic representation of the different parts the TPR1-TAP protein. The protein A and calmodulin binding (CBP) domains of the TAP sequence have been fused immediately downstream of the last residue of TPR1. *B*, Western-blot analyses. The recombinant proteins were expressed from p6*gro*-derived plasmids in LVS. The three proteins carry the TAPtag sequence at their C-terminal end. Western blot analysis was performed on whole cell extracts to verify production and stability of TAP-tagged proteins, using a polyclonal anti-TAPtag antibody. The three recombinant proteins were detected at the expected molecular weight (a, MoxR-TAP; b, VWA1-TAP; c, TPR1-TAP). The open arrow indicates the position of a probable degradation product of MoxR-TAP. Wild-type LVS strain was used as a negative control. *C*, TAP tag purification. TL, whole cell lysate; FT1, flow-through of the first purification column; FT2, flow-through of the second purification column; E2, final elution sample from the second column. The arrows indicate the protein band in which peptides corresponding to the bait were the most abundant. Molecular weight markers are indicated to the left of the figure (in kDa).

identified in the TAPtag approach. We focused in particular on the interactions of MoxR and TPR1 with the OGDH E2 subunit (FTL-1783 or SucB), as well as on the interactions of TPR1 with the three subunits of PDH (FTL_0309, FTL_0310, FTL_0311) and with the acetyl CoA carboxylase-α subunit (FTL_0295).

The FTL proteins moieties were fused to the proximal portion (designated CyaA-T25, vectors pKT25 and pKNT25) or to the distal portion (designated CyaA-T18, vector pUT18C) of the catalytic domain of adenylate cyclase (Table II). Briefly, genes *moxR* and *tpr1* were cloned into plasmid pKT25 (C-terminal fusions to CyaA-T25). The gene *tpr1* was also cloned into plasmid pKNT25 (N-terminal fusion to CyaA-T25). The genes *FTL-1783*, *FTL-0309*, *FTL-0310*, *FTL-0311*, *FTL-0295*, were cloned into plasmid pUT18C encoding the distal domain of CyaA (C-terminal fusions to CyaA-T18). Each pair of recombinant bait (CyaA-T25, pKT derivatives)/pray (CyaA-T18, pUT derivatives) plasmids was introduced into the *E. coli cya*- strain BTH101. The interaction CyaA-T25 + CyaA-T18, reconstituting catalytic CyaA activity and leading to the production

TABLE I

Accession UniProtKB	Gene name	FTL number	Protein description	Unique peptides
A. MoxR-TAP. Dieppedale *et al*.				
P94798	*groEL*	*FTL_1714*	60 kDa chaperonin**	36
Q2A5K6	*moxR*	*FTL_0200*	MoxR family ATPase**	23
Q9ZAW3	*ftsZ*	*FTL_1907*	Cell division protein FtsZ**	12
Q2A5L9	*pheC*	*FTL_0187*	Cyclohexadienyl dehydratase*	8
Q2A328	*dnaK*	*FTL_1191*	Chaperone protein DnaK*	8
Q2A1M4	*rplA*	*FTL_1747*	50S ribosomal protein L1*	7
Q2A1Z7	*pckA*	*FTL_1616*	Phosphoenolpyruvate carboxykinase*	7
Q2A358	*iglD*	*FTL_0114/FTL_1160*	Intracellular growth locus protein D*	7
Q2A3U7	*phoH*	*FTL_0885*	PhoH-like protein**	6
Q2A639	*dnaN*	*FTL_0002*	DNA polymerase III β subunit**	5
Q2A499		*FTL_0702*	Hypothetical protein*	5
Q2A5I2	*rpsB*	*FTL_0224*	30S ribosomal protein S2*	4
Q2A5G4	*rpsC*	*FTL_0242*	30S ribosomal protein S3*	4
Q2A360	*iglB*	*FTL_0112/FTL_1158*	Intracellular growth locus protein B*	4
Q2A5E6	*rpsD*	*FTL_0260*	30S ribosomal protein S4*	3
Q2A5H0	*rplC*	*FTL_0236*	50S ribosomal protein L3*	3
Q2A2S5		*FTL_1306*	Putative uncharacterized protein*	3
Q2A5E5	*rpoA1*	*FTL_0261*	DNA-directed RNA polymerase α_1 subunit*	3
Q2A198		*FTL_0265*	Glycosyltransferase containing DXD motif*	3
Q2A4H7	*rpoA2*	*FTL_0616*	DNA-directed RNA polymerase α_2 subunit*	3
Q2A1I0	*atpA*	*FTL_1797*	ATP synthase α subunit*	3
Q2A4R4	*minD*	*FTL_0519*	Septum site-determining protein MinD*	2
Q2A370		*FTL_1146*	Glyceraldehyde-3-phosphate dehydrogenase*	2
Q2A3K7	*mdh*	*FTL_0987*	Malate dehydrogenase*	2
Q2A253	*sucC*	*FTL_1553*	Succinyl-CoA ligase β subunit*	2
Q2A5I1	*tsf*	*FTL_0225*	Elongation factor Ts*	2
Q2A3U2	*tig*	*FTL_0891*	Trigger factor*	2
Q2A1J4	*sucB*	*FTL_1783*	Oxoglutarate dehydrogenase E2 component*	2
Q0BNJ4	*tolB*	*FTL_0334*	Protein TolB*	2
Q2A368	*pyk*	*FTL_1148*	Pyruvate kinase*	2
1*B*. VWA1-TAP. Dieppedale *et al*.				
P94798	*groEL*	*FTL_1714*	60 kDa chaperonin**	43
Q2A1J4	*sucB*	*FTL_1783*	Oxoglutarate dehydrogenase E2 component*	14
Q2A328	*dnaK*	*FTL_1191*	Chaperone protein DnaK**	8
Q2A5E0	*htpG*	*FTL_0267*	Chaperone protein HtpG*	4
Q2A5K5	*vwa1*	*FTL_0201*	Hypothetical protein	3
Q2A1M0	*tuf*	*FTL_1751*	Elongation factor Tu*	3
Q2A5K1	*tpr1*	*FTL_0205*	Tetratrico peptide repeat*	2
Q2A368	*pyk*	*FTL_1148*	Pyruvate kinase	2
1*C*. TPR1-TAP. Dieppedale *et al*.				
Q2A328	*dnaK*	*FTL_1191*	Chaperone protein DnaK*	55
Q2A5E0	*htpG*	*FTL_0267*	Chaperone protein HtpG*	34
P94798	*groEL*	*FTL_1714*	60 kDa chaperonin*	21
Q2A5A0	***aceE***	***FTL_0309***	**Pyruvate dehydrogenase E1 component**	**21**
Q2A5K1	*tpr1*	*FTL_0205*	Tetratrico peptide repeat*	19
Q2A4Q0	*gyrA*	*FTL_0533*	DNA gyrase, subunit A	17
Q2A5V6	*clpB*	*FTL_0094*	AAA superfamily ATPase ClpB	15
Q2A1M4	*rplA*	*FTL_1747*	50S ribosomal protein L1*	15
Q2A5I2	*rpsB*	*FTL_0224*	30S ribosomal protein S2*	15
Q2A1G8	*infB*	*FTL_1809*	Translation initiation factor IF-2*	14
Q2A1J3	***sucA***	***FTL_1784***	**Oxoglutarate dehydrogenase E1 component**	**14**
Q2A432		*FTL_0785*	GTP-binding protein	13
Q2A2S2	*accD*	*FTL_1309*	Acetyl-CoA carboxylase β subunit*	12
Q2A5B4	*accA*	*FTL_0295*	Acetyl-coA carboxylase α subunit	12
Q2A3T9	*lon*	*FTL_0894*	ATP-dependent protease La	12
Q2A1M8	*rpoC*	*FTL_1743*	DNA-directed RNA polymerase β subunit*	12
Q2A1K3	*acnA*	*FTL_1772*	Aconitate hydratase	11

TABLE I—*continued*

Accession UniProtKB	Gene name	FTL number	Protein description	Unique peptides
Q2A5G4	*rpsC*	*FTL_0242*	30S ribosomal protein S3*	11
Q2A360	*iglB*	*FTL_0112/FTL1158*	Intracellular growth locus protein B*	10
Q2A180	*rpsA*	*FTL_1912*	30S ribosomal protein S1*	9
Q2A298	*katG*	*FTL_1504*	Catalase-peroxidase*	9
Q2A2S5		*FTL_1306*	Hypothetical protein	9
Q2A5C7	*dnaJ*	*FTL_0281*	Chaperone DnaJ*	9
Q2A1J4	***sucB***	***FTL_1783***	**Oxoglutarate dehydrogenase E2 component***	**9**
Q2A632	*ompH*	*FTL_0009*	Outer membrane protein*	9
Q2A5E6	*rpsD*	*FTL_0260*	30S ribosomal protein S4*	9
Q2A3U2	*tig*	*FTL_0891*	Trigger factor*	9
Q2A2Z4		*FTL_1225*	Lipoprotein, putative*	8
Q2A598	***lpd***	***FTL_0311***	**Dihydrolipoyl dehydrogenase***	**8**
Q2A5J9	*pcp*	*FTL_0207*	Pyrrolidone-carboxylate peptidase*	8
Q2A5L9	*pheC*	*FTL_0187*	Cyclohexadienyl dehydratase*	8
Q2A3H1	*rluB*	*FTL_1030*	Pseudouridine synthase	7
Q2A427	*era*	*FTL_0790*	GTP-binding protein Era	6
Q2A4W8	*parC*	*FTL_0462*	DNA topoisomerase IV, α subunit	6
Q2A1U2		*FTL_1678*	Hypothetical protein	6
Q2A1M0	*tuf*	*FTL_1751*	Elongation factor Tu*	6
Q2A383	*suhB*	*FTL_1132*	Inositol-1-monophosphatase*	5
Q2A2M7	*iclR*	*FTL_1364*	Transcriptional regulator, IclR family*	5
Q9ZAW3	*ftsZ*	*FTL_1907*	Cell division protein FtsZ*	5
Q2A599	***aceF***	***FTL_0310***	**Pyruvate dehydrogenase E2 component***	**5**
Q2A1I0	*atpA*	*FTL_1797*	F0F1 ATP synthase α subunit*	5
Q2A2J1	*infC*	*FTL_1406*	Translation initiation factor IF-3	5
Q2A2H7		*FTL_1420*	Carbohydrate/purine kinase PkfB family	5
Q2A5F5	*rplF*	*FTL_0251*	50S ribosomal protein L6	5
Q2A193	*glnA*	*FTL_1899*	Glutamine synthetase*	4
Q2A4K8	*fadB/acbP*	*FTL_0584*	Hydroxacyl-CoA dehydrogenase/acyl-CoA-binding protein	4
Q2A377	*fabG*	*FTL_1139*	3-oxoacyl-(Acyl-carrier) reductase*	4
Q2A2C4		*FTL_1477*	Thiamine pyrophosphokinase	4
Q2A263	*mutM*	*FTL_1543*	Formamidopyrimidine-DNA glycosylase	4
Q2A2T8		*FTL_1293*	Hypothetical protein	4
Q2A502	*parB*	*FTL_0428*	Chromosome partition protein B	4
Q2A5X6	*lepA*	*FTL_0071*	GTP-binding protein LepA	4
Q2A269	*pnp*	*FTL_1537*	Polynucleotide phosphorylase/polyadenylase*	4
Q2A3I6		*FTL_1015*	AhpC/TSA family protein- Peroxiredoxin*	4
Q2A4M0		*FTL_0572*	Hypothetical protein*	4
Q2A1M7	*rpoB*	*FTL_1744*	DNA-directed RNA polymerase β subunit	4
Q2A2E3	*secA*	*FTL_1458*	Protein translocase subunit SecA	4
Q2A303		*FTL_1216*	Hypothetical protein	4
Q2A5S1	*ppdK*	*FTL_0132*	Pyruvate phosphate dikinase	3
Q2A259	*gyrB*	*FTL_1547*	DNA gyrase β subunit	3
Q2A2K5	*deaD*	*FTL_1392*	cold-shock DEAD-box protein A	3
Q2A3E5	*dacD*	*FTL_1060*	D-alanyl-D-alanine carboxypeptidase*	3
Q2A358	*iglD*	*FTL_0114/FTL_1160*	Intracellular growth locus protein D	3
Q2A346	*pdpA*	*FTL_0162/FTL_1172*	Pathogenicity deteminant protein PdpA	3
Q2A1F6	*nuoG*	*FTL_1824*	NADH dehydrogenase subunit G	3
Q2A4R4	*minD*	*FTL_0519*	Septum site-determining protein MinD	3
Q2A3U7	*phoH*	*FTL_0885*	PhoH-like protein	3
Q2A356	*pdpC*	*FTL_0116/FTL_1162*	Pathogenicity determinant protein PdpC	3
Q2A4B2	*araC*	*FTL_0689*	Transcriptional regulator AraC family	3
Q2A5H2	*fusA*	*FTL_0234*	Elongation factor G	3
Q2A329	*grpE*	*FTL_1190*	Heat shock protein GrpE*	3
Q2A374	*plsX*	*FTL_1142*	Glycerol-3-phosphate acyltransferase PlsX*	3
Q2A5P0	*usp*	*FTL_0166*	Universal stress protein*	3
Q2A415	*putA*	*FTL_0805*	Bifunctional proline dehydrogenase	3
Q2A580	*tolB*	*FTL_0334*	Protein TolB	3
Q2A639	*dnaN*	*FTL_0002*	DNA polymerase III β subunit	2
Q2A211	*hemB*	*FTL_1602*	Delta-aminolevulinic acid dehydratase	2

TABLE I—*continued*

Accession UniProtKB	Gene name	FTL number	Protein description	Unique peptides
Q2A264		*FTL_1542*	AMP-binding protein	2
Q2A2Q8	*fopA*	*FTL_1328*	OmpA family protein*	2
Q2A2U7	*gshB*	*FTL_1284*	Glutathione synthetase	2
Q2A3R1	*elbB*	*FTL_0928*	Isoprenoid biosynthesis protein	2
Q2A3Z9	*cphA*	*FTL_0831*	Cyanophycin synthetase	2
Q2A2F5	*fabL*	*FTL_1442*	Enoyl-[acyl-carrier-protein] reductase	2
Q2A368	*pyk*	*FTL_1148*	Pyruvate kinase*	2
-		*FTL_0629*	Pseudogene	2
Q2A4K6	*fadD*	*FTL_0586*	Long chain fatty acid CoA ligase	2
Q2A1B9	*pcm*	*FTL_1866*	L-isoaspartate O-methyltransferase*	2
Q2A4N4		*FTL_0552*	Two-component response regulator	2
Q2A378	*acpP*	*FTL_1138*	Acyl carrier protein	2
Q2A2H1		*FTL_1426*	Hypothetical protein	2
Q2A5X9	*gmhA*	*FTL_0068*	Phosphoheptose isomerase	2
Q2A484	*rne*	*FTL_0717*	Ribonuclease E	2
Q2A4B1	*fadD1*	*FTL_0690*	Long chain fatty acid CoA ligase	2
Q2A359	*iglC*	*FTL_0113/FTL_1159*	Intracellular growth locus protein C	2
Q2A3S7	*ysxC*	*FTL_0906*	Ribosome biogenesis protein YsxC	2
Q2A4C7	*panC*	*FTL_0673*	Pantoate-b-alanine ligase	2
Q2A4P4	*lpxA*	*FTL_0539*	UDP-N-acetylglucosamine acyltransferase	2
Q2A503	*parA*	*FTL_0427*	Chmomosome partition protein A	2
P18149	*lpnA*	*FTL_0421*	Lipoprotein*	2
Q2A265	*mraW*	*FTL_1541*	S-adenosyl-methyltransferase MraW	2

TABLE II
BACTH. Dieppedale et al.

pKT25	MoxR (C-ter)	TPR1 (C-ter)	TPR1 (N-ter)
pUT18			
-	-	-	-
FTL_1783 (C-ter)	++	+	+
FTL_0309 (C-ter)	nt	-	+
FTL_0310 (C-ter)	nt	-	+
FTL_0311 (C-ter)	nt	±	±
FTL_0295 (C-ter)	nt	+	++

of cAMP, was monitored by the hydrolysis of the lactose analog X-Gal on LB- X-Gal plates. As summarized in Table II, MoxR-CyaA-T25 and FTL_1783-CyaA-T18 recombinant proteins interacted together to produce cAMP. The TPR1-CyaA-T25 N-terminal fusion interacted with all the protein partners tested whereas the CyaA-T25-TPR1 C-terminal fusion interacted only with 3/5 of them. Altogether, this assay confirmed the interactions of MoxR with the E2 subunit of the OGDH complex; and of TPR1 with the OGDH E2 subunit, the PDH complex as well as with the ACC α subunit.

Construction and Characterization of a Δtpr1 Chromosomal Deletion—To further characterize the role of the protein TPR1 in *Francisella* pathogenesis, we constructed a clean chromosomal deletion of gene *tpr1* by allelic replacement, and a complemented strain by introducing a plasmid-born wild-type *tpr1* allele in LVSΔ*tpr1*. Expression of gene *tpr1* was monitored by quantitative reverse transcription PCR (qRT-PCR) in these strains. As expected, expression of *tpr1* was abolished in the deletion strain and introduction of a plasmid-born wild-type *tpr1* allele led to high level expression of the *tpr1* gene (supplemental Fig. S2). We also monitored expression of the gene *FTL_0206* lying immediately downstream of *tpr1* (Fig. 1), in these strains. An ~2-fold reduction in *FTL_0206* gene expression was recorded in the Δ*tpr1* mutant background (supplemental Fig. S2), reflecting a polar effect of the clean deletion. Reduced expression of *FTL_0206* was still observed in the *tpr1*-complemented strain. We therefore constructed a new complemented strain by introducing in the Δ*tpr1* mutant a plasmid expressing both *tpr1* and *FTL_0206* genes. In this new complemented strain, expression of both genes *tpr1* and *FTL_0206* was fully restored (supplemental Fig. S2). The characteristics of the wild-type, Δ*tpr1* mutant and complemented strains were followed in different stress conditions as well as in human macrophages and *in vivo*.

Sensitivity to Oxidative, pH and Other Stresses—Upon *Francisella* entry into cells, the phagosomal compartment transiently acidifies and the activation of NADPH oxidase leads to the production of noxious oxygen reactive species (23, 24). Thus, we first tested the survival of parental LVS, LVSΔ*tpr1* mutant and complemented strains, under oxidative stress conditions.

For this, bacteria were exposed to 0.03% H_2O_2 (~10 mM) (Fig. 3). The Δ*tpr1* deletion mutant strain (LVSΔ*tpr1*/p6*gro*) appeared to be extremely sensitive to oxidative stress as compared with the wild-type strain (LVS/p6*gro*) Indeed, it showed a 25-fold decrease in the number of viable bacteria already after 10 min, and an ~50,000-fold decrease after 30 min of exposure to H_2O_2. Remarkably, the two complemented

strains, harboring either a plasmid-born copy of gene *tpr1* alone (plasmid p6*gro-tpr1*) or of genes *tpr1* and *FTL_0206* (p6*gro-tpr1* or p6*gro-tpr1-FTL_0206*) showed wild-type bacterial viability (Fig. 3). This assay confirmed that protein TPR1 specifically contributes to the adaptation of *F. tularensis* to oxidative stress. Notably, we also evaluated the capacity of the protein TPR1-TAP to complement the Δ*tpr1* deletion mutant. This strain (LVSΔ*tpr1*/p6*gro-tpr1-TAP*) showed resistance to oxidative stress similar to LVS and complemented strains, indicating a normal activity of the TPR1-TAP protein despite the presence of the C-terminal tag.

We next evaluated the ability of the LVSΔ*tpr1* mutant to endure acid stress, by incubating the LVS, LVSΔ*tpr1* and of the complemented strain (LVSΔ*tpr1*/p6*gro-tpr1-FTL_0206*), in normal growth media adjusted to pH 4.0 (supplemental Fig. S3*A*). Both LVS and LVSΔ*tpr1* were sensitive to low pH, but the LVSΔ*tpr1* mutant strain showed a 2,300-fold increase of mortality after 4 h. The complemented strain exhibited viability at the same level as the wild-type parent.

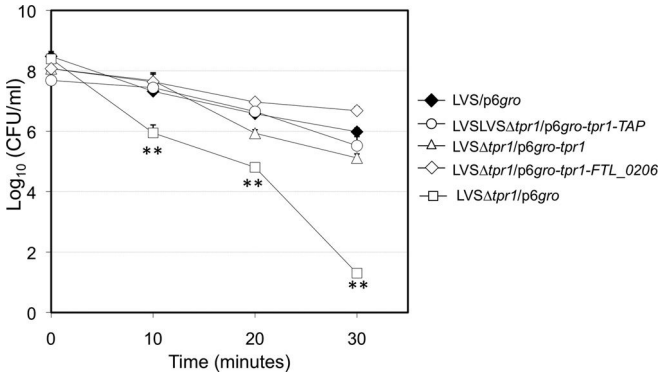

FIG. 3. **Sensitivity to oxidative stress of LVS, LVSΔ*tpr1* and complemented strains.** Exponential-phase bacteria were diluted to a final concentration of 10^8 bacteria/ml in fresh Schaedler-K3 broth and subjected to oxidative stresses (10 mM H_2O_2). The bacteria were plated on chocolate agar plates at different times, and viable bacteria were monitored 3 days after. Data are the average CFU/ml for three independent experiments for each condition. Results are shown as the averages of $\log_{10}$ (CFU/ml) ± standard deviations. ** $p < 0.01$ (as determined by Student's *t* test).

We also evaluated the impact of the Δ*tpr1* deletion on bacteria subjected to heat, ethanol and SDS stresses. When subjected to high temperature (50 °C) (supplemental Fig. S3*B*), the number of viable bacteria of the LVSΔ*tpr1* mutant was 14-fold lower than that of the wild type strain after 1 h. In media containing 0.05% SDS (supplemental Fig. S3*C*), the number of mutant bacteria was 350-fold lower than of LVS bacteria after 4 h and the mutant resisted 15-fold less than LVS after 2 h and in media containing a high concentration of ethanol (10%) (supplemental Fig. S3*D*). In all four assays, the complemented strain (LVSΔ*tpr1*/p6*gro-tpr1-FTL_0206*) exhibited viability at the same level as the wild-type parent.

Thus, the Δ*tpr1* mutant appeared to be more sensitive than the wild-type strain to all the stresses tested, a characteristic resembling that previously observed with the Δ*moxR* mutant (6). Remarkably, the Δ*moxR* and Δ*tpr1* mutants were both more sensitive to oxidative stress than to any other stress. Altogether, these data indicate that the proteins MoxR and TPR1 contribute to the adaptation of *F. tularensis* to a variety of stressful conditions and are particularly important for oxidative stress defense.

Intracellular Survival and Multiplication—We then examined the ability of the wild-type, Δ*tpr1* mutant, and complemented strains, to multiply in human macrophages (THP-1 cell line) over a 48-h period. The Δ*tpr1* mutant (LVSΔ*tpr1*/p6*gro*) showed an ~10-fold reduction of intracellular bacteria after 24 h and 48 h, as compared with the parental strain (LVS/p6*gro*) (Fig. 4*A*). Introduction of the complementing plasmid p6*gro-tpr1* restored partially bacterial multiplication in THP-1 cells. Indeed, after 24 h and 48 h of infection, multiplication of the complemented strain was improved as

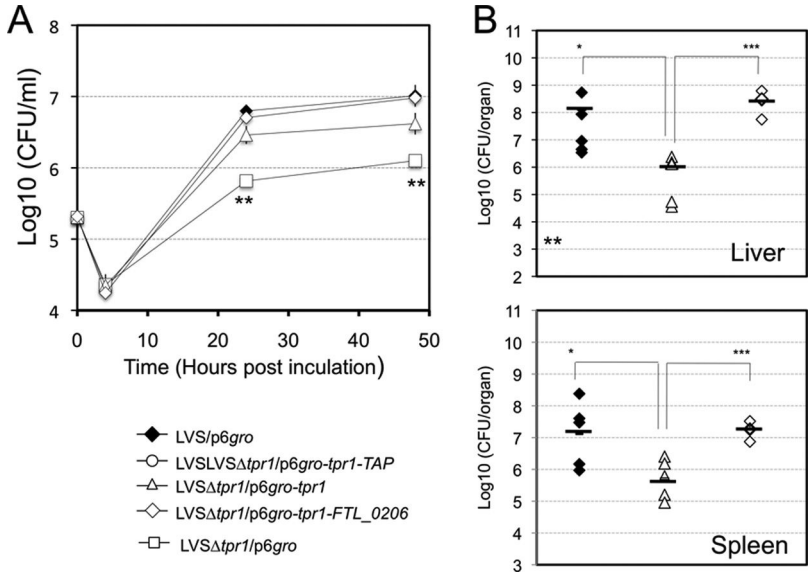

FIG. 4. **In vitro and vivo properties of LVSΔ*tpr1*.** *A*, Intracellular replication of LVS, LVSΔ*tpr1*and the complemented strains was monitored over a 48 h period in THP-1 human macrophages. Results are shown as the averages of $\log_{10}$ (CFU/ml) ± standard deviations. ** $p < 0.01$ (as determined by Student's *t* test). *B*, Bacterial burden in spleen and livers of mice infected with 250 CFU of wild-type LVS (LVS/p6*gro*, black diamonds), Δ*tpr1* mutant (LVSΔ*tpr1*/p6*gro*, open triangles) or complemented strain (LVSΔ*tpr1*/p6*gro-tpr1-FTL_0206*, open diamonds). Results are shown as $\log_{10}$ CFU per organ ± standard deviations. Liver and spleen data at day 4, for LVS and LVSΔ*tpr1* infections, represent five mice. *$p < 0.05$; ** $p < 0.01$; *** $p < 0.001$ (as determined by Student's *t* test).

compared with the deletion strain (~fivefold higher) but was still lower than that of the parental strain. The complemented strain expressing both *tpr1* and *FTL_0206* genes (LVSΔ*tpr1*/ p6*gro-tpr1-FTL0206*) showed wild-type intracellular survival and multiplication in macrophages (Fig. 4*A*), indicating that both *tpr1*and *FTL_0206* genes contribute to LVS intracellular multiplication.

In Vivo Properties—We examined the virulence of wild-type LVS (LVS/p6*gro*), Δ*tpr1* mutant (LVSΔ*tpr1*/p6*gro*) and complemented strain (LVSΔ*tpr1*/p6*gro-tpr1-FTL_0206*), in mice, by following the kinetics of bacterial multiplication in the target organs (spleen and liver) of infected animals (Fig. 4*B*). Groups of five BALB/c mice were infected with 250 bacteria by the intra-peritoneal route and mice were sacrificed at day 4 after the inoculation. At day 4, multiplication in the Δ*tpr1*mutant strain significant decreased as compared with the wild-type strain in both organs (25-fold and 63-fold, in the spleen and in the liver, respectively). Remarkably, complementation with plasmid p6*gro-tpr1-FTL_0206* restored full virulence. Indeed, similar counts were recorded in the spleens of animals infected with the wild-type and complemented strains ($\log_{10}$6.2 *versus* $\log_{10}$6.38, respectively). The counts recorded in the livers were even 10-fold higher with the complemented strain than with the wild-type strain (Fig. 4*B*). These results thus confirm our earlier preliminary observations (6) on the participation of genes *tpr1* and *FTL_0206* in *F. tularensis* virulence.

MoxR and TPR1 Modulate OGDH and PDH Enzymatic Activities—As mentioned above, all the subunits of the 2-oxoglutarate dehydrogenase (OGDH) and pyruvate dehydrogenase (PDH) complexes interacted with TPR1-TAP. The TPR-bearing motif protein also interacted with the two subunits of Acetyl-CoA carboxylase (ACC). This observation led us to test the impact of *moxR* or *tpr1* inactivation on the activity of these three enzymatic complexes. The OGDH complex is a key enzyme in the TCA cycle which catalyzes the conversion of 2-oxoglutarate to succinyl-CoA, NADH and CO_2 (25). The PDH complex, an enzyme linking the glycolysis pathway and the TCA cycle, catalyzes the conversion of pyruvate in acetyl-CoA, NADH and CO_2 (25, 26). Acetyl-CoA carboxylase (ACC) is a biotin-dependent multi-subunit enzyme (19) that catalyzes the irreversible carboxylation of acetyl-CoA to produce malonyl-CoA. This irreversible reaction is involved in fatty acid synthesis.

OGDH activity was assayed on bacterial lysates by measuring the reduction of NAD^+ at 340 nm in the presence of 16 mM oxoglutarate. PDH activity was assayed in the same conditions in the presence of 16 mM pyruvate. ACC activity was assayed on bacterial lysates by measuring the amount of coenzyme A formed at 412 nm, in the presence of malonyl-CoA (see Experimental procedures).

The protein TPR1 also interacted with the catalase KatG, responsible for the detoxification of bactericidal compounds such as H_2O_2. The fact that KatG has been shown previously to participate to *F. tularensis* oxidative stress response ((4) and references therein), prompted us to monitor the catalase enzymatic activity in wild-type, Δ*tpr1* and complemented strains. Catalase activity was assayed on bacterial lysates by measuring the conversion of H_2O_2 into H_20 and O_2, using the Amplite™ Fluorimetric Catalase Assay Kit (see Experimental procedures).

As shown in Fig. 5, PDH and OGDH activities dropped down to 30% of the wild-type activity in the lysate from the LVSΔ*moxR* mutant strain. Both enzymatic activities were also significantly reduced in the lysate from LVSΔ*tpr1* (18 and 29% reduction of activity for PDH and OGDH, respectively). We monitored expression of genes *FTL_0309* and *FTL_1784* (encoding PDH- and OGDH- E1 subunits, respectively) by qRT-PCR, in LVS and in the LVSΔ*tpr1*, strains (supplemental Fig. S4). Transcription of these two genes was unaffected in the Δ*tpr1* mutant, strongly suggesting that the decrease in PDH and OGDH activities in this strain was not due to reduced protein expression.

KatG activity was also moderately but significantly reduced in the Δ*tpr1* mutant strain (17% reduction of activity) and wild-type activity was fully restored in the complemented strain (Fig. 5*F*). The background activity recorded in the Δ*tpr1* strain is likely to be due to the remaining H_2O_2 detoxifying activity of glutathione peroxidase and alkyl-hydroperoxide reductase. This assay confirmed, thus, the functional relevance of the interaction between the proteins TPR1 and KatG. Of note, inactivation of *katG*, in both *F. tularensis* subsp. *tularensis* strain SCHU S4 or *F. tularensis* subsp. *holarctica* strain LVS, resulted in enhanced susceptibility to H_2O_2 *in vitro*. The oxidative stress defect of the LVSΔ*tpr1* mutant (see above) might thus be accounted by, at least in part, to an effect on this protein.

In contrast, ACC activity was not significantly affected in any of the two mutants as compared with LVS. Hence, the interaction of TPR1 with this enzyme is not critical for its activity, at least in the conditions tested.

DISCUSSION

Using *in vivo* tandem affinity purification, combined with high-resolution mass spectrometry, we identified the interactomes of MoxR, VWA1 and TPR1, three proteins encoded by the *moxR* locus of *F. tularensis* LVS. The interacting proteins belonged to various functional categories, notably including key metabolic enzymes such as PDH and OGDH. We show here that inactivation of *tpr1* impairs bacterial virulence and affects bacterial stress defense. Remarkably, in both *moxR* and *tpr1* mutants, the activities of PDH and OGDH were altered, suggesting a possible link between stress defense and the tricarboxylic acid cycle in *F. tularensis* virulence.

The Interactomes Show Partial Overlap—We successfully identified some interactions between *moxR*-encoded proteins (VWA1 with TPR1, and TPR1 with FTL_0207). However, we did not identify the reciprocal interactions (*e.g.* VWA1 was not identified in the TPR1-TAP interactome), possibly due to hin-

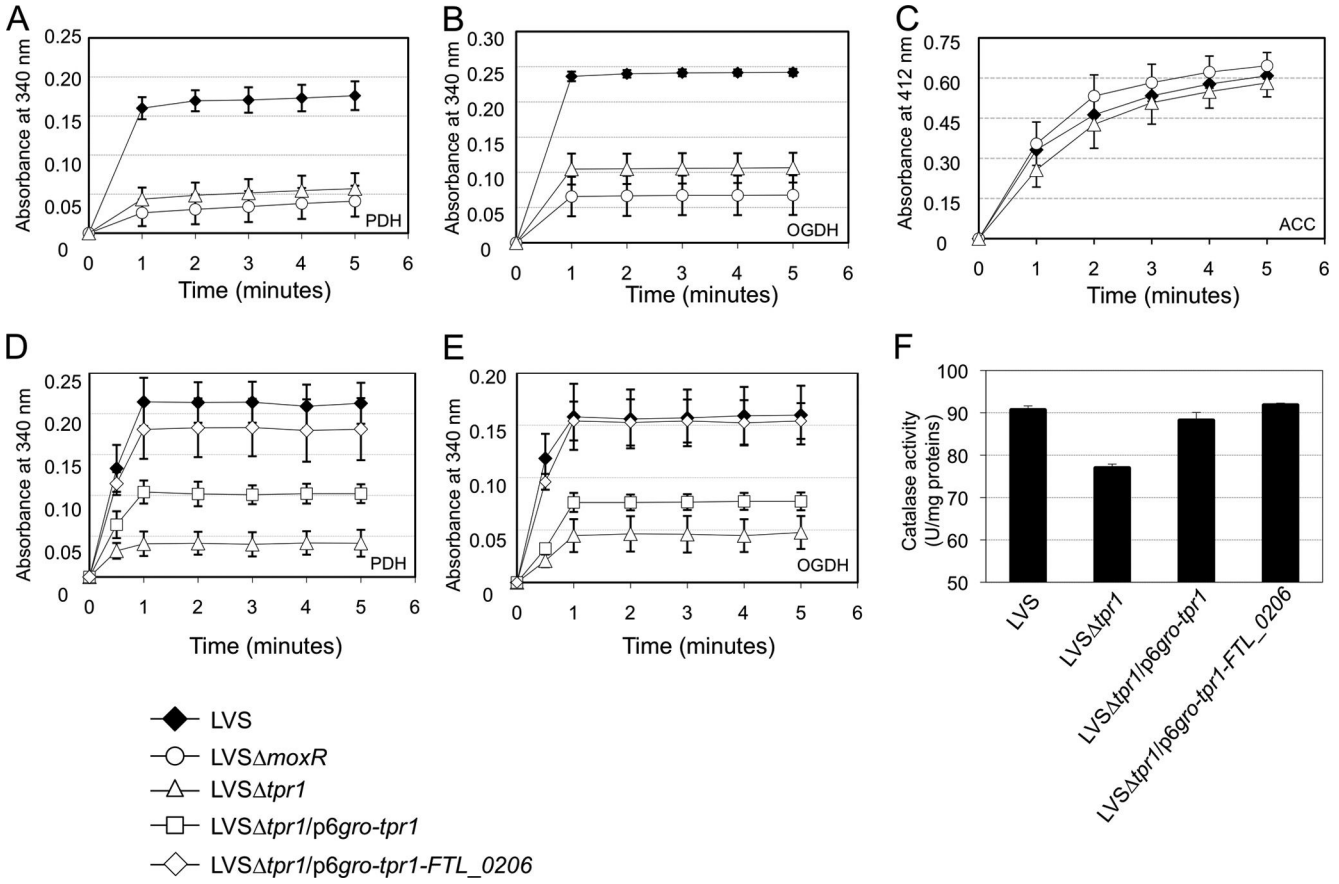

FIG. 5. **Enzymatic assays.** The assays were performed on total protein lysates. Panels *A*, *B*, *C*, compared the activities in wild-type LVS to those in Δ*moxR* and Δ*tpr1* mutant strains. Panels *D*, *E*, *F*, compared the activities in wild-type LVS to those in Δ*tpr1* and complemented strains (*LVS*Δ*tpr1*/p6*gro-tpr1* and *LVS*Δ*tpr1*/p6*gro-tpr1-FTL_0206*). (*A*, *D*) Pyruvate dehydrogenase assays were realized at 340 nm, over a reaction time of 10 min. (*B*, *E*) Oxoglutarate dehydrogenase assays were realized at 340 nm, over a reaction time of 5 min. (*C*) Acetyl-CoA carboxylase assay was realized at 412 nm over a reaction time of 5 min. Values were collected every minute. Each assay was performed on three independent protein lysates and each experiment was repeated twice. The average of absorbance ± standard deviations, recorded for the wild-type LVS and mutant strains at the end of the reaction were significantly different (PDH, $p < 0.05$; OGDH, $p < 0.01$, as determined by Student's *t* test). Ordinate, variation of absorbance. Abcissa, time (in min) of the reaction. *F*, Catalase activity assay was realized at 576 nm, using the Amplite™ Fluorimetric Catalase Assay Kit. The assay was performed according to manufacturer's recommendation. Each assay was performed on three independent protein lysates and each experiment was repeated twice. The average of catalase activity (in unit/mg of total proteins) ± standard deviations, recorded for the wild-type LVS and mutant strains at the end of the reaction were significantly different ($p < 0.01$, as determined by Student's *t* test). Ordinate, catalase activity.

drance caused by the presence of the C-terminal Tag. Further biochemical and structural studies will be required to characterize the nature of the oligomeric structures comprising these proteins.

In addition, to the *moxR*-encoded proteins, the three interactomes comprised a subset of common proteins. Remarkably, most of the proteins interacting with MoxR-TAP also interacted with either one or both of the two other TAP-tagged proteins. For example, two-third of the proteins interacting with MoxR-TAP (19/31) also interacted with TPR1-TAP. These included: 1) the general chaperones GroEL and DnaK; 2) trigger factor (Tig) and EF-Tu, involved in polypeptide chain elongation; 3) FtsZ and MinD, involved in cell division; 4) the pyruvate kinase (Pyk) and the OGDH E2 component, involved in metabolism; and v) the *Francisella* pathogenicity island proteins IglB and IglD. Similarly, all the proteins interacting with VWA1-TAP also interacted with proteins from the two other TAP-tagged interactomes. The proteins GroEL and DnaK constituted the most abundant peptides in most interactomes. It cannot be excluded that they correspond to non-specific protein–protein interactions because these two proteins are highly abundant in *F. tularensis* (27, 28).

The protein TPR1-TAP interacted with numerous proteins, including several enzymes or enzymatic complexes that were not detected in the other two interactomes.

In particular, if one considers as relevant interacting partners only the proteins identified with at least 10 peptides (Fig. 6), TPR1 appears to interact with: the PDH E1, and E2 subunits (AceE, AceF), the OGDH E1 and E2 subunits (SucA, SucB), their common E3 subunit (Lpd), the two subunits of

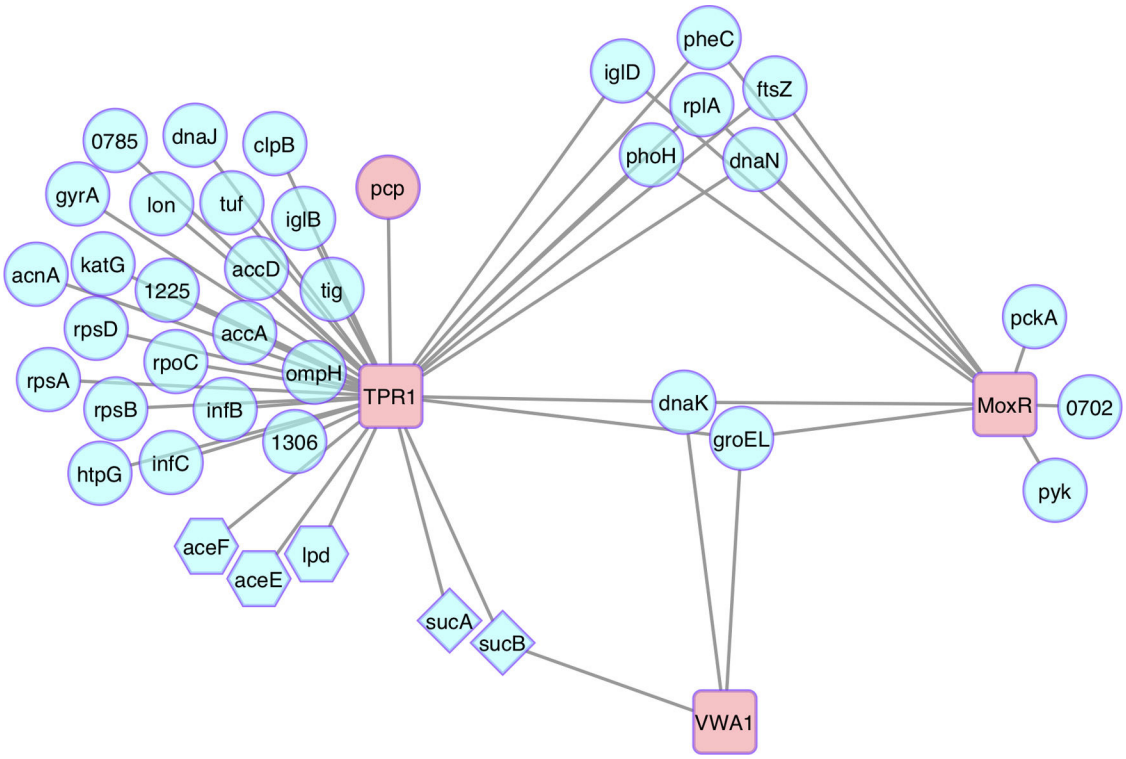

FIG. 6. **The MoxR-TAP, VWA1-TAP and TPR1-TAP interactomes.** MoxR-TAP, VWA1-TAP, and TPR1-TAP proteins were used as baits and are represented within red squares In contrast, for the proteins identified with a unique bait, only the most abundant proteins are represented (identified with ≥ 10 total peptides). SucA and SucB (OGDH subunits) are in diamond shape. AceE, AceF and LpD (PHD subunits) are in hexagon shape. Pcp, encoded by the distal part of the *moxR* locus, is in red. This graphical representation was generated by using the Cytoscape software (freely available at http://www. cytoscape.org).

acetyl-CoA carboxylase (AccA, AccD), and KatG. Among these only the OGDH E2 subunit (SucB) belonged to another interactome (VWA1). This may reflect peculiar biochemical and/or structural properties of TPR1, favoring protein–protein interactions. The contribution of the other *moxR*-encoded proteins to these other enzymatic activities, if needed, might not require direct binding. Using the same threshold of 10 peptides, the TPR1 interactome shares eight proteins with the MoxR interactome and only three proteins with the VWA1 interactome (Fig. 6). The chaperones DnaK and GroEL are the only two proteins identified in the three interactomes.

Stress Response, the TCA Cycle and Virulence—Inactivation of either *moxR* or *tpr1* impaired bacterial stress defenses and also significantly altered PDH and OGDH activities. OGDH is an enzymatic complex composed of multiple copies of three different subunits: the 2-oxoglutarate dehydrogenase (E1, FTL_1784), the dihydrolipoamide succinyltransferase (E2, FTL_1783), and the lipoamide dehydrogenase (lpd or E3, FTL_0311) that is shared with pyruvate dehydrogenase (supplemental Fig. S4). The OGDH complex, which constitutes the primary site of control of the metabolic flux through the TCA cycle, has been also shown to be involved in the protection of the bacterium against reactive nitrogen intermediates and oxidative stress generated by the host immune system (see for a review (29)). The PDH enzymatic complex is composed of three components: the pyruvate dehydrogenase (E1 component, FTL_0309), the dihydrolipoamide transacetylase (E2 component, FTL_0310) and the dihydrolipoamide dehydrogenase (E3 component, FTL_0311). In both complexes the E2 component forms a multimeric core, which binds the peripheral E1 and E3 subunits. The substrate is decarboxylated by the E1 component dependant of thiamine pyrophosphate. Then, it is oxidized and transiently acetylated by E2 component.

In *F. tularensis*, the genes encoding the E1 and E2 subunits of OGDH complex are predicted to be essential genes (30) which probably accounts for the fact that they have not been identified in earlier *in vitro* and *in vivo* genetic screens as potential virulence factors. In contrast, the genes encoding the E1 and E2 subunits of PDH, as well as that encoding the shared E3 subunit are not essential. Indeed, the gene *aceE*, encoding PDH E1 subunit in *F. novicida* (*FTN_1494*), was identified in a recent screen as important for intracellular survival (31). Inactivation of the *lpd* gene (encoding the E3 subunit) was also found to affect the virulence of *F. tularensis* LVS (32). Interestingly, in *Mycobacterium tuberculosis*, the Lpd protein is part of an antioxidant defense system in addition to its role in intermediary metabolism (33). Hence, it is also possible that Lpd participates in defense against oxidative stress in *F. tularensis*. Of note, in *S. typhimurium*, a

Δ*sucAB* mutant (lacking OGDH E1 and E2, and thus unable to make succinyl-CoA) was shown to be avirulent in the mouse model (34). Interestingly, Richardson *et al.* recently showed that *S. typhimurium* became auxotroph for methionine and lysine under nitrosative stress, because of reduced succinyl-CoA availability (35).

Our work suggested possible connections between stress response and metabolism in pathogenic *F. tularensis*. The proteins MoxR, VWA1, TPR1, and possibly other *moxR*-encoded proteins, might assist multiple enzymatic activities, including the tricarboxylic acid cycle-related PDH and OGDH. Further work will be required to make precise the molecular mechanisms involved in these interactions and their importance for intracellular survival and multiplication of the bacterium. More generally, the fact that similar *moxR*-like loci exists in several other intracellular bacteria, such as for example *Legionella* species, suggest functions carried by *moxR*-encoded proteins might be shared by other pathogenic organisms.

Acknowledgments—We thank Monique Barel for careful reading of the manuscript. We thank all the personnel of the 3P5 Proteomics facility, University Paris Descartes, Sorbonne Paris Cité.

* This study was supported by INSERM, CNRS, and Université Paris Descartes Paris V. Jennifer Dieppedale and Gael Gesbert were funded by a fellowship from the Délégation Générale à l'Armement (DGA) and Elodie Ramond by a fellowship from the "Région Ile de France."

S This article contains supplemental material.

** The authors contributed equally to this work.

‖ To whom correspondence should be addressed: Bâtiment Leriche. 96 rue Didot 75993 Paris Cedex 14 France. Tel.: 0033-1-72606511; E-mail: alain.charbit@inserm.fr.

REFERENCES

1. Bossi, P., Tegnell, A., Baka, A., Van Loock, F., Hendriks, J., Werner, A., Maidhof, H., and Gouvras, G. (2004) Bichat guidelines for the clinical management of tularaemia and bioterrorism-related tularaemia. *Euro. Surveill.* **9**, E9–E10
2. McLendon,, M. K., Apicella, M. A., and Allen, L. A. (2006) *Francisella tularensis*: taxonomy, genetics, and Immunopathogenesis of a potential agent of biowarfare. *Annu. Rev. Microbiol.* **60,** 167–185
3. Keim, P., Johansson, A., and Wagner, D. M. (2007) Molecular epidemiolgy, evolution, and ecology of Francisella. *Ann. N. Y. Acad. Sci.* **1105,** 30–66
4. Sjostedt, A., (Ed.) (2011) *Francisella tularensis* and tularemia. *Fontiers Media* SA
5. Oyston, P. C. (2008) *Francisella tularensis*: unravelling the secrets of an intracellular pathogen. *J. Med. Microbiol.* **57,** 921–930
6. Dieppedale, J., Sobral, D., Dupuis, M., Dubail, I., Klimentova, J., Stulik, J., Postic, G., Frapy, E., Meibom, K. L., Barel, M., and Charbit, A. (2011) Identification of a putative chaperone involved in stress resistance and virulence in *Francisella tularensis*. *Infect. Immun.* **79,** 1428–1439
7. Wong, K. S., and Houry, W. A. (2012) Novel structural and functional insights into the MoxR family of AAA+ ATPases. *J. Struct. Biol.* **179,** 211–221
8. Li, Y. (2011) The tandem affinity purification technology: an overview. *Biotechnol. Lett.* **33,** 1487–1499
9. Whittaker, C. A., and Hynes, R. O. (2002) Distribution and evolution of von Willebrand/integrin A domains: widely dispersed domains with roles in cell adhesion and elsewhere. *Mol. Biol. Cell* **13,** 3369–3387
10. Main, E. R., Xiong, Y., Cocco, M. J., D'Andrea, L., and Regan, L. (2003) Design of stable alpha-helical arrays from an idealized TPR motif. *Structure* **11,** 497–508
11. Cerveny, L., Straskova, A., Dankova, V., Hartlova, A., Ceckova, M., Staud, F., and Stulik, J. (2013) Tetratricopeptide repeat motifs in the world of bacterial pathogens: role in virulence mechanisms. *Infect. Immun.* **81,** 629–635
12. Golovliov, I., Sjostedt, A., Mokrievich, A., and Pavlov, V. (2003) A method for allelic replacement in *Francisella tularensis*. *FEMS Microbiol. Lett.* **222,** 273–280
13. Maier, T. M., Pechous, R., Casey, M., Zahrt, T. C., and Frank, D. W. (2006) In vivo Himar1-based transposon mutagenesis of *Francisella tularensis*. *Appl. Environ. Microbiol.* **72,** 1878–1885
14. Gully, D., and Bouveret, E. (2006) A protein network for phospholipid synthesis uncovered by a variant of the tandem affinity purification method in *Escherichia coli*. *Proteomics* **6,** 282–293
15. Stingl, K., Schauer, K., Ecobichon, C., Labigne, A., Lenormand, P., Rousselle, J. C., Namane, A., and de Reuse, H. (2008) *In vivo* interactome of *Helicobacter pylori* urease revealed by tandem affinity purification. *Mol. Cell. Proteomics* **7,** 2429–2441
16. Ladant, D., and Karimova, G. (2000) Genetic systems for analyzing protein-protein interactions in bacteria. *Res. Microbiol.* **151,** 711–720
17. Humphries, K. M., and Szweda, L. I. (1998) Selective inactivation of alpha-ketoglutarate dehydrogenase and pyruvate dehydrogenase: reaction of lipoic acid with 4-hydroxy-2-nonenal. *Biochemistry* **37,** 15835–15841
18. Hoffman, P. S., Sisson, G., Croxen, M. A., Welch, K., Harman, W. D., Cremades, N., and Morash, M. G. (2007) Antiparasitic drug nitazoxanide inhibits the pyruvate oxidoreductases of *Helicobacter pylori*, selected anaerobic bacteria and parasites, and *Campylobacter jejuni*. *Antimicrob. Agents Chemother.* **51,** 868–876
19. Santoro, N., Brtva, T., Roest, S. V., Siegel, K., and Waldrop, G. L. (2006) A high-throughput screening assay for the carboxyltransferase subunit of acetyl-CoA carboxylase. *Anal. Biochem.* **354,** 70–77
20. Sasse, J., and Gallagher, S. R. (2008) Detection of proteins on blot transfer membranes. *Curr. Protoc. Immunol.* Chapter 8: Unit 8 10B
21. Johansson, A., Goransson, I., Larsson, P., and Sjostedt, A. (2001) Extensive allelic variation among *Francisella tularensis* strains in a short-sequence tandem repeat region. *J. Clin. Microbiol.* **39,** 3140–3146
22. Wehrly, T. D., Chong, A., Virtaneva, K., Sturdevant, D. E., Child, R., Edwards, J. A., Brouwer, D., Nair, V., Fischer, E. R., Wicke, L., Curda, A. J., Kupko, J. J. 3rd, Martens, C., Crane, D. D., Bosio, C. M., Porcella, S. F., and Celli, J. (2009) Intracellular biology and virulence determinants of *Francisella tularensis* revealed by transcriptional profiling inside macrophages. *Cell Microbiol.* **11,** 1128–1150
23. Elkins, K. L, Cowley, S. C., and Bosio, C. M. (2007) Innate and adaptive immunity to *Francisella*. *Ann. N. Y. Acad. Sci.* **1105,** 284–324
24. McCaffrey, R. L., Schwartz, J. T., Lindemann, S. R., Moreland, J. G., Buchan, B. W., Jones, B. D., and Allen, L. A. (2010) Multiple mechanisms of NADPH oxidase inhibition by type A and type B *Francisella tularensis*. *J. Leukoc. Biol.* **88,** 791–805
25. Stobbe, M. D., Houten, S. M., van Kampen, A. H., Wanders, R. J., and Moerland, P. D. (2012) Improving the description of metabolic networks: the TCA cycle as example. *FASEB J.* **26,** 3625–3633
26. Song, J., and Jordan, F. (2012) Interchain acetyl transfer in the E2 component of bacterial pyruvate dehydrogenase suggests a model with different roles for each chain in a trimer of the homooligomeric component. *Biochemistry* **51,** 2795–2803
27. Ericsson, M., Tarnvik, A., Kuoppa, K., Sandstrom, G., and Sjostedt, A. (1994) Increased synthesis of DnaK, GroEL, and GroES homologs by *Francisella tularensis* LVS in response to heat and hydrogen peroxide. *Infect. Immun.* **62,** 178–183
28. Hubalek, M., Hernychova, L., Havlasova, J., Kasalova, I., Neubauerova, V., Stulik, J., Macela, A., Lundqvist, M., and Larsson, P. (2003) Towards proteome database of *Francisella tularensis*. *J. Chromatogr.* **787,** 149–177
29. Spalding, M. D., and Prigge, S. T. (2010) Lipoic acid metabolism in microbial pathogens. *Microbiol. Mol. Biol. Rev.* **74,** 200–228
30. Gallagher, L. A., Ramage, E., Jacobs, M. A., Kaul, R., Brittnacher, M., and Manoil, C. (2007) A comprehensive transposon mutant library of *Francisella novicida*, a bioweapon surrogate. *Proc. Natl. Acad. Sci. U. S. A.* **104,** 1009–1014
31. Asare, R., and Kwaik, Y. A. (2010) Molecular complexity orchestrates modulation of phagosome biogenesis and escape to the cytosol of macrophages by *Francisella tularensis*. *Environ. Microbiol.* **12,** 2559–2586

32. Meibom, K. L., Dubail, I., Dupuis, M., Barel, M., Lenco, J., Stulik,J., Golovliov, I., Sjöstedt, A., and Charbit, A. (2008) The heat-shock protein ClpB of *Francisella tularensis* is involved in stress tolerance and is required for multiplication in target organs of infected mice. *Mol. Microbiol.* **67,** 1384–1401
33. Venugopal, A., Bryk, R., Shi, S., Rhee, K., Rath, P., Schnappinger, D., Ehrt, S., and Nathan, C. (2011) Virulence of *Mycobacterium tuberculosis* depends on lipoamide dehydrogenase, a member of three multienzyme complexes. *Cell Host Microbe.* **9,** 21–31
34. Mercado-Lubo, R., Leatham, M. P., Conway, T., and Cohen, P. S. (2009) *Salmonella enterica* serovar Typhimurium mutants unable to convert malate to pyruvate and oxaloacetate are avirulent and immunogenic in BALB/c mice. *Infect. Immun.* **77,** 1397–1405
35. Richardson, A. R., Payne, E. C., Younger, N., Karlinsey, J. E., Thomas, V. C., Becker, L. A., Navarre, W. W., Castor, M. E., Libby, S. J., and Fang, F. C. (2011) Multiple targets of nitric oxide in the tricarboxylic acid cycle of *Salmonella enterica* serovar Typhimurium. *Cell Host Microbe.* **10,** 33–43

Review
Future Microbiology

Proteins involved in *Francisella tularensis* survival and replication inside macrophages

Elodie Ramond[1,2‡], Gael Gesbert[1,2‡], Monique Barel[1,2] & Alain Charbit*[1,2]

[1]Université Paris Descartes, Faculté de Médecine Necker, 156, rue de Vaugirard, 75730, Paris, Cedex 15, France

[2]INSERM U1002, Unité de Pathogénie des Infections Systémiques, Paris, France

*Author for correspondence: alain.charbit@inserm.fr

‡Authors contributed equally

Francisella tularensis, the etiological agent of tularemia, is a member of the γ-proteobacteria class of Gram-negative bacteria. This highly virulent bacterium can infect a large range of mammalian species and has been recognized as a human pathogen for a century. *F. tularensis* is able to survive *in vitro* in a variety of cell types. *In vivo*, the bacterium replicates mainly in infected macrophages, using the cytoplasmic compartment as a replicative niche. To successfully adapt to this stressful environment, *F. tularensis* must simultaneously: produce and regulate the expression of a series of dedicated virulence factors; adapt its metabolic needs to the nutritional context of the host cytosol; and control the innate immune cytosolic surveillance pathways to avoid premature cell death. We will focus here on the secretion or release of bacterial proteins in the host, as well as on the envelope proteins, involved in bacterial survival inside macrophages.

Francisella tularensis is a small Gram-negative bacterium responsible for tularemia, a zoonotic disease that includes several clinical manifestations and various levels of severity depending on the route of entry of the bacteria [1]. The most common route of infection is through the skin, leading to ulceroglandular tularemia. Inhalation of the bacteria can lead to pneumonic tularemia, which is a life-threatening disease. In the absence of antibiotic treatment or if treatment is not taken early enough, mortality during pneumonic tularemia can be as high as 30% [2]. Furthermore, *F. tularensis* is one of the most highly infectious pathogens for humans. Indeed, the lethal dose for humans is estimated to be less than ten bacteria upon inhalation. In addition, *F. tularensis* is naturally resistant to penicillin due to the expression of β-lactamase. These features have led the CDC to classify *F. tularensis* as a category A bioterrorism agent [3].

Four different subspecies of *F. tularensis* that differ in virulence and geographic distribution exist, designated *F. tularensis* subsp. *tularensis*, *F. tularensis* subsp. *holarctica*, *F. tularensis* subsp. *novicida* and *F. tularensis* subsp. *mediasiatica*. *F. tularensis* subsp. *tularensis* is the most virulent subspecies, causing severe disease in humans, whereas *F. tularensis* subsp. *holarctica* causes a disease that is similar but less severe [4]. While subsp. *mediasiatica* may cause human disease, it is rare that subsp. *novicida* does so. However, *F. tularensis* subsp. *novicida*, which is still highly virulent for mice, is often used as a surrogate model to study the molecular basis of *F. tularensis* pathogenesis [5]. *F. tularensis* is a facultative intracellular pathogen that infects a variety of cell types within the host, such as phagocytes (including neutrophils), epithelial cells and hepatocytes. Mutant strains that are unable to replicate inside phagocytic cells are generally severely attenuated for virulence, and the ability of the bacterium to enter and replicate inside macrophages is essential for the pathogenicity of *F. tularensis* [6].

F. tularensis replicates in the cytosolic compartment of infected cells. Until recently, the host cytosol was considered to be a safe and nutrient-replete haven for the few bacterial pathogens that have chosen this cellular compartment for survival and multiplication [7]. It is now clear that cytosolic bacteria have to face a highly stressful environment in which they must:

- Adapt their metabolism to the nutritional context of the host cytosol;
- Control the innate immune mechanisms, in particular the cytosolic surveillance pathways, to avoid premature cell death;
- Produce and regulate the optimal expression of dedicated virulence factors at the different steps of its infectious cycle.

The capacity of a macrophage to deprive intracellular pathogens of required nutrients [8] is now viewed as an intrinsic antimicrobial innate immune defense mechanism, often referred to

Keywords

bacterial pathogen ■ *Francisella tularensis* ■ intracellular survival ■ protein secretion systems ■ virulence

Future Medicine part of fsg

as 'nutritional immunity' (e.g., see [9]). We have recently discussed the importance of metabolism and nutrition for *F. tularensis* pathogenesis [10], and so this aspect will not be discussed here. Cytosolic surveillance systems, which exist to monitor the presence of microbial molecules within the host cytosol and mount antibacterial responses, include capturing by autophagy [11,12] and triggering cell death pathways, including apoptosis and pyroptosis. *F. tularensis* largely escapes autophagy [13], delays cytosolic innate immune responses [14] and is able to perform approximately seven to eight replication cycles in the host cytosol [15]. The mechanisms and attributes used by *F. tularensis* to avoid/manipulate host surveillance pathways have been recently reviewed elsewhere (for reviews, see [16–18]).

In this review, we aim to provide a comprehensive update of the proteins involved in *F. tularensis* replication inside macrophages. Special attention will be paid to the mechanisms involved in the secretion and/or release of proteins in the host cell.

Secreted proteins

In bacteria, secreted proteins cross the cytoplasmic membrane either via the general secretory pathway (or Sec translocon, for the secretion of unfolded proteins) or the twin arginine translocation pathway (Tat, for the secretion of folded proteins). These two pathways, dedicated to the secretion of proteins bearing typical N-terminal signal sequences [19], are present in all domains of life. In addition, bacteria possess more dedicated protein secretion systems and appendages to secrete molecules in the external milieu. In Gram-negative bacteria, eight different protein secretion pathways have been described thus far, designated type I (T1SS) to type VIII (T8SS) secretion systems [20–23]. Some of these systems (T3SS, T4SS and T6SS, in particular) have been implicated in interactions between bacterial and eukaryotic cells and in the translocation of bacterial effectors directly into the eukaryotic cytosol [24].

In silico analysis of *Francisella* genomes reveals, in addition to the classical components of the general Sec pathway, the presence of at least three specific secretion machineries:

- A putative T1SS, including the channel-forming protein TolC;
- A type II-like secretion system, represented by type IV pili (or Tfp);
- A type VI-like secretion system, encoded by the *Francisella* pathogenicity island (FPI) (Figure 1).

By contrast, there is currently no evidence of the presence of intact T3SS or T4SS in *Francisella* [25,26]. Although several putative substrates of a Tat pathway can be predicted, it is noteworthy that no evidence of a functional Tat system has been provided.

The contribution of the T1SS, T2SS-like and T6SS in *F. tularensis* intracellular survival will be discussed below.

Type I secretion

T1SS functions in the secretion of a variety of toxins and other virulence factors directly from the cytoplasm to the extracellular milieu in a single energized step. In *Escherichia coli*, the TolC protein is the outer membrane (OM) channel component of the T1SS involved in hemolysin secretion (via the HlyBD–TolC complex [27]) and in the efflux of small noxious molecules (via the AcrAB–TolC complex [28]). *F. tularensis* contains three TolC paralogs: TolC, FtlC and SilC [29]. Both TolC and FtlC participate in multidrug resistance in *F. tularensis*, but only TolC is a critical virulence factor in *F. tularensis* subsp. *holarctica* strain LVS [30]. Moreover, a Δ*tolC* mutant is hypercytotoxic to both murine and human macrophages, and elicits increased secretion of proinflammatory chemokines from human macrophages and endothelial cells. Hence, *F. tularensis* TolC is assumed to contribute to inhibition of host cell death and delaying host innate immune responses. Inhibition of host cell death is generally considered to be a strategy used by intracellular pathogens to prolong their survival and replication time in their intracellular niche. Remarkably, the targeted deletion of the *tolC* gene in *F. tularensis* subsp. *tularensis* strain SCHU S4 resulted in significantly prolonged time to death [31], suggesting a similar role in both subspecies. The exact mechanism by which TolC participates to these processes is not known. One can speculate that, since TolC is located in the bacterial OM, it may interact directly with host cell components. Alternatively, TolC may constitute a genuine T1SS that delivers effector(s) (toxins or other molecules) that are responsible for the control of the host innate immune response.

Type II secretion & type IV pili

The T2SS, also known as the main terminal branch of the general secretory (Sec) pathway, mediates the translocation of proteins from the periplasm across the OM of Gram-negative bacteria. The best-characterized T2SS is the pullulanase secretion apparatus of *Klebsiella* species,

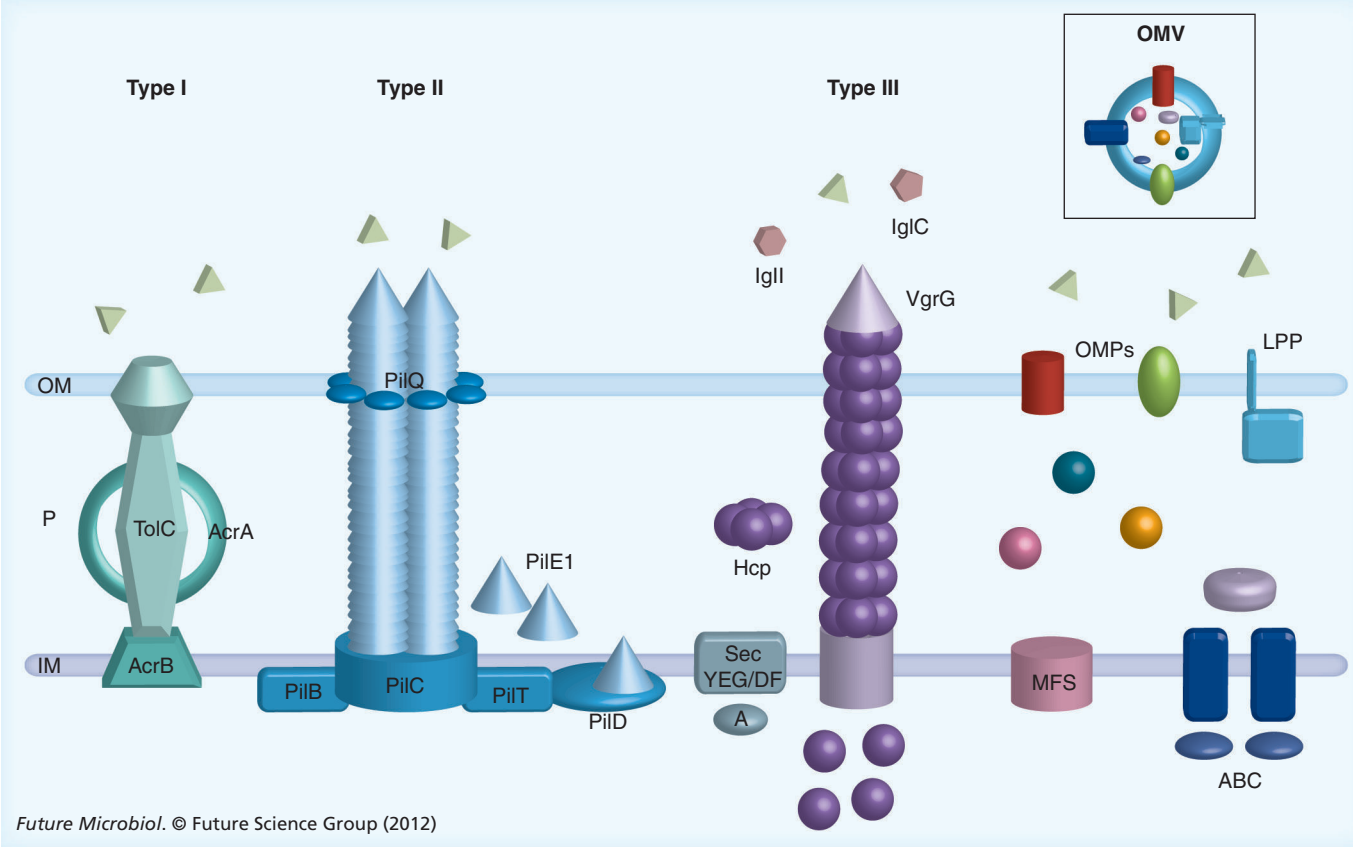

Figure 1. The secretion systems of *Francisella tularensis*. From left to right: the type I secretion system; the type II-like sectetion system (Tfp); the general secretory apparatus (Sec); the type VI-like secretion system (*Francisella* pathogenicity island-encoded); and MFS and ABC transporters (IM), as well as OMPs and LPPs (OM). Inset depicts an OMV.
IM: Inner membrane; LPP: Lipoprotein; MFS: Major facilitator superfamily; OM: Outer membrane; OMP: Outer membrane protein; OMV: Outer membrane vesicle; P: Periplasm.

which is composed of 15 components, several of which are similar to Tfp proteins [32]. Tfp are multifunctional filamentous appendages that are involved in the virulence of many Gram-negative pathogenic bacteria, generally by promoting attachment to host cells [33]. Tfp and T2SS use homologous components to mediate substrate release [32]. However, in spite of their common origin, these systems have diverged and acquired unique properties to perform distinct biological functions.

The different subspecies of *F. tularensis* have different secretion capacities in broth [21,22]. Indeed, significant protein secretion in the extracellular medium has only been observed with *F. tularensis* subsp. *novicida* and is specifically mediated by Tfp. *F. tularensis* genomes contain numerous genes with similarity to known Tfp genes, including secretin (PilQ) and six genes predicted to encode major type IV pilin subunits, designated *pilE1* (or *pilA*) to *pilE6*. Surface fiber expression has been observed in both *F. tularensis* subsp. *holarctica* LVS, *F. tularensis* subsp. *tularensis* SCHU S4 and in *F. tularensis* subsp. *novicida* U112 [34–36]. There is strong evidence in U112 and SCHU S4 strains that *pilE4* encodes the pilin subunit [35,36]. However, LVS completely lacks *pilE1* (*pilA*), has mutations in *pilE2* and *pilE3* (implying that the remaining functional pilin genes contribute to surface fiber expression) and expresses a nonfunctional PilT (the ATPase involved in pilus retraction).

At present, the role that Tfp-mediated secretion could play in *F. tularensis* virulence is still not fully understood. The very low level of protein secretion in pathogenic *F. tularensis* subsp. *holarctica* during growth in broth has been mainly attributed to the presence of pseudogenes of Tfp-encoding genes. However, in pathogenic *F. tularensis* subsp. *tularensis* species, the Tfp-encoding genes are intact, yet the bacterium secretes very low amounts of protein in the external milieu during growth in broth.

Of note, a recent proteomic analysis revealed the presence of low amounts of more than 100 proteins in cell culture filtrates of *F. tularensis* subsp. *tularensis* SCHU S4 and *F. tularensis* subsp. *holarctica* LVS [37]. Many of these proteins are not

predicted to be secreted, suggesting alternative secretion mechanisms in these bacteria.

The Tfp biogenesis genes *pilC* and *pilQ* both contribute to virulence in the highly virulent type A strain SCHU S4 [38]. The pilin PilE1 (PilA) is the only pilin that has been shown to be required for full virulence in both type A and type B strains [38,39]. However, the molecular mechanism whereby PilE1 promotes infection is not known. One might speculate that pilin subunits may constitute, or be part of, a type II-like secretion system required during intracellular growth to promote secretion of yet to be identified effectors.

Type VI secretion

The T6SS was first discovered in *Vibrio cholerae* and has now been identified in more than a quarter of all sequenced bacterial genomes [40]. Pathogenic bacteria use T6SS to inject effector proteins into infected host cells. In spite of a heterogeneous overall genetic organization, most T6SS systems encode homologs of *V. cholerae* proteins: IcmF (TssM), IcmH/DotU (TssL), ClpV, VipA (TssB), VipB (TssC), VgrG (TssI) and Hcp (TssD) proteins [41–43]. VgrG and Hcp are the two main proteins secreted by T6SS. They show structural resemblance to proteins of the cell-puncturing apparatus used by the T4 bacteriophage. Hence, Hcp may form a tubule-like hollow structure with a trimeric membrane-puncturing VgrG complex situated at the tip, through which macromolecules may be delivered directly into target cells [44]. In addition to Hcp and VgrG proteins, RbsB in *Rhizobium leguminosarum*, Evp in *Edwardsiella tarda* and TssM in *Burkholderia pseudomallei* have been identified as secreted T6SS effectors [45]. Their roles are still largely unknown. Very recently, the T6SS has also been shown to be involved in delivery of toxins to other bacteria [46].

The FPI

The 33-kb FPI consists of 16–19 open reading frames and plays a crucial role in the virulence of *F. tularensis* [47]. Notably, the FPI is duplicated in all the subspecies of *F. tularensis* except *F. tularensis* subsp. *novicida*, where it is present in a single copy. The species *Francisella philomiragia* also possesses a single copy of the FPI. Systematic mutational analyses of the FPI-encoded genes have shown that most of them participate in bacterial virulence. Many of the FPI genes have also been repeatedly identified in various genetic screens [15], confirming the critical role of this locus in *F. tularensis* pathogenesis.

In *F. tularensis* subsp. *novicida*, 14 out of the 18 genes within the FPI are required for intramacrophage multiplication [48]. *In silico* analyses have suggested that proteins encoded by the FPI might constitute a T6SS that is phylogenetically distinct from all other T6SS clusters described so far [49]. Indeed, it encodes proteins with limited homology to IcmF (PdpB), IcmH/DotU, VipA (IglA), VipB (IglB) and VgrG. IglC is suggested to be structurally homologous to Hcp [50]. The *F. tularensis* VgrG homolog is significantly smaller than any described VgrG and without an active C-terminal domain. Although it is not yet fully established that the *F. tularensis* FPI encodes a true T6SS, the current hypothesis is that it might secrete effector proteins into the host cytosol. IglC (the Hcp homolog) was the first FPI protein shown to be highly expressed in the host cytosol during *F. tularensis* subsp. *holarctica* LVS infection [51]. Although predominantly cytoplasmic [51], a small fraction of IglC localizes to the bacterial surface [52]. IglC export does not occur in *pdpB*, *dotU*, *iglA* or *iglB* mutants of *F. tularensis* subsp. *novicida*, supporting the notion that its export is T6SS dependent [50]. More recently, Barker *et al.* demonstrated secretion of two additional *F. tularensis* subsp. *novicida* proteins, VgrG and IglI, into the cytosol of infected macrophages [53]. Secretion of these two proteins was demonstrated by using C-terminal CyaA fusions (following the accumulation of cAMP in the host cell cytosol, see below) and N-terminally FLAG-tagged proteins. Strikingly, in contrast to all VgrG proteins reported so far, *F. tularensis* VgrG appeared to be exported into the extracellular milieu in an FPI-independent fashion [53], suggesting a unique mechanism of export. It is still unclear whether IglI secretion into host cells is dependent on core FPI components.

In spite of all the efforts devoted to the FPI and to its potential secreted effectors, its functional role in *F. tularensis* virulence is still largely unknown. At this stage, it is reasonable to assume that (any) FPI-dependent secreted proteins interact with host partner proteins to modify the host (metabolism and/or innate immunity) to the benefit of the bacterium.

OM vesicles

Membrane vesicle release is a universal phenomenon shared by bacteria, archae and eukaryotes. The release of vesicles provides a simple and rapid means to respond to many different situations, including environmental changes, as well as for pathogenic bacteria to secrete

virulence factors and deliver toxins or effectors for interacting with the host. OM vesicles (OMVs) are spherical structures (50–250 nm in diameter) released from the surface of many Gram-negative bacteria during cell growth [54]. On their surface, OMVs comprise the same components as the OM from which they derive (i.e., an asymmetric lipid bilayer with lipopolysaccharide [LPS] on the outer leaflet), as well as all the OM-associated proteins (e.g., β-barrels, lipoproteins [LPPs]). The interior of OMVs contains both periplasmic and cytoplasmic proteins. Although they have been observed for more than three decades, their release mechanism has not yet been fully understood [55].

Francisella spp. have recently been shown to produce OMVs when grown to stationary phase in liquid broth [56]. Mass spectrometry analyses of OMVs from *F. tularensis* subsp. *novicida* and *F. philomiragia* led to the identification of hundreds of different proteins, including 166 proteins common to both species. The *Francisella* OMVs also contained significant amounts of chromosomal DNA. In agreement with earlier studies, the *F. tularensis* subsp. *novicida* OMV proteome was composed mainly (60%) of predicted cytoplasmic proteins, including the chaperone GroEL (which was the most abundant protein identified), DnaK and KatG. It also contained predicted OM proteins, including notably PilQ (the Tfp secretin) and TolC, as well as predicted periplasmic and extracellular proteins. Six proteins encoded by the FPI were also identified (PdpA, B and D, and IglA, B and C). Many of the OMV proteins have a demonstrated role in *Francisella* pathogenesis. Hence, OMVs may constitute a genuine 'vesicle-mediated secretion system' employed by *Francisella* to deliver virulence factors in the host cytosol. Further experimental work will be required to test this tempting hypothesis.

Other secreted/released proteins

In 2006, Lee *et al.* compared the proteins released in the culture medium of the virulent isolate *F. tularensis* subsp. *tularensis* RCI to that of *F. tularensis* subsp. *holarctica* LVS, grown in chemically defined medium [57]. The catalase-peroxidases KatG, DnaK and GroEL were among the 12 most abundant proteins found in culture filtrates from both strains. Interestingly, western blot analysis of bacterial proteins released after 10 h of infection of THP-1 macrophages with the virulent RCI strain identified both KatG and GroEL. At present, this observation, suggesting that these two proteins are indeed released in the cytosol of infected cells, has not been confirmed by other studies.

The *F. tularensis* KatG has the capacity to detoxify bactericidal compounds such as H_2O_2 and $ONOO^-$ [58]. In this respect, *katG* mutants of both *F. tularensis* subsp. *tularensis* SCHU S4 and *F. tularensis* subsp. *holarctica* LVS show enhanced susceptibility to H_2O_2 *in vitro* [59]. However, *katG* inactivation has no effect on intracellular survival of the mutants in macrophages, and only little or no effect *in vivo*. These observations suggest that KatG might protect *Francisella* against reactive oxygen and nitrogen species in other cell types than macrophages and that virulent species possess additional resistance mechanisms.

As mentioned above, the proteomic analysis of OMVs revealed that DnaK, GroEL and KatG were among the major proteins identified in *F. tularensis* subsp. *novicida* [56]. Moreover, KatG has also been detected in *F. tularensis* OM fractions by Huntley *et al.* [60].

The acid phosphatase AcpA

Acid phosphatases hydrolyze the phosphoryl groups of phosphomonoesters at acidic pH. *Francisella* subspecies possess at least four acid phosphatases (designated AcpA, B and C, and Hap). The simultaneous loss of all four acid phosphatases in *F. tularensis* subsp. *novicida* has been shown to dramatically affect phagosomal escape, intramacrophage survival and virulence [61]. These effects are less pronounced in *F. tularensis* subsp. *holarctica* and *tularensis* (SCHU S4) [62]. The four acid phosphatases were shown to directly participate to dephosphorylation of the Phox components of the NADPH oxidase, thus preventing their functional assembly and, ultimately, the production of reactive oxygen species. The structure of AcpA, the major acid phosphatase, has been determined [63], and its phosphatase activity has been demonstrated *in vitro*, with purified phosphorylated NADPH oxidase components p40phox and p47phox [62]. AcpA, initially described as an OM protein [64], has also been found in the culture supernatant [56]. Recent studies revealed that AcpA was also secreted by *F. tularensis* subsp. *novicida* U112 within macrophages [65]. Remarkably, immunofluorescence microscopy experiments performed in human monocyte-derived macrophages revealed that as early as 30 min after infection, a minor fraction of AcpA was able to diffuse across the phagosomal membrane into the host cell cytosol with both *F. tularensis* subsp.

novicida and *F. tularensis* subsp. *tularensis* SCHU S4 strains [65].

However, studies from two different groups of mutants generated in *F. tularensis* subsp. *tularensis* SCHU S4 have demonstrated that acid phosphatases are completely dispensable for phagosomal escape and intramacrophagic growth, disruption of NADPH oxidase activity in neutrophils and virulence in mice [66,67]. Thus, the significance and relevance of rapid AcpA secretion by *F. tularensis* subsp. *novicida* remains unclear. At this stage, the molecular mechanisms underlying this release are still unknown but have been hypothesized to correspond to fusion events between OMVs and the phagosomal membrane.

Altogether, these data support the notion that the vast majority of the proteins released by *Francisella* in culture originate from OMVs.

Surface structures

The importance of extramembranous surface structures (e.g., LPS, capsular material and surface glycoproteins) in *F. tularensis* virulence has been clearly established. The biogenesis of the *Francisella* LPS, its biochemical composition and its role in pathogenesis have been extensively studied (reviewed in [68–70]; see also [71–75] for recent studies) and, therefore, will not be discussed here. We will briefly discuss the production of a peptidic capsular material and surface protein glycosylation.

Poly-γ-glutamate or not poly-γ-glutamate: the *cap* enigma

The existence and composition of the *F. tularensis* capsule(s) is still a subject of great controversy. Several electron microscopic analyses supported the existence of a *F. tularensis* capsule, whereas other unsuccessful attempts suggested that LPS O-antigen might be the only capsule-like structure [76–78].

The *capBCA* locus was the first gene cluster possibly encoding a capsule that was identified in a signature mutagenesis screen performed in *F. tularensis* subsp. *holarctica* LVS [79]. The three genes of this locus share significant similarities with genes within the *capBCADE* locus of *Bacillus anthracis* [80,81], which are responsible for poly-γ-glutamate (PGA) synthesis. In *B. anthracis,* PGA synthesis depends primarily on the proteins CapB and CapC, whereas PGA transport requires the presence of the proteins CapA and CapE. Finally, PGA is either anchored to the bacterial surface, via the action of the γ-glutamyl transpeptidase CapD, or released in the extracellular milieu. The *F. tularensis capBCA* locus (*FTT_0805–FTT_0807* in *F. tularensis* subsp. *tularensis* SCHU S4 strain) has been shown to be necessary for the infection of LVS in a respiratory infection mouse model [82]. More recent studies confirmed the role of this locus in the virulence of the SCHU S4 strain [79,82,83]. Furthermore, deletion of *capB* alone was shown to impair virulence in both *holarctica* and *tularensis* subspecies [79,83]. Confocal microscopy experiments with Δ*capB* and Δ*capBCA* mutants of LVS indicated that these mutants were severely impaired in their ability to escape from the phagosomal compartment of infected human macrophages. Hence, the *capBCA* genes are likely to contribute mainly to the early step of *F. tularensis* intracellular survival, perhaps by producing some kind of PGA. However, no PGA-like material could be detected from *F. tularensis* cultures, even in broth, in experiments performed to date [81,83]. Further studies will be required to conclusively establish the functional role of the *capBCA* locus in the production of a capsular material.

Notably, the recent development of a specific monoclonal antibody led Apicella *et al.* to identify an O-antigen capsular polysaccharide around all *F. tularensis* type A and B strains tested [77]. Mass spectrometry, compositional analysis and nuclear magnetic resonance indicated that the capsule was composed of a polymer of the tetrasaccharide repeat, identical in composition to the LPS O-antigen subunit but corresponding to a structure that was distinct from LPS. Indeed, mutations in genes encoding for O-antigen glycosyltransferases blocked LPS O-antigen and capsule biosynthesis, but mutations in genes encoding for O-antigen polymerase or acyltransferase only prevented LPS O-antigen synthesis, not capsule synthesis.

Envelope protein glycosylation

The genetic locus *FTT_0789–FTT_0800* of *F. tularensis* subsp. *tularensis* (*FTL_1432–FTL_1421* in *F. tularensis* subsp. *holarctica* LVS) contains genes that are potentially involved in polysaccharide biosynthesis, including:

- Four genes encoding putative glycosyltransferases;
- A *galE* homolog (encoding a putative UDP-glucose 4-epimerase);
- One gene encoding a putative ABC transport protein (*FTT_0793*).

The whole cluster is conserved in subspecies *tularensis* and *holarctica*, whereas the genome of subsp. *novicida* possesses only the four proximal genes of the cluster (corresponding to *FTT_0789–FTT_0792*). Most of the genes within this locus have been hit in at least one genetic screen searching for attenuated mutants [72,84–86], strongly supporting the notion that this locus plays an important role in *F. tularensis* virulence. Interestingly, Bandara *et al.* recently isolated a capsule-like material (CLM) in *F. tularensis* subsp. *holarctica* LVS after repeated passages in defined medium [78]. The authors found that the *FTL_1432–FTL_1421* locus contributed to CLM production. Although the nature of the CLM was not fully characterized, the data revealed that the CLM was distinct from LPS, contained glucose, galactose and mannose and suggested that it might be a glycoprotein.

In a search for genes that are responsible for protein glycosylation in *F. tularensis* subsp. *tularensis* SCHU S4, Thomas *et al.* recently reported that inactivation of *FTT_0791* and *FTT_0798* genes resulted in loss of glycosylation of the LPP DsbA, an essential virulence factor of *F. tularensis* [87–89]. The mutations had no effect on LPS O-antigen biosynthesis. Remarkably, they did not impair bacterial virulence in the mouse model of subcutaneous tularemia, indicating that glycosylation of DsbA does not play a major role in SCHU S4 virulence under these conditions.

A very recent study identified another protein (PglA , FTT_0905, annotated as a type IV pilus glycosylation protein) to be responsible for the glycosylation of DsbA in the *F. tularensis* subsp. *holarctica* virulent strain FSC200 [90]. In addition, Peng *et al*. reported that inactivation of the ortholog of *FTT_0793* in *F. tularensis* subsp. *novicida* (which also impaired *in vivo* survival [84]) caused increased intracellular bacterial lysis, thus increasing nonspecifically AIM2-dependent pyroptosis and other innate immune signaling pathways [72]. Hence, at least in subsp. *novicida*, the putative ABC transport protein FTN_1217 (FTT_0793 in SCHU S4) contributes to bacterial membrane integrity during cytosolic growth of the bacterium.

Other envelope proteins

Several OM proteins have been shown to contribute to *F. tularensis* intracellular survival. These include a OmpA-like protein (FTT_0831c in *F. tularensis* subsp. *tularensis* SCHU S4 [91]) and FopC (FTN_0444 in *F. tularensis* subsp. *novicida* [92,93]), as well as LPPs such as LpnA (Tul4) and the newly identified LPP encoded by the *FTN_1103* gene in *F. tularensis* subsp. *novicida* [94]. These proteins influence/control the host cell innate immune defenses, either by silencing bacterial recognition by surface TLR2 (LPPs) or by interfering with the intracellular activation pathways (OmpA-like protein and FopC). The mechanisms of host defense subversion have been recently reviewed [95] and will not be discussed further here.

Transporters

The intracellular niche contains numerous utilizable carbon substrates in variable amounts, various nitrogen, phosphorus and sulfur sources and variable (and most often scarce) sources of essential ions, such as iron, magnesium, zinc and manganese [7,96]. The efficient transport of nutrients is thus critical for intracellular survival. Therefore, these bacteria generally possess multiple specific nutrient uptake systems, many of which are tightly regulated to promote their optimal temporal expression.

Here, we will first recall our current understanding of iron uptake by intracellular *Francisella* and then discuss recent studies on efflux pumps.

Iron uptake

Iron is an essential cofactor for many enzymes and the ability to acquire iron has been demonstrated to play a critical role in the outcome of numerous bacterial infections. However, many fundamental mechanistic questions about bacterial iron uptake remain unanswered. Ferric iron (Fe^{3+}) is water insoluble and thus requires specialized proteins for its solubilization and to facilitate its mobilization. Mammalian species possess several iron binding and storage proteins (e.g., lactoferrin, transferrin, ferritin and lipocalin) but the majority of mammalian iron exists as heme and hemoglobin. The production of siderophores, which generally chelate iron with a higher affinity than eukaryotic proteins, is one way that pathogenic bacteria utilizes to overcome iron sequestration. Gram-negative bacteria notably possess dedicated envelope uptake systems to bind and internalize ferric siderophore complexes and, in some cases, heme and iron binding proteins [97].

Unlike other intracellular pathogens, which possess numerous iron uptake systems [98], the *F. tularensis* genomes encode only two iron transport systems: a siderophore production and capture system encoded by the *fsl* operon (for *Francisella* siderophore locus; also called *fig*

in the subsp. *novicida*); and a putative ferrous (Fe^{2+}) iron transport system encoded by the *feoA* and *feoB* genes (*FTT_1403c* and *FTT_0249,* respectively, in *F. tularensis* subsp. *tularensis*) [99]. Intriguingly, the *F. tularensis* genomes do not encode orthologs of the inner membrane proteins TonB, ExbB and ExbD, which are generally required to energize the iron uptake process in Gram-negative bacteria [100]. In addition, translocation of the ferric siderophore across the inner membrane requires a periplasmic binding protein and specific ABC transporters. The *F. tularensis* subsp. *tularensis* SCHU S4 genome encodes only 15 complete ABC transporters, and only three of them are predicted to be importers. Their possible role in iron uptake has not been studied so far. In particular, the *FTT_0207c–FTT_0208c–FTT_0209c* locus is the only locus predicted to encode a divalent ion transport system (predicted zinc/manganese transport system permease protein in the Kyoto Encyclopedia of Genes and Genomes [KEGG] database) that has been identified in earlier genetic screens [10].

As in other bacterial species, these two loci are under the negative control of the Fur repressor (encoded by the *fur* gene, *FTT_0030c*, in *F. tularensis* subsp. *tularensis*, located immediately upstream of the *fsl* operon) (Figure 2). The *fsl* operon is composed of six genes (*fslA* to *fslF*) [101]. The genes *fslA* and *fslC* (*FTT_0029c* and *FTT_0027c*, encoding a putative siderophore synthase and a pyridoxal-dependent decarboxylase, respectively) are responsible for the production of a siderophore that is similar in structure to rhizoferrin [102]. The gene *fslE* (*FTT_0025c*) is assumed to encode the siderophore receptor [91,103,104]. Of note, FslB and FslD contain putative major facilitator superfamily (MFS) domains (FTT_0028c and FTT_0026c) and, thus, could be involved in siderophore release. Mutants in *fslA, fslB* and *fslC* have been found repeatedly in various screens (for reviews, see [15,105]), supporting the notion of the importance of this operon in *F. tularensis* pathogenesis. The *F. tularensis* subsp. *tularensis* genome encodes one FslE paralog, designated FupA (FTT_0918), which shares 59% amino acid identity with FslE. Unlike genes of the Fur-regulated *fsl* operon, expression of *FTT_0918* is not affected by the iron concentration, implying a different regulation [103]. Both FslE and FupA proteins are predicted to form β-barrels in the bacterial OM. It was recently demonstrated that these two paralogs function in concert to promote siderophore-dependent and -independent iron uptake [91]. The authors notably showed that FupA, but not FslE, facilitated high-affinity Fe^{2+} uptake. In J774A.1 macrophage-like cells, only the Δ*fslE*–Δ*fupA* double mutant showed significantly impaired multiplication. In a mouse model, the Δ*fslE*–Δ*fupA* double mutant was also significantly more attenuated than the single mutant, suggesting that the two systems function in concert to facilitate iron capture and, hence, contribute to bacterial virulence.

Efflux pumps

ABC transporters, the MFS of transporters and the resistance–nodulation–division (RND) efflux systems constitute the major modes of resistance to antibacterial drugs. These complexes are generally associated with the OM TolC channel (see above). The MFS (31 proteins) represents the larger subclass of secondary transporters in *F. tularensis* [10]. They are predicted to transport a broad variety of substrates across the inner membrane (via import, export, symport or antiport mechanisms). At present, none of these family members have been functionally characterized. The RND efflux system consists of a tripartite transporter with a cytoplasmic membrane protein (AcrB) and a periplasmic membrane fusion protein (AcrA) coupled to OM TolC. The *F. tularensis* subsp. *tularensis* SCHU S4 genome encodes only four putative RND genes. The AcrA–AcrB system is encoded by an operon (*FTT_0105c* to *FTT_0107c*) that also comprises the *dsbA* gene (*FTT_0107c*) that is involved in virulence (see above). In *F. tularensis* subsp. *holarctica* LVS, an *acrB* mutant showed attenuated virulence [106]. By contrast, in *F. tularensis* subsp. *tularensis* SCHU S4, deletions in *acrA* and *acrB* had no impact on either intracellular growth or on virulence in a mouse (when given intranasally) [107]. In spite of these apparently conflicting observations, this RND system might contribute to virulence under other infectious conditions (e.g., other cell types, other routes of infection and/or animal models). The other two RND-like proteins, FTT_1115c and FTT_1114c, are orthologs of the preprotein translocase subunits SecD and SecF, which associate with the secretory translocon SecYEG (Sec system) [108].

At present, it cannot be excluded that one (or several) of these efflux systems might be involved in the intracellular delivery of proteins (or peptides) involved in bacterial adaptation to the host cell environment.

Other proteins

The recent follow-up of a genome-wide *in vivo* negative selection of *F. tularensis* subsp. *novicida* mutants led to the identification of numerous

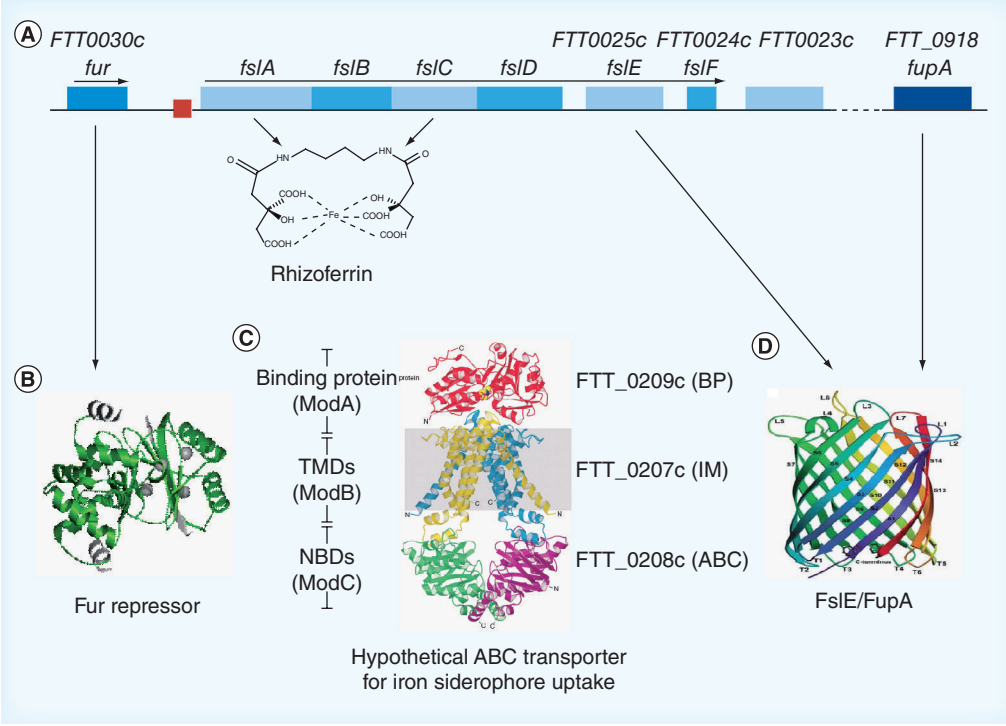

Figure 2. Iron uptake in *Francisella tularensis*. (A) Schematic genetic organization of the *fur–fsl* locus. The red box indicates the Fur binding site. The arrows below selected genes indicate their participation to the production of the Fur repressor (*fur*), the synthesis of the rhizoferrin-like siderophore (*fslA*, *flsC*) and the OM proteins involved in the uptake of the iron-bound siderophore (*fslE*, *fupA*). **(B–D)** 3D structures of proteins showing sequence similarities to the *Francisella* proteins. **(B)** The Fur repressor. The structure shown is that of *Vibrio cholerae* (PDB 2w57). The *Francisella* Fur protein shares 38.3% amino acid identity with Fur of *V. cholerae*. **(D)** FslE and FupA. The structure shown is that of the *Escherichia coli* OmpG barrel (PDB 2iwv). FslE and FupA, which share 59% amino acid identity, are predicted to form a similar 14-stranded β-barrel. **(C)** The hypothetical ABC transporter that is possibly involved in the translocation of the iron-bound siderophore across the inner membrane. The structure shown is that of the molybdate transporter from *Archaeoglobus fulgidus* (PDB 2ONK), a prototypical bacterial ABC transporter.
BP: Periplasmic binding protein; IM: Inner membrane permease.

mutants with impaired intramacrophage survival [109]. One of these mutants, in gene *FTN_1133*, was particularly studied. FTN_1133 is a small protein of 127 amino acid residues in length that shows similarity to the C-terminal domain of the organic hydroperoxide resistance protein (Ohr) from *Bacillus megaterium*. This protein contributes to resistance to reactive oxygen species. Favoring a similar role in *Francisella* species, the mutant *FTN_1133* showed increased susceptibility to organic hyperoxides, as well as resistance to the action of the NADPH oxidase *in vitro* and *in vivo*. The subcellular localization and precise contribution of FTN_1133 (FTT_1152 in SCHU S4) to intracellular survival and multiplication remains to be determined. At this stage, one would assume that it might be particularly important during the phagosomal stage of the intracellular life cycle by reducing the amount of reactive oxygen species in this compartment and interfering with NADPH oxidase assembly.

RipA is a cytoplasmic membrane protein that is conserved among *Francisella* species [110]. Deletion of the *ripA* gene in *F. tularensis* subsp. *holarctica* LVS (*FTL_1914*) results in a mutant that escapes the phagosome but is defective for intracellular replication in both macrophages and epithelial cells. The mutant is also attenuated in a pulmonary mouse model of tularemia. Deletion of *ripA* in *F. tularensis* subsp *tularensis* SCHU S4 (*FTT_0181c*) also results in a mutant that is defective for intracellular replication and is attenuated in a mouse model [111]. Although the topological organization of the protein has recently been determined [111], it is not known whether this integral membrane protein is involved in transport activities, and its biological function(s) remain completely obscure.

Conclusion

F. tularensis intracellular adaptation implies the existence of sophisticated regulatory circuits

for the temporal control of numerous virulence genes. Indeed, many transcriptional factors have been shown to regulate the expression of FPI genes, as well as of numerous other genes scattered along the chromosome, including MglA, SspA, FevR (PigR), MigR, PmrA and Hfq (see [112,113]). Remarkably, the intracellular concentration of guanosine tetraphosphate, the alarmone involved in the stringent response in bacteria (which is determined by the products of the *relA* and *spoT* genes) has also been shown to promote the interaction between FevR (PigR) and the RNA polymerase-associated MglA–SspA complex [114]. Hence, it is clear that bacterial metabolic adaptation and expression of so-called 'virulence' genes are two interconnected mechanisms that are essential for intracellular survival. Thus, the secretion/release of bacterial proteins, as well as modification of the bacterial envelope, respond to the simultaneous need to adapt to the intracellular lifestyle conditions and control the host defense mechanisms at the different steps of its infectious cycle.

Acknowledgement

The authors would like to thank K Meibom for careful reading of the manuscript and helpful comments.

Financial & competing interests disclosure

This study was funded by INSERM, CNRS and Université René Descartes, Sorbonne Paris Cité. E Ramond is supported by a doctoral fellowship from the 'Région Ile-de-France' (DIM-Malinf). G Gesbert is funded by a doctoral fellowship from the 'Délégation Générale à l'Armement' (DGA). The authors have no other relevant affiliations or financial involvement with any organization or entity with a financial interest in or financial conflict with the subject matter or materials discussed in the manuscript apart from those disclosed.

No writing assistance was utilized in the production of this manuscript.

Executive summary

Secreted proteins

- *Francisella* genomes encode the classical components of the general Sec pathway and three specific secretion machineries: a putative type I secretion system (T1SS), a type II-like secretion system and a type VI-like sectetion system, encoded by the *Francisella* pathogenicity island.
- There is no evidence of the presence of intact T3SS or T4SS in *Francisella*.

The Francisella *pathogenicity island*

- Cytosolic secretion of two *Francisella* pathogenicity island-encoded proteins was demonstrated: VgrG and IglI.
- The secretion of IglI is likely to be T6SS dependent, whereas that of VgrG appears to be T6SS independent.
- IglC is one of the most upregulated proteins during intramacrophagic growth. IglC is predominantly cytoplasmic, but a fraction of the protein is exported to the bacterial surface.

Other secreted proteins

- *Francisella* spp. produce outer membrane vesicles. The *Francisella tularensis* subsp. *novicida* outer membrane vesicle/proteome is composed mainly of cytoplasmic proteins, but also contains outer membrane proteins as well as periplasmic and extracellular proteins.
- Several proteins encoded by the *Francisella* pathogenicity island were also identified in outer membrane vesicles.

Surface structures

- *F. tularensis* genomes encode several putative polysaccharide and/or polypeptide biogenesis loci that are possibly involved in protein glycosylation and/or capsular material production.
- The nature and genetic basis of the capsule-like surrounding of *F. tularensis* are still not clearly defined.

Other envelope proteins

- *F. tularensis* genomes encode numerous putative transporters and efflux pumps that may also contribute to the release of peptide or proteins in the host.

References

Papers of special note have been highlighted as:
- ▪ of interest
- ▪▪ of considerable interest

1. Francisella tularensis *and Tularemia*. Sjostedt A (Ed.). Fontiers Media SA, Switzerland (2011).

▪▪ **Reviews the major aspects of *Francisella tularensis* pathogenesis.**

2. Keim P, Johansson A, Wagner DM. Molecular epidemiolgy, evolution, and ecology of *Francisella*. *Ann. NY Acad. Sci.* 1105, 30–66 (2007).
3. McLendon MK, Apicella MA, Allen LA. *Francisella tularensis*: taxonomy, genetics, and immunopathogenesis of a potential agent of biowarfare. *Annu. Rev. Microbiol.* 60, 167–185 (2006).
4. Johansson A, Petersen JM. Genotyping of *Francisella tularensis*, the causative agent of tularemia. *J. AOAC Int.* 93, 1930–1943 (2010).
5. Gallagher LA, Ramage E, Jacobs MA *et al.* A comprehensive transposon mutant library of *Francisella novicida*, a bioweapon surrogate. *Proc. Natl Acad. Sci. USA* 104, 1009–1014 (2007).
6. Chong A, Celli J. The *Francisella* intracellular life cycle: toward molecular mechanisms of intracellular survival and proliferation. *Front. Microbiol.* 1, 138 (2010).

▪ **Comprehensive review on the mechanisms of *F. tularensis* intracellular survival.**

7. Ray K, Marteyn B, Sansonetti PJ, Tang CM. Life on the inside: the intracellular lifestyle of cytosolic bacteria. *Nat. Rev. Microbiol.* 7, 333–340 (2009).
8. Appelberg R. Macrophage nutriprive antimicrobial mechanisms. *J. Leukoc. Biol.* 79, 1117–1128 (2006).

▪▪ **First review linking nutrition and intramacrophage survival.**

9. Hammer ND, Skaar EP. The impact of metal sequestration on *Staphylococcus aureus* metabolism. *Curr. Opin. Microbiol.* 15, 10–14 (2012).

▪ **Comprehensive review on iron captation mechanisms in *Staphylococcus aureus*.**

10. Meibom KL, Charbit A. *Francisella tularensis* metabolism and its relation to virulence. *Front. Microbiol.* 1, 140 (2010).
11. Knodler LA, Celli J. Eating the strangers within: host control of intracellular bacteria via xenophagy. *Cell. Microbiol.* 13, 1319–1327 (2011).
12. Ligeon LA, Temime-Smaali N, Lafont F. Ubiquitylation and autophagy in the control of bacterial infections and related inflammatory responses. *Cell. Microbiol*. 13, 1303–1311 (2011).
13. Checroun C, Wehrly TD, Fischer ER, Hayes SF, Celli J. Autophagy-mediated reentry of *Francisella tularensis* into the endocytic compartment after cytoplasmic replication. *Proc. Natl Acad. Sci. USA* 103, 14578–14583 (2006).

▪ **Describes for the first time autophagy in *F. tularensis* intracellular survival.**

14. Henry T, Monack DM. Activation of the inflammasome upon *Francisella tularensis* infection: interplay of innate immune pathways and virulence factors. *Cell. Microbiol.* 9, 2543–2551 (2007).
15. Meibom KL, Charbit A. The unraveling panoply of *Francisella tularensis* virulence attributes. *Curr. Opin. Microbiol.* 13, 11–17 (2010).
16. Asare R, Kwaik YA. Exploitation of host cell biology and evasion of immunity by *Francisella tularensis. Front. Microbiol.* 1, 145 (2010).

▪ **Comprehensive review on the evasion of host cell defenses by *F. tularensis*.**

17. Jones JW, Broz P, Monack DM. Innate immune recognition of *Francisella tularensis*: activation of type-I interferons and the inflammasome. *Front. Microbiol.* 2, 16 (2011).

▪ **Comprehensive review on the innate immune recognition by *F. tularensis*.**

18. Pierini R, Juruj C, Perret M *et al.* AIM2/ASC triggers caspase-8-dependent apoptosis in *Francisella*-infected caspase-1-deficient macrophages. *Cell Death Differ.* 19(10), 1709–1721 (2012).
19. Natale P, Bruser T, Driessen AJ. Sec- and Tat-mediated protein secretion across the bacterial cytoplasmic membrane – distinct translocases and mechanisms. *Biochim. Biophys. Acta* 1778, 1735–1756 (2008).

▪ **Recent review on the Sec and Tat pathways.**

20. Desvaux M, Hebraud M, Talon R, Henderson IR. Secretion and subcellular localizations of bacterial proteins: a semantic awareness issue. *Trends Microbiol.* 17, 139–145 (2009).
21. Forsberg A, Guina T. Type II secretion and type IV pili of *Francisella*. *Ann. NY Acad. Sci.* 1105, 187–201 (2007).

▪ **Comprehensive review on the role of type IV pili in *F. tularensis* pathogenesis.**

22. Chandler JC, Molins CR, Petersen JM, Belisle JT. Differential chitinase activity and production within *Francisella* species, subspecies, and subpopulations. *J. Bacteriol.* 193, 3265–3275 (2011).
23. Thanassi DG, Bliska JB, Christie PJ. Surface organelles assembled by secretion systems of Gram-negative bacteria: diversity in structure and function. *FEMS Microbiol. Rev.* doi:10.1111/j.1574-6976.2012.00342.x (2012) (Epub ahead of print).

▪ **Comprehensive review on the surface organelles of Gram-negative bacteria.**

24. Schwarz S, Hood RD, Mougous JD. What is type VI secretion doing in all those bugs? *Trends Microbiol.* 18, 531–537 (2010).
25. Titball RW, Petrosino JF. *Francisella tularensis* genomics and proteomics. *Ann. NY Acad. Sci.* 1105, 98–121 (2007).
26. Champion MD, Zeng Q, Nix EB *et al.* Comparative genomic characterization of *Francisella tularensis* strains belonging to low and high virulence subspecies. *PLoS Pathog.* 5, e1000459 (2009).
27. Holland IB, Schmitt L, Young J. Type 1 protein secretion in bacteria, the ABC-transporter dependent pathway (review). *Mol. Membr. Biol.* 22, 29–39 (2005).
28. Eicher T, Cha HJ, Seeger MA *et al.* Transport of drugs by the multidrug transporter AcrB involves an access and a deep binding pocket that are separated by a switch-loop. *Proc. Natl Acad. Sci. USA* 109, 5687–5692 (2012).
29. Gil H, Platz GJ, Forestal CA *et al.* Deletion of TolC orthologs in *Francisella tularensis* identifies roles in multidrug resistance and virulence. *Proc. Natl Acad. Sci. USA* 103, 12897–12902 (2006).
30. Platz GJ, Bublitz DC, Mena P *et al.* A *tolC* mutant of *Francisella tularensis* is hypercytotoxic compared to the wild type and elicits increased proinflammatory responses from host cells. *Infect. Immun.* 78, 1022–1031 (2010).
31. Kadzhaev K, Zingmark C, Golovliov I *et al.* Identification of genes contributing to the virulence of *Francisella tularensis* SCHU S4 in a mouse intradermal infection model. *PLoS One* 4, e5463 (2009).
32. Chen I, Dubnau D. DNA uptake during bacterial transformation. *Nat. Rev. Microbiol.* 2, 241–249 (2004).
33. Ayers M, Howell PL, Burrows LL. Architecture of the type II secretion and type IV pilus machineries. *Future Microbiol.* 5, 1203–1218 (2010).
34. Chakraborty S, Monfett M, Maier TM *et al.* Type IV pili in *Francisella tularensis*: roles of *pilF* and *pilT* in fiber assembly, host cell adherence, and virulence. *Infect. Immun.* 76, 2852–2861 (2008).
35. Zogaj X, Chakraborty S, Liu J, Thanassi DG, Klose KE. Characterization of the *Francisella tularensis* subsp. *novicida* type IV pilus. *Microbiology* 154, 2139–2150 (2008).
36. Ark NM, Mann BJ. Impact of *Francisella tularensis* pilin homologs on pilus formation and virulence. *Microb. Pathog.* 51, 110–120 (2011).
37. Konecna K, Hernychova L, Reichelova M *et al.* Comparative proteomic profiling of culture filtrate proteins of less and highly virulent *Francisella tularensis* strains. *Proteomics* 10, 4501–4511 (2010).
38. Forslund AL, Salomonsson EN, Golovliov I *et al.* The type IV pilin, PilA, is required for full virulence of *Francisella tularensis* subspecies *tularensis*. *BMC Microbiol.* 10, 227 (2010).
39. Forslund AL, Kuoppa K, Svensson K *et al.* Direct repeat-mediated deletion of a type IV pilin gene results in major virulence attenuation of *Francisella tularensis*. *Mol. Microbiol.* 59, 1818–1830 (2006).
40. Cascales E. The type VI secretion toolkit. *EMBO Rep.* 9, 735–741 (2008).
41. Pukatzki S, McAuley SB, Miyata ST. The type VI secretion system: translocation of effectors and effector-domains. *Curr. Opin. Microbiol.* 12, 11–17 (2009).
42. Miyata ST, Kitaoka M, Wieteska L *et al.* The *Vibrio cholerae* type VI secretion system: evaluating its role in the human disease cholera. *Front. Microbiol.* 1, 117 (2010).
43. Filloux A. Protein secretion systems in *Pseudomonas aeruginosa*: an essay on diversity,

evolution, and function. *Front. Microbiol.* 2, 155 (2011).

- **Comprehensive review on the protein secretion systems of *Pseudomonas aeruginosa*.**

44. Bonemann G, Pietrosiuk A, Mogk A. Tubules and donuts: a type VI secretion story. *Mol. Microbiol.* 76, 815–821 (2010).
45. Schwarz S, West TE, Boyer F *et al.* Burkholderia type VI secretion systems have distinct roles in eukaryotic and bacterial cell interactions. *PLoS Pathog.* 6, e1001068 (2010).
46. Russell AB, Hood RD, Bui NK *et al.* Type VI secretion delivers bacteriolytic effectors to target cells. *Nature* 475, 343–347 (2011).
47. Nano FE, Schmerk C. The *Francisella* pathogenicity island. *Ann. NY Acad. Sci.* 1105, 122–137 (2007).
48. Broms JE, Meyer L, Lavander M, Larsson P, Sjostedt A. DotU and VgrG, core components of type VI secretion systems, are essential for *Francisella* LVS pathogenicity. *PLoS One* 7, e34639 (2012).
49. Bröms JE, Sjöstedt A, Lavander M. The role of the *Francisella tularensis* pathogenicity island in type VI secretion, intracellular survival, and modulation of host cell signaling. *Front. Microbiol.* 1, 136 (2010).
50. de Bruin OM, Duplantis BN, Ludu JS *et al.* The biochemical properties of the *Francisella* pathogenicity island (FPI)-encoded proteins, IglA, IglB, IglC, PdpB and DotU, suggest roles in type VI secretion. *Microbiology* 157, 3483–3491 (2011).
51. Golovliov I, Ericsson M, Sandstrom G, Tarnvik A, Sjostedt A. Identification of proteins of *Francisella tularensis* induced during growth in macrophages and cloning of the gene encoding a prominently induced 23-kilodalton protein. *Infect. Immun.* 65, 2183–2189 (1997).

- **First identification of IglC overexpression by cytosolic bacteria.**

52. Ludu JS, de Bruin OM, Duplantis BN *et al.* The *Francisella* pathogenicity island protein PdpD is required for full virulence and associates with homologues of the type VI secretion system. *J. Bacteriol.* 190, 4584–4595 (2008).
53. Barker JR, Chong A, Wehrly TD *et al.* The *Francisella tularensis* pathogenicity island encodes a secretion system that is required for phagosome escape and virulence. *Mol. Microbiol.* 74, 1459–1470 (2009).

- **First demonstration of the secretion of VgrG and IglI in the host cell cytosol.**

54. Deatherage BL, Cookson BT. Membrane vesicle release in bacteria, eukaryotes, and archaea: a conserved yet underappreciated aspect of microbial life. *Infect. Immun.* 80, 1948–1957 (2012).
55. Kulp A, Kuehn MJ. Biological functions and biogenesis of secreted bacterial outer membrane vesicles. *Annu. Rev. Microbiol.* 64, 163–184 (2010).

- **Comprehensive review on the biogenesis of outer membrane vesicles.**

56. Pierson T, Matrakas D, Taylor YU *et al.* Proteomic characterization and functional analysis of outer membrane vesicles of *Francisella novicida* suggests possible role in virulence and use as a vaccine. *J. Proteome Res.* 10, 954–967 (2011).
57. Lee BY, Horwitz MA, Clemens DL. Identification, recombinant expression, immunolocalization in macrophages, and T-cell responsiveness of the major extracellular proteins of *Francisella tularensis*. *Infect. Immun.* 74, 4002–4013 (2006).
58. Lindgren H, Shen H, Zingmark C *et al.* Resistance of *Francisella* strains against reactive nitrogen and oxygen species with special reference to the role of KatG. *Infect. Immun.* 75, 1303–1309 (2007).
59. Melillo AA, Bakshi CS, Melendez JA. *Francisella tularensis* antioxidants harness reactive oxygen species to restrict macrophage signaling and cytokine production. *J. Biol. Chem.* 285, 27553–27560 (2010).
60. Huntley JF, Conley PG, Hagman KE, Norgard MV. Characterization of *Francisella tularensis* outer membrane proteins. *J. Bacteriol.* 189, 561–574 (2007).
61. Mohapatra NP, Soni S, Reilly TJ *et al.* Combined deletion of four *Francisella novicida* acid phosphatases attenuates virulence and macrophage vacuolar escape. *Infect. Immun.* 76, 3690–3699 (2008).
62. Mohapatra NP, Soni S, Rajaram MV *et al.* *Francisella* acid phosphatases inactivate the NADPH oxidase in human phagocytes. *J. Immunol.* 184, 5141–5150 (2010).
63. Felts RL, Reilly TJ, Tanner JJ. Structure of *Francisella tularensis* AcpA: prototype of a unique superfamily of acid phosphatases and phospholipases C. *J. Biol. Chem.* 281, 30289–30298 (2006).
64. Mohapatra N, Balagopal A, Soni S, Schlesinger L, Gunn J. AcpA is a *Francisella* acid phosphatase that affects intramacrophage survival and virulence. *Infect. Immun.* 75, 390–396 (2007).
65. Dai S, Mohapatra NP, Schlesinger LS, Gunn JS. The acid phosphatase AcpA is secreted *in vitro* and in macrophages by *Francisella* spp. *Infect. Immun.* 80, 1088–1097 (2012).

- **Reports the secretion of AcpA in macrophages.**

66. Child R, Wehrly TD, Rockx-Brouwer D, Dorward DW, Celli J. Acid phosphatases do not contribute to the pathogenesis of type A *Francisella tularensis*. *Infect. Immun.* 78, 59–67 (2010).
67. McCaffrey RL, Schwartz JT, Lindemann SR *et al.* Multiple mechanisms of NADPH oxidase inhibition by type A and type B *Francisella tularensis*. *J. Leukoc. Biol.* 88, 791–805 (2010).
68. Gunn JS, Ernst RK. The structure and function of *Francisella* lipopolysaccharide. *Ann. NY Acad. Sci.* 1105, 202–218 (2007).
69. Raetz CR, Guan Z, Ingram BO *et al.* Discovery of new biosynthetic pathways: the lipid A story. *J. Lipid Res.* 50(Suppl.), S103–S108 (2009).

- **Reviews the biosynthetic pathways of the *F. tularensis* lipopolysaccharide.**

70. Soni S, Ernst RK, Muszynski A *et al.* *Francisella tularensis* blue–gray phase variation involves structural modifications of lipopolysaccharide O-antigen, core and lipid a and affects intramacrophage survival and vaccine efficacy. *Front. Microbiol.* 1, 129 (2010).
71. Lindemann SR, Peng K, Long ME *et al.* *Francisella tularensis* SCHU S4 O-antigen and capsule biosynthesis gene mutants induce early cell death in human macrophages. *Infect. Immun.* 79, 581–594 (2011).
72. Peng K, Broz P, Jones J, Joubert LM, Monack D. Elevated AIM2-mediated pyroptosis triggered by hypercytotoxic *Francisella* mutant strains is attributed to increased intracellular bacteriolysis. *Cell. Microbiol.* 13, 1586–1600 (2011).
73. Clemens DL, Lee BY, Horwitz MA. O-antigen-deficient *Francisella tularensis* live vaccine strain mutants are ingested via an aberrant form of looping phagocytosis and show altered kinetics of intracellular trafficking in human macrophages. *Infect. Immun.* 80, 952–967 (2012).
74. Li Y, Powell DA, Shaffer SA *et al.* LPS remodeling is an evolved survival strategy for bacteria. *Proc. Natl Acad. Sci. USA* 109, 8716–8721 (2012).
75. Beasley AS, Cotter RJ, Vogel SN *et al.* A variety of novel lipid A structures obtained from *Francisella tularensis* live vaccine strain. *Innate Immun.* 18, 268–278 (2012).
76. Zarrella TM, Singh A, Bitsaktsis C *et al.* Host-adaptation of *Francisella tularensis* alters the bacterium's surface-carbohydrates

to hinder effectors of innate and adaptive immunity. *PLoS One* 6, e22335 (2011).

77. Apicella MA, Post DM, Fowler AC *et al.* Identification, characterization and immunogenicity of an O-antigen capsular polysaccharide of *Francisella tularensis*. *PLoS One* 5, e11060 (2010).
78. Bandara AB, Champion AE, Wang X *et al.* Isolation and mutagenesis of a capsule-like complex (CLC) from *Francisella tularensis*, and contribution of the CLC to *F. tularensis* virulence in mice. *PLoS One* 6, e19003 (2011).
79. Su J, Asare R, Yang J *et al.* The *capBCA* locus is required for intracellular growth of *Francisella tularensis* LVS. *Front. Microbiol.* 2, 83 (2011).
80. Candela T, Fouet A. Poly-γ-glutamate in bacteria. *Mol. Microbiol.* 60, 1091–1098 (2006).
81. Raynaud C, Meibom KL, Lety MA *et al.* Role of the *wbt* locus of *Francisella tularensis* in lipopolysaccharide O-antigen biogenesis and pathogenicity. *Infect. Immun.* 75, 536–541 (2007).
82. Jia Q, Lee BY, Bowen R *et al.* A *Francisella tularensis* live vaccine strain (LVS) mutant with a deletion in *capB*, encoding a putative capsular biosynthesis protein, is significantly more attenuated than LVS yet induces potent protective immunity in mice against *F. tularensis* challenge. *Infect. Immun.* 78, 4341–4355 (2010).
83. Michell SL, Dean RE, Eyles JE *et al.* Deletion of the *Bacillus anthracis capB* homologue in *Francisella tularensis* subspecies *tularensis* generates an attenuated strain that protects mice against virulent tularaemia. *J. Med. Microbiol.* 59, 1275–1284 (2010).
84. Weiss DS, Brotcke A, Henry T *et al. In vivo* negative selection screen identifies genes required for *Francisella* virulence. *Proc. Natl Acad. Sci. USA* 104, 6037–6042 (2007).

▪ **First *in vivo* negative screening of banks of *F. tularensis* mutants.**

85. Kraemer PS, Mitchell A, Pelletier MR *et al.* Genome-wide screen in *Francisella novicida* for genes required for pulmonary and systemic infection in mice. *Infect. Immun.* 77, 232–244 (2009).
86. Moule MG, Monack DM, Schneider DS. Reciprocal analysis of *Francisella novicida* infections of a *Drosophila melanogaster* model reveal host–pathogen conflicts mediated by reactive oxygen and *imd*-regulated innate immune response. *PLoS Pathog.* 6, e1001065 (2010).
87. Straskova A, Pavkova I, Link M *et al.* Proteome analysis of an attenuated *Francisella tularensis dsbA* mutant: identification of potential DsbA substrate proteins. *J. Proteome Res.* 8, 5336–5346 (2009).
88. Qin A, Scott DW, Rabideau MM, Moore EA, Mann BJ. Requirement of the CXXC motif of novel *Francisella* infectivity potentiator protein B FipB, and FipA in virulence of *F. tularensis* subsp. *tularensis*. *PLoS One* 6, e24611 (2011).
89. Thomas RM, Twine SM, Fulton KM *et al.* Glycosylation of DsbA in *Francisella tularensis* subsp. *tularensis*. *J. Bacteriol.* 193, 5498–5509 (2011).
90. Balonova L, Mann BF, Cerveny L *et al.* Characterization of protein glycosylation in *Francisella tularensis* subsp. *holarctica*; identification of a novel glycosylated lipoprotein required for virulence. *Mol. Cell Proteomics* 11, M111.015016 (2012).
91. Ramakrishnan G, Sen B, Johnson R. Paralogous outer membrane proteins mediate uptake of different forms of iron and synergistically govern virulence in *Francisella tularensis tularensis*. *J. Biol. Chem.* 287, 25191–25202 (2012).
92. Nallaparaju KC, Yu JJ, Rodriguez SA *et al.* Evasion of IFN-γ signaling by *Francisella novicida* is dependent upon *Francisella* outer membrane protein C. *PLoS One* 6, e18201 (2011).
93. Sanapala S, Yu JJ, Murthy AK *et al.* Perforin- and granzyme-mediated cytotoxic effector functions are essential for protection against *Francisella tularensis* following vaccination by the defined *F. tularensis* subsp. *novicida* Δ*fopC* vaccine strain. *Infect. Immun.* 80, 2177–2185 (2012).
94. Jones CL, Sampson TR, Nakaya HI, Pulendran B, Weiss DS. Repression of bacterial lipoprotein production by *F. novicida* facilitates evasion of innate immune recognition. *Cell. Microbiol.* 14(10), 1531–1543 (2012).
95. Jones CL, Napier BA, Sampson TR *et al.* Subversion of host recognition and defense systems by *Francisella* spp. *Microbiol. Mol. Biol. Rev.* 76(2), 383–404 (2012).

▪▪ **Comprehensive review on the subversion of host cell defenses by intracellular *Francisella*.**

96. Eisenreich W, Dandekar T, Heesemann J, Goebel W. Carbon metabolism of intracellular bacterial pathogens and possible links to virulence. *Nat. Rev. Microbiol.* 8, 401–412 (2010).

▪▪ **Comprehensive review on the relationship between carbon metabolism and intracellular bacterial survival.**

97. Krewulak KD, Vogel HJ. Structural biology of bacterial iron uptake. *Biochim. Biophys. Acta* 1778, 1781–1804 (2008).
98. Hammer ND, Skaar EP. Molecular mechanisms of *Staphylococcus aureus* iron acquisition. *Annu. Rev. Microbiol.* 65, 129–147 (2011).
99. Sullivan JT, Jeffery EF, Shannon JD, Ramakrishnan G. Characterization of the siderophore of *Francisella tularensis* and role of *fslA* in siderophore production. *J. Bacteriol.* 188, 3785–3795 (2006).
100. Noinaj N, Guillier M, Barnard TJ, Buchanan SK. TonB-dependent transporters: regulation, structure, and function. *Annu. Rev. Microbiol.* 64, 43–60 (2010).
101. Deng K, Blick RJ, Liu W, Hansen EJ. Identification of *Francisella tularensis* genes affected by iron limitation. *Infect. Immun.* 74, 4224–4236 (2006).
102. Ramakrishnan G, Meeker A, Dragulev B. *fslE* is necessary for siderophore-mediated iron acquisition in *Francisella tularensis* SCHU S4. *J. Bacteriol.* 190, 5353–5361 (2008).
103. Lindgren H, Honn M, Golovlev I *et al.* The 58-kilodalton major virulence factor of *Francisella tularensis* is required for efficient utilization of iron. *Infect. Immun.* 77, 4429–4436 (2009).
104. Sen B, Meeker A, Ramakrishnan G. The *fslE* homolog, *FTL_0439* (*fupA/B*), mediates siderophore-dependent iron uptake in *Francisella tularensis* LVS. *Infect. Immun.* 78, 4276–4285 (2010).
105. Pechous RD, McCarthy TR, Zahrt TC. Working toward the future: insights into *Francisella tularensis* pathogenesis and vaccine development. *Microbiol. Mol. Biol. Rev.* 73, 684–711 (2009).
106. Bina XR, Lavine CL, Miller MA, Bina JE. The AcrAB RND efflux system from the live vaccine strain of *Francisella tularensis* is a multiple drug efflux system that is required for virulence in mice. *FEMS Microbiol. Lett.* 279, 226–233 (2008).
107. Qin A, Scott DW, Mann BJ. *Francisella tularensis* subsp. *tularensis* SCHU S4 disulfide bond formation protein B, but not an RND-type efflux pump, is required for virulence. *Infect. Immun.* 76, 3086–3092 (2008).
108. Tsukazaki T, Mori H, Echizen Y *et al.* Structure and function of a membrane component SecDF that enhances protein export. *Nature* 474, 235–238 (2011).
109. Llewellyn AC, Jones CL, Napier BA, Bina JE, Weiss DS. Macrophage replication screen identifies a novel *Francisella* hydroperoxide resistance protein involved in virulence. *PLoS One* 6, e24201 (2011).
110. Huang MT, Mortensen BL, Taxman DJ *et al.* Deletion of *ripA* alleviates suppression of the

inflammasome and MAPK by *Francisella tularensis*. *J. Immunol.* 185, 5476–5485 (2010).

111. Mortensen BL, Fuller JR, Taft-Benz S, Collins EJ, Kawula TH. *Francisella tularensis* RipA protein topology and identification of functional domains. *J. Bacteriol.* 194, 1474–1484 (2012).

112. Meibom KL, Barel M, Charbit A. Loops and networks in control of *Francisella tularensis* virulence. *Future Microbiol.* 4, 713–729 (2009).

113. Dai S, Mohapatra NP, Schlesinger LS, Gunn JS. Regulation of *Francisella tularensis* virulence. *Front. Microbiol.* 1, 144 (2010).

▪ **Comprehensive review on the regulatory systems of *F. tularensis*.**

114. Charity JC, Blalock LT, Costante-Hamm MM, Kasper DL, Dove SL. Small molecule control of virulence gene expression in *Francisella tularensis*. *PLoS Pathog.* 5, e1000641 (2009).

▪▪ **Demonstrates the role of guanosine tetraphosphate in *F. tularensis* gene regulation and virulence.**

Bibliographie

Abu Kwaik, Y. (1996). The phagosome containing Legionella pneumophila within the protozoan Hartmannella vermiformis is surrounded by the rough endoplasmic reticulum. Appl Environ Microbiol, *62*(6), 2022-2028.
Ahlund, M. K., Ryden, P., et al. (2010). Directed screen of Francisella novicida virulence determinants using Drosophila melanogaster. Infect Immun, *78*(7), 3118-3128.
Akimana, C., Al-Khodor, S., et al. (2010). Host factors required for modulation of phagosome biogenesis and proliferation of Francisella tularensis within the cytosol. PLoS One, *5*(6), e11025.
Al Dahouk, S., Jubier-Maurin, V., et al. (2013). Quantitative analysis of the Brucella suis proteome reveals metabolic adaptation to long-term nutrient starvation. BMC Microbiol, *13*199.
Alkhuder, K., Meibom, K. L., et al. (2009). Glutathione provides a source of cysteine essential for intracellular multiplication of Francisella tularensis. PLoS Pathog, *5*(1), e1000284.
Amores-Sanchez, M. I., & Medina, M. A. (1999). Glutamine, as a precursor of glutathione, and oxidative stress. Mol Genet Metab, *67*(2), 100-105.
Andersson, H., Hartmanova, B., et al. (2006). A microarray analysis of the murine macrophage response to infection with Francisella tularensis LVS. J Med Microbiol, *55*(Pt 8), 1023-1033.
Andersson, J. O., & Andersson, S. G. (1999). Insights into the evolutionary process of genome degradation. Curr Opin Genet Dev, *9*(6), 664-671.
Andrew, P. J., & Mayer, B. (1999). Enzymatic function of nitric oxide synthases. Cardiovasc Res, *43*(3), 521-531.
Anthony, L. S., & Kongshavn, P. A. (1988). H-2 restriction in acquired cell-mediated immunity to infection with Francisella tularensis LVS. Infect Immun, *56*(2), 452-456.
Apicella, M. A., Post, D. M., et al. (2010). Identification, characterization and immunogenicity of an O-antigen capsular polysaccharide of Francisella tularensis. PLoS One, *5*(7), e11060.
Arnoult, D., Soares, F., et al. (2011). Mitochondria in innate immunity. EMBO Rep, *12*(9), 901-910.
Asare, R., & Abu Kwaik, Y. (2010a). Molecular complexity orchestrates modulation of phagosome biogenesis and escape to the cytosol of macrophages by Francisella tularensis. Environ Microbiol, *12*(9), 2559-2586.
Asare, R., & Kwaik, Y. A. (2010b). Exploitation of host cell biology and evasion of immunity by francisella tularensis. Front Microbiol, *1*145.
Atkins, H. S., Dassa, E., et al. (2006). The identification and evaluation of ATP binding cassette systems in the intracellular bacterium Francisella tularensis. Res Microbiol, *157*(6), 593-604.
Babior, B. M. (2004). NADPH oxidase. Curr Opin Immunol, *16*(1), 42-47.
Baca, O. G., Roman, M. J., et al. (1993). Acid phosphatase activity in Coxiella burnetii: a possible virulence factor. Infect Immun, *61*(10), 4232-4239.
Bakshi, C. S., Malik, M., et al. (2006). Superoxide dismutase B gene (sodB)-deficient mutants of Francisella tularensis demonstrate hypersensitivity to oxidative stress and attenuated virulence. J Bacteriol, *188*(17), 6443-6448.
Balagopal, A., MacFarlane, A. S., et al. (2006). Characterization of the receptor-ligand pathways important for entry and survival of Francisella tularensis in human macrophages. Infect Immun, *74*(9), 5114-5125.

Baldridge, C. W., & Gerard, R. W. (1932). The extra respirtion of phagocytosis. American Journal of Physiology, *103*235-236.

Balonova, L., Hernychova, L., et al. (2010). Multimethodological approach to identification of glycoproteins from the proteome of Francisella tularensis, an intracellular microorganism. J Proteome Res, *9*(4), 1995-2005.

Banga, S., Gao, P., et al. (2007). Legionella pneumophila inhibits macrophage apoptosis by targeting pro-death members of the Bcl2 protein family. Proc Natl Acad Sci U S A, *104*(12), 5121-5126.

Barel, M., Hovanessian, A. G., et al. (2008). A novel receptor - ligand pathway for entry of Francisella tularensis in monocyte-like THP-1 cells: interaction between surface nucleolin and bacterial elongation factor Tu. BMC Microbiol, *8*145.

Barel, M., Meibom, K., et al. (2012). Francisella tularensis regulates the expression of the amino acid transporter SLC1A5 in infected THP-1 human monocytes. Cell Microbiol, *14*(11), 1769-1783.

Barker, J. R., Chong, A., et al. (2009). The Francisella tularensis pathogenicity island encodes a secretion system that is required for phagosome escape and virulence. Mol Microbiol, *74*(6), 1459-1470.

Barker, J. R., & Klose, K. E. (2007). Molecular and genetic basis of pathogenesis in Francisella tularensis. Ann N Y Acad Sci, *1105*138-159.

Baron, G. S., & Nano, F. E. (1998). MglA and MglB are required for the intramacrophage growth of Francisella novicida. Mol Microbiol, *29*(1), 247-259.

Bearson, B. L., Lee, I. S., et al. (2009). Escherichia coli O157 : H7 glutamate- and arginine-dependent acid-resistance systems protect against oxidative stress during extreme acid challenge. Microbiology, *155*(Pt 3), 805-812.

Beisel, W. R. (1975). Metabolic response to infection. Annu Rev Med, *26*9-20.

Bell, B. L., Mohapatra, N. P., et al. (2010). Regulation of virulence gene transcripts by the Francisella novicida orphan response regulator PmrA: role of phosphorylation and evidence of MglA/SspA interaction. Infect Immun, *78*(5), 2189-2198.

Berlett, B. S., & Stadtman, E. R. (1997). Protein oxidation in aging, disease, and oxidative stress. J Biol Chem, *272*(33), 20313-20316.

Bethani, I., Lang, T., et al. (2007). The specificity of SNARE pairing in biological membranes is mediated by both proof-reading and spatial segregation. EMBO J, *26*(17), 3981-3992.

Biteau, B., Labarre, J., et al. (2003). ATP-dependent reduction of cysteine-sulphinic acid by S. cerevisiae sulphiredoxin. Nature, *425*(6961), 980-984.

Bonquist, L., Lindgren, H., et al. (2008). MglA and Igl proteins contribute to the modulation of Francisella tularensis live vaccine strain-containing phagosomes in murine macrophages. Infect Immun, *76*(8), 3502-3510.

Borregaard, N., Kjeldsen, L., et al. (1995). Granules and secretory vesicles of the human neutrophil. Clin Exp Immunol, *101 Suppl 1*6-9.

Bowater, R., & Doherty, A. J. (2006). Making ends meet: repairing breaks in bacterial DNA by non-homologous end-joining. PLoS Genet, *2*(2), e8.

Bozzi, M., Mignogna, G., et al. (1997). A novel non-heme iron-binding ferritin related to the DNA-binding proteins of the Dps family in Listeria innocua. J Biol Chem, *272*(6), 3259-3265.

Bradbury, A. J., Gruer, M. J., et al. (1996). The second aconitase (AcnB) of Escherichia coli. Microbiology, *142 (Pt 2)*389-400.

Braeken, K., Moris, M., et al. (2006). New horizons for (p)ppGpp in bacterial and plant physiology. Trends Microbiol, *14*(1), 45-54.

Broekhuijsen, M., Larsson, P., et al. (2003). Genome-wide DNA microarray analysis of Francisella tularensis strains demonstrates extensive genetic conservation within the species but identifies regions that are unique to the highly virulent F. tularensis subsp. tularensis. J Clin Microbiol, *41*(7), 2924-2931.

Broms, J. E., Lavander, M., et al. (2011). IglG and IglI of the Francisella pathogenicity island are important virulence determinants of Francisella tularensis LVS. Infect Immun, *79*(9), 3683-3696.

Broms, J. E., Meyer, L., et al. (2012). DotU and VgrG, core components of type VI secretion systems, are essential for Francisella LVS pathogenicity. PLoS One, *7*(4), e34639.

Brotcke, A., & Monack, D. M. (2008). Identification of fevR, a novel regulator of virulence gene expression in Francisella novicida. Infect Immun, *76*(8), 3473-3480.

Brotcke, A., Weiss, D. S., et al. (2006). Identification of MglA-regulated genes reveals novel virulence factors in Francisella tularensis. Infect Immun, *74*(12), 6642-6655.

Bubert, A., Riebe, J., et al. (1997). Isolation of catalase-negative Listeria monocytogenes strains from listeriosis patients and their rapid identification by anti-p60 antibodies and/or PCR. J Clin Microbiol, *35*(1), 179-183.

Bubici, C., Papa, S., et al. (2006). The NF-kappaB-mediated control of ROS and JNK signaling. Histol Histopathol, *21*(1), 69-80.

Buchan, B. W., McCaffrey, R. L., et al. (2009). Identification of migR, a regulatory element of the Francisella tularensis live vaccine strain iglABCD virulence operon required for normal replication and trafficking in macrophages. Infect Immun, *77*(6), 2517-2529.

Buchmeier, N. A., Libby, S. J., et al. (1995). DNA repair is more important than catalase for Salmonella virulence in mice. J Clin Invest, *95*(3), 1047-1053.

Butala, M., Zgur-Bertok, D., et al. (2009). The bacterial LexA transcriptional repressor. Cell Mol Life Sci, *66*(1), 82-93.

Cabiscol, E., Tamarit, J., et al. (2000). Oxidative stress in bacteria and protein damage by reactive oxygen species. Int Microbiol, *3*(1), 3-8.

Caipang, C. M., Kulkarni, A., et al. (2010). Detection of Francisella piscicida in Atlantic cod (Gadus morhua L) by the loop-mediated isothermal amplification (LAMP) reaction. Vet J, *184*(3), 357-361.

Carlisle, H. N., & Saslaw, S. (1962). Studies with tularemia vaccines in volunteers. VI. Assessment of role of properdin in resistance. Proc Soc Exp Biol Med, *110*603-605.

Carlson, P. E., Jr., Horzempa, J., et al. (2009). Global transcriptional response to spermine, a component of the intramacrophage environment, reveals regulation of Francisella gene expression through insertion sequence elements. J Bacteriol, *191*(22), 6855-6864.

Casadevall, A. (2008). Evolution of intracellular pathogens. Annu Rev Microbiol, *62*19-33.

Cashel, M., & Kalbacher, B. (1970). The control of ribonucleic acid synthesis in Escherichia coli. V. Characterization of a nucleotide associated with the stringent response. J Biol Chem, *245*(9), 2309-2318.

Cassat, J. E., & Skaar, E. P. (2013). Iron in infection and immunity. Cell Host Microbe, *13*(5), 509-519.

Castanie-Cornet, M. P., Penfound, T. A., et al. (1999). Control of acid resistance in Escherichia coli. J Bacteriol, *181*(11), 3525-3535.

Ceci, P., Ilari, A., et al. (2005). Reassessment of protein stability, DNA binding, and protection of Mycobacterium smegmatis Dps. J Biol Chem, *280*(41), 34776-34785.
Cellier, M. F., Courville, P., et al. (2007). Nramp1 phagocyte intracellular metal withdrawal defense. Microbes Infect, *9*(14-15), 1662-1670.
Chamberlain, R. E. (1965). Evaluation of Live Tularemia Vaccine Prepared in a Chemically Defined Medium. Appl Microbiol, *13*232-235.
Champion, M. D., Zeng, Q., et al. (2009). Comparative genomic characterization of Francisella tularensis strains belonging to low and high virulence subspecies. PLoS Pathog, *5*(5), e1000459.
Charity, J. C., Blalock, L. T., et al. (2009). Small molecule control of virulence gene expression in Francisella tularensis. PLoS Pathog, *5*(10), e1000641.
Charity, J. C., Costante-Hamm, M. M., et al. (2007). Twin RNA polymerase-associated proteins control virulence gene expression in Francisella tularensis. PLoS Pathog, *3*(6), e84.
Chatgilialoglu, C., & O'Neill, P. (2001). Free radicals associated with DNA damage. Exp Gerontol, *36*(9), 1459-1471.
Chatterjee, S. S., Hossain, H., et al. (2006). Intracellular gene expression profile of Listeria monocytogenes. Infect Immun, *74*(2), 1323-1338.
Checroun, C., Wehrly, T. D., et al. (2006). Autophagy-mediated reentry of Francisella tularensis into the endocytic compartment after cytoplasmic replication. Proc Natl Acad Sci U S A, *103*(39), 14578-14583.
Chen, Y., Bystricky, P., et al. (2007). The capsule polysaccharide structure and biogenesis for non-O1 Vibrio cholerae NRT36S: genes are embedded in the LPS region. BMC Microbiol, *7*20.
Chong, A., & Celli, J. (2010). The francisella intracellular life cycle: toward molecular mechanisms of intracellular survival and proliferation. Front Microbiol, *1*138.
Chong, A., Wehrly, T. D., et al. (2008a). The early phagosomal stage of Francisella tularensis determines optimal phagosomal escape and Francisella pathogenicity island protein expression. Infect Immun, *76*(12), 5488-5499.
Chong, A., Wehrly, T. D., et al. (2008b). The early phagosomal stage of Francisella tularensis determines optimal phagosomal escape and Francisella pathogenicity island protein expression. Infect Immun, *76*(12), 5488-5499.
Choy, A., Dancourt, J., et al. (2012). The Legionella effector RavZ inhibits host autophagy through irreversible Atg8 deconjugation. Science, *338*(6110), 1072-1076.
Christiansen, J. K., Larsen, M. H., et al. (2004). The RNA-binding protein Hfq of Listeria monocytogenes: role in stress tolerance and virulence. J Bacteriol, *186*(11), 3355-3362.
Christman, M. F., Morgan, R. W., et al. (1985). Positive control of a regulon for defenses against oxidative stress and some heat-shock proteins in Salmonella typhimurium. Cell, *41*(3), 753-762.
Christoforidis, S., Miaczynska, M., et al. (1999). Phosphatidylinositol-3-OH kinases are Rab5 effectors. Nat Cell Biol, *1*(4), 249-252.
Chung, C. H. (1993). Proteases in Escherichia coli. Science, *262*(5132), 372-374.
Clemens, D. L., & Horwitz, M. A. (2007). Uptake and intracellular fate of Francisella tularensis in human macrophages. Ann N Y Acad Sci, *1105*160-186.
Clemens, D. L., Lee, B. Y., et al. (2004). Virulent and avirulent strains of Francisella tularensis prevent acidification and maturation of their phagosomes and escape into the cytoplasm in human macrophages. Infect Immun, *72*(6), 3204-3217.

Clemens, D. L., Lee, B. Y., et al. (2005). Francisella tularensis enters macrophages via a novel process involving pseudopod loops. Infect Immun, *73*(9), 5892-5902.
Clemens, D. L., Lee, B. Y., et al. (2009). Francisella tularensis phagosomal escape does not require acidification of the phagosome. Infect Immun, *77*(5), 1757-1773.
Collins, H. L. (2003). The role of iron in infections with intracellular bacteria. Immunol Lett, *85*(2), 193-195.
Colquhoun, D. J., & Duodu, S. (2011). Francisella infections in farmed and wild aquatic organisms. Vet Res, *42*47.
Cunningham, L., Gruer, M. J., et al. (1997). Transcriptional regulation of the aconitase genes (acnA and acnB) of Escherichia coli. Microbiology, *143 (Pt 12)*3795-3805.
Dallo, S. F., & Weitao, T. (2010). Bacteria under SOS evolve anticancer phenotypes. Infect Agent Cancer, *5*(1), 3.
Das, P., Lahiri, A., et al. (2010). Modulation of the arginase pathway in the context of microbial pathogenesis: a metabolic enzyme moonlighting as an immune modulator. PLoS Pathog, *6*(6), e1000899.
de Bruin, O. M., Ludu, J. S., et al. (2007). The Francisella pathogenicity island protein IglA localizes to the bacterial cytoplasm and is needed for intracellular growth. BMC Microbiol, *7*1.
Dean, R. E., Ireland, P. M., et al. (2009). RelA regulates virulence and intracellular survival of Francisella novicida. Microbiology, *155*(Pt 12), 4104-4113.
Dean, R. T., Fu, S., et al. (1997). Biochemistry and pathology of radical-mediated protein oxidation. Biochem J, *324 (Pt 1)*1-18.
Della, M., Palmbos, P. L., et al. (2004). Mycobacterial Ku and ligase proteins constitute a two-component NHEJ repair machine. Science, *306*(5696), 683-685.
Deng, K., Blick, R. J., et al. (2006). Identification of Francisella tularensis genes affected by iron limitation. Infect Immun, *74*(7), 4224-4236.
Dennis, D. T., Inglesby, T. V., et al. (2001). Tularemia as a biological weapon: medical and public health management. JAMA, *285*(21), 2763-2773.
Desvaux, M., Hebraud, M., et al. (2009). Secretion and subcellular localizations of bacterial proteins: a semantic awareness issue. Trends Microbiol, *17*(4), 139-145.
Deussing, J., Roth, W., et al. (1998). Cathepsins B and D are dispensable for major histocompatibility complex class II-mediated antigen presentation. Proc Natl Acad Sci U S A, *95*(8), 4516-4521.
Dianov, G. L., Sleeth, K. M., et al. (2003). Repair of abasic sites in DNA. Mutat Res, *531*(1-2), 157-163.
Diekmann, D., Abo, A., et al. (1994). Interaction of Rac with p67phox and regulation of phagocytic NADPH oxidase activity. Science, *265*(5171), 531-533.
Dieppedale, J., Sobral, D., et al. (2011). Identification of a putative chaperone involved in stress resistance and virulence in Francisella tularensis. Infect Immun, *79*(4), 1428-1439.
Dizdaroglu, M. (2012). Oxidatively induced DNA damage: mechanisms, repair and disease. Cancer Lett, *327*(1-2), 26-47.
Doumith, M., Cazalet, C., et al. (2004). New aspects regarding evolution and virulence of Listeria monocytogenes revealed by comparative genomics and DNA arrays. Infect Immun, *72*(2), 1072-1083.
Dunn, W. A., Jr. (1990). Studies on the mechanisms of autophagy: formation of the autophagic vacuole. J Cell Biol, *110*(6), 1923-1933.

Edwards, J. A., Rockx-Brouwer, D., et al. (2010). Restricted cytosolic growth of Francisella tularensis subsp. tularensis by IFN-gamma activation of macrophages. Microbiology, *156*(Pt 2), 327-339.

Egge-Jacobsen, W., Salomonsson, E. N., et al. (2011). O-linked glycosylation of the PilA pilin protein of Francisella tularensis: identification of the endogenous protein-targeting oligosaccharyltransferase and characterization of the native oligosaccharide. J Bacteriol, *193*(19), 5487-5497.

Eisenreich, W., Dandekar, T., et al. (2010). Carbon metabolism of intracellular bacterial pathogens and possible links to virulence. Nat Rev Microbiol, *8*(6), 401-412.

Eisenreich, W., Heesemann, J., et al. (2013). Metabolic host responses to infection by intracellular bacterial pathogens. Front Cell Infect Microbiol, *3*24.

Eliasson, H., Lindback, J., et al. (2002). The 2000 tularemia outbreak: a case-control study of risk factors in disease-endemic and emergent areas, Sweden. Emerg Infect Dis, *8*(9), 956-960.

Ericsson, M., Tarnvik, A., et al. (1994). Increased synthesis of DnaK, GroEL, and GroES homologs by Francisella tularensis LVS in response to heat and hydrogen peroxide. Infect Immun, *62*(1), 178-183.

Eswarappa, S. M. (2009). Location of pathogenic bacteria during persistent infections: insights from an analysis using game theory. PLoS One, *4*(4), e5383.

Fang, F. C. (2004). Antimicrobial reactive oxygen and nitrogen species: concepts and controversies. Nat Rev Microbiol, *2*(10), 820-832.

Fang, F. C., Libby, S. J., et al. (2005). Isocitrate lyase (AceA) is required for Salmonella persistence but not for acute lethal infection in mice. Infect Immun, *73*(4), 2547-2549.

Feehily, C., & Karatzas, K. A. (2013). Role of glutamate metabolism in bacterial responses towards acid and other stresses. J Appl Microbiol, *114*(1), 11-24.

Forsman, M., Sandstrom, G., et al. (1994). Analysis of 16S ribosomal DNA sequences of Francisella strains and utilization for determination of the phylogeny of the genus and for identification of strains by PCR. Int J Syst Bacteriol, *44*(1), 38-46.

Fuchs, T. M., Eisenreich, W., et al. (2012). Metabolic adaptation of human pathogenic and related nonpathogenic bacteria to extra- and intracellular habitats. FEMS Microbiol Rev, *36*(2), 435-462.

Ganley, I. G., Carroll, K., et al. (2004). Rab9 GTPase regulates late endosome size and requires effector interaction for its stability. Mol Biol Cell, *15*(12), 5420-5430.

Gee, J. M., Valderas, M. W., et al. (2005). The Brucella abortus Cu,Zn superoxide dismutase is required for optimal resistance to oxidative killing by murine macrophages and wild-type virulence in experimentally infected mice. Infect Immun, *73*(5), 2873-2880.

Gibbings, S., Elkins, N. D., et al. (2011). Xanthine oxidoreductase promotes the inflammatory state of mononuclear phagocytes through effects on chemokine expression, peroxisome proliferator-activated receptor-{gamma} sumoylation, and HIF-1{alpha}. J Biol Chem, *286*(2), 961-975.

Gil, H., Benach, J. L., et al. (2004). Presence of pili on the surface of Francisella tularensis. Infect Immun, *72*(5), 3042-3047.

Girotti, A. W. (1998). Lipid hydroperoxide generation, turnover, and effector action in biological systems. J Lipid Res, *39*(8), 1529-1542.

Goetz, M., Bubert, A., et al. (2001). Microinjection and growth of bacteria in the cytosol of mammalian host cells. Proc Natl Acad Sci U S A, *98*(21), 12221-12226.

Goldberg, I., & Hochman, A. (1989). Three different types of catalases in Klebsiella pneumoniae. Arch Biochem Biophys, *268*(1), 124-128.
Golovliov, I., Ericsson, M., et al. (1997). Identification of proteins of Francisella tularensis induced during growth in macrophages and cloning of the gene encoding a prominently induced 23-kilodalton protein. Infect Immun, *65*(6), 2183-2189.
Goon, S., Kelly, J. F., et al. (2003). Pseudaminic acid, the major modification on Campylobacter flagellin, is synthesized via the Cj1293 gene. Mol Microbiol, *50*(2), 659-671.
Grall, N., Livny, J., et al. (2009). Pivotal role of the Francisella tularensis heat-shock sigma factor RpoH. Microbiology, *155*(Pt 8), 2560-2572.
Grant, R. A., Filman, D. J., et al. (1998). The crystal structure of Dps, a ferritin homolog that binds and protects DNA. Nat Struct Biol, *5*(4), 294-303.
Gray, C. G., Cowley, S. C., et al. (2002). The identification of five genetic loci of Francisella novicida associated with intracellular growth. FEMS Microbiol Lett, *215*(1), 53-56.
Green, J., & Paget, M. S. (2004). Bacterial redox sensors. Nat Rev Microbiol, *2*(12), 954-966.
Grune, T., Reinheckel, T., et al. (1997). Degradation of oxidized proteins in mammalian cells. FASEB J, *11*(7), 526-534.
Guina, T., Radulovic, D., et al. (2007). MglA regulates Francisella tularensis subsp. novicida (Francisella novicida) response to starvation and oxidative stress. J Bacteriol, *189*(18), 6580-6586.
Gunn, J. S. (2008). The Salmonella PmrAB regulon: lipopolysaccharide modifications, antimicrobial peptide resistance and more. Trends Microbiol, *16*(6), 284-290.
Haas, A., & Goebel, W. (1992). Cloning of a superoxide dismutase gene from Listeria ivanovii by functional complementation in Escherichia coli and characterization of the gene product. Mol Gen Genet, *231*(2), 313-322.
Halsey, T. A., Vazquez-Torres, A., et al. (2004). The ferritin-like Dps protein is required for Salmonella enterica serovar Typhimurium oxidative stress resistance and virulence. Infect Immun, *72*(2), 1155-1158.
Hanada, T., Noda, N. N., et al. (2007). The Atg12-Atg5 conjugate has a novel E3-like activity for protein lipidation in autophagy. J Biol Chem, *282*(52), 37298-37302.
Hancock, R. E., & Diamond, G. (2000). The role of cationic antimicrobial peptides in innate host defences. Trends Microbiol, *8*(9), 402-410.
Hansson, C., & Ingvarsson, T. (2002). Two cases of tularaemia after an orienteering contest on the non-endemic Island of Bornholm. Scand J Infect Dis, *34*(1), 76.
Hayashi-Nishino, M., Fukushima, A., et al. (2012). Impact of hfq on the intrinsic drug resistance of salmonella enterica serovar typhimurium. Front Microbiol, *3*205.
He, C., & Klionsky, D. J. (2009). Regulation mechanisms and signaling pathways of autophagy. Annu Rev Genet, *43*67-93.
Hébrard, M. (2010). *Etude des systèmes antioxydants dans le métabolisme et la virulence de Salmonella typhimurium.* Aix-Marseille 2.
Hebrard, M., Viala, J. P., et al. (2009). Redundant hydrogen peroxide scavengers contribute to Salmonella virulence and oxidative stress resistance. J Bacteriol, *191*(14), 4605-4614.
Heinzen, R. A., Howe, D., et al. (1996). Developmentally regulated synthesis of an unusually small, basic peptide by Coxiella burnetii. Mol Microbiol, *22*(1), 9-19.
Henry, T., Brotcke, A., et al. (2007). Type I interferon signaling is required for activation of the inflammasome during Francisella infection. J Exp Med, *204*(5), 987-994.

Holland, I. B., Schmitt, L., et al. (2005). Type 1 protein secretion in bacteria, the ABC-transporter dependent pathway (review). Mol Membr Biol, *22*(1-2), 29-39.
Hollis, D. G., Weaver, R. E., et al. (1989). Francisella philomiragia comb. nov. (formerly Yersinia philomiragia) and Francisella tularensis biogroup novicida (formerly Francisella novicida) associated with human disease. J Clin Microbiol, *27*(7), 1601-1608.
Honer zu Bentrup, K., & Russell, D. G. (2001). Mycobacterial persistence: adaptation to a changing environment. Trends Microbiol, *9*(12), 597-605.
Honn, M., Lindgren, H., et al. (2012). The role of MglA for adaptation to oxidative stress of Francisella tularensis LVS. BMC Microbiol, *12*14.
Horwitz, M. A. (1984). Phagocytosis of the Legionnaires' disease bacterium (Legionella pneumophila) occurs by a novel mechanism: engulfment within a pseudopod coil. Cell, *36*(1), 27-33.
Horzempa, J., Carlson, P. E., Jr., et al. (2008). Global transcriptional response to mammalian temperature provides new insight into Francisella tularensis pathogenesis. BMC Microbiol, *8*172.
Huber, B., Escudero, R., et al. (2010). Description of Francisella hispaniensis sp. nov., isolated from human blood, reclassification of Francisella novicida (Larson et al. 1955) Olsufiev et al. 1959 as Francisella tularensis subsp. novicida comb. nov. and emended description of the genus Francisella. Int J Syst Evol Microbiol, *60*(Pt 8), 1887-1896.
Huynh, K. K., Eskelinen, E. L., et al. (2007). LAMP proteins are required for fusion of lysosomes with phagosomes. EMBO J, *26*(2), 313-324.
Ireton, K. (2013). Molecular mechanisms of cell-cell spread of intracellular bacterial pathogens. Open Biol, *3*(7), 130079.
Jackson, S. M., & Cooper, J. B. (1998). An analysis of structural similarity in the iron and manganese superoxide dismutases based on known structures and sequences. Biometals, *11*(2), 159-173.
Jacobs, A. L., & Schar, P. (2012). DNA glycosylases: in DNA repair and beyond. Chromosoma, *121*(1), 1-20.
Jain, V., Kumar, M., et al. (2006). ppGpp: stringent response and survival. J Microbiol, *44*(1), 1-10.
Jeong, W., Cha, M. K., et al. (2000). Thioredoxin-dependent hydroperoxide peroxidase activity of bacterioferritin comigratory protein (BCP) as a new member of the thiol-specific antioxidant protein (TSA)/Alkyl hydroperoxide peroxidase C (AhpC) family. J Biol Chem, *275*(4), 2924-2930.
Jones, J. W., Broz, P., et al. (2011). Innate immune recognition of francisella tularensis: activation of type-I interferons and the inflammasome. Front Microbiol, *2*16.
Josenhans, C., Vossebein, L., et al. (2002). The neuA/flmD gene cluster of Helicobacter pylori is involved in flagellar biosynthesis and flagellin glycosylation. FEMS Microbiol Lett, *210*(2), 165-172.
Kadzhaev, K., Zingmark, C., et al. (2009). Identification of genes contributing to the virulence of Francisella tularensis SCHU S4 in a mouse intradermal infection model. PLoS One, *4*(5), e5463.
Kanemori, M., Nishihara, K., et al. (1997). Synergistic roles of HslVU and other ATP-dependent proteases in controlling in vivo turnover of sigma32 and abnormal proteins in Escherichia coli. J Bacteriol, *179*(23), 7219-7225.
Kayal, S., & Charbit, A. (2006). Listeriolysin O: a key protein of Listeria monocytogenes with multiple functions. FEMS Microbiol Rev, *30*(4), 514-529.

Kim, J. A., & Mayfield, J. (2000). Identification of Brucella abortus OxyR and its role in control of catalase expression. J Bacteriol, *182*(19), 5631-5633.
Kingry, L. C., & Petersen, J. M. (2014). Comparative review of Francisella tularensis and Francisella novicida. Front Cell Infect Microbiol, *4*35.
Kiss, K., Liu, W., et al. (2008). Characterization of fig operon mutants of Francisella novicida U112. FEMS Microbiol Lett, *285*(2), 270-277.
Koay, M. A., Christman, J. W., et al. (2001). Impaired pulmonary NF-kappaB activation in response to lipopolysaccharide in NADPH oxidase-deficient mice. Infect Immun, *69*(10), 5991-5996.
Kraemer, P. S., Mitchell, A., et al. (2009). Genome-wide screen in Francisella novicida for genes required for pulmonary and systemic infection in mice. Infect Immun, *77*(1), 232-244.
Kulp, A., & Kuehn, M. J. (2010). Biological functions and biogenesis of secreted bacterial outer membrane vesicles. Annu Rev Microbiol, *64*163-184.
Kummel, D., & Ungermann, C. (2014). Principles of membrane tethering and fusion in endosome and lysosome biogenesis. Curr Opin Cell Biol, *29C*61-66.
Kurokawa, T., Masuda, H., et al. (1961). Studies on the skin test of Yato-Byo (Ohara's disease, tularemia in Japan). 4th. Results of the skin test in Miyagi Prefecture. Tohoku J Exp Med, *73*268-273.
Laguna, R. K., Creasey, E. A., et al. (2006). A Legionella pneumophila-translocated substrate that is required for growth within macrophages and protection from host cell death. Proc Natl Acad Sci U S A, *103*(49), 18745-18750.
Lai, X. H., Golovliov, I., et al. (2001). Francisella tularensis induces cytopathogenicity and apoptosis in murine macrophages via a mechanism that requires intracellular bacterial multiplication. Infect Immun, *69*(7), 4691-4694.
Lai, X. H., Shirley, R. L., et al. (2010). Mutations of Francisella novicida that alter the mechanism of its phagocytosis by murine macrophages. PLoS One, *5*(7), e11857.
Larsson, P., Oyston, P. C., et al. (2005). The complete genome sequence of Francisella tularensis, the causative agent of tularemia. Nat Genet, *37*(2), 153-159.
Lauriano, C. M., Barker, J. R., et al. (2004). MglA regulates transcription of virulence factors necessary for Francisella tularensis intraamoebae and intramacrophage survival. Proc Natl Acad Sci U S A, *101*(12), 4246-4249.
Lee, I., & Suzuki, C. K. (2008). Functional mechanics of the ATP-dependent Lon protease-lessons from endogenous protein and synthetic peptide substrates. Biochim Biophys Acta, *1784*(5), 727-735.
Lehrer, R. I., Lichtenstein, A. K., et al. (1993). Defensins: antimicrobial and cytotoxic peptides of mammalian cells. Annu Rev Immunol, *11*105-128.
Lemire, J., Milandu, Y., et al. (2010). Histidine is a source of the antioxidant, alpha-ketoglutarate, in Pseudomonas fluorescens challenged by oxidative stress. FEMS Microbiol Lett, *309*(2), 170-177.
Lenco, J., Hubalek, M., et al. (2007). Proteomics analysis of the Francisella tularensis LVS response to iron restriction: induction of the F. tularensis pathogenicity island proteins IglABC. FEMS Microbiol Lett, *269*(1), 11-21.
Lenco, J., Link, M., et al. (2009). iTRAQ quantitative analysis of Francisella tularensis ssp. holarctica live vaccine strain and Francisella tularensis ssp. tularensis SCHU S4 response to different temperatures and stationary phases of growth. Proteomics, *9*(10), 2875-2882.

Lenco, J., Pavkova, I., et al. (2005). Insights into the oxidative stress response in Francisella tularensis LVS and its mutant DeltaiglC1+2 by proteomics analysis. FEMS Microbiol Lett, *246*(1), 47-54.

Levesque, B., De Serres, G., et al. (1995). Seroepidemiologic study of three zoonoses (leptospirosis, Q fever, and tularemia) among trappers in Quebec, Canada. Clin Diagn Lab Immunol, *2*(4), 496-498.

Li, J. M., & Shah, A. M. (2001). Differential NADPH- versus NADH-dependent superoxide production by phagocyte-type endothelial cell NADPH oxidase. Cardiovasc Res, *52*(3), 477-486.

Lieu, P. T., Heiskala, M., et al. (2001). The roles of iron in health and disease. Mol Aspects Med, *22*(1-2), 1-87.

Lindgren, H., Golovliov, I., et al. (2004a). Factors affecting the escape of Francisella tularensis from the phagolysosome. J Med Microbiol, *53*(Pt 10), 953-958.

Lindgren, H., Shen, H., et al. (2007). Resistance of Francisella tularensis strains against reactive nitrogen and oxygen species with special reference to the role of KatG. Infect Immun, *75*(3), 1303-1309.

Lindgren, H., Stenmark, S., et al. (2004b). Distinct roles of reactive nitrogen and oxygen species to control infection with the facultative intracellular bacterium Francisella tularensis. Infect Immun, *72*(12), 7172-7182.

Lindgren, M., Broms, J. E., et al. (2013a). The Francisella tularensis LVS DeltapdpC mutant exhibits a unique phenotype during intracellular infection. BMC Microbiol, *13*20.

Lindgren, M., Eneslatt, K., et al. (2013b). Importance of PdpC, IglC, IglI, and IglG for modulation of a host cell death pathway induced by Francisella tularensis. Infect Immun, *81*(6), 2076-2084.

Loeuillet, C., Martinon, F., et al. (2006). Mycobacterium tuberculosis subverts innate immunity to evade specific effectors. J Immunol, *177*(9), 6245-6255.

Lofgren, S., Tarnvik, A., et al. (1980). Demonstration of opsonizing antibodies to Francisella tularensis by leukocyte chemiluminescence. Infect Immun, *29*(2), 329-334.

Long, M. E., Lindemann, S. R., et al. (2013). Disruption of Francisella tularensis Schu S4 iglI, iglJ, and pdpC genes results in attenuation for growth in human macrophages and in vivo virulence in mice and reveals a unique phenotype for pdpC. Infect Immun, *81*(3), 850-861.

Ludu, J. S., de Bruin, O. M., et al. (2008). The Francisella pathogenicity island protein PdpD is required for full virulence and associates with homologues of the type VI secretion system. J Bacteriol, *190*(13), 4584-4595.

Luo, S., & Levine, R. L. (2009). Methionine in proteins defends against oxidative stress. FASEB J, *23*(2), 464-472.

Lushchak, V. I. (2011). Adaptive response to oxidative stress: Bacteria, fungi, plants and animals. Comp Biochem Physiol C Toxicol Pharmacol, *153*(2), 175-190.

Ma, D., Lu, P., et al. (2012). Structure and mechanism of a glutamate-GABA antiporter. Nature, *483*(7391), 632-636.

Macela, A., Stulik, J., et al. (1996). The immune response against Francisella tularensis live vaccine strain in Lps(n) and Lps(d) mice. FEMS Immunol Med Microbiol, *13*(3), 235-238.

Maier, T. M., Casey, M. S., et al. (2007). Identification of Francisella tularensis Himar1-based transposon mutants defective for replication in macrophages. Infect Immun, *75*(11), 5376-5389.

Maier, T. M., Pechous, R., et al. (2006). In vivo Himar1-based transposon mutagenesis of Francisella tularensis. Appl Environ Microbiol, *72*(3), 1878-1885.
Mailloux, R. J., Singh, R., et al. (2009). Alpha-ketoglutarate dehydrogenase and glutamate dehydrogenase work in tandem to modulate the antioxidant alpha-ketoglutarate during oxidative stress in Pseudomonas fluorescens. J Bacteriol, *191*(12), 3804-3810.
Maly, F. E., Quilliam, L. A., et al. (1994). Activated or dominant inhibitory mutants of Rap1A decrease the oxidative burst of Epstein-Barr virus-transformed human B lymphocytes. J Biol Chem, *269*(29), 18743-18746.
Mariathasan, S., & Monack, D. M. (2007). Inflammasome adaptors and sensors: intracellular regulators of infection and inflammation. Nat Rev Immunol, *7*(1), 31-40.
Mariathasan, S., Weiss, D. S., et al. (2005). Innate immunity against Francisella tularensis is dependent on the ASC/caspase-1 axis. J Exp Med, *202*(8), 1043-1049.
Mariathasan, S., Weiss, D. S., et al. (2006). Cryopyrin activates the inflammasome in response to toxins and ATP. Nature, *440*(7081), 228-232.
Marnett, L. J. (1999). Lipid peroxidation-DNA damage by malondialdehyde. Mutat Res, *424*(1-2), 83-95.
Martin, D. W., Baumgartner, J. E., et al. (2012). SodA is a major metabolic antioxidant in Brucella abortus 2308 that plays a significant, but limited, role in the virulence of this strain in the mouse model. Microbiology, *158*(Pt 7), 1767-1774.
Maxfield, F. R., & Yamashiro, D. J. (1987). Endosome acidification and the pathways of receptor-mediated endocytosis. Adv Exp Med Biol, *225*189-198.
McBride, H. M., Rybin, V., et al. (1999). Oligomeric complexes link Rab5 effectors with NSF and drive membrane fusion via interactions between EEA1 and syntaxin 13. Cell, *98*(3), 377-386.
McCaffrey, R. L., & Allen, L. A. (2006). Francisella tularensis LVS evades killing by human neutrophils via inhibition of the respiratory burst and phagosome escape. J Leukoc Biol, *80*(6), 1224-1230.
McCaffrey, R. L., Schwartz, J. T., et al. (2010). Multiple mechanisms of NADPH oxidase inhibition by type A and type B Francisella tularensis. J Leukoc Biol, *88*(4), 791-805.
McCaig, W. D., Koller, A., et al. (2013). Production of outer membrane vesicles and outer membrane tubes by Francisella novicida. J Bacteriol, *195*(6), 1120-1132.
McCrumb, F. R. (1961). Aerosol Infection of Man with Pasteurella Tularensis. Bacteriol Rev, *25*(3), 262-267.
McDonough, K. A., Kress, Y., et al. (1993). Pathogenesis of tuberculosis: interaction of Mycobacterium tuberculosis with macrophages. Infect Immun, *61*(7), 2763-2773.
McNealy, T. L., Forsbach-Birk, V., et al. (2005). The Hfq homolog in Legionella pneumophila demonstrates regulation by LetA and RpoS and interacts with the global regulator CsrA. J Bacteriol, *187*(4), 1527-1532.
Meibom, K. L., & Charbit, A. (2010). Francisella tularensis metabolism and its relation to virulence. Front Microbiol, *1*140.
Meibom, K. L., Forslund, A. L., et al. (2009). Hfq, a novel pleiotropic regulator of virulence-associated genes in Francisella tularensis. Infect Immun, *77*(5), 1866-1880.
Meireles Dde, A., Alegria, T. G., et al. (2014). A 14.7 kDa Protein from Francisella tularensis subsp. novicida (Named FTN_1133), Involved in the Response to

Oxidative Stress Induced by Organic Peroxides, Is Not Endowed with Thiol-Dependent Peroxidase Activity. PLoS One, *9*(6), e99492.
Melillo, A., Sledjeski, D. D., et al. (2006). Identification of a Francisella tularensis LVS outer membrane protein that confers adherence to A549 human lung cells. FEMS Microbiol Lett, *263*(1), 102-108.
Melillo, A. A., Bakshi, C. S., et al. (2010). Francisella tularensis antioxidants harness reactive oxygen species to restrict macrophage signaling and cytokine production. J Biol Chem, *285*(36), 27553-27560.
Melillo, A. A., Mahawar, M., et al. (2009). Identification of Francisella tularensis live vaccine strain CuZn superoxide dismutase as critical for resistance to extracellularly generated reactive oxygen species. J Bacteriol, *191*(20), 6447-6456.
Mendez-Samperio, P. (2008). Expression and regulation of chemokines in mycobacterial infection. J Infect, *57*(5), 374-384.
Metschnikoff. (1884). Ueber die Beziehung der Phagocyten zu Milzbrandbacillen
Miller, S. I., Ernst, R. K., et al. (2005). LPS, TLR4 and infectious disease diversity. Nat Rev Microbiol, *3*(1), 36-46.
Mohapatra, N. P., Balagopal, A., et al. (2007a). AcpA is a Francisella acid phosphatase that affects intramacrophage survival and virulence. Infect Immun, *75*(1), 390-396.
Mohapatra, N. P., Soni, S., et al. (2007b). Identification of an orphan response regulator required for the virulence of Francisella spp. and transcription of pathogenicity island genes. Infect Immun, *75*(7), 3305-3314.
Mohapatra, N. P., Soni, S., et al. (2013). Type A Francisella tularensis acid phosphatases contribute to pathogenesis. PLoS One, *8*(2), e56834.
Monteiro, C., Papenfort, K., et al. (2012). Hfq and Hfq-dependent small RNAs are major contributors to multicellular development in Salmonella enterica serovar Typhimurium. RNA Biol, *9*(4), 489-502.
Morgan, M. J., & Liu, Z. G. (2011). Crosstalk of reactive oxygen species and NF-kappaB signaling. Cell Res, *21*(1), 103-115.
Morner, T. (1992). The ecology of tularaemia. Rev Sci Tech, *11*(4), 1123-1130.
Mostowy, S., Sancho-Shimizu, V., et al. (2011). p62 and NDP52 proteins target intracytosolic Shigella and Listeria to different autophagy pathways. J Biol Chem, *286*(30), 26987-26995.
Moule, M. G., Monack, D. M., et al. (2010). Reciprocal analysis of Francisella novicida infections of a Drosophila melanogaster model reveal host-pathogen conflicts mediated by reactive oxygen and imd-regulated innate immune response. PLoS Pathog, *6*(8), e1001065.
Nano, F. E., Zhang, N., et al. (2004). A Francisella tularensis pathogenicity island required for intramacrophage growth. J Bacteriol, *186*(19), 6430-6436.
Newsholme, P., Procopio, J., et al. (2003). Glutamine and glutamate--their central role in cell metabolism and function. Cell Biochem Funct, *21*(1), 1-9.
Nguyen, L., & Pieters, J. (2005). The Trojan horse: survival tactics of pathogenic mycobacteria in macrophages. Trends Cell Biol, *15*(5), 269-276.
Noguchi, T., Ishii, K., et al. (2008). Requirement of reactive oxygen species-dependent activation of ASK1-p38 MAPK pathway for extracellular ATP-induced apoptosis in macrophage. J Biol Chem, *283*(12), 7657-7665.
Nunn, D. (1999). Bacterial type II protein export and pilus biogenesis: more than just homologies? Trends Cell Biol, *9*(10), 402-408.
Ogawa, M., & Sasakawa, C. (2006). Shigella and autophagy. Autophagy, *2*(3), 171-174.

Ohya, T., Miaczynska, M., et al. (2009). Reconstitution of Rab- and SNARE-dependent membrane fusion by synthetic endosomes. Nature, *459*(7250), 1091-1097.
Okan, N. A., & Kasper, D. L. (2013). The atypical lipopolysaccharide of Francisella. Carbohydr Res, *378*79-83.
Olsufjev, N. G. (1970). Taxonomy and characteristic of the genus Francisella Dorofeev, 1947. J Hyg Epidemiol Microbiol Immunol, *14*(1), 67-74.
Ottem, K. F., Nylund, A., et al. (2007a). Characterization of Francisella sp., GM2212, the first Francisella isolate from marine fish, Atlantic cod (Gadus morhua). Arch Microbiol, *187*(5), 343-350.
Ottem, K. F., Nylund, A., et al. (2007b). New species in the genus Francisella (Gammaproteobacteria; Francisellaceae); Francisella piscicida sp. nov. isolated from cod (Gadus morhua). Arch Microbiol, *188*(5), 547-550.
Otto, G. P., Wu, M. Y., et al. (2004). Macroautophagy is dispensable for intracellular replication of Legionella pneumophila in Dictyostelium discoideum. Mol Microbiol, *51*(1), 63-72.
Oyston, P. C., Sjostedt, A., et al. (2004). Tularaemia: bioterrorism defence renews interest in Francisella tularensis. Nat Rev Microbiol, *2*(12), 967-978.
Pagan-Ramos, E., Song, J., et al. (1998). Oxidative stress response and characterization of the oxyR-ahpC and furA-katG loci in Mycobacterium marinum. J Bacteriol, *180*(18), 4856-4864.
Patel, R. P., McAndrew, J., et al. (1999). Biological aspects of reactive nitrogen species. Biochim Biophys Acta, *1411*(2-3), 385-400.
Pechous, R. D., McCarthy, T. R., et al. (2009). Working toward the future: insights into Francisella tularensis pathogenesis and vaccine development. Microbiol Mol Biol Rev, *73*(4), 684-711.
Peng, K., & Monack, D. M. (2010). Indoleamine 2,3-dioxygenase 1 is a lung-specific innate immune defense mechanism that inhibits growth of Francisella tularensis tryptophan auxotrophs. Infect Immun, *78*(6), 2723-2733.
Petersen, J. M., & Schriefer, M. E. (2005). Tularemia: emergence/re-emergence. Vet Res, *36*(3), 455-467.
Pham, T. N., Rahman, P., et al. (2003). Elevated serum nitric oxide levels in patients with inflammatory arthritis associated with co-expression of inducible nitric oxide synthase and protein kinase C-eta in peripheral blood monocyte-derived macrophages. J Rheumatol, *30*(12), 2529-2534.
Piddington, D. L., Fang, F. C., et al. (2001). Cu,Zn superoxide dismutase of Mycobacterium tuberculosis contributes to survival in activated macrophages that are generating an oxidative burst. Infect Immun, *69*(8), 4980-4987.
Pierini, L. M. (2006). Uptake of serum-opsonized Francisella tularensis by macrophages can be mediated by class A scavenger receptors. Cell Microbiol, *8*(8), 1361-1370.
Pierson, T., Matrakas, D., et al. (2011). Proteomic characterization and functional analysis of outer membrane vesicles of Francisella novicida suggests possible role in virulence and use as a vaccine. J Proteome Res, *10*(3), 954-967.
Pillay, C. S., Elliott, E., et al. (2002). Endolysosomal proteolysis and its regulation. Biochem J, *363*(Pt 3), 417-429.
Pitt, A., Mayorga, L. S., et al. (1992). Assays for phagosome-endosome fusion and phagosome protein recycling. Methods Enzymol, *219*21-31.
Platz, G. J., Bublitz, D. C., et al. (2010). A tolC mutant of Francisella tularensis is hypercytotoxic compared to the wild type and elicits increased proinflammatory responses from host cells. Infect Immun, *78*(3), 1022-1031.

Pollak, N., Niere, M., et al. (2007). NAD kinase levels control the NADPH concentration in human cells. J Biol Chem, *282*(46), 33562-33571.
Popa, O., Hazkani-Covo, E., et al. (2011). Directed networks reveal genomic barriers and DNA repair bypasses to lateral gene transfer among prokaryotes. Genome Res, *21*(4), 599-609.
Price, D. R., Feng, H., et al. (2014). Aphid amino acid transporter regulates glutamine supply to intracellular bacterial symbionts. Proc Natl Acad Sci U S A, *111*(1), 320-325.
Prior, K., Hautefort, I., et al. (2009). All stressed out. Salmonella pathogenesis and reactive nitrogen species. Adv Microb Physiol, *56*1-28.
Proctor, R. A., White, J. D., et al. (1975). Phagocytosis of Francisella tularensis by Rhesus monkey peripheral leukocytes. Infect Immun, *11*(1), 146-151.
Pukatzki, S., Ma, A. T., et al. (2006). Identification of a conserved bacterial protein secretion system in Vibrio cholerae using the Dictyostelium host model system. Proc Natl Acad Sci U S A, *103*(5), 1528-1533.
Qin, A., Scott, D. W., et al. (2009). Identification of an essential Francisella tularensis subsp. tularensis virulence factor. Infect Immun, *77*(1), 152-161.
Raetz, C. R., Guan, Z., et al. (2009). Discovery of new biosynthetic pathways: the lipid A story. J Lipid Res, *50 Suppl*S103-108.
Raghunathan, A., Shin, S., et al. (2010). Systems approach to investigating host-pathogen interactions in infections with the biothreat agent Francisella. Constraints-based model of Francisella tularensis. BMC Syst Biol, *4*118.
Rajaram, M. V., Butchar, J. P., et al. (2009). Akt and SHIP modulate Francisella escape from the phagosome and induction of the Fas-mediated death pathway. PLoS One, *4*(11), e7919.
Ramakrishnan, G., Meeker, A., et al. (2008). fslE is necessary for siderophore-mediated iron acquisition in Francisella tularensis Schu S4. J Bacteriol, *190*(15), 5353-5361.
Read, A., Vogl, S. J., et al. (2008). Francisella genes required for replication in mosquito cells. J Med Entomol, *45*(6), 1108-1116.
Reilly, T. J., Baron, G. S., et al. (1996). Characterization and sequencing of a respiratory burst-inhibiting acid phosphatase from Francisella tularensis. J Biol Chem, *271*(18), 10973-10983.
Renesto, P., Ogata, H., et al. (2005). Some lessons from Rickettsia genomics. FEMS Microbiol Rev, *29*(1), 99-117.
Rink, J., Ghigo, E., et al. (2005). Rab conversion as a mechanism of progression from early to late endosomes. Cell, *122*(5), 735-749.
Robb, C. S., Nano, F. E., et al. (2012). The structure of the conserved type six secretion protein TssL (DotU) from Francisella novicida. J Mol Biol, *419*(5), 277-283.
Robertson, G. T., Child, R., et al. (2013). IglE is an outer membrane-associated lipoprotein essential for intracellular survival and murine virulence of type A Francisella tularensis. Infect Immun, *81*(11), 4026-4040.
Rohlfing, A. E., & Dove, S. L. (2014). Coordinate control of virulence gene expression in Francisella tularensis involves direct interaction between key regulators. J Bacteriol
Rohmer, L., Brittnacher, M., et al. (2006). Potential source of Francisella tularensis live vaccine strain attenuation determined by genome comparison. Infect Immun, *74*(12), 6895-6906.

Rohmer, L., Fong, C., et al. (2007). Comparison of Francisella tularensis genomes reveals evolutionary events associated with the emergence of human pathogenic strains. Genome Biol, *8*(6), R102.
Roy, C. R., Berger, K. H., et al. (1998). Legionella pneumophila DotA protein is required for early phagosome trafficking decisions that occur within minutes of bacterial uptake. Mol Microbiol, *28*(3), 663-674.
Rubinsztein, D. C., Shpilka, T., et al. (2012). Mechanisms of autophagosome biogenesis. Curr Biol, *22*(1), R29-34.
Rupp, J., Hellwig-Burgel, T., et al. (2005). Chlamydia pneumoniae infection promotes a proliferative phenotype in the vasculature through Egr-1 activation in vitro and in vivo. Proc Natl Acad Sci U S A, *102*(9), 3447-3452.
Sadosky, A. B., Wilson, J. W., et al. (1994). The iron superoxide dismutase of Legionella pneumophila is essential for viability. J Bacteriol, *176*(12), 3790-3799.
Saha, A. K., Dowling, J. N., et al. (1985). Properties of an acid phosphatase from Legionella micdadei which blocks superoxide anion production by human neutrophils. Arch Biochem Biophys, *243*(1), 150-160.
Sammons-Jackson, W. L., McClelland, K., et al. (2008). Generation and characterization of an attenuated mutant in a response regulator gene of Francisella tularensis live vaccine strain (LVS). DNA Cell Biol, *27*(7), 387-403.
Sandstrom, G. (1994). The tularaemia vaccine. J Chem Technol Biotechnol, *59*(4), 315-320.
Santic, M., & Abu Kwaik, Y. (2013). Nutritional virulence of Francisella tularensis. Front Cell Infect Microbiol, *3*112.
Santic, M., Asare, R., et al. (2008). Acquisition of the vacuolar ATPase proton pump and phagosome acidification are essential for escape of Francisella tularensis into the macrophage cytosol. Infect Immun, *76*(6), 2671-2677.
Santic, M., Molmeret, M., et al. (2005a). Modulation of biogenesis of the Francisella tularensis subsp. novicida-containing phagosome in quiescent human macrophages and its maturation into a phagolysosome upon activation by IFN-gamma. Cell Microbiol, *7*(7), 957-967.
Santic, M., Molmeret, M., et al. (2007). A Francisella tularensis pathogenicity island protein essential for bacterial proliferation within the host cell cytosol. Cell Microbiol, *9*(10), 2391-2403.
Santic, M., Molmeret, M., et al. (2005b). The Francisella tularensis pathogenicity island protein IglC and its regulator MglA are essential for modulating phagosome biogenesis and subsequent bacterial escape into the cytoplasm. Cell Microbiol, *7*(7), 969-979.
Sarkar, S., Ulett, G. C., et al. (2014). Role of capsule and O antigen in the virulence of uropathogenic Escherichia coli. PLoS One, *9*(4), e94786.
Sbarra, A. J., & Karnovsky, M. L. (1959). The biochemical basis of phagocytosis. I. Metabolic changes during the ingestion of particles by polymorphonuclear leukocytes. J Biol Chem, *234*(6), 1355-1362.
Schmerk, C. L., Duplantis, B. N., et al. (2009). Characterization of the pathogenicity island protein PdpA and its role in the virulence of Francisella novicida. Microbiology, *155*(Pt 5), 1489-1497.
Schulert, G. S., & Allen, L. A. (2006). Differential infection of mononuclear phagocytes by Francisella tularensis: role of the macrophage mannose receptor. J Leukoc Biol, *80*(3), 563-571.

Schulert, G. S., McCaffrey, R. L., et al. (2009). Francisella tularensis genes required for inhibition of the neutrophil respiratory burst and intramacrophage growth identified by random transposon mutagenesis of strain LVS. Infect Immun, *77*(4), 1324-1336.
Shackelford, D. B., & Shaw, R. J. (2009). The LKB1-AMPK pathway: metabolism and growth control in tumour suppression. Nat Rev Cancer, *9*(8), 563-575.
Shaffer, S. A., Harvey, M. D., et al. (2007). Structural heterogeneity and environmentally regulated remodeling of Francisella tularensis subspecies novicida lipid A characterized by tandem mass spectrometry. J Am Soc Mass Spectrom, *18*(6), 1080-1092.
Singh, R., Mailloux, R. J., et al. (2007). Oxidative stress evokes a metabolic adaptation that favors increased NADPH synthesis and decreased NADH production in Pseudomonas fluorescens. J Bacteriol, *189*(18), 6665-6675.
Sittka, A., Pfeiffer, V., et al. (2007). The RNA chaperone Hfq is essential for the virulence of Salmonella typhimurium. Mol Microbiol, *63*(1), 193-217.
Sjostedt, A. (2007). Tularemia: history, epidemiology, pathogen physiology, and clinical manifestations. Ann N Y Acad Sci, *1105*1-29.
Sobrero, P., & Valverde, C. (2012). The bacterial protein Hfq: much more than a mere RNA-binding factor. Crit Rev Microbiol, *38*(4), 276-299.
St John, G., & Steinman, H. M. (1996). Periplasmic copper-zinc superoxide dismutase of Legionella pneumophila: role in stationary-phase survival. J Bacteriol, *178*(6), 1578-1584.
Starr, T., Ng, T. W., et al. (2008). Brucella intracellular replication requires trafficking through the late endosomal/lysosomal compartment. Traffic, *9*(5), 678-694.
Steele, S., Brunton, J., et al. (2013). Francisella tularensis harvests nutrients derived via ATG5-independent autophagy to support intracellular growth. PLoS Pathog, *9*(8), e1003562.
Steinman, H. M. (1992). Construction of an Escherichia coli K-12 strain deleted for manganese and iron superoxide dismutase genes and its use in cloning the iron superoxide dismutase gene of Legionella pneumophila. Mol Gen Genet, *232*(3), 427-430.
Stenmark, H. (2009). Rab GTPases as coordinators of vesicle traffic. Nat Rev Mol Cell Biol, *10*(8), 513-525.
Storz, G., & Imlay, J. A. (1999). Oxidative stress. Curr Opin Microbiol, *2*(2), 188-194.
Straskova, A., Cerveny, L., et al. (2012). Deletion of IglH in virulent Francisella tularensis subsp. holarctica FSC200 strain results in attenuation and provides protection against the challenge with the parental strain. Microbes Infect, *14*(2), 177-187.
Su, J., Asare, R., et al. (2011). The capBCA Locus is Required for Intracellular Growth of Francisella tularensis LVS. Front Microbiol, *2*83.
Su, J., Yang, J., et al. (2007). Genome-wide identification of Francisella tularensis virulence determinants. Infect Immun, *75*(6), 3089-3101.
Sugano, Y., Muramatsu, R., et al. (2007). DyP, a unique dye-decolorizing peroxidase, represents a novel heme peroxidase family: ASP171 replaces the distal histidine of classical peroxidases. J Biol Chem, *282*(50), 36652-36658.
Suter, E. (1956). Interaction between phagocytes and pathogenic microorganisms. Bacteriol Rev, *20*(2), 94-132.
Svensson, K., Larsson, P., et al. (2005). Evolution of subspecies of Francisella tularensis. J Bacteriol, *187*(11), 3903-3908.

Swanson, J. A., & Baer, S. C. (1995). Phagocytosis by zippers and triggers. Trends Cell Biol, *5*(3), 89-93.
Takaya, A., Suzuki, M., et al. (2003). Lon, a stress-induced ATP-dependent protease, is critically important for systemic Salmonella enterica serovar typhimurium infection of mice. Infect Immun, *71*(2), 690-696.
Tamilselvam, B., & Daefler, S. (2008). Francisella targets cholesterol-rich host cell membrane domains for entry into macrophages. J Immunol, *180*(12), 8262-8271.
Tang, Y., Guest, J. R., et al. (2004). Post-transcriptional regulation of bacterial motility by aconitase proteins. Mol Microbiol, *51*(6), 1817-1826.
Tempel, R., Lai, X. H., et al. (2006). Attenuated Francisella novicida transposon mutants protect mice against wild-type challenge. Infect Immun, *74*(9), 5095-5105.
Thanassi, D. G., Bliska, J. B., et al. (2012). Surface organelles assembled by secretion systems of Gram-negative bacteria: diversity in structure and function. FEMS Microbiol Rev, *36*(6), 1046-1082.
Titball, R. W., Johansson, A., et al. (2003). Will the enigma of Francisella tularensis virulence soon be solved? Trends Microbiol, *11*(3), 118-123.
Toledano, M. B., Kullik, I., et al. (1994). Redox-dependent shift of OxyR-DNA contacts along an extended DNA-binding site: a mechanism for differential promoter selection. Cell, *78*(5), 897-909.
Travassos, L. H., Carneiro, L. A., et al. (2010). Nod1 and Nod2 direct autophagy by recruiting ATG16L1 to the plasma membrane at the site of bacterial entry. Nat Immunol, *11*(1), 55-62.
Tsolis, R. M., Baumler, A. J., et al. (1995). Role of Salmonella typhimurium Mn-superoxide dismutase (SodA) in protection against early killing by J774 macrophages. Infect Immun, *63*(5), 1739-1744.
Tsui, H. C., Leung, H. C., et al. (1994). Characterization of broadly pleiotropic phenotypes caused by an hfq insertion mutation in Escherichia coli K-12. Mol Microbiol, *13*(1), 35-49.
Tujulin, E., Macellaro, A., et al. (1998). Effect of endocytosis inhibitors on Coxiella burnetii interaction with host cells. Acta Virol, *42*(3), 125-131.
van der Wel, N., Hava, D., et al. (2007). M. tuberculosis and M. leprae translocate from the phagolysosome to the cytosol in myeloid cells. Cell, *129*(7), 1287-1298.
Vestvik, N., Ronneseth, A., et al. (2013). Francisella noatunensis subsp. noatunensis replicates within Atlantic cod (Gadus morhua L.) leucocytes and inhibits respiratory burst activity. Fish Shellfish Immunol, *35*(3), 725-733.
Via, L. E., Deretic, D., et al. (1997). Arrest of mycobacterial phagosome maturation is caused by a block in vesicle fusion between stages controlled by rab5 and rab7. J Biol Chem, *272*(20), 13326-13331.
Vieira, O. V., Bucci, C., et al. (2003). Modulation of Rab5 and Rab7 recruitment to phagosomes by phosphatidylinositol 3-kinase. Mol Cell Biol, *23*(7), 2501-2514.
Vonderheit, A., & Helenius, A. (2005). Rab7 associates with early endosomes to mediate sorting and transport of Semliki forest virus to late endosomes. PLoS Biol, *3*(7), e233.
Wang, X., Ribeiro, A. A., et al. (2007). Attenuated virulence of a Francisella mutant lacking the lipid A 4'-phosphatase. Proc Natl Acad Sci U S A, *104*(10), 4136-4141.
Wayne, L. G., & Diaz, G. A. (1988). Detection of a novel catalase in extracts of Mycobacterium avium and Mycobacterium intracellulare. Infect Immun, *56*(4), 936-941.

Wehrly, T. D., Chong, A., et al. (2009). Intracellular biology and virulence determinants of Francisella tularensis revealed by transcriptional profiling inside macrophages. Cell Microbiol, *11*(7), 1128-1150.
Weiss, D. S., Brotcke, A., et al. (2007). In vivo negative selection screen identifies genes required for Francisella virulence. Proc Natl Acad Sci U S A, *104*(14), 6037-6042.
Wherry, W. B., & Lamb, B. H. (2004). Infection of man with Bacterium tularense. 1914. J Infect Dis, *189*(7), 1321-1329.
Wren, J. D., Forgacs, E., et al. (2000). Repeat polymorphisms within gene regions: phenotypic and evolutionary implications. Am J Hum Genet, *67*(2), 345-356.
Wu, S., Ye, Z., et al. (2010). Salmonella typhimurium infection increases p53 acetylation in intestinal epithelial cells. Am J Physiol Gastrointest Liver Physiol, *298*(5), G784-794.
Yildiz, F. H. (2007). Processes controlling the transmission of bacterial pathogens in the environment. Res Microbiol, *158*(3), 195-202.
Yoshikawa, Y., Ogawa, M., et al. (2009). Listeria monocytogenes ActA-mediated escape from autophagic recognition. Nat Cell Biol, *11*(10), 1233-1240.
Yu, M. J., Ren, J., et al. (2009). The Legionella pneumophila Dps homolog is regulated by iron and involved in multiple stress tolerance. J Basic Microbiol, *49 Suppl 1*S79-86.
Zheng, M., Aslund, F., et al. (1998). Activation of the OxyR transcription factor by reversible disulfide bond formation. Science, *279*(5357), 1718-1721.
Zheng, Y. T., Shahnazari, S., et al. (2009). The adaptor protein p62/SQSTM1 targets invading bacteria to the autophagy pathway. J Immunol, *183*(9), 5909-5916.

Résumé

Francisella tularensis, l'agent étiologique de la tularémie, est une bactérie à multiplication intracellulaire facultative capable d'infecter de nombreux types cellulaires avec un tropisme particulier pour les macrophages. Cette bactérie est responsable d'infections graves chez de nombreuses espèces animales mais aussi chez l'homme. En particulier, la sous-espèce *F. tularensis* ssp *tularensis* a été classée comme agent de bioterrorisme de type A du fait de son pouvoir pathogène extrêmement élevé avec une faible dose infectieuse.

Des approches de mutagénèse aléatoire et de criblage de banques de mutants ont suggéré l'importance des gènes impliqués dans les fonctions métaboliques et nutritionnelles dans le cycle intracellulaire de *Francisella.* Parmi ces gènes, on retrouve de très nombreux systèmes de transport d'acides aminés dont la sous-famille de transporteurs amino-polyamine-organocation (APC).

Dans un premier temps, nous nous sommes intéressés à un transporteur APC codé par le gène *FTN_0571*, que nous avons appelé GadC. Pour comprendre l'importance de GadC dans la virulence de *F. tularensis*, nous avons réalisé un mutant chromosomique, délété du gène *gadC*, chez la sous-espèce *novicida*. Nous avons démontré que GadC est un importeur de glutamate et qu'il est nécessaire à la multiplication intracellulaire et à la virulence de *Francisella*, en assurant une sortie normale de la bactérie du phagosome. Ce phénomène s'explique par l'implication de GadC dans la résistance au stress oxydant généré dans le phagosome. De façon remarquable, la multiplication du mutant *gadC* est restaurée dans un contexte gp91phox$^{-/-}$, incapable de générer des espèces réactives de l'oxygène, aussi bien *in vitro* qu'*in vivo*. Enfin, nous avons montré que l'activité de GadC modifie la production de certains intermédiaires du cycle de Krebs, et la transcription de l'enzyme qui leur est associée, démontrant un lien étroit entre la résistance au stress oxydant, le métabolisme du glutamate et la virulence de *F. tularensis*.

Ces résultats nous ont conduits à nous intéresser à un autre transporteur appartenant à la sous-famille APC, présentant une homologie de 33% avec GadC, et que nous avons nommé ArgP. Nous montrons qu'un mutant *argP* présente un défaut de multiplication intracellulaire et de virulence résultant d'un retard sévère de sortie du phagosome. Ce phénotype s'explique par un défaut d'import d'arginine. L'inactivation du gène *argP* dans sous-espèce *holarctica* LVS provoque des défauts de multiplication intracellulaire similaires à ceux observés dans la sous-espèce *novicida*, suggérant un rôle conservé du transporteur ArgP dans les différentes sous-espèces de *F. tularensis*.

Comme l'arginine constitue un acide aminé essentiel pour la bactérie, nous nous sommes posés la question de l'importance de cet acide aminé durant la phase phagosomale. Une analyse du protéome bactérien du mutant *argP* de *F. novicida*, dans des conditions mimant les conditions nutritionnelles phagosomales, révèle que l'arginine joue un rôle prépondérant dans la traduction des protéines en affectant la synthèse des protéines ribosomales.

L'ensemble des travaux réalisés au cours de cette thèse constitue la première démonstration de l'importance de l'acquisition d'acides aminés durant la phase phagosomale du cycle intracellulaire de *F. tularensis*.

Mots-clés : *F. tularensis*, GadC, ArgP, échappement phagosomal